A Novel Long-Range Passive UHF RFID System over Twisted-pair Cable

Zhe Fu

Department of Engineering

University of Cambridge

This dissertation is submitted for the degree of

Doctor of Philosophy

St. Catharine's College November 2018

Abstract

Dissertation Title	A Novel Long-Range Passive UHF RFID System over Twisted-pair Cable
Name	Zhe Fu

Radio Frequency Identification (RFID) is one of the most representative, rapidly growing, and highly extendable technologies, which uses electromagnetic waves in accordance with specific communications standards and regulations to identify, track, or even localise desired objects. However, due to its high cost, limited read range, and uncertain reliability, its adoption still lags, especially in large-scale organisations. Even though an RFID distributed antenna system (DAS) can greatly improve the detection range and read rate of a single reader when the system uses different combinations of antenna states with frequency and phase hopping, the lossy and heavy coaxial cables between reader and antennas still limits the system coverage and design flexibility for wide-area passive UHF RFID applications.

In order to develop a cost-efficient and flexibly-installed passive RFID DAS, a novel large-range passive UHF RFID system over twisted-pair cable is proposed in this dissertation. This new system consists of one baseband central controller and one antenna subsystem, connected by a commonly used twisted-pair cable. It is shown that transmitting/receiving low frequency baseband signals over a twisted-pair cable can significantly reduce cable attenuation and extend the communication distance. A simulation is conducted to demonstrate that frequency and phase hopping can also be remotely controlled to fit this system structure by slightly varying the frequency or phase of the input reference signal of the frequency synthesis system. The features of twisted-pair cable in terms of its low cost, light weight, and bend radius greatly improve the design and installation flexibility of an RFID system.

The implemented system is designed based on the ISO 18000-6C and EPC Class 1 Generation 2 standards, and can operate according to FCC (902-928 MHz) and ETSI (865-868MHz) regulations. The results of the measurement show the reader can achieve a sensitivity of - 94.5 dBm over 30 m Cat5e cable, and its sensitivity can still remain at around -94.2 dBm over 150 m Cat5e cable. The experimental results of tag detection show that the passive tags can be successfully detected over a 6 m wireless range following a 300 m length of twisted-pair cable

between the central controller and antenna. This detection range cannot be achieved by existing commercial RFID systems.

Since the transmission and reception in a RFID system are simultaneous, finite isolation of the circulator/directional coupler and environmentally dependent reflection ratio of the antenna lead to serious leakage problems. Leakage can directly cause sensitivity degradation due to saturation of the RF components. A fast leakage suppression block is developed in efforts to solve this problem. Measurements show that this new canceller can deliver an average suppression of 36.9 dB, and this excellent performance remains when the system uses frequency hopping. With help of an improved scanning algorithm, this canceller can find its optimal status within 38 ms, and this settling time is short enough for most commercial RFID readers. By reducing the number of voltage samples taken, the convergence time can be further improved.

To fully investigate this new passive UHF RFID system value, a comparison study between the new system and a commercial system is conducted. This new automatic passive UHF RFID system is confirmed to deliver high performance long-range passive tag detection. Particular advantages are shown in the fast tag read rate and capability of uplink SNR improvement. This novel system is also superior to conventional RFID systems in terms of link distance, link cost, and installation flexibility.

Declaration of Originality

This dissertation is the result of my own work and includes nothing which is the outcome of work done in collaboration except as declared in the Preface and specified in the text.

It is not substantially the same as any that I have submitted, or, is being concurrently submitted for a degree or diploma or other qualification at the University of Cambridge or any other University or similar institution except as declared in the Preface and specified in the text. I further state that no substantial part of my dissertation has already been submitted, or, is being concurrently submitted for any such degree, diploma or other qualification at the University of Cambridge or any other University or similar institution except as declared in the Preface and specified in the text

It does not exceed the prescribed word limit for the relevant Degree Committee. This dissertation contains 42,580 words and 95 figures, including appendices, bibliography, footnotes, tables and equations.

1st November 2018

Acknowledgements

I would like to thank my supervisor Prof. Ian White and advisor Prof. Richard Penty for guidance and advice throughout my Ph.D. work. I would also like to thank Cambridge Trust, China Scholarship Council, and St. Catharine's College for their financial support.

In addition, I would like to thank Dr. Michael Crisp, Dr. Tongyun Li, and other group colleagues for communication and discussion of my research work. I would also like to thank Adrian Wonfor for his help in my experimental studies.

Finally, I would like to thank my parents for their support and encouragement. I would also like to particularly thank my wife for giving me great support and patience during my Ph.D. study. I feel grateful that my daughter and my doctoral research can grow up together during these years.

Contents

List of Figures

List of Tables

List of Acronyms

ACK	Acknowledgement
ADC	Analog to Digital Converter
AI	Artificial Intelligence
AMC	Artificial Magnetic Conductor
ASIC	Application-Specific Integrated Circuit
BER	Bit Error Rate
CDF	Cumulative Distribution Function
CPS	Cyber Physical System
CRC	Cyclic Redundancy Check
DAC	Digital to Analog Converter
DAS	Distributed Antenna System
DCOC	DC-Offset Cancellation
DCR	Direct Convert Receiver
DSB-ASK	Double Sideband Amplitude Shift Key
DRM	Dense Reader Mode
EAS	Electronic Article Surveillance
EIA	Electronic Industries Association
EPC	Electronic Product Code
ERO	European Radio Organisation
ERP	Effective Radiated Power
EIRP	Equivalent Isotropic Radiated Power
ETSI	European Telecommunications Standards Institute
FBAR	Film Bulk Acoustic Resonators
FCC	Federal Communications Commission
FDM	Frequency Division Multiplexing
FER	Frame Error Rate
IC	Integrated Circuit
IIP3	Input Third-Order Intercept Point
IoT	Internet of Things
ISO	International Organization for Standardization

LCC	Leaky Coupling Circuit
LF	Low Frequency
LNA	Low Noise Amplifier
LO	Local Oscillator
LPF	Low Pass Filter
LSB	Leakage Suppression Block
MCU	Micro-programmable Control Units
NF	Noise Figure
NFRA	Neighbour-Friendly Reader Anti-collision
OIP3	Output Third-Order Intercept Point
P1dB	1-dB Compressed Power
PCB	Printed circuit board
PD	Powered Devices
PIE	Pulse Interval Encoding
PLL	Phase-Locked Loop
PMU	Power Management Unit
PoE	Power over Ethernet
PPE	Pulse Position Encoding
PR-ASK	Phase Reverse Amplitude Shift Key
PSE	Power Source Equipment
RAIN	RAdio frequency IdentificatioN Organisations
RF	Radio Frequency
RFID	Radio Frequency Identification
ROI	Return of Investment
RSSI	Received Signal Strength Indicator
SAW	Surface Acoustic Wave
SCM	Supply Chain Management
SDR	Software defined radio
SFDR	Spur-Free Dynamic Range
SNR	Signal to Noise Ratio
SPDT	Single Pole Double Throw
STP	Shielded Twisted-Pair Cable
TDM	Time Division Multiplexing
TIA	Telecommunications Industries Association

TOTAL	Tag only Talks after Listening
UHF	Ultra-High Frequency
USB	Universal Serial Bus
UTP	Unshielded Twisted-Pair Cable
VCO	Voltage Controlled Oscillator
VHF	Very High Frequency
VNA	Vector Network Analyser

Publications

Z. Fu, M. J. Crisp, S. Yang, R. V. Penty and I. H. White, “Long distance passive UHF RFID system over ethernet cable,” in IEEE RFID-TA, Warsaw, Poland, 2017.

Fu, Z., Crisp, M.J., Penty, R.V., White, I.H., 2019, A novel wide-are passive UHF RFID system over twisted-pari cable, IEEE RFID Journal. (Filing)

Patent

Fu, Z., Crisp, M.J., Penty, R.V., White, I.H., 2018, A method for the transmission of UHF RFID signals over twisted pair cables to reduce installation costs of RFID distributed antenna systems. (Under Review)

Chapter 1

1. Introduction

1.1. Overview and Motivation

Radio Frequency Identification (RFID) is part and parcel of the Internet of Things (IoT). It uses electromagnetic waves to identify objects, animals or persons within a certain range [1]. The impact of RFID in emerging applications has been gradually changing people's lifestyles. For example, by simply using a contactless card, people are able to access office buildings, prove their personal ID, or borrow a book from a library. Figure 1.1 depicts these RFID applications.

Figure 1.1 RFID applications in different areas [2, 3, 4]

In addition to these benefits, the biggest change using RFID has been making payments. Today, in many stores and supermarkets, barcodes are still widely used for identifying products. They require a scanner with a beam of light to translate those black and white lines into information and send it to a database. The barcode can be directly printed onto the product overwrap at a tiny cost, and it has high detection accuracy. Over the past 25 years it has become a globally universal norm for retail products [5]. However, with the increasing requirements for highly-

efficient payment approaches, the barcode based system has revealed its limitations. In order to successfully identify a barcode, a scanner is needed to read the full barcode with a direct line of sight within 15 ft [6]. Products with ripped or damaged barcodes are impossible to be scanned. Additionally, the barcode payment process is very labour intensive and time consuming since all the products have to be scanned manually and individually. Most printed barcodes only contain limited product information such as manufacturer and product, and cannot be modified.

With the advent of RFID technology, the limitations of barcodes can be overcome and people can enjoy a better and more convenient shopping and payment experience. Low frequency (30 kHz to 300 kHz) RFID techniques help to improve payment efficiency. For example, people can quickly pay bills or tickets by tapping their authorised bank cards against a reader at stores, restaurants, or underground stations [7]. High frequency (3 MHz to 30 MHz) RFID applications are able to help the retailer to monitor and track the quality of their products. For instance, temperature sensing tags can provide real-time temperature indications for each shelf to ensure wine quality [8]. Ultra-high frequency (860 to 960 MHz) RFID applications are most widely used since they provide many new functions in the shopping experience, such as locating desired products and automatically identifying multiple products [9].

A new kind of store using RFID technology has merged in recent years. Alibaba, which is a financial technology arm of a Chinese internet giant, and Tencent, which is one of the biggest Chinese Internet services providers, opened their own personnel-free stores in early 2018 [2]. In such stores, customers are only required to be personally recognised when they enter the store. After their purchases, they can leave the store directly since the payment for their needs is automatically completed by the RFID systems. This easy-pay and unmanned store encourages more investment in developing new technology-based retail services. In addition to the retail industry, RFID applications are also used in other areas including pharma and healthcare, surveillance systems, and flora and fauna identification [3].

Based on the marketing report from IDTechEx, the world RFID market in 2018 is estimated to reach around $11.5 billion [3]. RFID technology is expected to maintain this rapid growth over the next four years due to faster developing sectors (healthcare, energy and security management, payments), wider deployment, and higher volumes. As shown in Figure 1.2, it is forecast that the global RFID market will rise to over $14 billion by 2022. The report also reveals that the passive RFID market constitutes more than 80 percent of the entire RFID

market. Passive RFID interrogators, which are worth around $2.8 billion, account for nearly a third of the passive RFID market revenue.

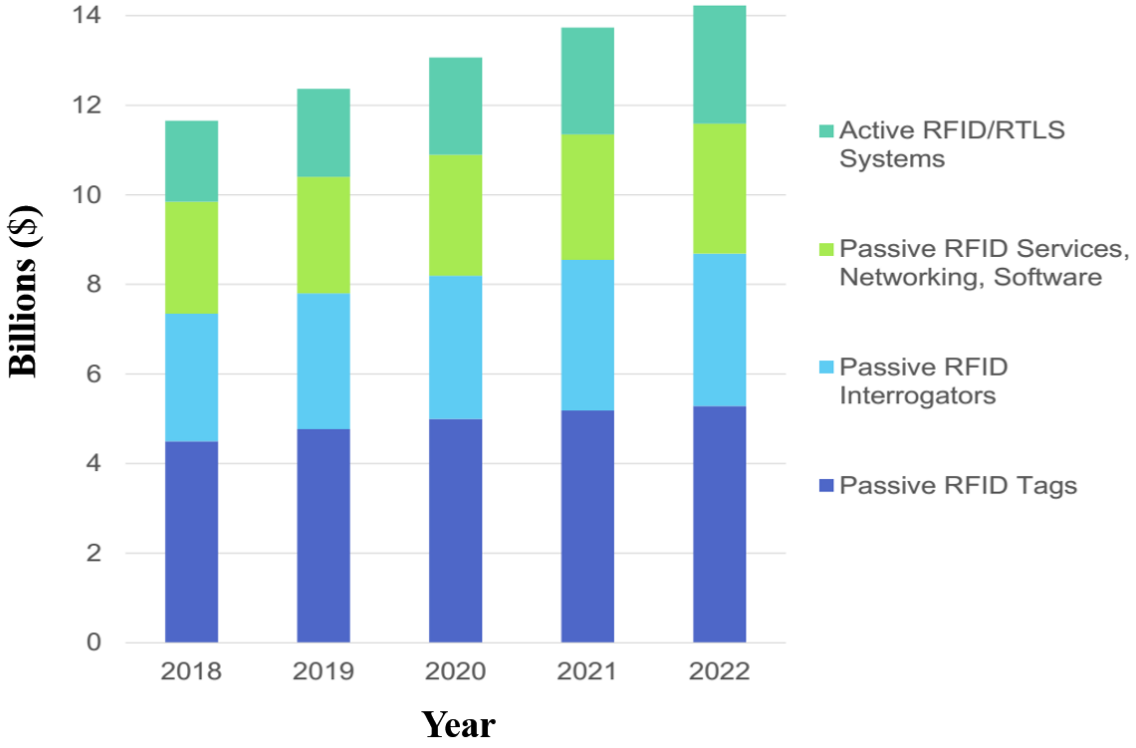

Figure 1.2 Entire RFID market outlook [3]

The high demands of passive RFID applications require more sophisticated hardware and software design since the businesses adopting this technology are becoming more competitive. Due to the growing demand from the government, transportation and retail sectors, cost-efficient, highly-reliable and installation-flexible passive UHF RFID systems are urgently needed for large-area detection [10]. This is because the maximum detection range of a conventional RFID reader is limited. The approach of using multiple readers for coverage extension results in high hardware costs (Figure 1.3(a)). In addition, operating multiple readers can lead to reliability issues due to serious tag collision problems. Re-installation and cable organisation can also be inflexible.

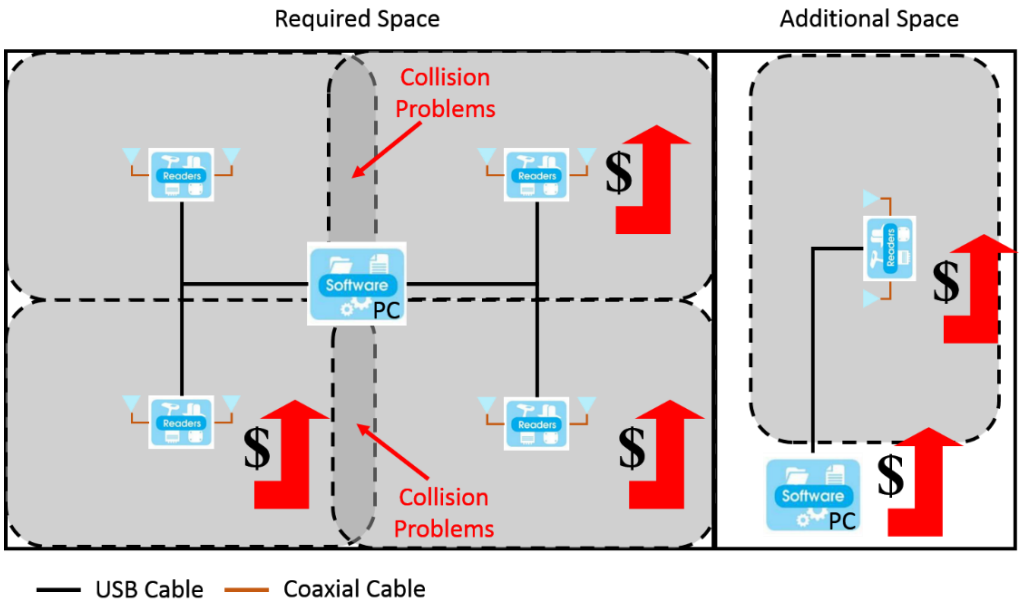

(a) A conventional RFID reader system for large-area detection

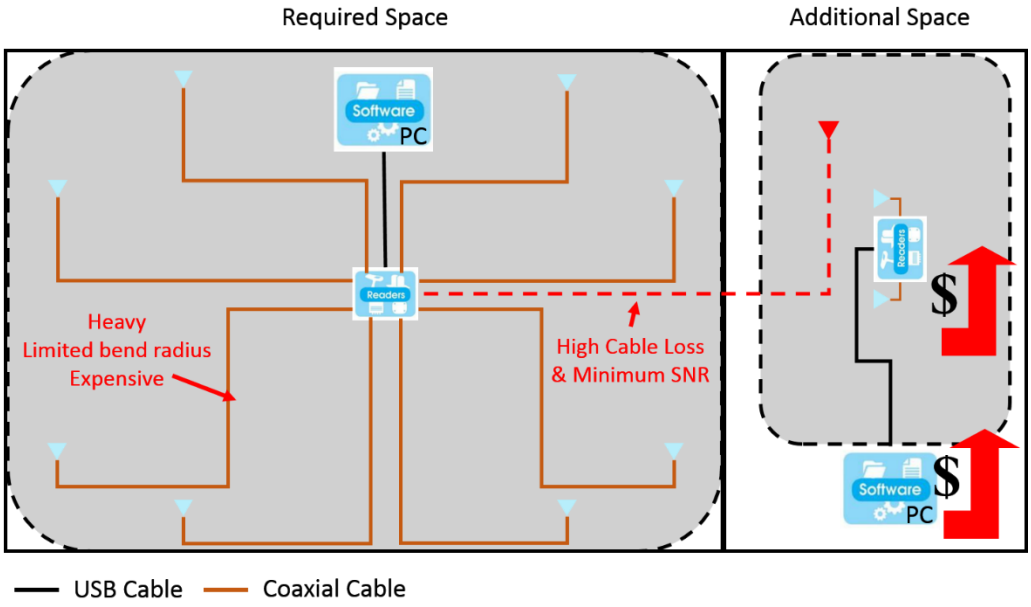

(b) A DAS reader system for large-area detection [11]

Figure 1.3 Limitations of current RFID systems for large-area detection

Communication technique such as distributed antenna systems (DAS) can reduce hardware cost and improve the detection range of single RFID readers. A comparison in terms of system cost between conventional RFID system and RFID DAS has been made in Table 1.1. Based on this conservative estimates, the RFID DAS is able to save almost half of the cost to achieve tag detection in the same area.

Table 1.1 Cost estimation between conventional RFID system and DAS [1] [3] [10]

Conversional RFID System			**RFID DAS**		
Name	Quantity	Ave. Unit Cost (£)	Name	Quantity	Ave. Unit Cost (£)
UHF RFID Reader (1 or 2 port)	4	750	UHF RFID Reader (Multi-port)	1	900
UHF Antenna	8	90	UHF Antenna	8	90
Coaxial Cable (5m)	8	15	Coaxial Cable (15m)	8	45
PC	1	300	PC	1	300
Total Cost	4140		Total Cost	2280	

However, the coverage of single RFID DAS is still not enough for major commercial wide-area applications [12]. As shown in Figure 1.3(b), the coverage of a DAS reader is limited by the maximum cable length they can support. High cable attenuation and uplink minimum SNR are the main factors that limit the cable length. Therefore, for additional space coverage, extra hardware sets are still required throughout the measurement scale. The deployment flexibility of this system is therefore impaired due to the use of expensive, heavy and limited bend coaxial cables. Thus, research is needed to provide a cost-efficient, highly flexible, and reliable RFID system for large-area tag detections. This is the focus of research in this thesis.

1.2. Aims and Objectives

This aim of this thesis therefore is to design a novel low-cost single-reader-based RFID system, which can provide reliable detection in large-scale organisations or wide-area applications. In order to achieve this design, there is a need to find solutions to overcome limitations such as high cable attenuation and SNR degradation. In addition, this new system should have deployment flexibility regardless of whether it is a first-time installation or a later modification. This system should also maintain high detection reliability even if the tag is far from the reader. The designed system must deliver low-cost options for extending the detection range. Moreover, the system should form the basis for developing future cyber-physical RFID systems.

Inspired by the development of the Ethernet, twisted-pair cable is widely used to connect in-building devices to the Internet. There are four pairs of wires available for the data communication. Twisted-pair cable is superior to coaxial cable in several respects, such as its low cost, light weight, and small bend radius. Although it suffers from significant cable loss when signals are transmitted at RFID carrier frequencies, it experiences little attenuation when baseband signals are transmitted. In terms of deployment, many buildings have already installed sockets for the Ethernet cable, and wiring designs for twisted-pair cable are much

easier than for coaxial cable. Based on these features, it is worthy investigating an RFID system that operates over a twisted-pair cable. To fully use the advantages of twisted-pair cable and improve the conventional RFID system for large-range passive tag detection, this thesis attempts to address the following issues:

- How to add twisted-pair cable to a conventional RFID system?
- How to allow the twisted-pair cable to achieve its potential for long-range detection?
- How to examine the feasibility of this new RFID configuration?
- How to implement this novel RFID system over a twisted-pair cable?
- How to measure the performance of this new system?
- How to understand the advantages and limitations of this new configuration?
- How to further explore this system to achieve its final potential?

1.3. Dissertation Outline and Original Contributions

The next five chapters of this thesis are described as follows and the original contributions are expressed in italics.

Chapter 2 presents three review studies relating to RFID technology. The first review describes the historical development of RFID, and the second review introduces the most recent RFID applications in different industrial sectors. The details in the third review focus on techniques used for advanced RFID system design. Challenges and opportunities are also discussed in this chapter.

Chapter 3 provides *a novel design of a passive UHF RFID system over twisted-pair cable*. *This system* is able to *deliver cost-efficient, highly-flexible, and simply-installed features*, and it is capable of being used for *wide-area detection*. Relevant theoretical simulations such as *link budgets and RF spreadsheets* prove the feasibility of this new design. In addition, *a new baseband-controlled frequency and phase hopping method* is demonstrated. According to the simulations and studies, this method not only can provide accurate frequency hopping and phase dithering, but also reduce the hardware cost and board in the RF transceiver.

Chapter 4 analyses the performance of the proposed RFID system. This new system is shown to provide excellent performance within the relevant industrial standards and regulations. *An investigation in sensitivity degradation over increasing twisted-pair cable length* is introduced

afterwards. The results show that the system can operate without sensitivity degradation over 180 m of Ethernet cable. A 300 metre long-range tag detection is also demonstrated. *This is the first demonstration of a passive RFID system over twisted-pair cable to achieve real tag detection over such a long distance, and this is also the first system to achieve long-range detection without performance degradation.*

Chapter 5 delivers *an automatic passive tag detection RFID system for long-range applications with a leakage suppression block*. A technical review is presented of the leakage canceller in terms of the cancelling methods and optimal scanning algorithms. Though the measurements, this *leakage canceller is shown to be able to find its optimal status within 38 ms and provide a stable suppression effect when the system operates with frequency hopping*. With help of this leakage canceller, *the proposed RFID system can operate in a monostatic antenna configuration and achieves as high detection rate as other commercial readers even over long-distance detection.*

Chapter 6 provides the overall conclusion of this thesis, and ideas for future work.

Chapter 2

2. Overview of RFID Systems

Over the past few decades, radio frequency identification (RFID) technology has been widely adopted for localisation, tracking, and monitoring in logistics, retail, manufacturing, and other areas. It is regarded as a key technology to enable "Industry 4.0" [13] or the "4th industrial revolution" [14], and is referred to as next generation cyber-physical systems (CPS). These advanced systems can provide unprecedented levels of flexibility and efficiency for industry. RFID also plays a vital role within systems that contribute real-world information about objects for artificial intelligence (AI) analysis.

In order to fully understand the importance of RFID technology, this chapter provides a detailed introduction to the history of RFID, and also describes its most recent developments and research challenges. After that, the basic operational principle and classification of RFID systems is explained. Finally, existing RFID standards and regulations are summarised before providing a technical review of the techniques and algorithms for RFID reader design.

2.1. The Development of RFID

This subchapter concerns the history of RFID development. The progress in RFID research (in different application categories) during the past five years is reviewed, and the challenges and opportunities in RFID research are discussed.

2.1.1. RFID History

The studies of electromagnetic waves and of radio frequency technology are the initial physical theories underlying RFID technology. In 1846, the initial research into electromagnetism was proposed by Michael Faraday [15]. He found that both light and radio waves are a form of electromagnetic energy. Based on his finding, James Maxwell published the preliminary electromagnetic theory in 1864, and Heinrich Hertz confirmed the theory in 1886 [15]. In 1906, Ernst F. W. Alexanderson illustrated how radio waves could be continuously generated and transmitted, and his hypothesis formed the technical foundation of RFID technology. Around two decades later, Evenor Brard [16] introduced the earliest passive communication system

based on an inductively coupled transceiver in his US patent (US 1744036), but, due to the limited description, its practical employment remains unclear.

During the Second World War, there were dramatic and rapid developments in radar systems. However, early radar was only capable of warning a local base of an approaching airplane from miles away. It was therefore difficult to distinguish which airplanes belonged to the enemy and which were 'friendly'. The German air force found an ingenious way to solve this problem. German pilots were asked to roll their airplanes in certain patterns when close to the base. This action allowed the radar signals from the airplane to be reflected in correlation with the patterns, and the modulated blips on the radar screen became an indication to identify friendly targets [1]. This is generally known as the first practical implementation of passive RFID. In Britain, the Royal Air Force invented the world's-first active RFID system to distinguish between friendly or enemy planes ('friend or foe', or IFF) in battle through the installation of active beacons on airplanes [1]. Once the signal from the radar was received, those beacons began to broadcast a signal that the identified airplane as friendly.

In 1948, Harry Stockman [17] proposed the basic theory of communication by means of reflected power. This great work provided the first example of using backscattered radiation to transmit information, and it inspired other researchers, including Vernon, who published "Application of the Microwave Homdyne" and Harris, who developed "Radio Transmission Systems with Modulatable Passive Transponder" [18]. Although RFID development bottlenecked in the following years due to its high cost, size and complexity, some important concepts and theories for forming modern RFID were nevertheless established. The first public description of an RFID integrated circuit (IC) was presented by Geoffrey Dummer [19] in 1952 and the matched filter theory, which helps to optimise the detection of weak signals, was demonstrated by Woodward [20] in 1953.

Many studies of electromagnetic theory relating to RFID emerged in the 1960s. Roger Harrington [16], known as the pioneer of computational electromagnetics, illustrated his works of "Field Measurement Using Active Scatterers" and "Theory of Loaded Scatterers" in 1963 and 1964 respectively. There were inventors like Jorgen Vinding [16], who devised an interrogator-responder identification system in 1967, and Robert Richardson [18], who introduced his remotely activated radio frequency devices in 1969. Meanwhile, RFID began to be commercialised. A practical anti-theft surveillance system, also known as Electronic Article

Surveillance (EAS), was developed by companies such as Sensormatic, Checkpoint and Knogo in 1960 [21]. They used inexpensive 1-bit tags to counter thefts by detecting the presence or absence of a tag. This system was the first commercial application of RFID technology.

During the 1970s and 1980s, RFID technology development progressed more quickly and drew more attention. The first conference on RFID was held in 1973 [22], and the Schlage Lock Company implemented one of the first major commercial applications of RFID in the same year [1]. With advances in semiconductor design and the decreasing prices of electronic goods, some large companies, such as Raytheon Co., RCA Co., and Fairchild, successfully produced their own RFID modules [23]. In 1973, William Arnold [24] published a remarkable article, in which he presented an attractive and foreseeable vision of potential RFID applications. In 1975, Koelle *et al.* [25] demonstrated a short-range radio telemetry system for electronic identification using modulated backscattering. This system had many features similar to the modern passive UHF RFID system.

By the 1980s, some of the uses listed in Arnold's paper were already a part of people's daily lives. For example, smart ID cards and motorway tolls were being rolled out in the United States, and industrial and business RFID applications and short-range tracking were being applied in Europe [23]. However, since most RFID systems were proprietorily implemented in the period, systems from different companies or inventors were difficult to interoperate [16]. Thus, there was low competition in the RFID industry, and the cost of RFID systems remained high. This slowed down the pace of RFID industry development.

In the early 1990s, the International Organization for Standardization (ISO) began to initialise standards and protocols for RFID communication [23]. These shed light on the diverse range of RFID applications, especially commercial requirements, including shipping container tracking and localisation [1]. By then, the information storage capacity of a single tag integrated circuit had increased, and RFID systems could therefore be used for more complicated tasks including traffic management and tracking library books [1]. However, due to the relatively high cost of the tags and incompatible standards, RFID systems had not yet been embraced in the retail supply chain. In 1999, the Auto-ID Centre was established in MIT, with the aim of accessing the product information from tag ICs and exchanging the obtained information on the Internet. In the same year, Kevin Ashton [26] coined the term 'Internet of Things' at the Auto-ID Center, a term which is still popular today.

In 2003, another important corporation, EPCglobal Inc., was founded. It provided standards for RFIDs in the supply chain, as well as standards for RFID training, marketing and installation. EPCglobal also pushed for the advancement of RFID public policy [1]. The ISO-18000C Class 1 Generation 2 standard, which was proposed by EPCglobal and ISO in 2006, is now a widely accepted protocol for UHF RFID communications. One of the world's largest retailers, Wal-Mart, installed RFID technology in its supply and delivery chains in 2005 and has enjoyed substantial benefits as a result of this new technology, particularly in inventory management [27]. Some other large retailers, including Tesco, Metro, and Target, are planning to install RFID technology [23]. During the last few years, RFID technology has continued to spread around the world, and is still undergoing rapid development. It is already focusing on some specific priorities, such as low-cost design, anti-collision protocols, and RFID data processing [28].

In more recent years, people have continued to explore the potential of RFID to reduce the system costs and expand its adoption more broadly. In 2012, Mojix [29] delivered its STAR (enhanced space time array) RFID system, which was able to achieve a very large detection coverage of 200,000 square feet. This innovation provided the possibility for installing a single RFID system to cover large-scale organisations. In 2013, due to the rapid growth of RFID applications and urgent need of additional operation spectrum, CEPT (the European Conference of Postal and Telecommunications Administrations) and ETSI (the European Telecommunications Standards Institute) allocated an extra spectrum 915-921MHz band for RFID devices [30]. In 2014, RAIN (the RAdio frequency IdentificatioN) was found as a wireless technology organisation for promoting the global adoption of UHF RFID technology. RAIN has already attached more than 155 members from all segments in the RFID industry chain [31].

The major events of RFID technology development from the 1940s to 2010s are summarised in Figure 2.1.

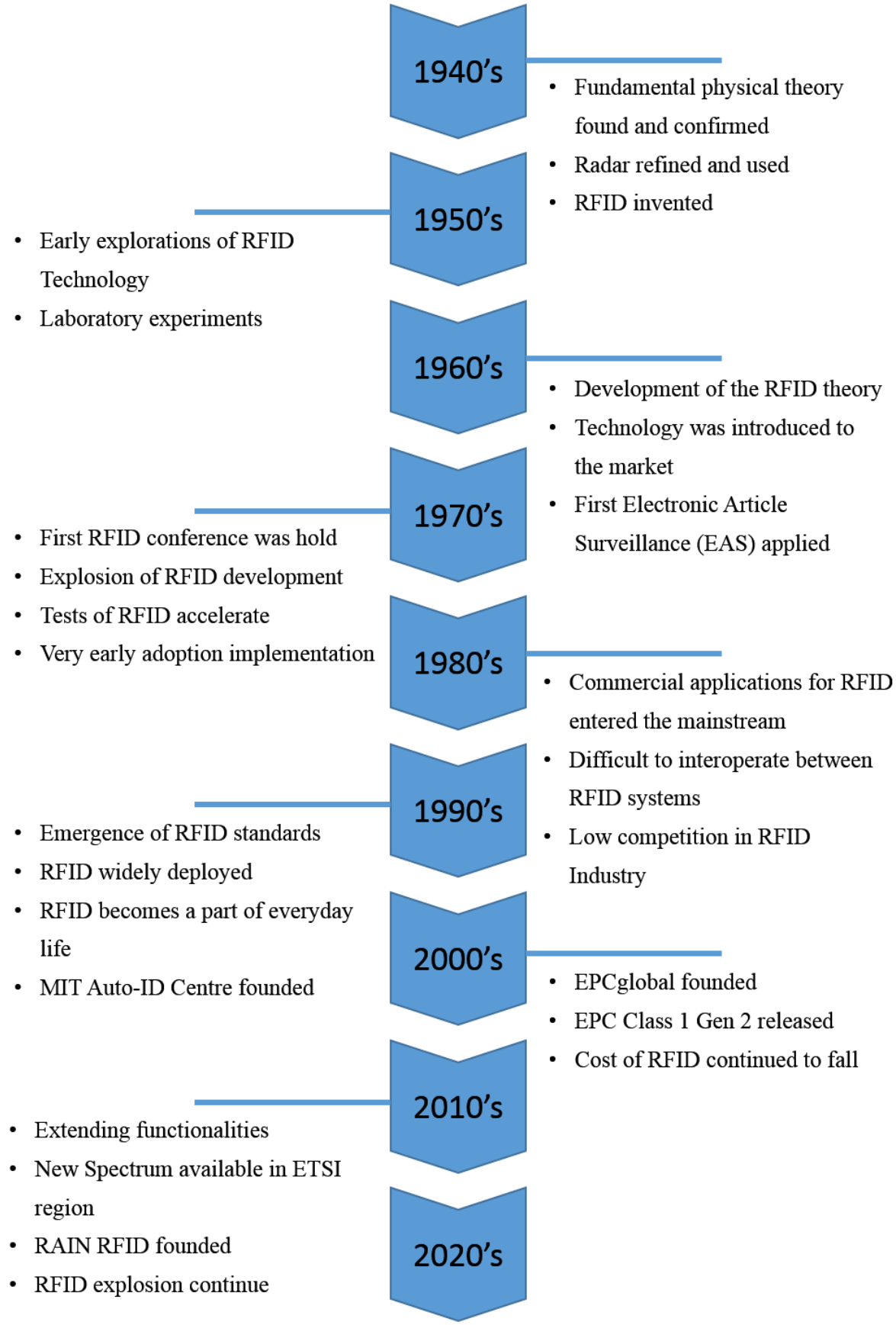

Figure 2.1 Brief history of RFID

2.1.2. Research Trend and Applications

RFID has become a widely used technology, to which extensive research is devoted. Researchers have explored and enhanced RFID technologies, and have reported many interesting applications and research findings. Some brief surveys of RFID publications have been reported in [22, 32, 33].

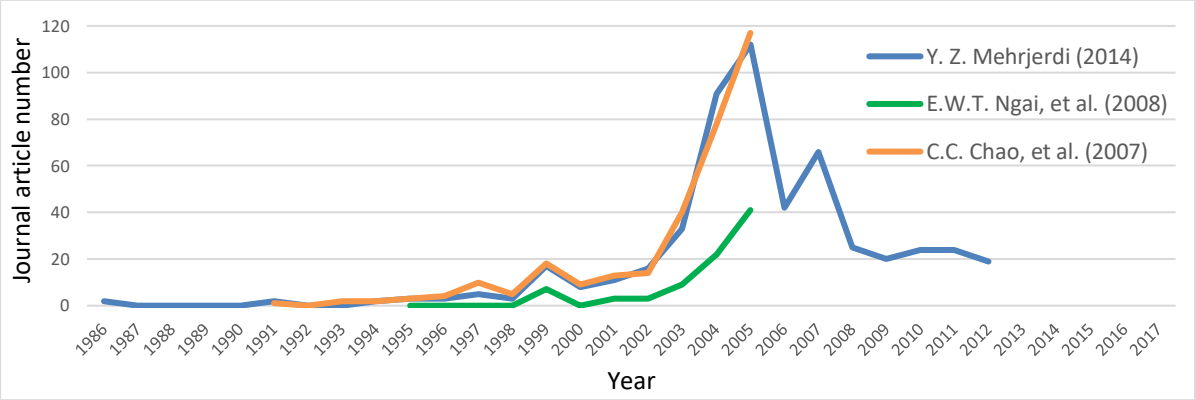

(a) Journal articles by year based on the review studies [22, 32, 33]

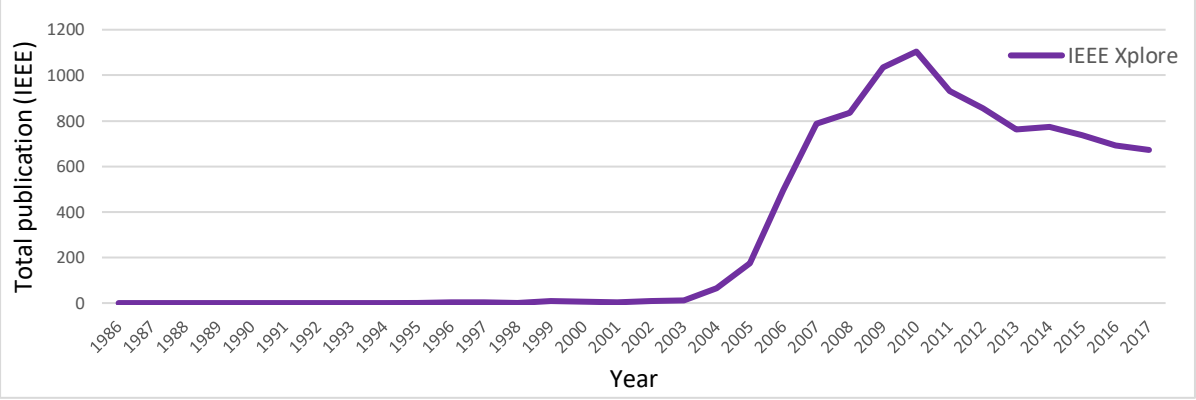

(b) Total publications relating to RFID based on the IEEE database

Figure 2.2 Distribution of RFID publications by years

As shown in Figure 2.2(a), there was a significant increase in RFID journal articles after 2002 which then reached maximum in 2005 with 112 publications. However, the number of journal papers rapidly decreased to 42 within two years. Although it rose again to 66 in 2007, there was a second reduction in publications in 2008. Since 2012, the number of RFID articles has remained at around 20. Another survey based on the IEEE database is shown in Figure 2.2(b). The publications include all books, magazines, journal articles, and conference papers relating to RFID. The number of publications in this survey is much larger and the studies regarding to RFID increased from only 3 in 2001 to 1104 in 2010. Even though the number of RFID

publications has gradually decreased in the last five years, it still consistently more than 600 publications per year.

Studies of RFID technology in the last five years can be broadly divided into four categories: (I) RFID technology; (II) RFID applications; (III) RFID privacy, policy and protocols; and (IV) others. The following content will discuss each category in detail.

(I) RFID technology

The vast majority of the publications focus on technology, aiming to provide technically advanced, better-performing, and lower-cost designs of RFID readers, tags, and antennas. Power transmission or energy harvesting approaches are also included in this category.

Software defined radio (SDR) based RFID readers have become increasingly popular in recent years. The advantages of such readers include their high flexibility through software upgrades and multi-standards capabilities [34]. More importantly, SDR-based readers provide the possibility for accessing and controlling the parameters of signals at each operational stage, whereas commercial readers only allow one to configure restricted parameters. Protocol evaluation and exploration [35], high-efficiency coding [36], and baseband synchronisation schemes [37] have therefore been extensively researched. Other recent studies on RFID readers, which are composed of discrete components or specific chipsets, have mainly focused on low cost design [38, 39], reliability improvement approaches [40, 41], and coverage extension scenarios [42, 12]. Current popular research topics relating to RFID tags include surface acoustic wave (SAW) tag design [43, 44], inkjet-printed tag design [45, 46] and sensor tag design [47, 48]. Additionally, during the past five years there has been encouraging progress in the development of flexible metal [49], dielectrics (water-filled containers) [50] and wall mountable tags [51].

Most recent studies regarding reader antennas have been primarily concentrated on low cost design [52] and multi-frequency band propagation [53]. Recently published research articles have addressed wearable tag antennas [54], where the focus has been on tag antenna design. New high performance antenna designs for tags and readers, and the design of multi-antenna configurations have conferred substantial advantages for RFID systems, including improved coverage [55], higher operational reliability [56] and higher localisation capability [57].

RFID-based sensor networks have shown great market potential, especially in healthcare and real-time monitoring [58]. Advanced energy-harvesting circuit design has accordingly become one of the major research directions supporting RFID-based sensing applications as power supply availability is often limited. In recent studies, challenges such as low power transmission efficiency [59], violable communication reliability [60], and product safety [61] have been fully discussed and addressed.

(II) RFID applications

Approximately a quarter of RFID articles concern RFID applications [32]. It is not possible to list each and every proposed application, therefore only some typical applications studies are considered here.

RFID healthcare applications have attracted much concern during the last five years. These not only lead to a reduction in medication error rates by 55 per cent, but they can also be used for access control and patient localising [22], [62]. Tracking is another popular application in various fields. For example, RFID systems are commonly used in the airline industry for luggage tracking [22], in the agricultural industry for food quality monitoring [63], in the manufacturing industry for enhancing return and maintenance efficiency [22], and in animal studies for monitoring the behaviour of animals [64]. Supply chain management (SCM) can be greatly improved by the installation of RFID technology. RFID technology is capable of solving SCM issues relating to data synchronisation, real-time tracking, planning, scheduling and reporting [65]. Furthermore, thanks to the development of anti-collision techniques and high reliable multi-antenna configurations, many low-cost and high-accuracy indoor object localisation applications are now available [66], [67].

(III) RFID privacy, policy and protocol

The importance of privacy, policy and protocol have increased due to the depth, breadth and speed of RFID development. The security of RFID communications has therefore been the focus of widespread research during the past five years. Chang *et al.* [68], Wang *et al.* [69], Sun *et al.* [70] and Mubarak [71] have clearly illustrated the security limitations of the current EPCglobal Class 1 Generation 2 protocol, and have proposed improvements in order to address issues relating to forward and reverse communication links. Some other protocols have been proposed in response to the anti-collision problem [72], distributed sensor networks [73], and tag read rate enhancement [74].

(IV) Others

Other RFID papers provide a general introduction to the subject area [15], [75] or are literature review studies [22], [32], [33] on RFID technology. In recent years, instead of reviewing the overall progress of RFID research, authors of review papers have tended to focus on specific RFID techniques or applications, for instance, RFID chipless tag design [76], RFID modelling and optimization problems [77], applications in agriculture and food supply chain [63], or applications in ornithology [64].

2.1.3. Challenges and Opportunities

As a widely adopted but not yet mature technology, RFID still has a long way to go to achieve its full potential. This subchapter mainly discusses the challenges and opportunities in relation to RFID system design. Other issues, such as return of investment (ROI), barcode-RFID migration, and management strategies, are beyond the scope of this study.

As shown in Figure 2.3, many obstacles need to be overcome before the full benefit of RFID can be realized. In terms of protocols, these are still under development and at present are not thorough enough for protecting the tag information. This deficiency can result in serious privacy and security problems, especially with people-tracking RFID systems, such as patient tracking and employee localising applications. Researchers have not yet successfully designed a universally compatible RFID reader that is capable of detecting all types of tags over different frequency bands, a breakthrough which would lead to reduced costs and enhanced flexibility. Another, less widely researched, problem is the compatibility of RFID and legacy systems. This critical problem should also be taken into account since it undermines the performance and reliability of RFID systems.

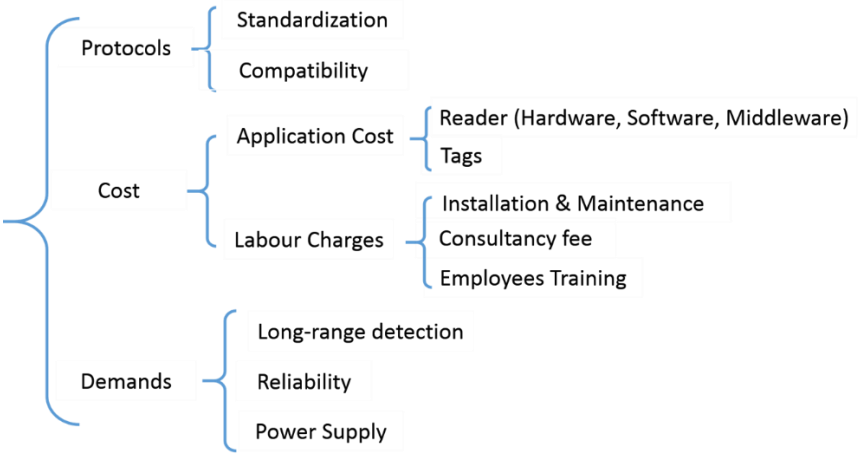

Figure 2.3 Main challenges of RFID system design

The high cost of RFID systems presents a considerable barrier to many potential clients. The most expensive component in an RFID system is the central reader, which usually costs around US$1000-2000 [22]. Tags also make up a significant proportion of costs since a large number of them need to be used in an RFID system. According to the study by Mehrjerdi [22], tags that operate in the low-frequency range (120 – 140 kHz) are generally more expensive (ranging from US $3 to $10), while tags that operate in the high-frequency (13.56 MHz) and ultra-high ranges (868 – 956 MHz) are relatively cheaper (around US $0.5 to $5 and ⩾US$0.75, respectively). Due to the shortage of experienced staff and qualified technical professionals, the cost of system installation and maintenance, technical consultancy, and employee training cannot be ignored.

In recent years, RFID technology has been increasingly applied in large-scale workplaces including warehouses, libraries and hospitals. The complexity and cost of RFID systems that cover the necessary detection range pose intractable problems, for which technical solutions are urgently needed. Another critical factor regarding long-range RFID systems is their reliability. Therefore appropriate approaches are needed in order to maintain a high detection rate. Power supply is another critical aspect of RFID systems. Longer detection distance and stricter communication regulations require advanced architecture and transceivers that can successfully activate passive tags. None of these improvements can be achieved without a smart power supply unit.

2.2. RFID Systems Architecture

This chapter provides an introduction to RFID systems, including system architectures, operational principles, and classes of system.

2.2.1. Conventional System and Operation Principles

A conventional RFID system consists of an interrogator (known as a reader) and transponders (known as tags). The reader can be further divided into several specific blocks, each providing particular functions to serve the entire system (Figure 2.4). For example, the radio block is typically employed as a front-end transceiver, which receives baseband commands and generates sufficient radio power to the tags via a reader antenna. It also decodes the backscattered signals from the tags and returns them to the reader baseband modules. Well-designed software and firmware are essential for a RFID reader. Interface infrastructure is important as it allows users to directly access or control the reader physical layer blocks by

simply clicking the buttons on their PC. The Universal Serial Bus (USB) and RS-232 cables are typically used to connect a reader to a user's PC. In addition, Ethernet cable can also be used to allow the reader to connect to other networks when Ethernet protocols are contained.

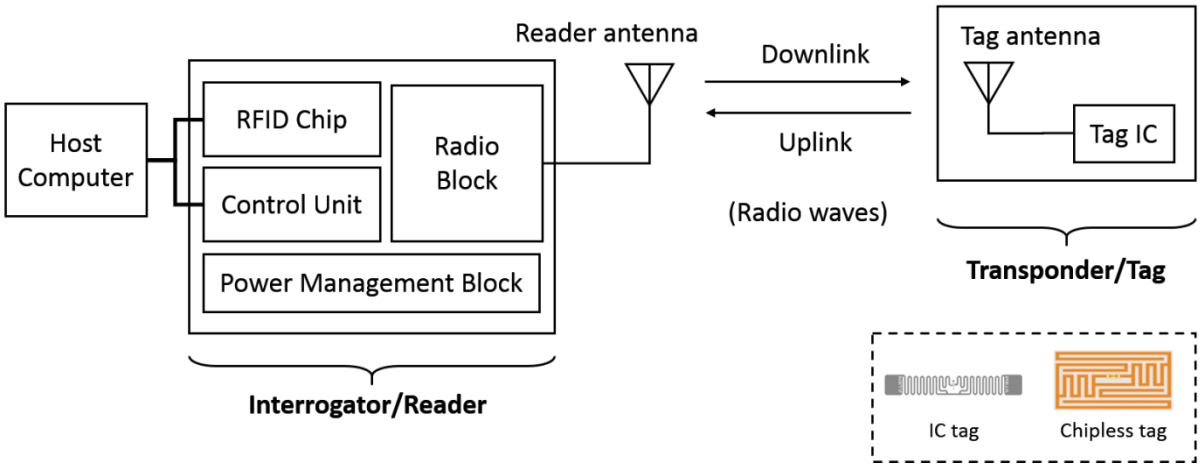

Figure 2.4 The components of a conventional RFID system

The power management block is a very common hardware unit, which offers a stable power source and provides methods for optimising power consumption. However, in recent years, the idea of developing auto- or remote-controlled RFID systems, which allow readers to automatically move following a track on the ceiling or flying in the sky carried by a Drone [78], has become important: This has led to more research into power management units. Techniques such as wireless charging and efficient charging are urgently needed to enable the adoption of exciting new RFID systems.

An application-specific integrated circuit (ASIC) and an antenna form a typical RFID tag. There are three main functional blocks in the tag IC: the backscatter block for signal modulation, the power supply block for energy storage, and the detector block for signal decoding [1]. With advanced electronic techniques, tag ICs can be produced in a very small size. However, the size of the tag antenna should remain large enough to satisfy specific RF requirements such as antenna gain or bandwidth. In the ultra-high frequency band, the half-wavelength dipole antenna is mostly used for passive tags due to its ease of fabrication and high power transmission efficiency. Since the entire length of the antenna equals the half-wavelength of the operation frequency, the size of this kind of tag is around 16 cm. Research into chipless tags such as surface acoustic wave (SAW) tags are also popular in the RFID industry. The SAW tag uses a series of reflectors on its antenna surface to modulate the approaching reader signals, and then re-radiate them back to the reader. Compared with an IC-based tag, a SAW tag is

superior in its low cost, low transmission power requirement, and longer detection range [79]. However, due to the absence of the IC, the illuminated SAW tags respond to a reader simultaneously, resulting in serious collision problems. In addition, a SAW tag is read-only and its storage capability is limited. Examples of both practical IC-based and chipless tags are shown in the bottom right of Figure 2.4.

The basic operational principles of an RFID system can be clearly explained by considering the signal transmission path. In the forward link, some crucial parameters such as output power, operational frequency, and modulation schemes have to be first defined. After that, the RFID chip starts to generate baseband signals and transmits them to the radio block. In the radio block, the signals pass through radio components including amplifiers, mixers, switches and filters, and then produce the desired radio source to the reader antenna. Communication between the reader and the tags is in the form of electromagnetic waves. The principle of this connection is similar to that of a magnetic transformer. The current flowing in the reader antenna provides radiative or inductive coupling, which leads to sufficient voltage across the tag. A certain proportion of the transmitted signals received by the tag are modulated so that they are added to the tag information. Amplitude and phase modulation methods are commonly applied in the tag's integrated circuits by changing the value of its load resistor [1].

In the reverse link, the reflected signals (backscattering signals) received by the reader antenna also go through a series of radio components. These components enable the reader to eliminate unwanted noise, react to a pre-set frequency band, down-convert the received signals, and send the received tag electronic product code (EPC) to the RFID chip. After signal processing in the firmware and software, users can view the detection results, including detecting speed and received signal strength indicator (RSSI), as well as the information from the tags.

2.2.2. Classification of RFID Systems

A modern RFID system can be broadly classified into various categories in terms of the types of tag which system uses, the types of reader which system deploys, and the frequency band in which system operates.

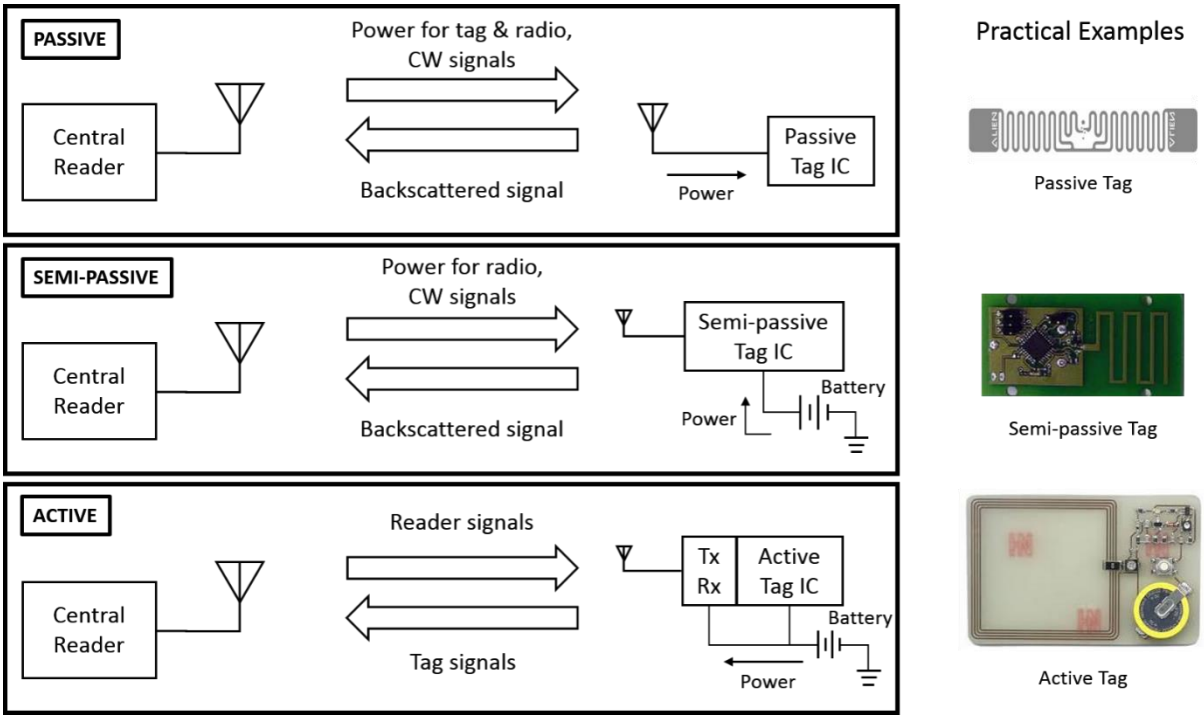

Figure 2.5 RFID systems with different tag options

RFID systems can be distinguished on the basis of the passive, semi-passive and active tags which they read (see Figure 2.5). A passive tag has no independent power source to support the operation of its circuit. The only means of self-activation is via electromagnetic waves sent from the reader. RFID systems with passive tags are quite popular today. The great advantage of a passive tag is the simplicity of its circuit, and its low cost. However, some typical problems of using such tags include their unreliability in terms of detection and their limited detection range, especially in the ultra-high frequency (UHF) band [1].

A semi-passive tag is more reliable, and its detection range can extend up to around 100 metres [22]. It contains a battery that powers up its circuit, but the tag still communicates with the reader via scattered and modulated electromagnetic waves. However, this better performance is accompanied by its larger size and higher cost.

Unlike a semi-passive tag, an active tag not only has a local power source, but also contains its own transceiver. The reader and tags in this kind of system can be used to achieve bidirectional communication with more sophisticated phase modulation schemes, and the read range can extend to hundreds of metres. However, in addition to the size and cost issues, active tags require extra maintenance, and also tend to suffer from serious time delays in long-distance detection.

Figure 2.6 RFID systems with different readers [80] [81] [82]

RFID systems can be also divided into three groups based on the readers they use, including fixed reader, portable/handheld reader, and auto-/remote-controlled reader. The most commonly used RFID reader for retail security and inventory applications is the reader with fixed antennas. As shown in Figure 2.6, the fixed reader is usually deployed on the ceiling or mounted on portals accompanied by several antennas nearby. These installation locations allow the fixed antennas to maximize the probability of line of sight to the tags so as to optimise the system detection rate.

A portable reader (shown bottom left of Figure 2.6) allows reduced cost and deployment time, since it can be placed close enough to the tags. In addition, a portable reader often provides interfaces for other devices such as a mobile phone or a barcode scanner to work cooperatively. However, since a fixed reader is capable of collecting specific information such as RSSI and phase differences between the tags and the antennas at different locations, these systems offer the possibility of fulfilling complex tasks such as object tracking and item localization where the portable reader cannot so flexibly.

With help of more sophisticated artificial intelligence (AI) and software solutions, robot RFID readers and Drone-reliant readers have emerged [80] [82]. These auto-/remote-controlled RFID systems (shown bottom right of Figure 2.6) enjoy the advantages of both fixed and portable readers in terms of powerful functionality and high mobility. In addition, these intelligent RFID

systems can further replace conventional non-RFID techniques and extend adoption of RFID technology.

Table 2.1 RFID systems based on different operation frequency bands [1], [83]

Frequency Band	*Detection Range*	*Coupling Mode*	*Application*	*Merits*	*Disadvantages*
LF (125/134 KHz)	0-1 m	Inductive	Animal ID Access control	Insensitive to environmental effects, Low cost of reader	Low data rate, Relatively high cost of tags
HF (13.56 MHz)	0-1 m	Inductive	Oyster card e-passport	High data rate, Secure communication	Require larger antenna for reader and tags
UHF (860-960 MHz)	1-10 m	Inductive Radiative	Motorway tolls Asset tracking	Low cost of tag Longer reader range	Dense reader interference, Discontinuous and unpredictable read zone
UHF (2.4 GHz)	1-100 m	Radiative	Inventory control Vehicle tracking	Smaller tag size, Lower cost of tag	Interference from other devices

The operational frequency band can also be a criteria for classifying RFID systems. Theoretically, the operational frequency of a system determines the antenna coupling mode, and the coupling mode directly affects the behaviour of the tags. Commonly, systems use frequency bands, from the low-frequency (LF) band (at around a few hundred KHz, where inductive coupling is used) to the very high-frequency (VHF) band (at several hundred MHz, where radiative coupling is usually employed). The main difference between these two coupling modes is the degradation of received signalling power over distance. With inductive coupling, the power falls smoothly but rapidly when the tag is moved away from the reader antenna. The read range of an inductive coupling system is mainly dependent on the antenna size. With radiative coupling, the power drops gradually but in a fluctuating manner. In view of these features, an RFID system that operates in a radiative coupling mode has a higher detection range, but is more likely to encounter interference. Furthermore, due to the fluctuation in power degradation, a radiative coupling system encounters discontinuous and unpredictable detection problems. More comparisons between RFID systems in relation to different frequency bands are detailed in Table 2.1.

Thus, the best way to select or design an RFID system is to optimise its requirements in terms of read range, cost budget, detection performance, local regulations and other environmental or special purposes. However, there is a common rule for devising an RFID system: the cost of identifying an object should be less than the value of the identified knowledge or object. Accordingly, there are several research projects that are concerned with the design of inexpensive (low-cost) identifying readers [84] or tags [85]. Generally, researchers aim to

simplify the reader and tag circuits, and they have been investigating low-cost components in order to reduce the overall cost of RFID systems.

2.3. Standards and Regulations

Before the 1990s, there was no specific standard for RFID communication. Systems developed in that period normally did not interoperate, and their cost remained very high due to little competition [15]. The RFID industry experienced slow development until standard-setting bodies such as the International Organization for Standardization (ISO) and EPCglobal Inc. provided agreed RFID standards. In getting an understanding of the field, there needs to be a good understanding of the RFID standards, since they not only provide basic communication agreements, but also they indicate the research trends, capital flows, and policy directions of the entire RFID industry. A standard such as Ethernet (IEEE 802.3) can greatly help the expansion of its industry and produce profits for further investment and development. RFID regulations can be regarded as regional rules, which mainly inform the allowable spectrum range, emission power level and maximum permissible interference of an RFID system. Due to the different development approaches, regulation of RFID differs between countries. It is important to acquire knowledge of local RFID regulations before designing or installing an RFID system in particular countries.

Table 2.2 ISO/IEC 18000 standards [86] [87]

Standard Code	Description		
ISO/IEC 18000-1	Generic parameters for air interfaces for globally accepted frequency		
ISO/IEC 18000-2	Air interface for 135 kHz		
ISO/IEC 18000-3	Air interface for 13.56 MHz		
ISO/IEC 18000-4	Air interface for 2.45 GHz		
ISO/IEC 18000-5	Air interface for 5.8 GHz		
ISO/IEC 18000-6	Air interface for 860-960 MHz	Type A	Pulse-Interval-Encoding (PIE) Adaptive ALOHA collision-arbitration algorithm
		Type B	Manchester Adaptive binary-tree collision-arbitration algorithm
		Type C	Pulse-Interval-Encoding (PIE) Random slotted collision-arbitration algorithm
		Type D	Pulse Position Encoding (PPE) / Miller 2 Encoding Tag only Talks After Listening (TOTAL)
ISO/IEC 18000-7	Air interface for 433 MHz		

2.3.1. ISO/IEC 18000 Standards

The International Organisation for Standardisation (IOS) is a global union which consists of national standardisation institutions. It has developed a series of standards relating to RFID in the last two decades. These standards, known as ISO/IEC 18000, are mainly set by the operational frequency of RFID applications. The details of these standards are shown in Table 2.2. In 2012, due to the rapid growth of the RFID market in the 860 – 960 MHz band, ISO explicated the Part 6 standard for supporting the new needs of the RFID industry. The main differences between these four types of standards are the symbol encoding schemes in the forward link and protocols of reader-tag communication.

2.3.2. EPCglobal Gen 2 Standards

The EPCglobal Gen2 standard is one of most globally accepted standards for RFID systems. It was first created to be compatible with ISO standards in 2004 [1]. This standard specifically introduces basic physical and logical guidelines such as symbol types, coding methods, modulation schemes and other specific parameters for RFID tags and readers. The EPC standard also includes the data format of the ID so that the tag information can be fully understood. Table 2.3 presents the existing EPC classes on the basis of the functionality of the tag.

Table 2.3 EPC tag classes [86]

EPC Classes	*Tag types*	*Features*
Class 0	Passive tag	Read only
Class 1	Passive tag	Read only, write once contains tag kill function
Class 2	Passive tag	Read only, write once Class 1 with additional memory
Class 3	Semi-passive tag	Read/Write with on-board energy Superior in wider range, collects sensor data
Class 4	Active tag	Read/Write with embedded battery Includes own RF transmitter
Class 5	Active tag	Read/Write with built-in battery Can activate Class 1, 2, 3 tags

2.3.3. Ultra-High Frequency Regulations

In addition to the RFID standards, RFID designs are usually affected by other local restrictions, which specify the available spectrum range, maximum transmission power, and permissible interference level for UHF RFID communications. Countries, in Europe, Middle East, and

North Africa, usually obey the regulations provided by the European Radio Organisation (ERO) and the European Telecommunications Standards Institute (ETSI). Countries in America such as the United States and Canada often conform to the regulations defined by the Federal Communications Commission (FCC). Countries in Asia differ widely in their regulation requirements. Since this thesis focuses on the ultra-high frequency band (860-960 MHz) RFID system design, the regulations relating to UHF are summarised in Table 2.4.

Table 2.4 Summary of UHF regulations in different countries [86] [88]

Country	**Frequency Band (MHz)**	**Emission Power**
United Kingdom	865.6-867.6 915-921	2W ERP 4W ERP
European Countries	865.6-867.6 915-921	2W ERP 4W ERP
United State & Canada	902-928	4W EIRP
China	920.5-924.5 865-868 (Hong Kong) 920-925 (Hong Kong)	2W ERP 2W ERP 4W EIRP
Japan	916.7-920.9 916.7-923.5	4W ERP 0.5W EIRP
Australia	920-926 918-926	4W EIRP 1W EIRP
New Zealand	864-868 921.5-928	4W EIRP 4W EIRP

(ERP: Effective Radiated Power, EIRP: Equivalent Isotropic Radiated Power, ERP=1.64 EIRP)

2.4. Review for Large-scale RFID system Design

Table 2.5 Structure of technique review chapter

Purposes	**Techniques / Protocols / Algorithms**
Range Extension	● Tag antenna ● Reader parameters ● Multi-antenna ● Booster or repeater
Reliability Enhancement	● Reader and tag anti-collision protocols ● Leakage and noise cancellation
Low Cost	● Low price ● Low power consumption ● Low complexity
Power Supply	● Power over Ethernet (PoE) ● Battery

This review chapter addresses the techniques and algorithms that are integral to passive UHF RFID system design. The advantages and disadvantages of each technique or algorithm are discussed. The structure of this review chapter is specified in Table 2.5.

2.4.1. Techniques for read range extension

The potential maximum read range of a UHF passive tag is 10 metres, which is sufficient for many indoor RFID systems. However, due to multi-path fading and environmental interference, the practical detection range is often substantially lower than the maximum. In order to overcome this problem and to provide more stable long-distance passive RFID reader systems, researchers have been designing new RFID tags and readers, RFID system configurations, and range-extended boosters and repeaters.

Kim and Yeo [89] designed a dual-band RFID tag antenna by using an artificial magnetic conductor (AMC) ground plane to increase the read range (Figure 2.7). Since this new tag was designed to be placed on metallic objects, such as vehicles, aircraft and containers, it was tested inside a metallic cavity. This new tag had a dipole-type antenna, and its chip was attached in between the bowtie loops. The researchers investigated the features of this tag by varying the tag depth (h), and the gap (l_{offset}) between the post and cavity dimensions (X_c or Y_c). After performing a series of tests, they were able to set two different resonant frequency bands (869 MHz and 913 MHz) by offsetting the above factors. More importantly, they discovered that this new tag exhibited a read distance that was 3.1 times longer (22.75 m at 864 MHz, and 23.74 m at 910 MHz) than that of the commercial ALN-9540-WR RFID tag. However, the aperture size of their tag was much larger than that of the commercial one.

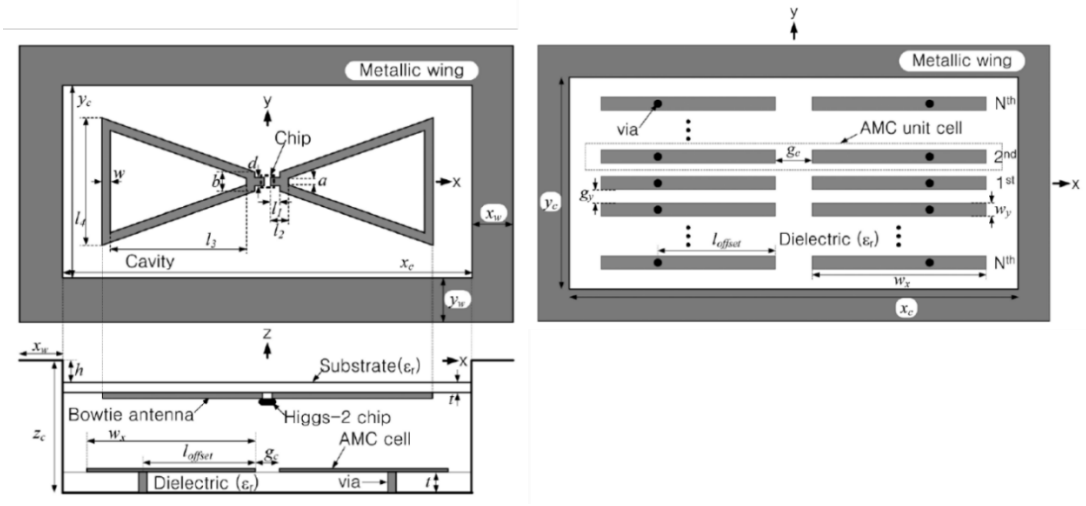

Figure 2.7 Geometry of the proposed RFID tag and the AMC substrate [89]

As well as making improvements to RFID tags, researchers have also investigated some reader-related parameters that can affect or limit the overall system performance (including the read range). Mayordomo *et al*. [90] thoroughly examined these issues in their study on long-range reader design. Transmission leakage is one of the main challenges in long-range reader design, as it increases the noise level and reduces reader sensitivity so that a very high dynamic range is required to avoid RF saturation. One of their solutions was to apply two antennas in order to reduce the leakage, and the other was to remove the low-noise amplifier (LNA) increase the threshold of the noise figure. Another serious problem mentioned in the paper was the DC offsets, but these can be easily eliminated by adding an AC coupling stage at the start of the baseband chain. The maximum read range of this design architecture has been measured up to 8.1m, which is the similar to the detection range (8.5m) of another recently designed long-range RFID reader by Liu and Zhang [91].

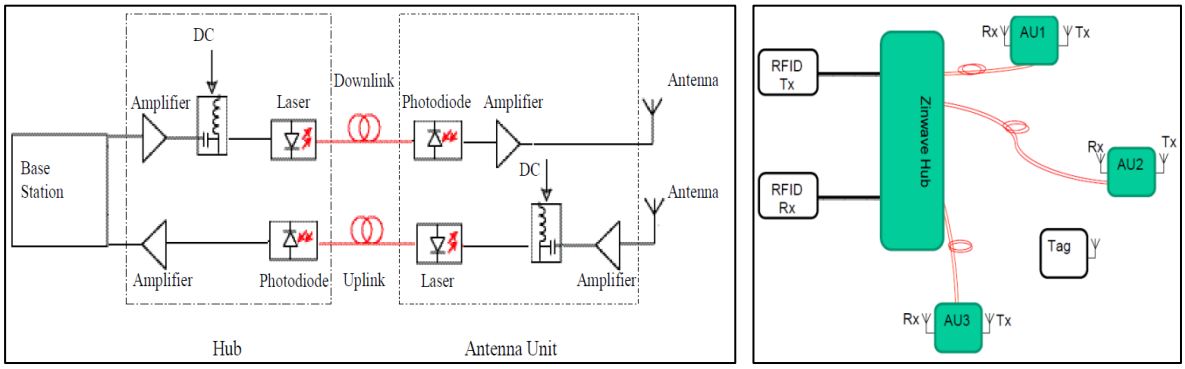

Figure 2.8 Typical duplex radio over fibre system and triple antenna DAS system [55]

An advanced system configuration can also be used to extend the read detection range. Sabesan *et al*. [55] proposed a new optically-fed antenna diversity configuration for an RFID system (Figure 2.8). In this work, they applied radio over optical fibres to replace the coaxial cables (which connected to the central reader and remote antennas). According to the results of their comparison experiments, the radio over fiber links exhibited a similar performance to that of conventional coaxial-based connections. Thus, they devised a triple antenna DAS RFID system, and demonstrated great improvement in terms of reducing the nulls from 62% to 28%. They also proved that this new system could achieve a 100% read rate in a 10m×8m conference room and a 20m×6m atrium. However, due to its large field of detection, this system tended to suffer from enhanced collision problems. They reported further improvements to their DAS RFID system in later studies [42], [92].

Just as with general wireless communications, techniques such as using repeaters or boosters are also capable of enhancing the detection coverage. Sabesan *et al.* [93] presented a novel repeater design for a passive UHF RFID interrogation system, which had a detection accuracy of 93% in a three-repeater system. With their design, the distance from a central reader antenna to a repeater could reach up to 20 m (Figure 2.9). However, there was a major antenna isolation problem due to the uplink and downlink using the same operating frequencies. It typically required antenna isolation of at least 10 dB greater than the gain provided by the repeater.

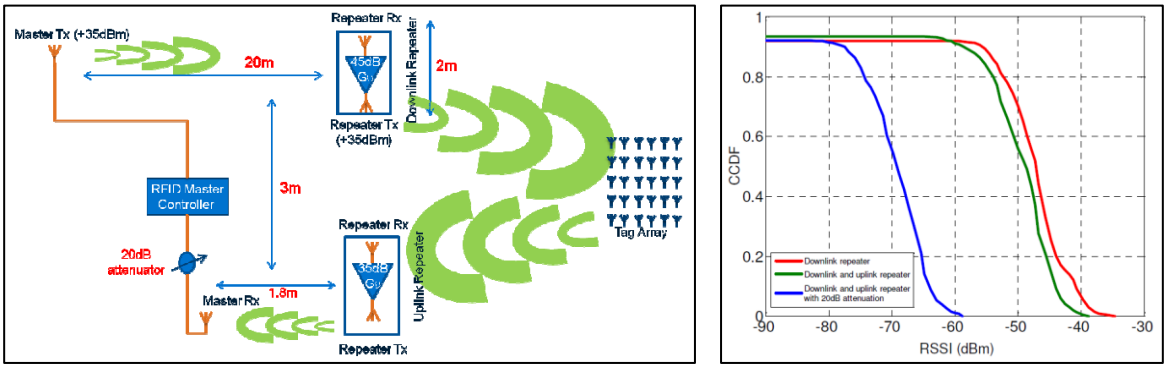

Figure 2.9 20m wireless RFID repeater system and comparison results of three different configurations (CCDF: cumulative probability distribution; RSSI: received signal strength indication) [93]

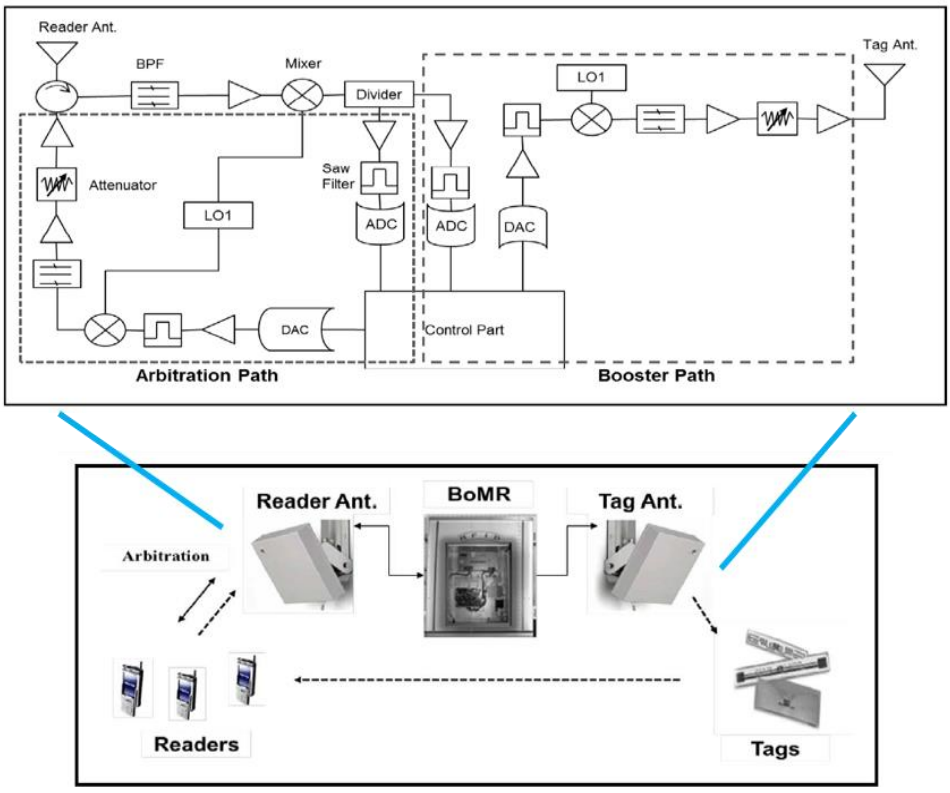

Figure 2.10 The system structure of a booster [94]

Another similar design of a mobile RFID reader booster, which was illustrated by Ahn *et al*. [94], is shown in Figure 2.10. With this booster, the detection range of the UCT-2300 reader could be extended from around 70 cm up to 6.5 m, and it could separate signals from the arbitration and booster paths by converting them into different frequencies so that the collision problem can be avoided. The advantage of these two devices is that they can be installed in an existing RFID system without having to modify the reader hardware. However, power supply and power consumption issues were not taken into account in these studies.

Based on this review study, most conventional methods using extra devices for extending the coverage of a single RFID reader suffer from high cost and high power consumption. Some other approaches in designing new reader or tag antennas to improve the read range usually require large antenna size or expensive fabrication schemes. Distributed antenna systems help a single reader to cover some indoor areas, but for large organizations or wide commercial areas its detection range is limited by the cable length they can support. Thus, cost-efficient methods or configurations for wide-area passive tag detection are still quite needed.

2.4.2. Techniques for reliability enhancement

The increasing adoption of RFID readers with even larger number of tags has been accompanied by rising reader-to-reader and reader-to-tag collision problems. These collision problems usually happen when more than one RFID tag exists in the range of a reader, or when a tag exists in the detection range of multiple readers. When a collision occurs, the reader may not receive the correct information from the tags, and the tags have to resend their data. Thus, in order to avoid the communications overhead and transmission delay caused by collisions, efficient anti-collision algorithms or protocols are needed.

There are two types of anti-collision protocols: tag anti-collision protocols, and reader anti-collision protocols. Tag anti-collision protocols include Aloha-based protocols (Slotted Aloha [95], Basic Frame Slotted Aloha [96], and Dynamic Frame Slotted Aloha [97]), and tree-based protocols (Binary Tree [98], Binary Search [98], and Query Tree [99]). In Aloha-based protocols, data from the tags can be transmitted during separate time slots within a frame. This way, the collision problems can be simply and robustly solved. However, this protocol design may suffer from synchronisation and starvation problems (some tags may not be detected over a certain duration), especially when there is a large number of tags [100]. In tree-based protocols, the reader splits the newly emerged tags into different subgroups so as to avoid

collisions, or uses a prefix in each communication round to identify particular prefix-matched tags. Generally, tree-based algorithms benefit from simplicity and low cost, but the long latency problems and frequent changes of the tree structure may constrain the serviceable range only to some static and small-scale identifying applications, like access control systems [101].

Regarding reader collisions, the most straightforward approach to solving this problem is to program colliding readers to operate at different frequencies or at different times. A typical example is the EPCglobal Class 1 Generation 2 protocol and the relevant European regulation which specify several frequencies for tag identification. There are other approaches, including a method for avoiding collision by disconnecting the overlapping readers [102], and an approach to minimise the overlapping zone by reducing the output power of collision-related readers [103]. Neighbour-Friendly Reader Anti-collision (NFRA) [104] is the preferred protocol, since it offers a relatively large mean number of reader transmissions per second. Some higher-performance protocols based on NFRA have been detailed by Bueno-Delgado *et al.* [105], and Li *et al.* [106].

In a passive UHF RFID system, the key problems include transmission leakage and noise, which significantly reduce the reader sensitivity and raise the noise level. As a result, the entire RFID system becomes unstable and unreliable. Generally a single antenna is used for a system in order to reduce reader cost and size. This single antenna performs both transmission and reception by using additional isolators to separate the reader and tag signals. However, its isolation features need to be improved before the performance of the reader can be considered acceptable [107]. Another option for isolation is to use a directional coupler, which can cancel the leakage by using reflection from the coupler isolation port. However, this may suffer from an impedance mismatch when the operation frequency is changed [108], and therefore an adaptive transmission leakage canceller is needed.

Jung *et al.* [109] and Xiong *et al.* [110] designed an adaptive leakage canceller, which consisted of a directional coupler, a power combiner, a variable attenuator and a variable phase shifter (Figure 2.11(a)). The magnitude and phase of the signal from the isolation port of the coupler can be tuned by an attenuator and a phase shifter. The transmission leakage can be successfully counteracted, since this signal possesses the same magnitude but exhibits a 180º phase difference compared to the leakage signal. However, this advanced design requires bulky and

costly components, and the coupling signal was usually not sufficient to protect against a strong leakage signal.

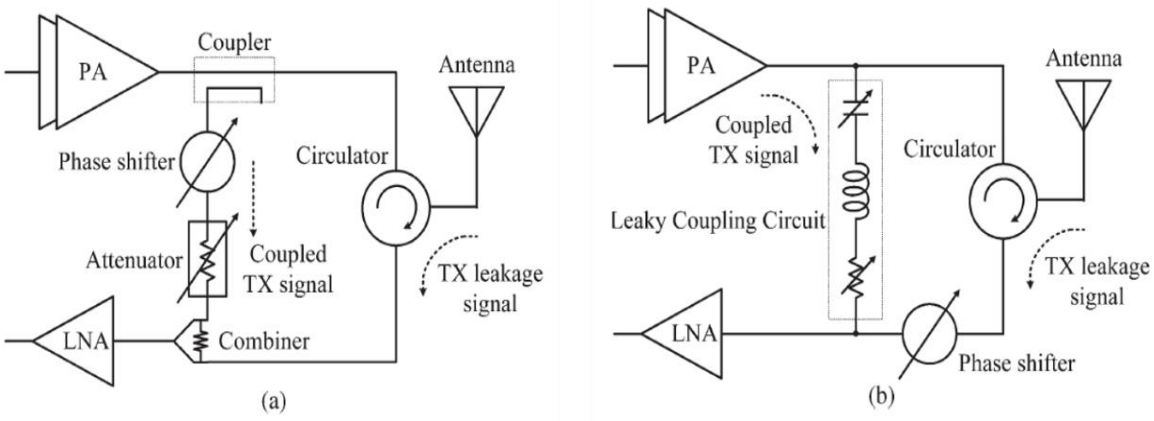

Figure 2.11 Circuits diagrams of conventional leakage canceller and direct leaky coupling canceller [92]

In view of this, Kim *et al*. [108] presented a canceller circuit with a higher signal coupling capability and better phase controllability, also known as a leaky coupling circuit (LCC). As shown in Figure 2.11(b), this LCC contained one alterable capacitor, one inductor and one variable resistor. This was not only a simplified circuit design, but also allowed for the elimination of transmission leakage. With this LCC leakage canceller, they found that UCODE G2XM passive tags could be successfully detected from a range of 2.7 m to 8.0 m using only 24.6dBm of transmit output power.

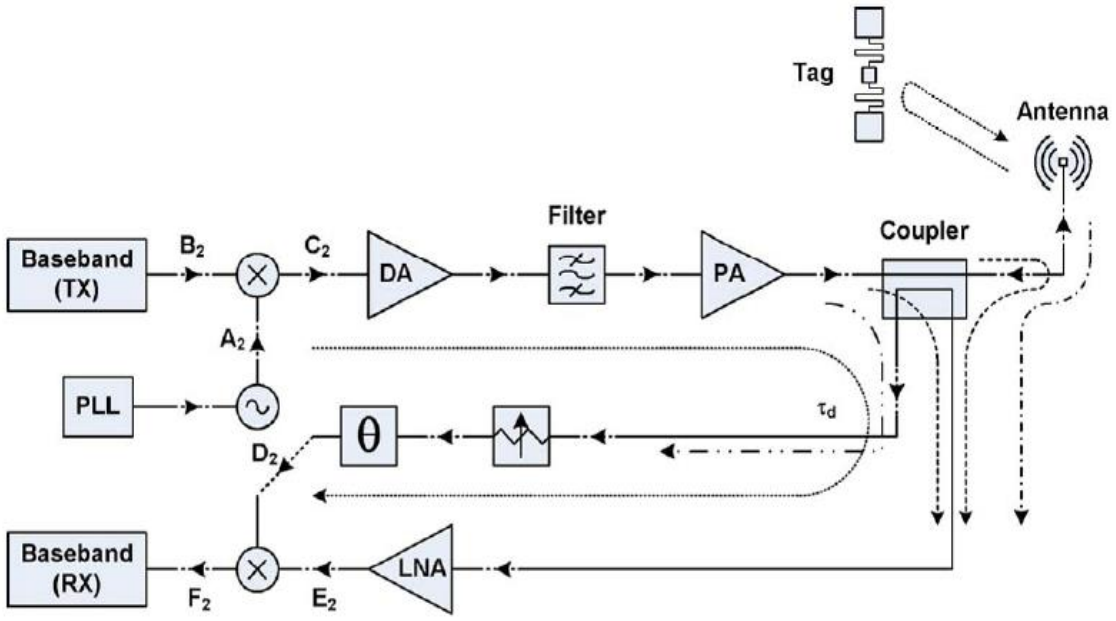

Figure 2.12 Schematic diagram of LO phase noise reduction method [111]

The mixing of local oscillator (LO) and residual TX leakage signals can produce LO phase noise. This kind of noise becomes problematic when sharp cut-off filters, like surface acoustic waves (SAW) and film bulk acoustic resonators (FBAR), are applied, since these filters induce significant time delays, and the resulting local signal and transmission leakage signal do not correlate with each other, which results in baseband noise. However, if the delay mismatch is negligible, this baseband signal can be significantly reduced within the range of a few hundred kHz. Jung *et al*. [111] presented a novel method using the capture transmission output signal as the LO signal for down-conversion in the receiver chain (Figure 2.12). With the help of this LO phase noise reduction method, the sensitivity of the reader was improved by 19 dB, and its reader range can achieve two metres.

Based on this review part, it was found that the collision problem caused by imperfect reader deployment directly results in poor reliability. Even though some algorithms can solve the collision problems, long latency and reduced read rate may not be acceptable in real-time detection. Leakage is another important reliability issue in an RFID system since it can greatly degrade the system sensitivity and increase the noise floor. Many designs of leakage suppression block are proposed with good suppression effects, but only few mention the settling time of the leakage canceller. Therefore, to deliver a reliable RFID system, reader antennas should be installed with a proper orientation and distance. In addition, an efficient closed-loop leakage canceller is required so as to maintain the best operating status.

2.4.3. Low-cost design scenarios

The number of designs of low-cost, low-power UHF RFID readers, transceivers for front-end mobile applications, has multiplied in recent years. These integrated single-chip readers are commonly implemented in a 0.18μm CMOS process or a SiGe BiCMOS process, and they have their own transceivers, PLL-based frequency synthesisers, digital basebands, micro-programmable control units (MCU), and other noise canceller blocks. This form of reader is highly popular in the current RFID reader market due to its low power consumption, small size, low price and ease of installation in mobile or handheld readers. A performance comparison of related designs in the last five years is presented in Table 2.6:

Table 2.6 RFID reader performance comparison

Reader	[112]	[113]	[114]	[115]	[116]	[84]
Year	2015	2014	2012	2010	2010	2010
Process	0.18 μm CMOS	0.25 μm SiGe BiCMOS	0.18 μm CMOS	0.18 μm CMOS	0.18 μm SiGe BiCMOS	0.18 μm CMOS
Integration Level	RF, BB modem, MCU	RF	RF, BB modem, MCU	RF, BB	RF, BB for physical layer	RF, BB modem, MCU
LO Phase noise (dBc/Hz)	-92@100 k; -125@1 M	-95@100 k	-93.7@100 k -117@1 M	-103@100 k -126@1 M	-126@250 k	-
Rx input P1dB	11.6 dBm	6 dBm	8 dBm	1 dBm	6 dBm	5 dBm
Sensitivity w/block	-67 dBm @ -1.3 dBm	-85 dBm	-55 dBm @ -1 dBm	-79 dBm @ 22 dBm	-82 dBm @ 10 dBm	-60 dBm
Output power	20 dBm	17 dBm	21 dBm	22 dBm	20 dBm	17.6 dBm
Die Size	19.2 mm^2	20×20 mm	19.2 mm^2	13.5 mm^2	(64-pin) 9×9 mm	19.38 mm^2
Total Power	500 mW	-	471 mW	660 mW	880 ~ 1100 mW	285.4 mW

(RF: Radio frequency block, BB: Baseband block, MCU: Micro-programmable control unit)

The most recent reader [112] (presented in Figure 2.13) is an improved version of the ones designed by Peng *et al.* [114] and Wang *et al.* [84]. It uses an integer-N PLL-based frequency synthesiser to convert the baseband signals to the carrier frequency (860 – 960 MHz), and these mixed signals are then passed through a single-ended pulse-modulation power amplifier (PA). The original idea of this direct-conversion structured PA was first proposed by Wang *et al.* in 2010 [84]. This PA is able to transmit the required output power and reduce power consumption and chip size, as mixer and digital-to-analog converters (DACs) are not required.

In addition, this reader uses I/Q paths to eliminate the residual phase noise in the receiver chain. An MCU controlled filter was inserted between these two components in order to remove the DC offset caused by the leakage signal. In the uplink, the first baseband LNA was employed to improve the noise performance, and the other two PGAs were integrated so as to amplify the received signals to a proper setting for 8-bit ADCs. As shown in Table 2.6, with the newest design, sensitivity has been improved from -55dBm to -67dBm. Compared to the devices created by Ye *et al.* [115] and the Impinj Company [116], this reader has a higher level of integration, and smaller power consumption (25% lower).

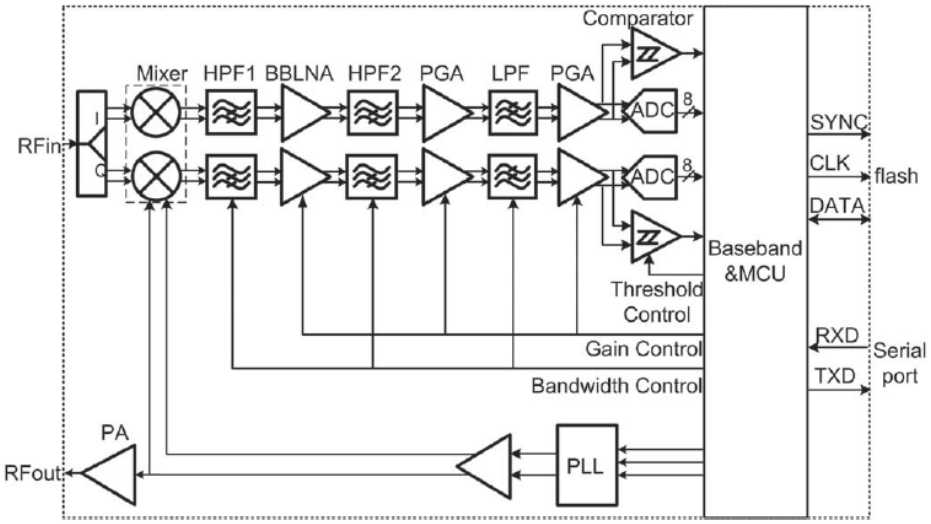

Figure 2.13 Block diagram of the RFID reader [112]

Two SiGe BiCMOS processed RFID modules were developed by Usachev *et al.* [113] and the Impinj Company [116]. In the former design, the authors only presented some features of the transceiver module in their article. Although the sensitivity of this new design is better than that of the others, its die size is significantly larger. The latter module introduced by the Impinj Company is now one of the most widely used commercial RFID modules, namely the Impinj R2000 chip. This module uses an I/Q modulation scheme and self-jammer cancellation block to reduce the impacts of noise, and it is flexible in terms of transmission mode (DSB, SSB, and PR-ASK) and system configuration (monostatic and bistatic) selection. In addition, the circuit is also able to support a dense reader mode operation, which makes it superior to other designs. However, all these functional blocks results in higher cost and power consumption.

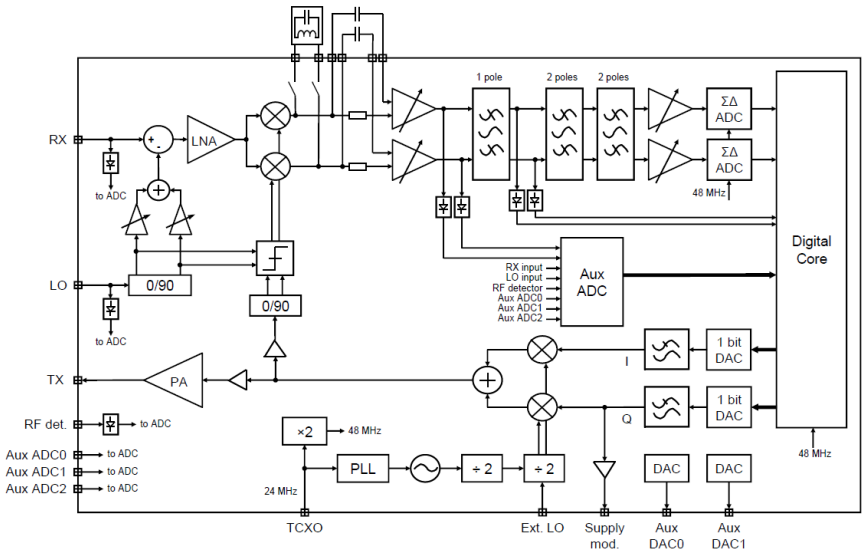

Figure 2.14 Block diagram of Impinj R2000 chip [116]

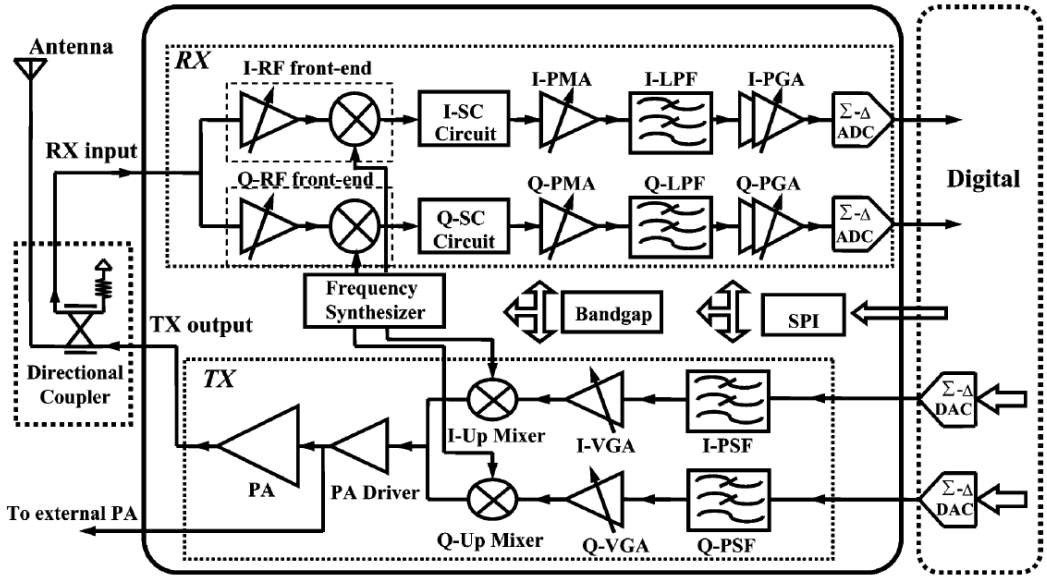

Figure 2.15 Block diagram of a single-chip reader transceiver [115]

Ye *et al.* [115] presented a single-chip CMOS transceiver with a relatively higher output transmission power and smaller chip size. In this chip, they adopted an on-chip self-jammer cancellation circuit with a rapidly time-varying cut-off frequency corner so as to prevent the DC leakage in the receiver chain. The post-mixer amplifier (PMA) and programmable gain amplifier are coupled with a DC-offset cancellation (DCOC) circuit in both the I and Q reverse links so as to remove residual DC leakage. However, this reader transceiver consumes relatively high levels of power (660 mW) when delivering around 22 dBm of output power, because its internal power amplifier operates on a 3.3 V voltage and consumes a great deal of power.

2.4.4. Power supply approaches

Power supply is always a critical part of a UHF RFID system design. A wired standard reader commonly relies on a standard commercial DC power brick, a USB, or Power over Ethernet (PoE) for access to a power source. A mobile or handheld reader usually relies on a battery or on energy harvesting blocks to support its entire circuitry. Compared to other power connections, the PoE systems have no need to charge or replace batteries, use fewer wires, and have a higher computing and communication capacity. Therefore, despite the initial cost of the wired network circuit being high, the long-term benefits for a fixed network are quite substantial [84]. Two standards for PoE connection for both power source equipment (PSE) and powered devices (PD) are shown in Table 2.7. Based on the listed parameters, the 802.3at Standard is greatly improved in every aspect compared to the 802.3af Standard.

Table 2.7 Two types of PoE Standards [117]

Standards	802.3af	802.3at
Published year	2003	2009
Maximum power at PSE	15.4W	30W
Maximum power at PD	12.95W	25.5W
Voltage range at PSE	44 – 57 V	55 – 57 V
Voltage range at PD	37 – 57 V	42 – 57V
Maximum current	350mA	600mA per mode
Cables	Category 3 or better	Category 5 or better
Typical impedance	20 Ω	12.5 Ω

There are four kinds of connections between PSE and PD. The two approaches in the top line of Figure 2.16 are the endspan modes. The method in Figure 2.16(a) can support the 10BASE-T and 100BASE-TX transmissions, whereas the top right-hand one in Figure 2.16(b) can support 10BASE-T, 100BASE-TX, and 1000BASE-T transmission. The bottom two connection approaches are the midspan modes. The connecting approach shown in Figure 2.16 (c) and (d) can support 10BASE-T/100BASE-TX and 10BASE-T/100BASE-TX/1000BASE-T transmissions respectively [117].

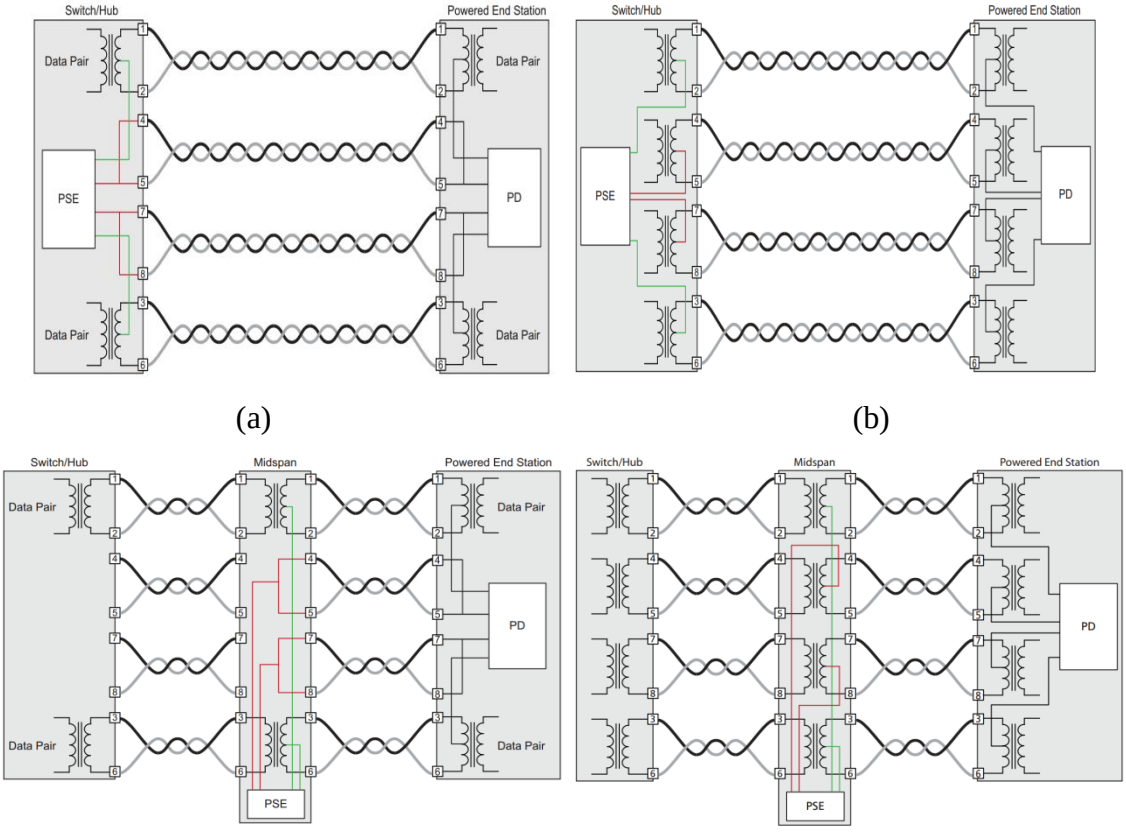

Figure 2.16 Endspan and midspan PSE power insertion methods [117]

Silva, *et al.* [118] proposed an automatic control RFID system to check the attendance of students. In their design, a PoE-powered K300 Proximity Card RFID reader from ZKsoftware was applied. This system was designed to monitor students' class attendance by identifying their personal IDs. Due to the large number of classrooms and buildings, such a system required a well-organized architecture to support all the RFID readers. The author omitted the use of RS-232, Wiegand and USBs in order to reduce the cost of the connections. Although they used PoE and TCP/IP communication to support their system, the total cost for installing the RFID readers in all the classrooms was considerable.

Another interesting application is the PoE-based RF switch box [118]. This switch box can be applied to existing 4-port or 2-port RFID readers so that the number of available ports can be increased, and more antennas can be connected in order to maximise the coverage of a single reader. As shown in Figure 2.17, this switch box uses an Ethernet cable to obtain the power, and Impinj Speedway Revolution RFID reader GPIO signals to control the T/R Switch. Those six SPDT T/R switches are employed to logically select the communication channel by setting the GPIO pins: VCC with V+, and GND with V-. By implementing this solution, the diversity can be increased, and the budget can be reduced by 4,300 euros for a 32-antenna RFID system [118].

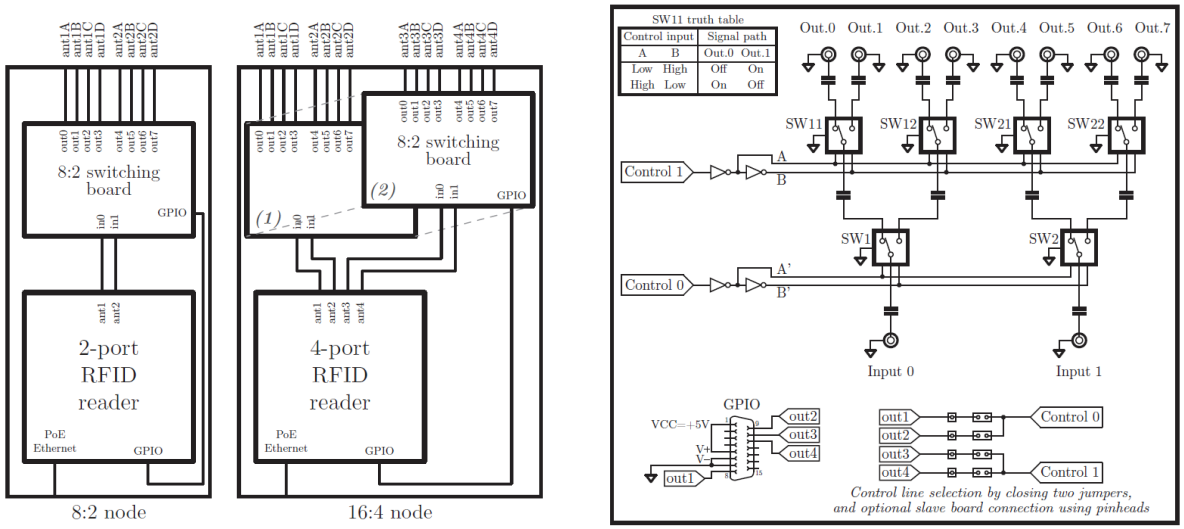

Figure 2.17 RF switch box diagram and schematic [118]

In addition to PoE techniques, there are some battery-based designs for mobile and handheld RFID readers. For example, Lei *et al.* [119] applied a power management chip (TPS65053) with a battery-based power management unit (PMU) to provide multiplex voltage DC-DC and

Low Dropout Regulator (LDO) output. Their PMU could be used to enable and disable the external power amplifier (SPA3118).

In another design, Hua *et al*. [120] employed a DC-DC power management chip (SMB122) to support the reader's operation within a sufficient power range. Their chip had three-way step-down channels that were used for an ARM chip (S3C2440); peripheral interface chips such as Nand Flash, SDRAM, and an SD Card; three-way step-up channels used for power amplifiers; voltage controlled oscillators; and an RFID chip (AS3990).

According to the review, an effective power management unit in an RFID reader can allow the system to deliver a stable performance. PoE is the most popular techniques used in RFID systems, being favoured over a conventional power supply and batteries. However, in most commercial readers, the PoE port is only used for supporting itself, and no RFID reader can use this twisted-pair cable to directly communicate with others. Therefore, a research gap still exists in simultaneous power management and communication of multiple reader modules for large area detection.

2.5. Conclusion

This chapter has described the historical development of RFID. With the rapid advances of RFID technology and the development of more sophisticated protocols and regulations, RFID is gaining greater public trust and driving its industry forward. However, existing RFID techniques and algorithms still need to be further enhanced to fully achieve their potential. Challenges such as high cost, inflexible installation, uncertain reliability, and limited read range still limit the widespread adoption of the RFID systems. In order to realise the next generation cyber-physical systems, more cost-efficient, flexible and cheap RFID systems are urgently required.

Chapter 3

3. Long-Range Passive RFID System over Ethernet Cable

Radio frequency identification is becoming an attractive technology to supersede barcode labels in retail and manufacturing, since objects can be detected without human intervention or light of sight. However, given the large number of tags involved, the high cost of the hardware is a challenge that limits widespread adoption, especially for large-area detection or large-scale organizations. Other issues such as system reliability, deployment difficulty, system maintenance, and data security have also created barriers. As a result, the adoption of RFID technology still lags. With the help of new materials for fabricating the tag antenna, the price of a passive tag has decreased over last few years, and is now approximately 5 US cents [116]. To overcome the remaining challenges and increase its practical adoption, solutions for developing cost-efficient, easily-installed, and highly-reliable RFID systems are urgently needed.

This chapter surveys wide-area UHF RFID systems, and then describes the design of a novel long-range passive RFID system over Ethernet cable, covering its key components, its basic communication theories and its preliminary system modelling. Following the design subchapter, a new baseband-controlled frequency and phase hopping method is proposed to achieve high detection performance and solve synchronization issues. Simulink tests are conducted to determine the feasibility of the approach.

3.1. Existing RFID Systems for Wide-area Detection

In a conventional RFID system, more than one fixed reader is needed to cover a required area due to the limited detection range of a single reader. The adoption of multiple fixed readers for wide-area detection increases the hardware cost. A system incorporating a handheld RFID reader can reduce the cost, since one remote reader can be easily carried to scan all the desired area. However, this kind of system generally supports offline detection and requires human assistance to identify those passive tags. Besides these requirements, human error and staff charges bring external issues to the handheld RFID reader system.

The distributed antenna system (DAS) technique was proposed in [121] for indoor radio communication. Research has shown that this multi-antenna configuration can significantly improve the multipath delay spread and alleviate signal attenuation problems. The coverage and diversity of indoor wireless systems has significantly increased. Studies relating to RFID in recent years have applied this technique to enhance the system detection performance and simultaneously reduce the hardware cost of the entire RFID system (Figure 3.1). The RFID system performance can be enhanced by adding frequency and phase hopping techniques, along with antenna diversity [42]. The demonstrated system can achieve near 100% tag detection rate over a 20 m × 15 m area. The system however uses individual coaxial cables to distribute raw RF signals to and from each antenna.

In part to avoid this, Buendia et al. [122] introduced a smart cable for a single reader RFID system, which allows the system to cover an area of 16 m × 2.5 m along a corridor. In this smart cable, single pole double throw (SPDT) switches and Wilkinson power combiners are applied to feed 5 rectangular patch antennas in a time division multiplexed approach. A similar solution is proposed by Rodas et al. [118]. They designed a Power-over-Ethernet (PoE) supported reader-plus-switch to extend a 2-port RFID reader to 8 ports or a 4-port RFID reader to 16 ports. The extended antenna ports are automatically switched by pre-programmed software so that the system can detect over a wide area without tag-to-reader and reader-to-reader interferences. In order to further reduce the cost of extra antenna control units, multiport RFID readers have been designed [123].

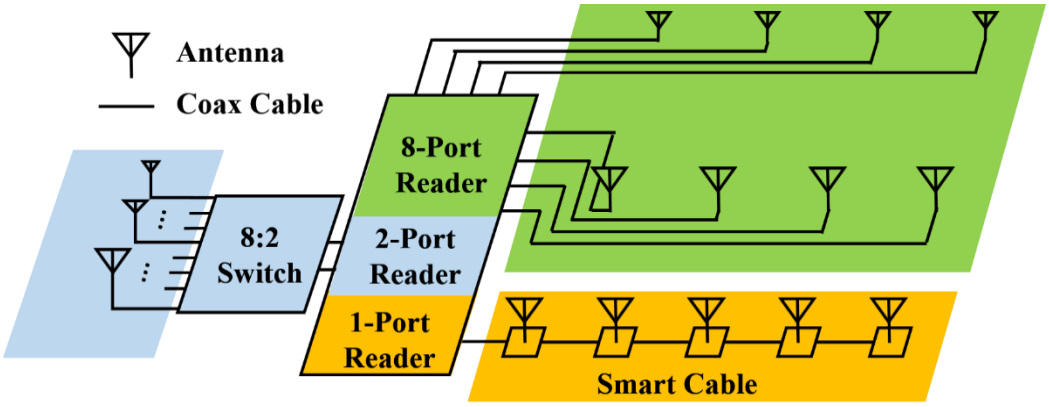

Figure 3.1 Multi-antenna solutions for single RFID reader

There are also some excellent approaches for wide-area detection from the RFID industry. A well-known RFID vendor, Mojix, offers an excellent long-range passive RFID Star system (see Figure 3.2(a)). This system consists of one Star receiver, which captures tag signals within an

interrogation space up to 250,000 sq. feet, and multiple eNodes, controlled by a central receiver, which provide energy to activate those passive tags for communication. eNodes can be easily deployed and arranged in a star network topology and the central receiver is directly connected to a Master Controller, able to access the Internet. As shown in Figure 3.2(b), PervasID, another RFID company, provides an RFID DAS with extremely high detection accuracy for areas up to 4,500 sq. feet. The 8-port Space Range 9100^{TM} reader can be controlled directly by an online server and achieves real-time zero null detection. The two products above from different RFID companies further confirm the value of using multiple antennas in an RFID system.

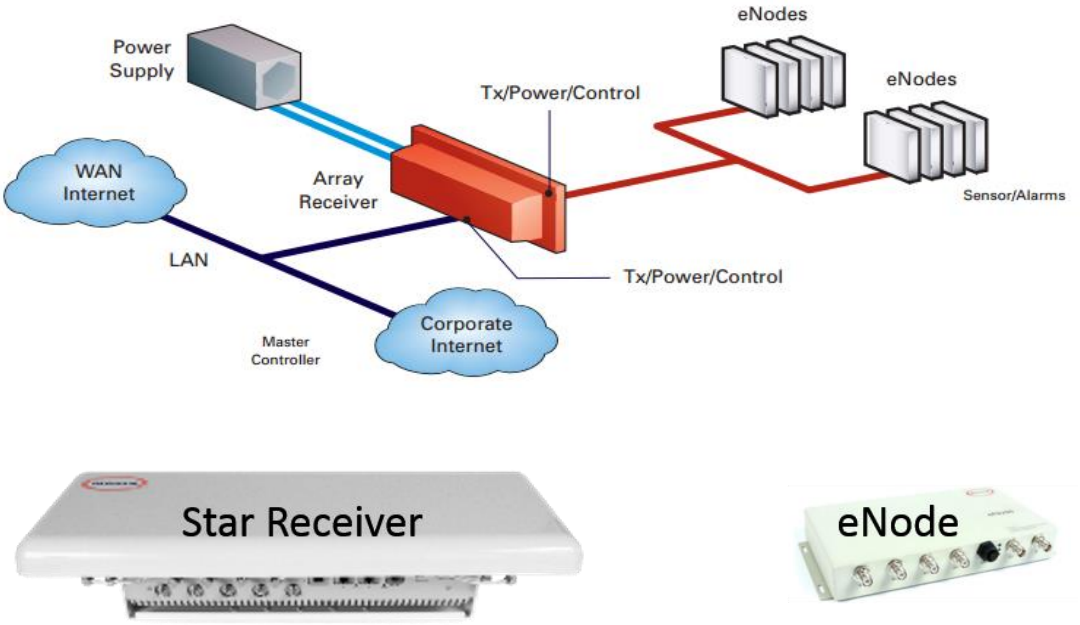

(a)

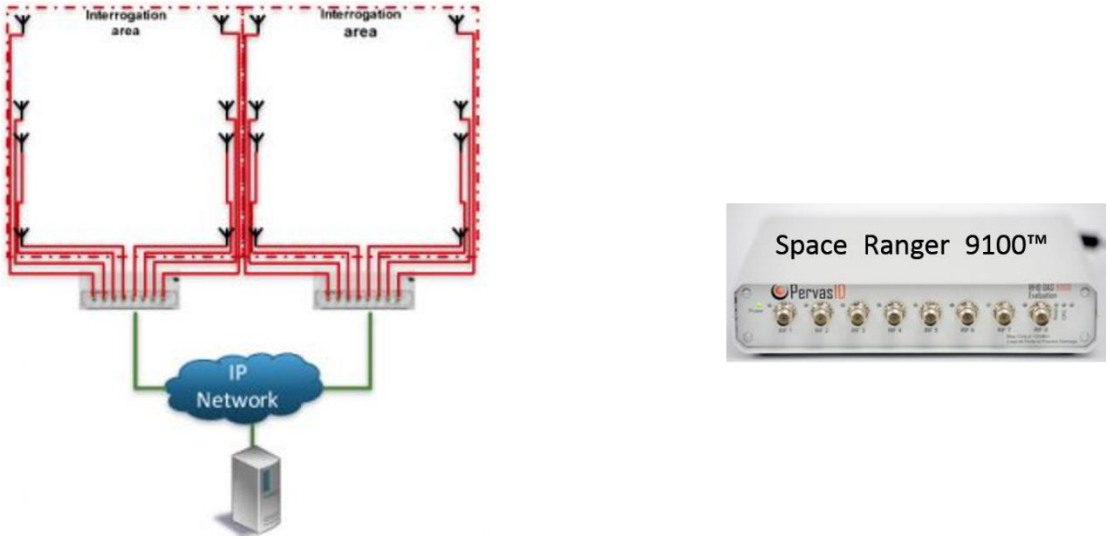

(b)

Figure 3.2 Multi-antenna solutions from the RFID industry [124] [125]

However, these systems on the market also require coaxial cables to connect the antennas to the RFID reader and other elements. Since coaxial cable is expensive and suffers high attenuation at around 900 MHz, the RFID systems discussed above are limited in the cable lengths they can support. The maximum cable length in the downlink can be increased by increasing the transmission power (at the expense of electrical power consumption), however, in the uplink the cable loss eventually results in noise that limits the link length and reduces sensitivity. Thus, the current system configuration is sufficient for small ranges, primarily for indoor applications, but, for commercial wide area applications, new connection approaches are reasonably required.

3.2. System Architecture

In a conventional RFID system, both the baseband block and radio frequency (RF) block (consisting of the RF front end and a frequency synthesizer) are integrated on a single PCB (or even IC) to form an RFID reader, and a short coaxial cable is applied to connect the reader to its antenna (Figure 3.3(1)). Since the cable loss is directly proportional to the cable length and is normally of the order of dB's per metre at frequencies around 900 MHz, the maximum reader output power and antenna gain limit the maximum allowable cable length if the maximum effective isotropic radiated power (EIRP) allowed by the local regulations is to be reached. For a typical 1 W conducted power and 6 dBi gain antenna, this is often only a few metres. Therefore, conventional RFID system architecture has its physical limitations in terms of its deployment flexibility and detection range.

Twisted-pair cable such as Category 5e (Cat5e) is an attractive option to form a new configuration of RFID system, since it has superior features such as cheap price, light weight, and high bend radius. However, this kind of cable suffers very high attenuation in the carrier frequency range (860 – 960 MHz). Nonetheless, this problem can be solved by converting the signal to a lower intermediate frequency band before transmission over the Cat5e cable. Early work in such a system configuration was conducted to determine the feasibility of the approach. By adding two frequency conversion blocks at either end of the Cat5e cable, lower intermediate frequency signals are transmitted in the twisted-pair cable so as to avoid serious attenuation (See Figure 3.3(2)). Through the measurement, a system using twisted-pair cables, like Cat5 cables, was able to detect the RFID tags. However, the extra components used for signal conversion directly increase system complexity and cost, and may also introduce extra

problems such as attenuation, nonlinearity, and delay. Hence, this system configuration is still imperfect for wide-area RFID systems.

The structure of this new system is shown in Figure 3.3(3). Unlike the second system configuration, this new configuration solves the previous problems by moving some RF blocks to the antenna side so only baseband signals need to be communicated over the Ethernet cable. Figure 3.3(3) shows that a central controller, addresses all the baseband related tasks, and the antenna subsystem, handles the radio frequency (RF) work. The operating scheme of this new system is very similar to the previous two versions, with the only difference being the transmission medium of the baseband signals.

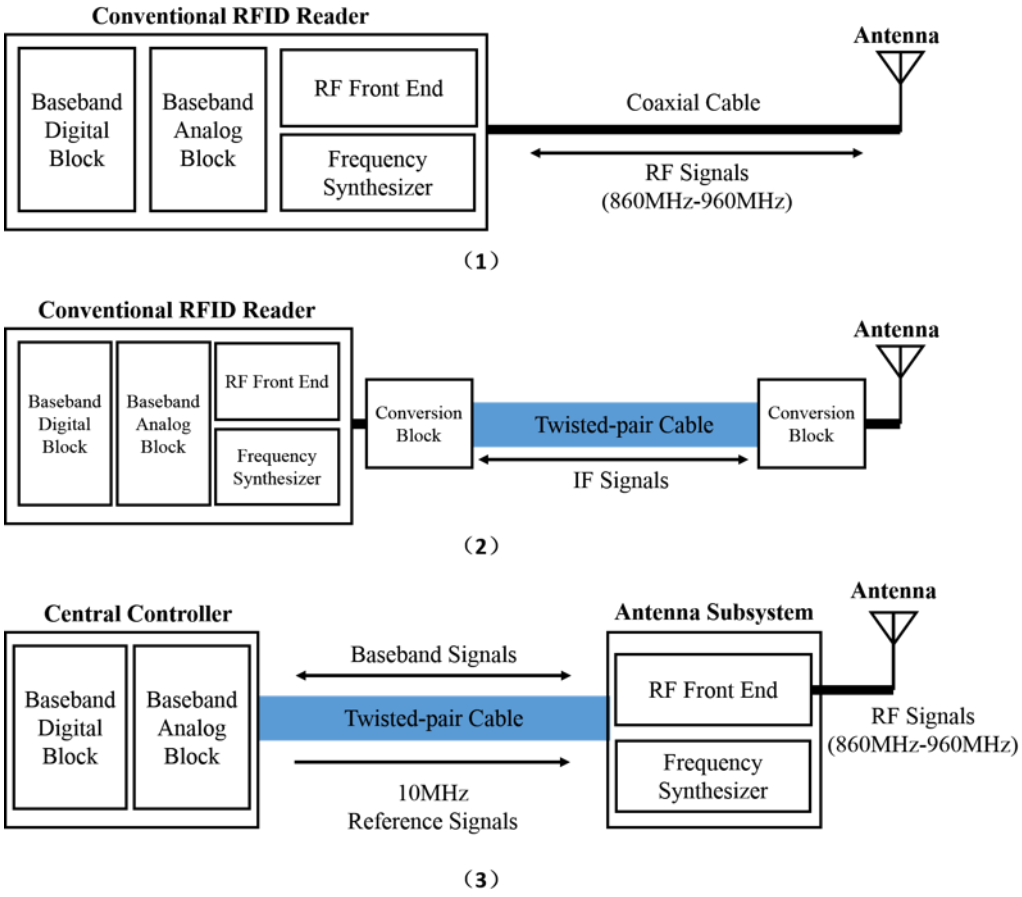

Figure 3.3 Conventional system configurations (1&2) and new system configuration (3)

In the forward link, the baseband transmit signals are generated in the digital block according to regulations and standards. After digital-to-analog conversion, the resulting analog baseband signals are transmitted to the remote antenna subsystem over a twisted-pair cable instead of the on-board internal bus. The up-conversion process is then performed in the RF front end. Coaxial cable is unnecessary in this new system for connecting the antenna. In the reverse link,

the backscattered signals experience a similar process but in the reverse order. They are received as RF at the antenna and directly mixed back to I and Q baseband channels in the antenna subsystem, before transmission over the Ethernet cable to the central controller where digitization and protocol operations are executed. The local oscillator for up and down conversion is generated in the antenna subsystem, but a reference tone is carried from the central controller, so multiple antenna subsystems can be potentially phase locked and new frequency and phase hopping can be possibly controlled in the user end.

3.3. Link Budget Analysis

The wireless detection range of a passive UHF RFID system is typically defined as the distance between the reader antenna and the passive tag. Link budget analysis allows determination of this maximum distance, in part by estimating the signal gain and loss between the RFID reader and passive tags link. Two separate links must be considered: the reader-to-tag communication (often known as the forward link or downlink), and the tag-to-reader communication (often described as the reverse link or uplink). The maximum read range is determined by the link with the smaller budget. An additional advantage of this analysis is to allow understanding of the limitations of each individual link. Specific solutions can be found to address those limits and improve the coverage of the entire system. However, some constraints such as maximum transmission power are set by the requirements of global standards and local regulations (as introduced in Chapter 2.3).

Complex environmental interferences are beyond the consideration of this chapter. Modelling of the maximum read distance is primarily based on the transmission power, free-space path loss, and the sensitivity of both reader and tag. Trade-offs to achieve the best system operating range are also discussed in the subsequent subchapters.

3.3.1. Forward Link Budget

In the forward link, there are four crucial parameters which should be defined to allow analysis of the system link budget (See Figure 3.4). The first parameter is the transmission power from the RFID reader. As mentioned previously, this value is set by a combination of global standards and local regulations. For instance, in the UK, the reader is allowed to transmit up to 2W ERP signals in the 865-868 MHz frequency band and 4W ERP signals in the 915 – 921 MHz frequency band. In many cases, the UHF readers operate at their legal limit to achieve the

maximum read range. The cable loss of the coaxial cable has to be considered in conventional systems especially for longer cable lengths. However, in the new system, this loss becomes negligible as lower frequencies are used.

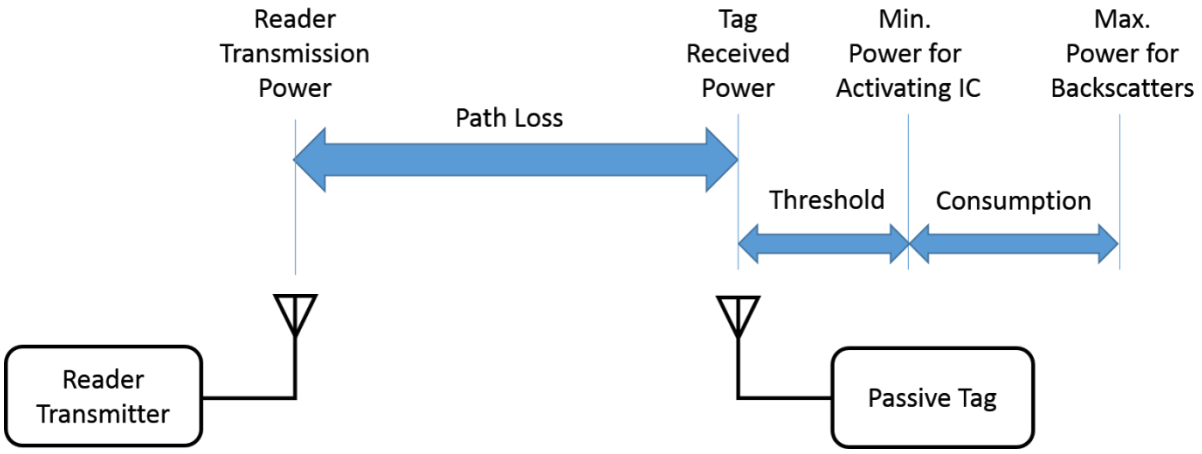

Figure 3.4 Critical parameters in the forward link

The second important parameter is the power received from the tag antenna. This parameter, P_{Rx} , can be calculated based on the path loss Equation 3.1 where:

$$P_{Rx} = G_{Tx}G_{Rx}P_{Tx}\frac{A_e}{4\pi r^2} \tag{3.1}$$

where G_{Tx} and G_{Rx} are the antenna gain of the reader and tag, respectively, P_{Tx} is the transmission power from the equipment. r is the distance between the reader antenna and tag antenna, and A_e is the effective aperture of the tag antenna, which can be further described as:

$$A_e = \frac{\lambda^2}{4\pi} \tag{3.2}$$

where λ is the wavelength of the transmission signal. In order to find the path loss as a function of distance, assume that the tag antenna gain is 1 dBi, and the maximum $G_{Tx}P_{Tx}$ can be represented as $P_{Max\ EIRP}$ according to the ETSI regulation. Thus, Equation 3.1 can be simplified to:

$$P_{Rx} = P_{Max\ EIRP}\frac{\lambda^2}{(4\pi r)^2} \tag{3.3}$$

and as a consequence the free-space communication distance can be depicted as

$$\mathrm{r} = \sqrt{\frac{P_{Max\,EIRP}\,\lambda^2}{P_{Rx}\,(4\pi)^2}} \tag{3.4}$$

The third parameter for the forward link analysis is the minimum power to activate the tag IC. This threshold, typically known as the tag sensitivity, is the minimum power strength to maintain tag-reader communication. Thus, according to Equation 3.4, if the operation

frequency is fixed and the tag sensitivity is given, then the forward link limited range can be estimated as

$$r = \sqrt{\frac{P_{Max\ EIRP}\ c^2}{P_{Min\ Rx}\ (4\pi f)^2}} = \frac{c}{4\pi f}\sqrt{\frac{P_{Max\ EIRP}}{P_{Min\ Rx}}} \tag{3.5}$$

where c is the speed of light at $3 \times 10^8\ m/s$, and f is the operation frequency.

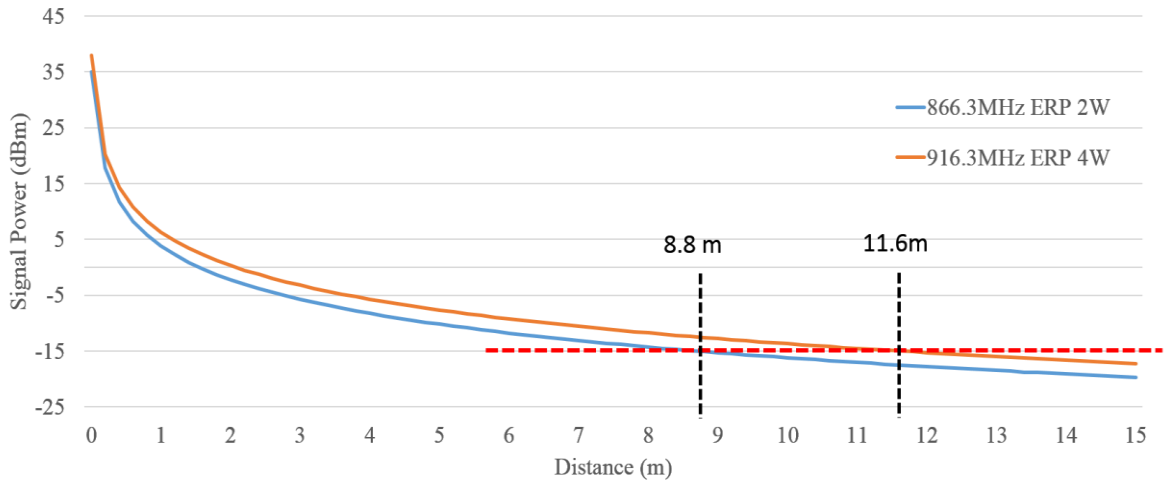

Figure 3.5 Forward link budget estimation for a passive RFID system

Figure 3.5 shows the theoretical maximum forward link distance based on Equation 3.5. It can be seen that both the lower (865 – 868 MHz) and upper (915 – 921 MHz) frequency bands have a similar slope of power decrease over distance. A passive tag with -15 dBm sensitivity can be successfully detected around 8.8m away from the reader antenna at an operational frequency of 866.3MHz. In the newly available ETSI spectrum, the maximum transmission power increases to 4W so that passive tags with the same sensitivity can be read at a longer distance of 11.6m.

A passive tag cannot generate its own carrier signals but simply modifies the received radio waves by changing the antenna loading. However, the tag backscatter modulation efficiency is limited as its internal rectifying circuit needs to generate sufficient current to pass through the diodes [126]. By knowing the power efficiency, it is possible to estimate the maximum power remaining (the fourth parameter) for backscattering. For example, if the modulation efficiency is 30% and the received power from the tag antenna is 31.6μW (-15dBm), then the modulated backscatter power is 9. 48μW (-20.2dBm).

3.3.2. Reverse Link Budget

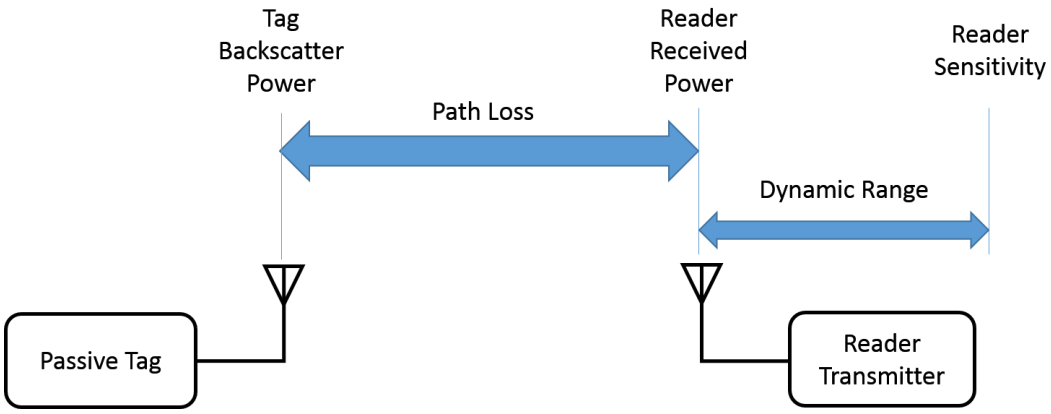

Figure 3.6 Parameters in the reverse link

In the reverse link, the passive RFID tag transmits the modulated radio waves back to the reader antenna (see Figure 3.6). The transmission process is similar to the forward link. Based on Equation 3.3, the received signal power at the reader side can be expressed as:

$$P'_{Rx} = \eta P_{Rx} \frac{\lambda^2}{(4\pi r')^2} \quad (P_{Rx} \geq P_{Min\,Rx}) \tag{3.6}$$

where η is the modulation efficiency, P_{Rx} is the tag received signal strength from reader radiations, and r' is the reverse link distance between reader and tag.

$$r' = \sqrt{\frac{\eta P_{Rx}\,\lambda^2}{P'_{Rx}\,(4\pi)^2}} \tag{3.7}$$

Equation 3.7 shows the relationship between the reverse link distance and the signal power at the antenna side.

The reader sensitivity, which is also known as the minimum backscattering signal threshold of the RFID reader, limits the communication distance. This is because the power of the backscattered signals must be higher than the noise floor of the reader, and it also requires enough power margin (dynamic range) for decoding the tag signals. The minimum received signal power P'_{Rx} can be represented as $G_{Tx}\,P'_{Min\,Sens}$. Thus, the maximum reverse link distance can be estimated by,

$$r' = \sqrt{\frac{\eta P_{Rx}\,\lambda^2}{G_{Tx}\,P'_{Min\,Sens}\,(4\pi)^2}} = \frac{c}{4\pi f}\sqrt{\frac{\eta P_{Rx}}{G_{Tx}\,P'_{Min\,Sens}}} \tag{3.8}$$

where G_{Tx} is the reader antenna gain and $P'_{Min\,Sens}$ is the reader sensitivity.

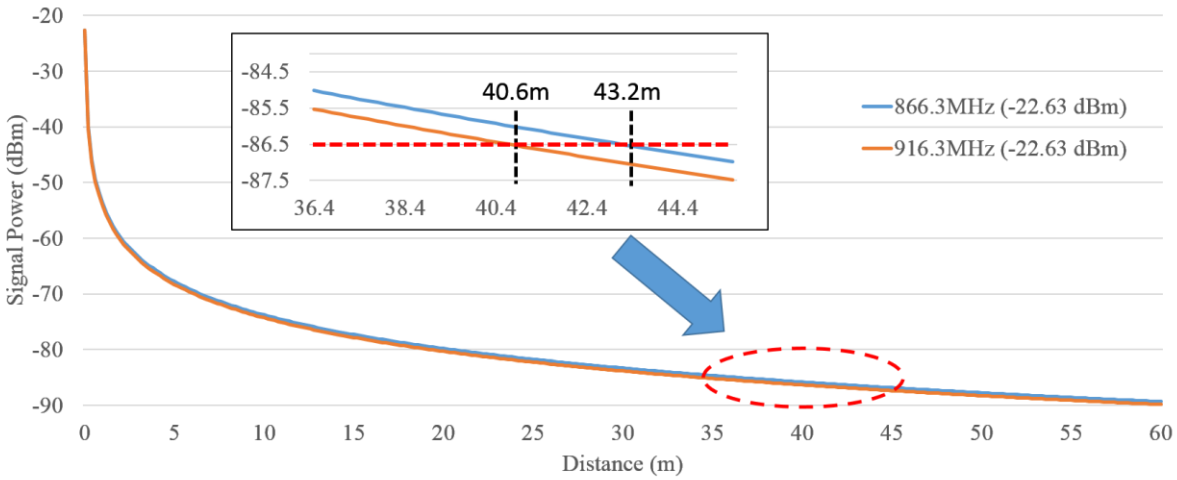

Figure 3.7 Reverse link budget estimation for a passive RFID system

The theoretical maximum reverse link distance based on Equation 3.8 is plotted in Figure 3.7. The two curves of signal power over distance are very similar to the curves in the forward link. However, in this graph, the assumed backscatter power from the passive tag at the two operation frequencies is the same, standing at -22.63 dBm. This value is calculated by assuming a passive tag with 30% modulation efficiency, and it absorbs -17.4 dBm signal power from the reader. In general, commercial readers have a sensitivity level from -70 dBm to -90 dBm [116]. If the minimum detection level is -86.5 dBm, from the enlarged figure, the system operating at the lower frequency has a longer detection range. This result can also be proved by Equation 3.8.

3.3.3. Limitations of Passive System Detection Range

The operating range is one of the key parameters used to assess the performance of a passive RFID system. In order to fully understand its limitations, a theoretical model of an entire passive RFID system link budget with typical parameters is discussed here. Assume that the carrier frequency of a system is 866.3 MHz and the transmission power is 35 dBm. Note that the gain of the antenna is set to 1 dBi for the ease of calculation and the sensitivity levels of the tag and reader are -17.4 dBm and -86.5 dBm, respectively. The modulation efficiency of the tag is 30% and only the free-space path loss is considered.

Based on the above assumptions, the entire link budget is plotted in Figure 3.8. It is clearly shown that the passive RFID system is a forward-link limited system since its reverse link distance has 40.6m whereas its forward link distance is only 11.6m. Thus, techniques to improve the forward link budget are required to enhance the read-tag communication distance.

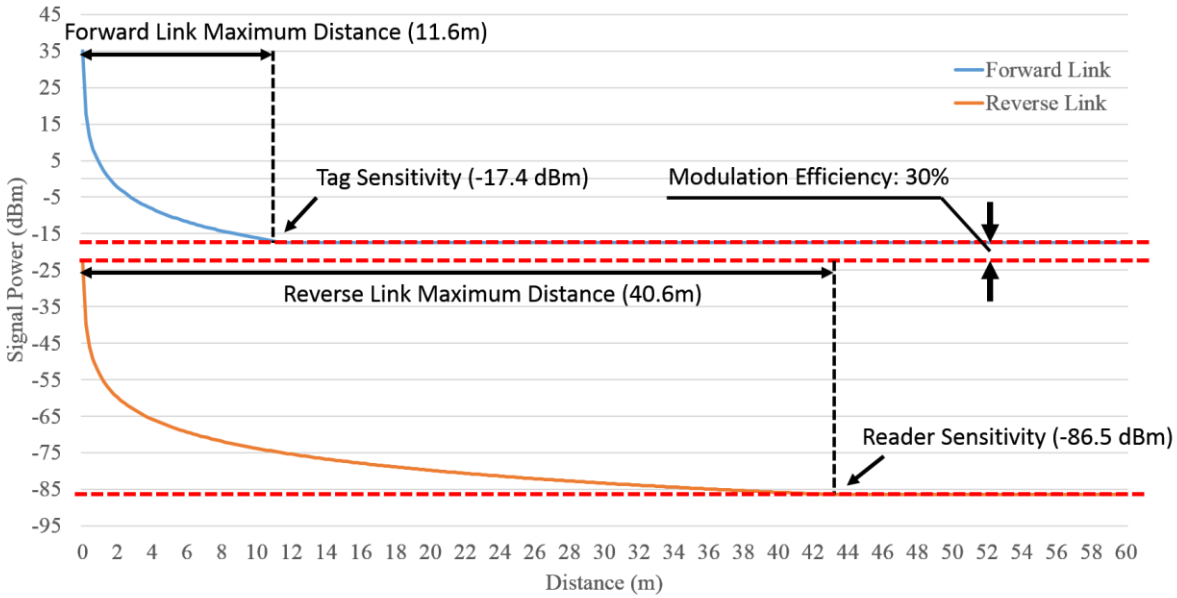

Figure 3.8 Link budget of a passive RFID system

Since the transmission power is fixed at its maximum limit, enhancement of the passive tag sensitivity is a good way of increasing the read-to-tag distance. According to the tag review in [127], the UHF RFID tag sensitivity has been improved from -8 dBm in 1997 to better than -20 dBm today. If the tag in the previous model is replaced by NXP's UCODE [128], which has -23 dBm read sensitivity, then the detection range can increase from 11.6 m to around 22 m. Another way of improving the read range is to redesign the tag antenna with higher gain. With help of this gain, more power can be received from the reader. However, the higher antenna gain usually results in larger antenna size or smaller antenna beamwidth. Another approach for extending the downlink read distance is to apply multiple antennas that simultaneously transmit the maximum allowable power. This approach increases the overall transmission power from the reader antennas to the passive tags, so that those tags are able to receive signal power several times larger than the power absorbed from a single antenna. However, this multi-antenna configuration brings higher cost in terms of cables, antennas, and power consumption.

In the reverse link, the read distance may be significantly decreased if the system suffers from leakage. This problem is mainly caused by the large carrier signal reflected back to the receiver chain, thus saturating the mixer or the downlink phase noise overlapping the weak tag signals. There are several methods, introduced in [129] [108], to avoid this kind of problem and maintain reliable tag-to-reader communication. Other methods relating to improving the reader sensitivity include the internal circuit design.

3.4. System Implementation

In a generic radio frequency identification system, baseband blocks (which provide the control interface and RFID reader commands for the passive tags) and radio frequency blocks (which offer specific functionalities such as modulation and demodulation) are essential. To build an RFID system, the functions of each component have to be fully understood. For instance, mixer and local oscillators help to convert the baseband commands to the required frequency. An amplifier is used to increase the amplitude of the weak backscattering signals for further processing.

However, in order to design a high performance RFID reader, additional processing has to be carried out. For example, parameters such as gain, noise floor, 1-dB compressed power (P1dB), and output third-order intercepts (OIP3) have to be carefully specified for every component. High performance can be achieved by keeping those parameters within an acceptable range. The following subchapters describe the components selected for both the central controller and antenna subsystem. Theoretical modelling, in terms of those parameters, is reported and the results for each component are summarised in a spreadsheet for initial evaluation of the proposed system.

3.4.1. Central Controller

The central controller in this new RFID system is required to transmit control symbols and process the received signals obeying the local regulations and standards. It also needs to provide an interface for users to initialise the system operating modes by simply setting the values in software. In many commercial readers, these requirements can be directly met by using two related functional chips: One is to support most recent Class 1 Generation 2 RFID protocol and local regulations; and the other one is to provide a data and control panel. In addition to the system set-up, the central controller also runs the operational program. When this program is correctly running and properly downloaded to the corresponding chips, the central controller is ready to provide its services.

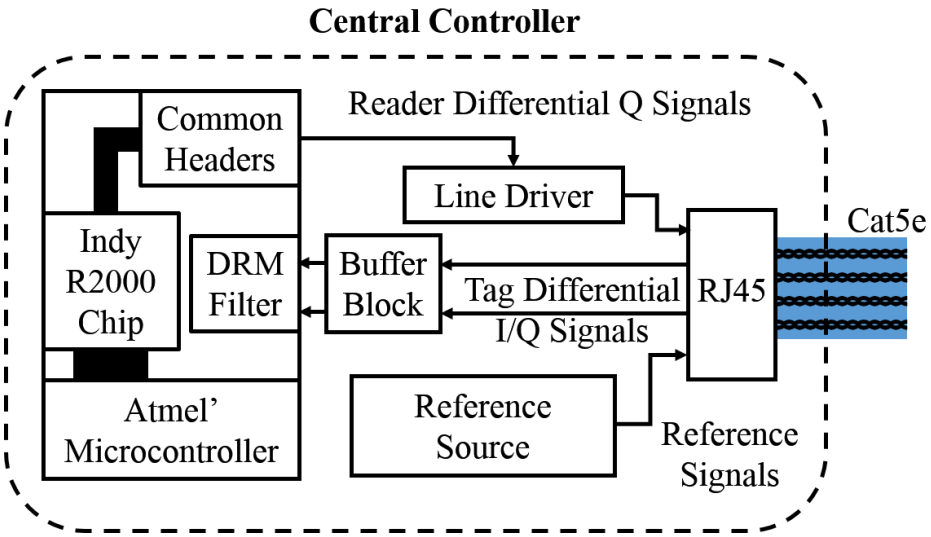

Figure 3.9 Block diagram of the central controller

The high-level block diagram of the proposed central controller is shown in Figure 3.9. Atmel's AT91SAM7S256-MU [130], which is based on a 32-bit ARM RISC processor, is selected as system microcontroller and monitor. It provides a 55 MHz operating frequency, 256 Kbytes flash memory, 64 Kbytes SRAM, and a peripheral set including USB, UART, SPI, ADC, and IO lines. This microcontroller comes in a 9 mm×9 mm QFN package with 64 pins. The microcontroller is used to implement the EPC Class 1 Gen 2 protocol and provide the interface for external control.

An Indy R2000 chip [116] from the Impinj Company is chosen to generate baseband reader signals based on the EPC global Gen 2/ISO 18000-6C standard (although in this implementation some of the functionality is unused). The Indy R2000 chip can deliver phase reverse amplitude shift key (PR-ASK) and double sideband amplitude shift key (DSB-ASK) modulation schemes. The baseband transmit signals can be accessed from the analog test pins of the R2000 as a differential signal. However, since these baseband signals are directly connected to the internal analog bus, they have little current driving capability. An external line driver is therefore designed to amplify these analog signals without loading down the signal bus in the chip. According to the datasheet of the Indy R2000, when operating the ASK modulation in the downlink, the data on the I channel is null (0) and signals only exist on the Q channel. In this way, only a single twisted pair is required to transmit the downlink signals.

With respect to the uplink, an analog buffer block in the central controller is employed to buffer the received baseband signals and provide noise filtering. After this block, the analog tag

signals are fed into the R2000 chip for additional filtering and processing via the inputs designed for the external dense reader mode (DRM) filters, thus allowing bypassing of the RF to IF conversion stages on the IC. The reference signal block allows for later frequency and phase hopping of the local oscillator in the antenna subsystem by varying the phase and frequency of the reference signal. Thus, a 10 MHz signal is generated as an external reference source in this block for the frequency synthesizer in the antenna subsystem. The details and block diagram of the selected components can be seen from Appendix A.

3.4.2. Antenna Subsystem

The antenna subsystem is primarily composed of radio components, which up-convert the baseband commands to the RF and also down-convert the backscattered signal to low frequency for symbol decoding. These two processes in the subsystem are generally known as modulation and demodulation. Components in this part must be carefully selected in order to produce a high-performed transceiver. Typically, in many RFID systems, high performance is defined in terms of its uplink sensitivity, dynamic range, and circuit linearity. In order to obtain these three indications, parameters such as noise figure (NF), 1 dB gain compression (P1dB), and third-order intercept point (IIP3) of each component must be calculated, as well as the cascaded results such as the signal to noise ratio (SNR) and noise floor. A summary table of these initial calculated results is able to provide system performance estimation. More details of these parameters will be discussed in the next chapter.

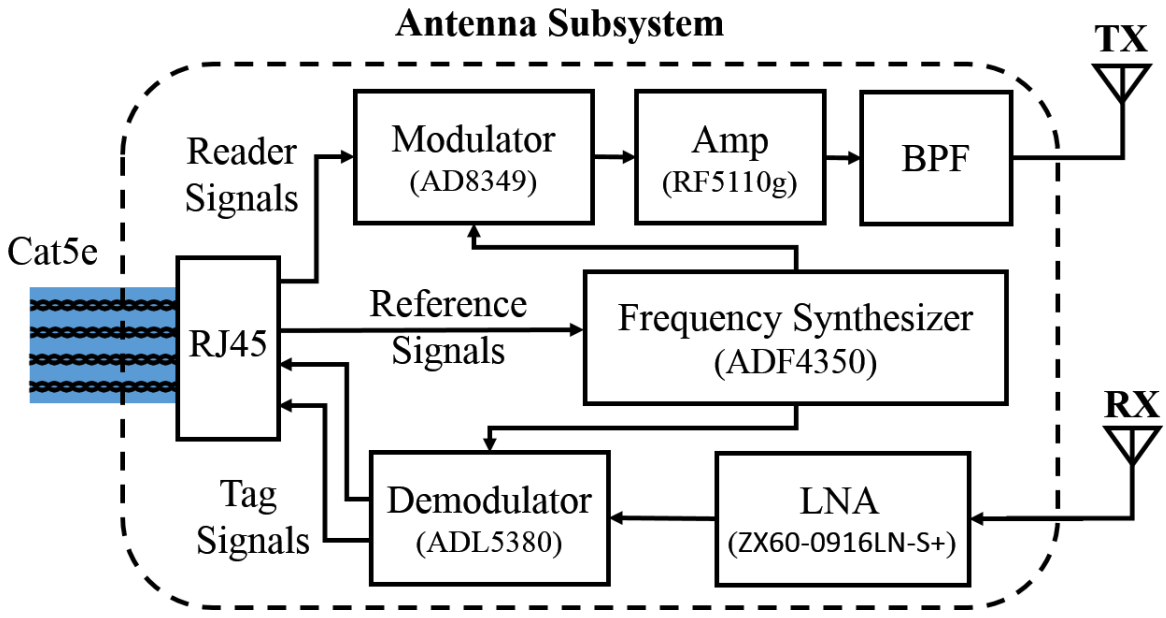

Figure 3.10 Block diagram of the antenna subsystem

As shown in Figure 3.10, the antenna subsystem is mainly composed of a quadrature modulator and demodulator, RF power amplifiers, and a PLL-based frequency synthesizer. The AD8349 [131] quadrature modulator and the ADL5380 [132] quadrature demodulator are used to fulfil up- and down-conversion tasks. These two products are produced by the Analog Device Company. They offer excellent dynamic range, amplitude and phase balance, and low noise floor for the direct-conversion system. The carrier frequency is generated by a fractional-N/integer-N PLL-based frequency synthesizer ADF4350 [133], which can work with either its internal oscillator or an external reference signal. This synthesizer has a wide output frequency range, low phase noise, and low rms jitter (< 0.4ps rms). In this implementation, an external 10 MHz reference signal from the central controller is applied. More details of this frequency synthesis setting is provided in Appendix B. An RF amplifiers (RF5110G [134]) is adopted to provide sufficient gain for the signals in the downlink. The amplifier can operate in all UHF RFID frequency bands and its output power can be controlled from -10 dBm to +35 dBm by changing the voltage level of the power control (Vapc).

3.4.3. Ethernet Cable

Ethernet cable usually refers to the twisted-pair cables in categories 5, 5e, 6 and higher levels, as defined by the Telecommunications Industries Association (TIA) and Electronic Industries Association (EIA) based on their performance. Ethernet cable is commonly found in offices, homes, and even some public places such as airports or restaurants where applications are required to access the Internet. The ease of installation, light weight, and low cost are other superior features of this type of cable.

Inside an Ethernet cable, there are commonly four pairs of wires. Each pair is tightly twisted with a specific twisting angle, so that different pairs are able to minimize crosstalk from each other. This twisted configuration also minimizes the noise and interference during the cable transmission. This is because two twisted wires experience almost the same external effects, and these unwanted effects can be easily removed when differential signals are carried. Some other characteristics such as the tightness of the twists, the diameter of the copper wire, and the insulation material of the twisted pair cable determine the transmission quality.

Originally, twisted-pair cable was developed for superseding the expensive coaxial cable of 10-Mbps Ethernet connection due to its lower cost and easier installation. Those types of Ethernet cables such as Categories 3, 4, 5 are accordingly classified by their performance in terms of the

attenuation at a frequency of 10 MHz in a 100 m cable. However, in recent years, more advanced twisted-pair cables have been produced for achieving faster transmission speed. Since the operating bandwidth of the new cables dramatically increases and the attenuation varies with operational frequency, the maximum bandwidth becomes an important criterion to classify those cables. Another way to classify twisted-pair cables is with reference to their shielding approaches: unshielded twisted-pair cable (UTP) and shielded twisted-pair cable (STP). The main difference between these two types is that the STP cable contains an additional layer of protection wrapped around the individual pair in the cable. The extra protection can further reduce the electromagnetic interference from the free space and crosstalk effects between pairs. Table 3.1 lists the parameters of popular twisted-pair cables, which are used for making the potential selections for an RFID system.

Table 3.1 Different categories of Ethernet cable [135]

Name	Maximum Bandwidth	Attenuation (10MHz,100m)	Maximum Length	Maximum Transmission Speed	Shielding Type
Cat3	16 MHz	≤98 dB/km	100 m	10 Mbps	UTP
Cat4	20 MHz	≤72 dB/km	100 m	16 Mbps	UTP
Cat5	100 MHz	≤65 dB/km	100 m	100 Mbps	UTP
Cat5e	100 MHz	-	100 m	1 Gbps	UTP
Cat6	250 MHz	-	100 m	10 Gbps	UTP/STP
Cat6a	500 MHz	-	100 m	10 Gbps	UTP/STP
Cat7	600 MHz	-	100 m	10 Gbps	STP

It is shown that the most recent developed cables including Cat6, Cat6e, and Cat7 have greater than 100 MHz bandwidth, and can support 10Gbps transmission speed. However, these superior features come at a high price. Cat3 and Cat4 cables have acceptable characteristics for transmitting the RFID baseband signals and reference signal, but these two versions of UTP were designed for early telephone networks. They are rarely used today and cannot be recognised by recent applications. Cat5 and Cat5e cables are extensively used in offices and personal homes, and their prices are relatively cheaper compared to other higher-bandwidth twisted-pair cables. Compared to the Cat5 version, the Cat5e cable has more test parameters including wire map, propagation delay, delay skew, attenuation, and crosstalk. Cat5e cable is more commonly used in offices and homes since it can be directly used for 1Gbps network connection whereas the Cat5 cannot. Accordingly, Cat5e has become the natural choice for new RFID systems.

Category-5e cable can be further divided into solid and stranded types depending on the internal copper conductors. In solid Cat5e cable, a single piece of copper is used for the electrical conductor. This type of cable is usually applied for permanent or semi-permanent installations, for example as horizontal and backbone cables, which are commonly installed in walls or outdoors with limited bend radius. Stranded Cat5e cable has multiple strands of copper conductors in each wire, and this type of cable is often used in patch cords and workstations, where the cable may be moved around quite often. Since this new RFID system requires highly flexible subsystem installation, stranded Cat5e should be used.

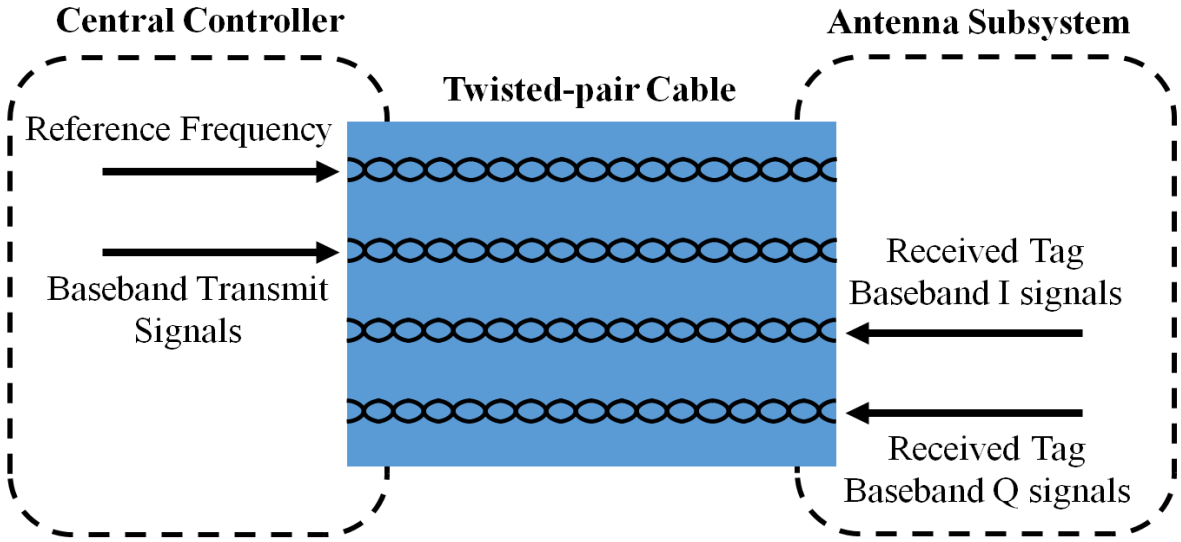

Figure 3.11 Signals in the Category 5e cable

It can be seen from Figure 3.11 that all pairs of the Cat5e cable are used: one for transmitting the baseband reader signals, one for the synthesizer reference frequency from the reader controller and two for receiving in-phase and quadrature down-converted tag signals from the antenna subsystem. Although not implemented for this proof of concept demonstration, it would be possible to transmit the DC power required for the antenna subsystem over the pairs in a manner similar to power over Ethernet (PoE). Since these Ethernet cables have the same wiring scheme, other types of twisted-pair cable such as Cat6 can also be used for the controller-subsystem connection.

3.5. System Modelling and Spreadsheet

To design a new system, it is essential to predict the system performance and understand the interactions of the components used. The system spreadsheet is an effective modelling method to reach this goal, since it can clearly provide segment or final cascaded system performance

based on the specifications of individual component. From this block-level analysis, the tolerance or margin between the requirement and current design results can be estimated. It is best to devise a system with this tolerance close to zero, but in practice it is usually difficult to achieve. Accordingly, in most cases a certain tolerance is acceptable, but its value should be a trade-off between component cost and any degradation in system performance. According to the initial design of the new RFID system in previous chapters, the critical parameters should be carefully considered in order to keep circuit linearity, avoid signal distortion, and reduce the noise floor.

Gain is an important parameter to describe the ratio of the output power over the input power. Generally, it is depicted in decibels (dB).

$$\text{Gain (dB)} = 10\log\frac{P_{out}}{P_{in}} = 20\log\frac{V_{out}}{V_{in}} \tag{3.9}$$

When a signal encounters the passive components such as mixer, filter or power splitter, negative gain or loss occurs. An amplifier is then required to provide enough gain to amplify the small signals to an acceptable level. For example, assume that a weak tag signal is received with a power of -65 dBm (0.177 mV peak voltage) in a 50-ohm RFID system. However, the minimum peak voltage of input needed to digitise the signal is 200 mV. Then, despite the loss, a voltage gain of 1130 or 61 dB is required before this tag signal reaches the analog-to-digital converter.

Nevertheless, devising a high-performance RFID reader cannot simply follow the principle that the bigger gain the better. Since the gain not only amplifies the desired tag signal but also enlarges the noise power, the reader dynamic range may degrade when the noise figure is high before the amplifier. In addition, large gains directly lead to large power consumption and also may cause nonlinearity problems. Taking the 1-dB compression point (P1dB) as an example, this usually occurs when the output power of an amplifier is saturated. The output power grows slowly and nonlinearly even though the input power continuously increases. P1dB usually defines the input power level of an amplifier where the gain drops 1 dB from the normal linear gain specifications. In the forward link, the amplifier should be chosen with a maximum output power within regulatory limit, while in the reverse link, the amplifier should be selected based on its P1dB and specifications of the components.

The output signal is a linear function of the input signal in an ideal linear circuit, but this is not feasible in practice. Distortion of the output signal occurs even for a slight non-linearity. New frequencies, usually known as harmonics and intermodulation products, are produced in the distorted signal arising from the amplified inputs. The second- and third-order harmonics of the components are usually listed in the specifications as the input second-order intercept (IIP2) and input third-order intercept (IIP3) points. Sometimes these parameters are depicted as the output second-order intercept (OIP2) and the output third-order intercept (OIP3), and the difference between them is the gain of the amplifier.

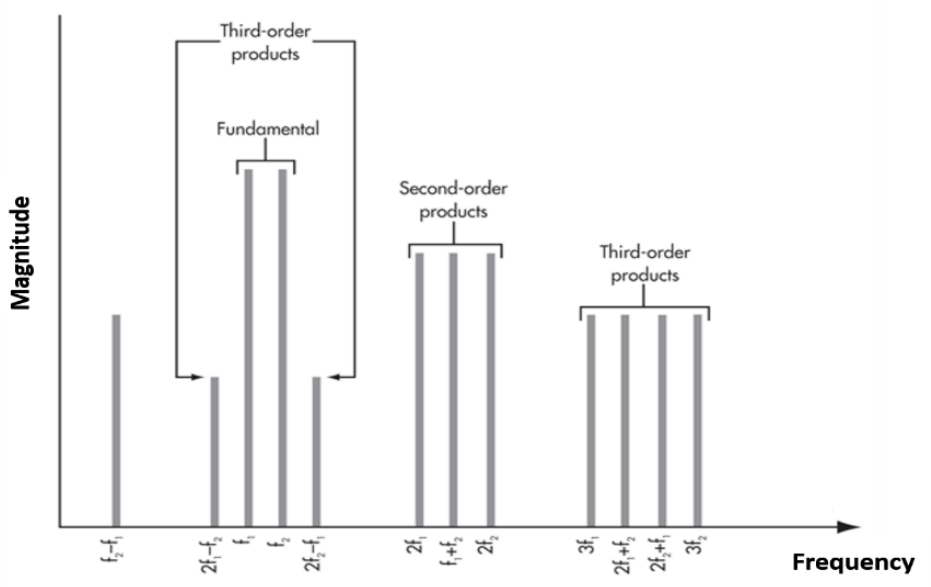

Figure 3.12 Spectrum of distorted signals with two input frequencies [1]

The second-order harmonics are easily removed by using the filter, since they double the operation frequency and usually lie outside the frequency band of interest. However, the third order is more difficult to filter out due to some of the distortion products being close to the main signals. For example, when two RFID readers operate at two close frequencies (see Figure 3.12), the intermodulation products at $(2f_2 - f_1)$ and $(2f_1 - f_2)$ become troublesome as they can no longer be filtered and may keep the reader from demodulating the desired backscattering signals. Therefore, to avoid these 3rd order harmonics affecting the neighbouring channels and eliminate circuit nonlinearity, the OIP3 or IIP3 are important indicators that should be considered during system design, especially under a dense-reader operation environment. Systems with higher intercept values are regarded as having better linearity.

Noise is another important criteria in component selection and system implementation. The most common noise is thermal noise, which is caused by the finite thermal excitation of the electrons. It is usually presented by the equation:

$$N_T = kTB \tag{3.10}$$

where k is Boltzmann's constant, T is the temperature in Kelvin and B is the bandwidth in Hz. Typically, in an RFID system, the channel bandwidth is 200 kHz. The noise floor at 300 K is equal to $-174 + 10\log(200000) = -121$ dBm. However, this is not the final noise value since it changes with gain and other noise sources from other components. Instead of measuring the noise itself, a system is usually characterized by its noise factor (f), which is the ratio of the signal-to-noise ratio on the input to that on the output:

$$f = \frac{(S/N)_{in}}{(S/N)_{out}} \tag{3.11}$$

Since the relative noise level on the output is impossible to be less than the level on the input, the noise factor is always greater than 1. Many specifications of the components report this value in dB, called the noise figure (*NF*):

$$NF = 10\log(f) \tag{3.12}$$

Similarly, for real devices, the NF is always greater than 0. If an amplifier has a noise figure of 8 dB, the output noise floor is -121 + 8 = - 113 dBm. Assuming that FM0 is applied and thermal noise dominates, an S/N of about 10 dB is required for reliable demodulation. The backscattered tag signal has to have a power equal to or greater than -103 dBm so that it can be successfully decoded. However, other noise sources such as the leakage from the transmitter may have a greater impact than thermal noise. For example, the Indy R2000 Reader has the broadband noise of -144 dBc/Hz of its output. If it operates with 35 dBm output power and 200 kHz signal bandwidth, the noise level from the transmitter is $35 - 144 + 10\log(200000) = -56$ dBm. When there is a 30 dB isolation between transmitter and receiver, the noise floor becomes – 86 dBm, which is worse than the thermal-noise-limited receiver environment.

Besides the impact of leakage, each selected component changes the total noise figure of the whole system. In order to calculate the noise figure at each stage, the equation for a cascaded noise figure is used.

$$NF_{cas} = 10\log(f_{cas}) = 10\log(f_1 + \frac{f_2 - 1}{G_1} + \frac{f_3 - 1}{G_1 G_2} + \cdots + \frac{f_n - 1}{G_1 G_2 \ldots G_{n-1}}) \tag{3.13}$$

where n is the number of cascaded components. This equation clearly shows that the effect of the noise figure at a later stage of the chain is decreased due to the increases in total gain. This

feature means that the cascaded noise figure is highly dependent on the noise figure of components at the first few stages. Thus, the total noise figure of the system can be reduced by selecting low noise figure components or adding a low noise amplifier (LNA) at the front.

The performance of the proposed system can be evaluated by calculating the parameters described above. In the system downlink, baseband signals from the central controller experience twisted-pair cable attenuation before they reach the quadrature modulator. This attenuation is commonly known as cable insertion loss and its value can be estimated using the equation set out in the TIA-568-C2 Standard [136]. According to the equation in Table 3.2, the maximum attenuation of a 100 m Cat5e cable is 1.31 dB when 250 kHz commands are transmitted. If the TX signal is large enough to overcome the cable loss and match the input requirement of the modulator, those commands can be successfully converted to the RF band. According to the specifications of the quadrature modulator, the output power is nearly a fixed value, staying around 4 dBm. This power level also matches the requirement of the RF amplifier input. With careful adjustment of the amplifier gain and selection of the antenna, the downlink of the proposed system can provide linear and stable transmission signals.

Table 3.2 Maximum insertion loss of 100m different types of twisted-pair cable [136]

Types	Frequency (MHz)	Insertion Loss (dB)
Cat3	$1 \leq f \leq 16$	$1.02\left(2.32\sqrt{f} + 0.238f\right)$
Cat5e	$1 \leq f \leq 100$	$1.02\left(1.967\sqrt{f} + 0.023f + \frac{0.05}{\sqrt{f}}\right)$
Cat6	$1 \leq f \leq 250$	$1.02\left(1.808\sqrt{f} + 0.017f + \frac{0.2}{\sqrt{f}}\right)$

The requirements for the system uplink are more complicated than those in the downlink, since it not only needs to enlarge the weak tag signals but also to maintain a required signal-to-noise ratio (SNR) for successful tag detection. Accordingly, despite the linearity problems, the noise figure has to be considered in the uplink. The spreadsheet of the proposed uplink is shown in Figure 3.13. The results show that the total uplink gain is 33 dB. This high gain can greatly enlarge the small tag signal to a desired level so that the later stages can correctly decode the received signals. However, high gain also brings the risk of saturation when a much higher power transmission signal leaks into the receiver chain. Therefore, lowering the RF amplifier

gain or adding a leakage cancellation block can help the current system to avoid the leakage problem. Based on the current design, the IIP3 of the uplink decreases to 1.76 dBm before it goes back to the Indy R2000 chip. In most RF systems, the lower power limit is determined by the noise floor and the upper limit is determined by the IIP3. The range between these two limits over which the system can work properly is called the spur-free dynamic range (SFDR). This value can be calculated by

$$\text{SFDR} = \frac{2}{3}[IIP_3 - (10\log_{10}(kTB) + NF - 174)] \tag{3.14}$$

In this design version, the uplink SFDR is 73.5 dB, which is enough for many RFID receivers. Equation 3.14 shows that the SFDR of the system is directly proportional to IIP_3 but inversely proportional to the NF. In order to design a high-SFDR uplink, the noise figure should be kept at a lower level. Based on Equation 3.13 and the spreadsheet results, the noise figure at the first few stages or before the high gain amplifier dominates the final noise figure. Thus, swapping the position of the BPF and amplifier and replacing the high-gain amplifier with a low-noise amplifier is able to further improve the system noise figure.

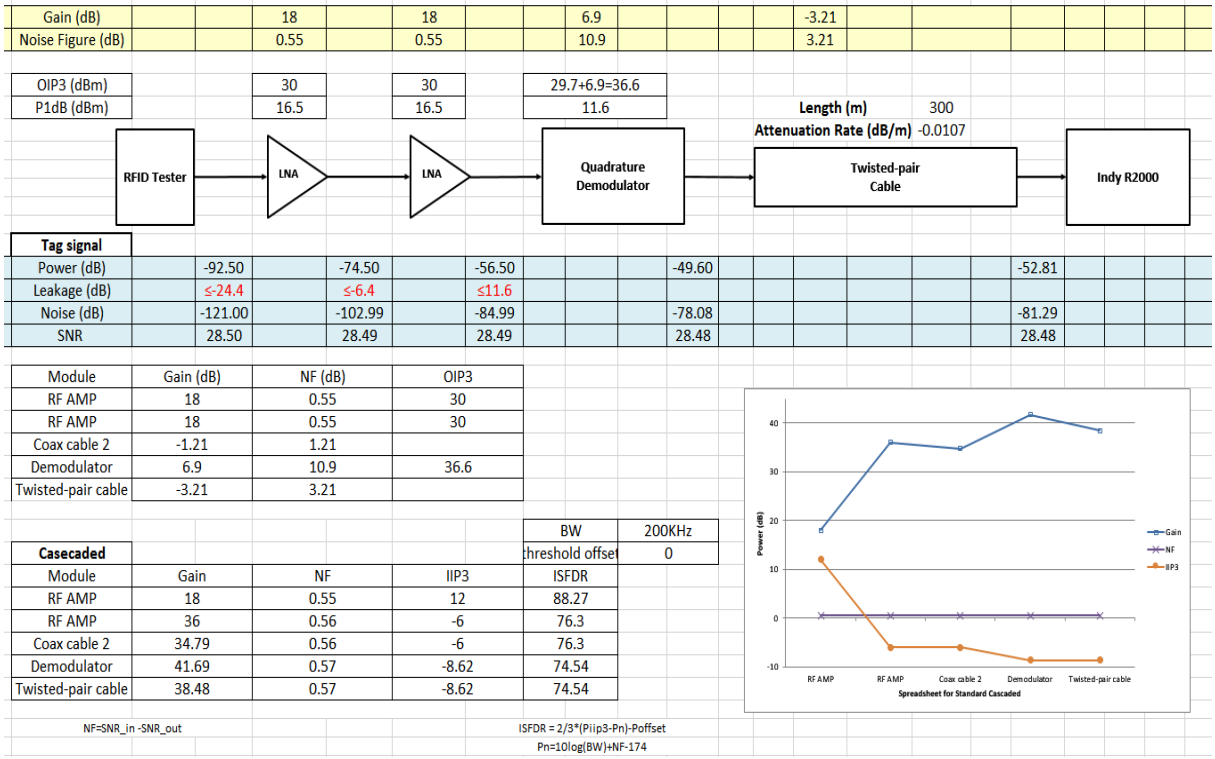

Figure 3.13 Spreadsheet of the preliminary system uplink

3.6. Frequency and Phase Hopping

Frequency hopping is required in RFID regulations and standards because of its advantages in eliminating collision problems between different RFID systems and avoiding interference from other wireless communication systems in the same frequency band. Hence the carrier frequency in such frequency hopping systems is designed to periodically change during operation. Generally, changes of frequency are achieved by tuning the frequency of the local oscillator, typically a frequency synthesiser. In the frequency synthesiser system, the frequency divider modulus and low-frequency input source can be a control signal to determine the carrier frequency. According to the results from [93], the frequency hopping technique can dramatically enhance the identification performance of the RFID system, in which the detection accuracy increases from less than 50 per cent to nearly 100 per cent.

Besides frequency hopping, the studies in [42] prove that phase hopping is also able to improve the system performance in terms of reducing destructive interference. If the phase of the transmission signal can be precisely controlled, constructive interference between backscattered signals can be achieved in the multi-path environment. As a result, the received signal power is maximised without adding any amplifiers. Controlling the phase of the transmission signals or local oscillator usually involves adding phase shifters, but this direct method brings extra cost and complexity to the circuit. However, if the phase of the synthesiser output signal can be tuned by changing the phase of the reference signal or phase offset of the phase detector, such phase shifters and extra commands can be avoided.

Thus the following simulation work attempts to investigate the feasibility of baseband controlled frequency and phase hopping as well as the limitations of this approach for the designed system.

3.6.1. PLL-based Frequency Synthesis Systems

Frequency Synthesis is an approach for generating a specific frequency by using a low-frequency signal (known as reference signal) which is multiplied by a range of modulus [137]. Usually, the reference frequency is very precise and obtained from a crystal oscillator. The modulus is selectable over a certain range, and can be an integer or fraction. A phase-locked loop (PLL) is used as a control technique that allows the phase of the generated frequency and reference frequency to be coherent so that the two frequencies are precisely correlated.

3.6.1.1. Phase-Locked Loop

The phase-locked loop is the basic control configuration for frequency synthesis. It is a nonlinear closed loop to lock the phase of the input and output signals. Typically, it consists of a phase detector, a loop filter, and a voltage-controlled oscillator (see Figure 3.14).

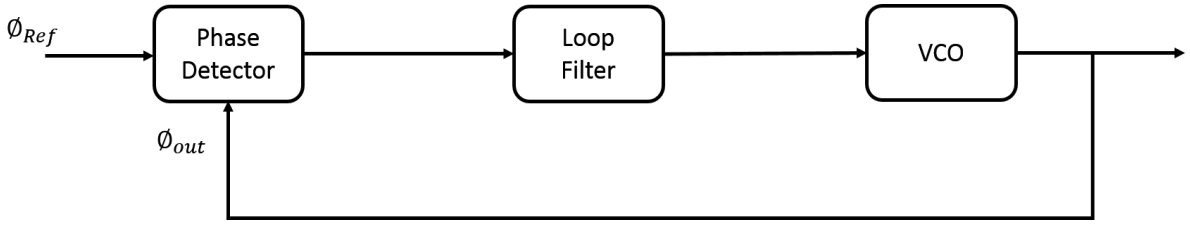

Figure 3.14 Typical Phase-locked loop structure

The phase detector compares the phase of the input signal and the phase of the VCO output, and then the differences between these two phases are generated as an error signal, which is transmitted to the loop filter. Ideally, the error signal is constrained to a fixed value after the loop filter over a period of time, and this stable value becomes a control signal for the VCO. Typically, the loop filter is a low pass filter, which is applied for noise suppression. More importantly, it determines the locking range, bandwidth and settling time of the entire loop. The VCO generates a sinusoidal signal, and the frequency of this signal is directly controlled by its input voltage. The phases of the input and output signals can be coherently locked through this control loop. When the loop becomes linear, the phase locked condition has been achieved and the phase error remains at a quiescent value.

3.6.1.2. Integer-N Frequency Synthesis

In the integer-N frequency synthesis, a divider is added to the phase-locked loop. The modulus of this divider has to be an integer. The functionality of this divider is to divide the phase and frequency of the VCO output signal. Accordingly, the relationship between the output and input can be expressed as the following two equations:

$$\emptyset_{out} = \mathrm{N} \times \emptyset_{Ref} \tag{3.15}$$

$$f_{out} = \mathrm{N} \times f_{Ref} \tag{3.16}$$

Equation 3.15 clearly shows that frequency synthesis generates a high-frequency signal from a low-frequency signal source. Generally, to achieve frequency hopping, control signals are sent to vary the modulus of the divider. Another method to hop the frequency is to tune the frequency of the input signal. The phase dithering technique can be achieved in the same way.

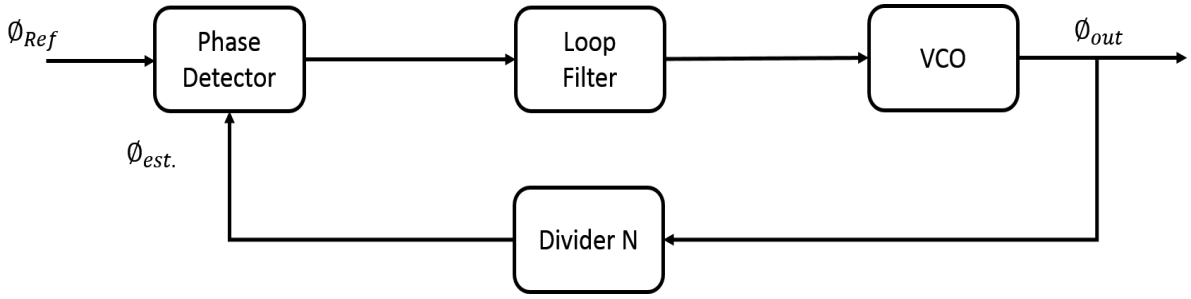

Figure 3.15 Integer-N frequency synthesis block diagram

Since the preliminary design of the baseband-controlled frequency and phase hopping attempts to simplify the remote subsystem, the frequency and phase reference signals are controlled on the baseband side.

3.6.1.3. Fractional-N Frequency Synthesis

Due to the regulations, there is only around a 3 MHz spectrum available for frequency and phase hopping. In order to avoid interference between the channels, a high resolution for the frequency selection is required. For the integer-N frequency synthesis, it is inflexible to tune the frequency of the input signal to achieve small frequency changes, especially when the divider modulus is very large. Thus, the fractional-N frequency synthesis becomes a reasonable choice for systems where high frequency resolution is required.

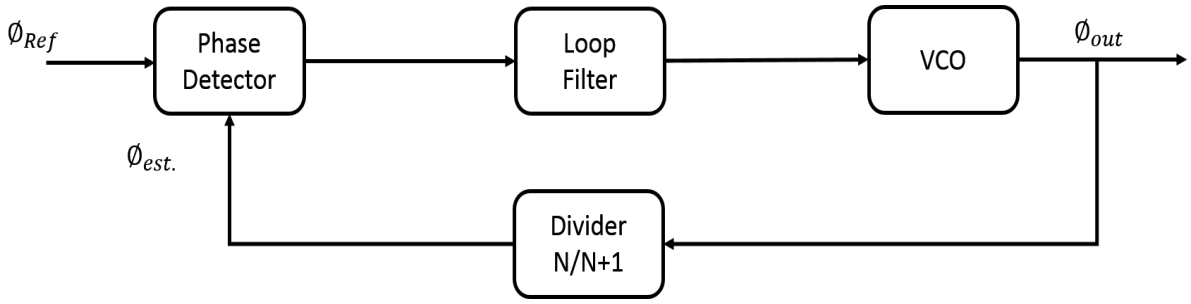

Figure 3.16 Integer-N frequency synthesis block diagram

A fractional divider is achieved by switching the modulus N and N+1 in a certain clock cycle time (see Figure 3.16). This time is set based on the fractional part of the modulus. Taking 866 MHz as an example, the overall divider modulus should equal 86.6 when the frequency of the input reference signal is 10 MHz. Thus, in each of the 10 periods of the reference signal, the accumulator provides six cycles for the system to divide 87 and four cycles to divide 86. The average divide modulus is: $(1 - 0.6) \times 86 + 0.6 \times (86 + 1) = 86.6$

3.6.2. Baseband-controlled Method Simulation

Based on the RFID regulations, there are four high power channels available for reader operation within the band from 865 MHz to 868 MHz. Each channel bandwidth is 200 kHz and they are usually placed on frequencies of 865.7 MHz, 866.3 MHz, 866.9 MHz, and 867.5 MHz. Besides the four high power channels, the rest of the channels are defined as the low power channels where the tag response is expected to be observed. In order to successfully obtain the tag signal, regulations also provide a spectrum mask envelope to limit the reader transmission power in a selected channel and adjacent channels. Figure 3.17 shows an example when the system operates at a frequency of 865.7 MHz.

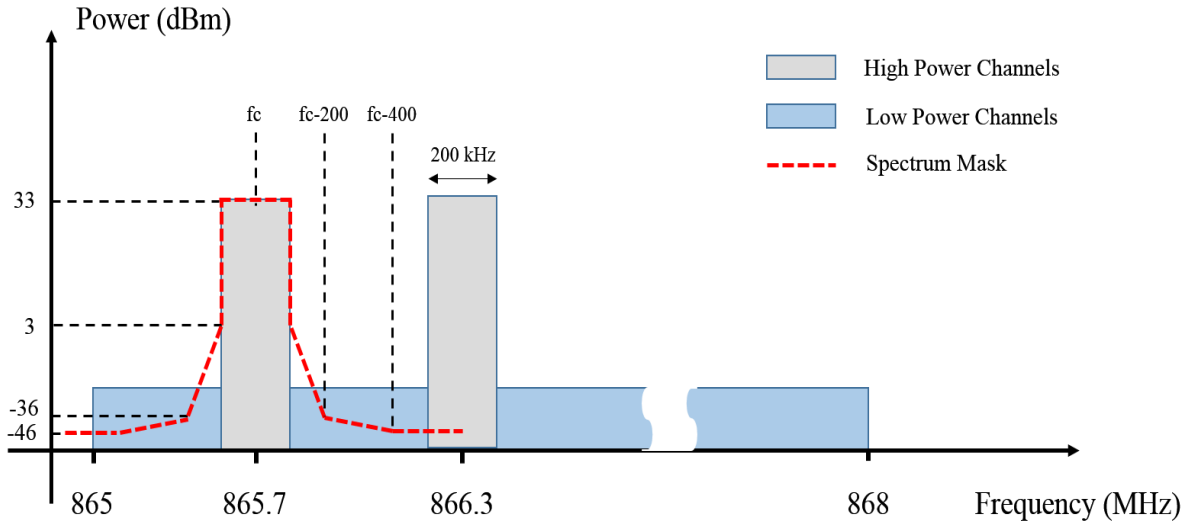

Figure 3.17 Limits in operational spectrum [88]

According to limits given by the European Telecommunications Standards Institute (ETSI) [88], an RFID system with sensitivity of -86 dBm and minimum SNR of 10 dB requires at least 6 dB above the sensitivity in the presence of an adjacent channel interference of -36 dBm at 200 kHz away. Based on these parameters, the phase noise in dimension of dBc/Hz can be estimated using the equation in [138]:

$$\mathrm{L}(\Delta \mathrm{f}) = S_d - S_{b@\Delta f} - S_I - 10\log(BW) \tag{3.17}$$

where $\mathrm{L}(\Delta \mathrm{f})$ is the phase noise at $\Delta \mathrm{f}$ away from the carrier frequency, S_d is the desired signal power, $S_{b@\Delta f}$ is the magnitude of blocker in dBm, S_I is the interference level in dBm, and BW is the receiver noise bandwidth. As a result, for the above example, the phase noise can be

estimated as $L(\Delta f) = \big((-86+6)-(-36)\big) - 10\log(200\times10^3) - 10 = -107\ dBc/Hz$. The maximum spurious tone of -54 dBc for this system can be also calculated.

In addition, the lock time of the PLL is another important parameter for RFID system performance. In [88], the standard describes the time limits for transmission on the same channel. For the on-duration, the maximum time is 4 s, and for the off-duration, the time should be not less than 100 ms. Although these two requirements can be simply achieved by most of the PLL-based frequency synthesisers, an RFID system still requires faster PLL lock times so as to retain the data rate and leave more time for processing in other blocks such as leakage cancellation. Hence, in this simulation work, the lock time has lower priority than phase noise and spectrum purity. The specifications of phase-locked loop frequency synthesis can be summarised in Table 3.3.

Table 3.3 Specifications for PLL design

Description	Value	Units
Frequency Range	860 - 960	MHz
Lock Time	≤ 1	ms
Output Power (minimum)	5	dBm
Phase Noise	-107	dBc/Hz @ 200 kHz
Spurious Tone	-54	dBc
Channel Spacing	200	kHz

3.6.2.1. Phase-locked Loop Design

Since the PLL is designed for achieving the minimum noise level, it is critical to find a proper loop bandwidth. A wider loop bandwidth usually leads to better lock time but worst spurs attenuation. In many cases, one-tenth of the phase detector frequency is the maximum limit for the loop bandwidth and one-third of the phase detector frequency can result in an unstable PLL system. VCO phase noise is attenuated inside the loop bandwidth but more is likely to dominate the noise level at the outside band. In this design case, the loop bandwidth for optimal noise level is the intersection point of the VCO phase noise curve and crystal oscillator phase noise curve. Based on the specifications of the reference oscillator and VCO in [139] and [133], these two curves are plotted in Figure 3.18 and the loop bandwidth is 160 kHz (or 10^6 rad).

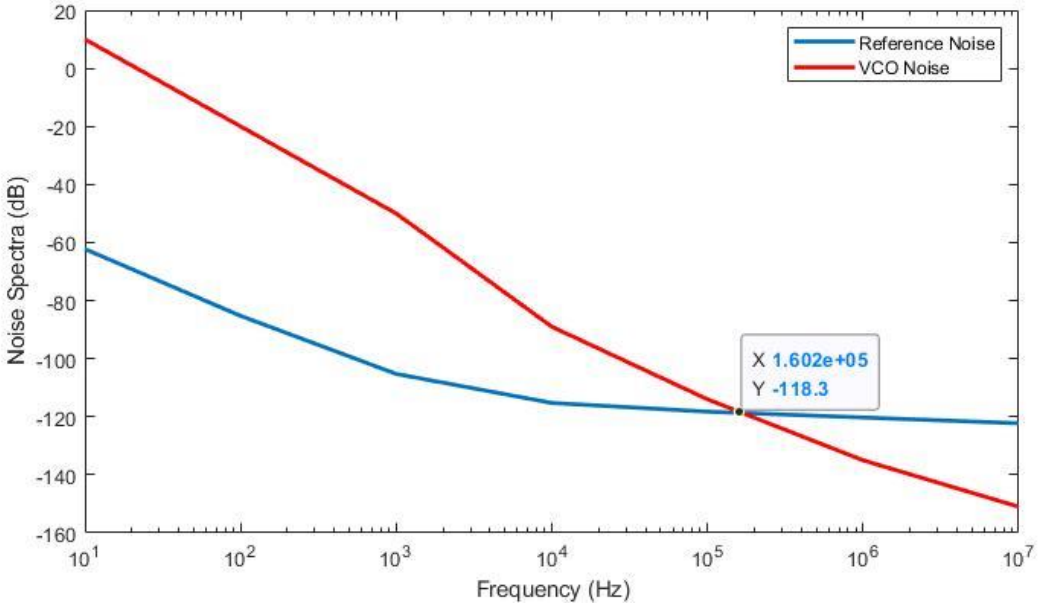

Figure 3.18 Oscillator and VCO phase noise curves

The PLL loop filter acts as an important connection between phase detector and VCO. It not only provides the conventional function of a low pass filter, but also it translates the proper tuning voltage to the VCO. Thus, in some architectures, the loop filter can further be divided into two parts: charge pump and low pass filter. The transfer function of the loop filter is the most important part of the entire closed loop PLL transfer function, and it significantly impacts on the switching speed, spur performance, phase noise, and stability of the entire synthesis system. Generally, the loop filter only consists of resistors and capacitors, but, if high power output is required, the filter can be also implemented by using an op-amp. Since the proposed the system aims to develop a low-cost block, the design of the loop filter (red dotted box) in this simulation only focuses on the passive type (Figure 3.19).

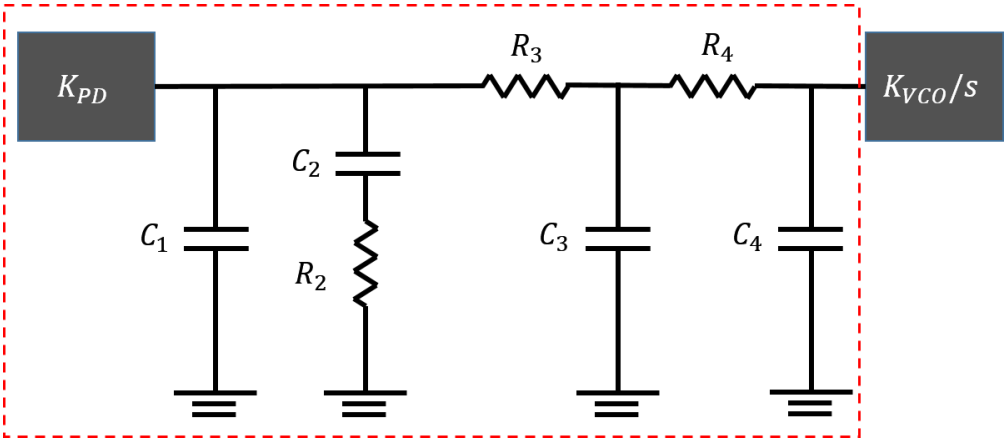

Figure 3.19 General passive loop filter

The transfer function of the PLL loop filter can be typically expressed as follows:

$$\mathrm{Z(s)} = \frac{1+s\times T2}{s\times(A3\times s^3+A2\times s^2+A1\times s+A0)}, T2 = R_2 \times C_2 \tag{3.18}$$

where A0, A1, A2, and A3 are the loop filter coefficients, T2 is the zero of the transfer function. The relationship between these coefficients and loop filter components are summarised in Table 3.4.

Table 3.4 Loop filter coefficients and components [139]

Filter Order	Coefficient	Components Value
2 (A2=A3=0)	A0	C1 + C2
	A1	C1 · C2 · R2
3 (A3=0)	A0	C1 + C2 + C3
	A1	C2 · R2 · (C1 + C3) + C3 · R3 · (C1 + C2)
	A2	C1 · C2 · C3 · R2 · R3
4	A0	C1 + C2 + C3 + C4
	A1	C2 · R2 · (C1 + C3 + C4) + R3 · (C1 + C2) · (C3 + C4) + C4 · R4 · (C1 + C2 + C3)
	A2	C1 · C2 · R2 · R3· (C3 + C4) + C4 · R4 · (C2 · C3 · R3 + C1 · C3 · R3 + C1 · C2 · R2 + C2 · C3 · R2)
	A3	C1 · C2 · C3 · C4 · R2 · R3 · R4

However, to calculate these coefficients, the loop filter needs to firstly determine the value of the divider N, phase detector gain (K_{PD}), and VCO gain (K_{VCO}) in the PLL. It is common in the PLL that the value of N is tuneable for generating different frequencies. Thus, to keep the loop filter dynamic or relatively stable loop gain, the K_{PD}, and K_{VCO} are normally used to compensate. In this simulation, these three parameters are fixed for simple calculation. Parameters such as phase margin are also important to determine loop filter performance. It has impacts on the loop transient response. Higher phase margin gives flatter response, whereas a lower phase margin is more likely to generate peaking in the response. 48 degrees is simulated as the optimal phase margin for lock time [139]. Since the lock time is not the priority in this simulation, the phase margin is set no less than 60 degrees. According to these discussions the requirements for this loop filter can be summarized in Table 3.5.

Table 3.5 Performance requirements for loop filter

Parameters	Value	Units
Phase Detector Frequency	10	MHz
Output Frequency	866	MHz
Divider N	86.6	-
VCO Gain	33	MHz/V
Phase Detector Gain	0.16	mA
Loop Bandwidth	10^6	Rad
Phase Margin (∅)	≥ 60	Degrees
Overshoot	≤ 20%	-

Take a type II 3rd order PLL as an example. The loop gain transfer function can be described as a polynomial:

$$\mathrm{T(s)} = \frac{K_{Loop} \times (1+s \times T2)}{s^2 \times (1+s \times T1)} \tag{3.13}$$

By removing VCO factors (K_{VCO}/s), the rest of the loop filter transfer function can be written as

$$\mathrm{Z(s)} = \frac{K_{PD}}{N \times A0} \times \frac{(1+s \times T2)}{s \times (1+s \times T1)} \tag{3.14}$$

According to Equation 3.14, the system is required to design a 2nd order loop filter and coefficients A0, A1 can be expressed as:

$$\mathrm{A0} = \mathrm{C1} + \mathrm{C2} \tag{3.15}$$

$$\mathrm{A1} = \mathrm{C1} \cdot \mathrm{C2} \cdot \mathrm{R2} \tag{3.16}$$

Based on the given parameters in Table 3.5, the unknown variant T1 can be calculated by solving the equations below:

$$\emptyset = 180 - \tan^{-1}(2\pi BW \cdot T2) - \tan^{-1}(2\pi BW \cdot T1) \tag{3.17}$$

$$\mathrm{T2} = \frac{1}{(2\pi BW)^2 \cdot T1} \tag{3.18}$$

$$\mathrm{A0} = \frac{K_{PD} \cdot K_{VCO}}{(2\pi BW)^2 \cdot N} \cdot \sqrt{\frac{1+(2\pi BW)^2 \cdot T2^2}{1+(2\pi BW)^2 \cdot T1^2}} \tag{3.19}$$

In order to further simplify the components selection, the C2 can be set to 1 nF. The rest of the components of the designed PLL are calculated and listed in Table 3.6.

Table 3.6 Components for the loop filter

Components		
C1	17.2	pF
C2	1	nF
R2	24.5	kΩ

The performance of the designed loop filter can be verified by using MATLAB software. The open and closed loop response of the designed filter have been plotted in Figure 3.20. The phase margin of the filter is the difference between the phase and 180 degrees when gain margin is at 0 dB gain. Thus, based on the open loop bode figure, the phase margin of this PLL is 64 degrees and its loop bandwidth is 1.06×10^6 rad. Based on the Equations 3.20 and 3.21, the damping factor (ζ) and natural frequency (W_n) of this PLL are 0.97 and 5.17×10^6 rad. Thus, this designed PLL is stable.

$$2 \times \zeta \times W_n = 2\pi BW \tag{3.20}$$

$$\sec\varphi - \tan\varphi = \frac{1}{4\times\zeta^2} \tag{3.21}$$

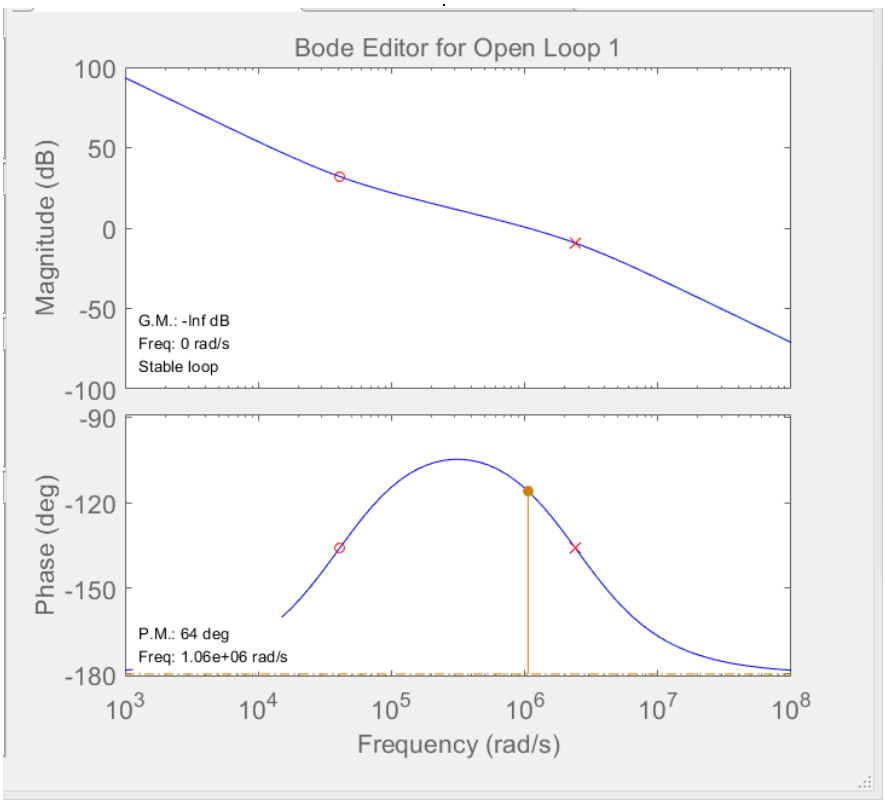

(a)

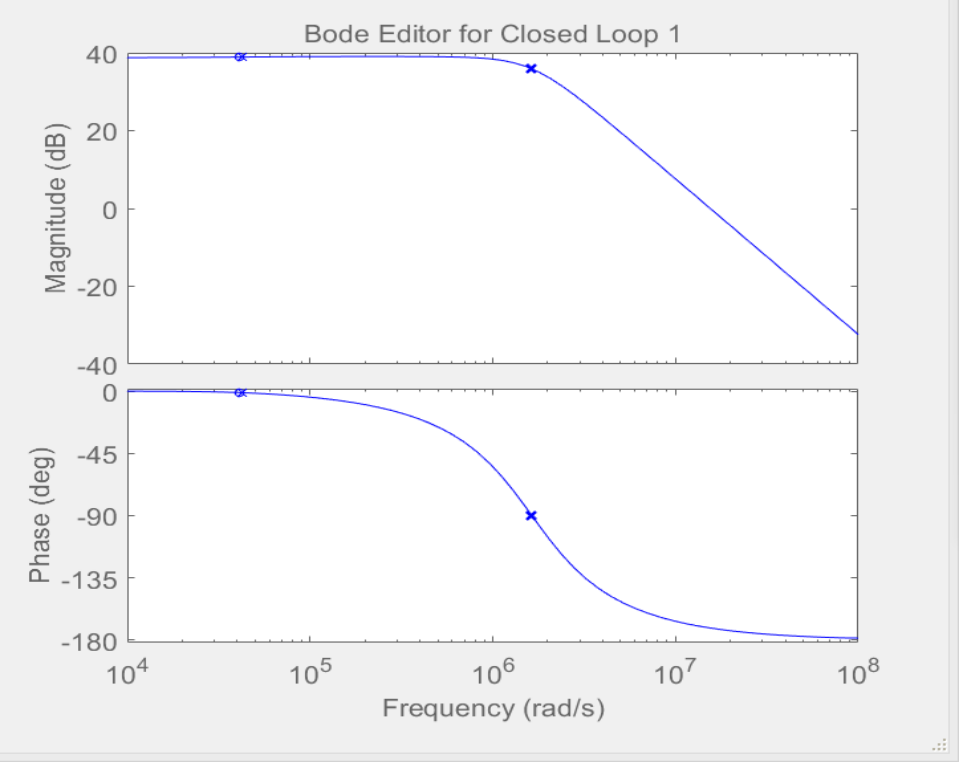

(b)

Figure 3.20 Open and closed loop response of the designed loop filter

The lock time and overshoot performance of this PLL are able to be determined by plotting its closed loop step response. As shown in Figure 3.21, the settling time of this designed PLL is 32 μs and its overshoot level is 7.39%.

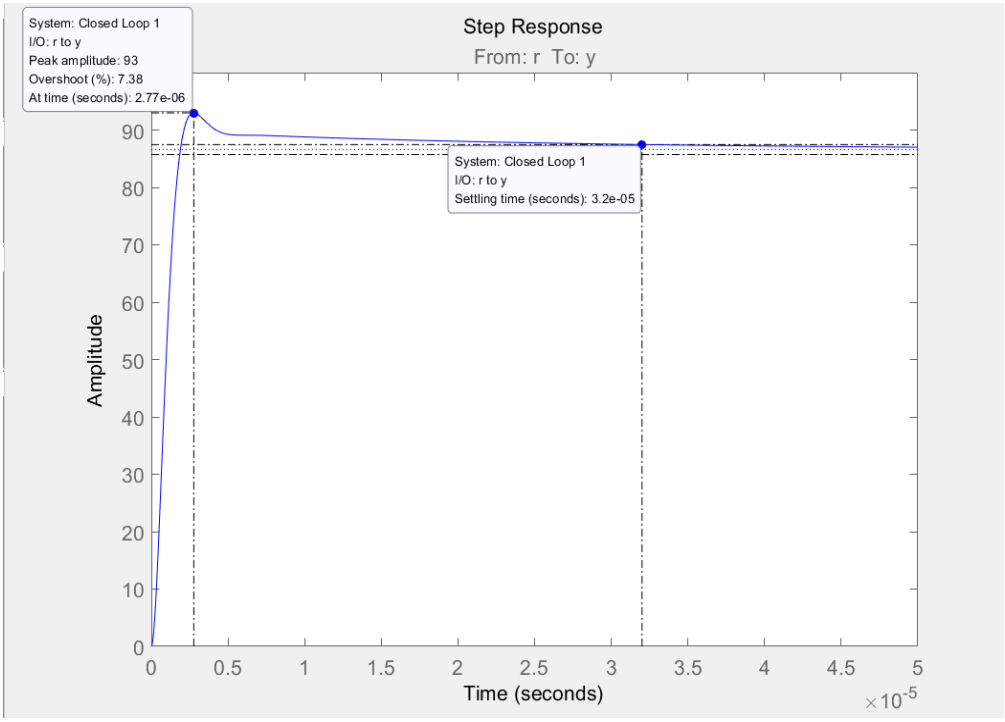

Figure 3.21 Step response of the designed loop filter

In addition, the PLL phase noise level is a critical part for achieving a high sensitivity RFID reader. By calculating and normalising the phase noise into dBc/Hz dimensions, the total PLL phase noise is plotted in Figure 3.22. Based on the calculation result, the designed PLL phase noise at frequency 200 kHz is -116.8 dBc/Hz, which is much smaller than the requirements of -107 dBc/Hz.

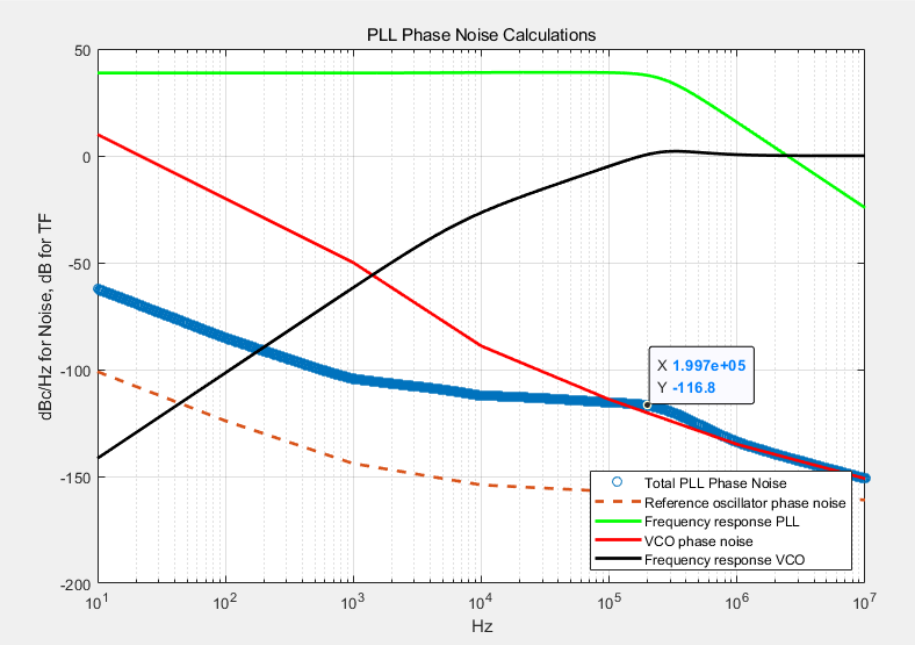

Figure 3.22 PLL phase noise calculation

Regarding the spectrum purity of the PLL frequency synthesis, a MATLAB Simulink simulation has been conducted to determine its performance. The block diagram of the frequency synthesis is shown in Figure 3.23. All the essential parameters are set based on the simulated results, and the output spectrum is plotted in Figure 3.34.

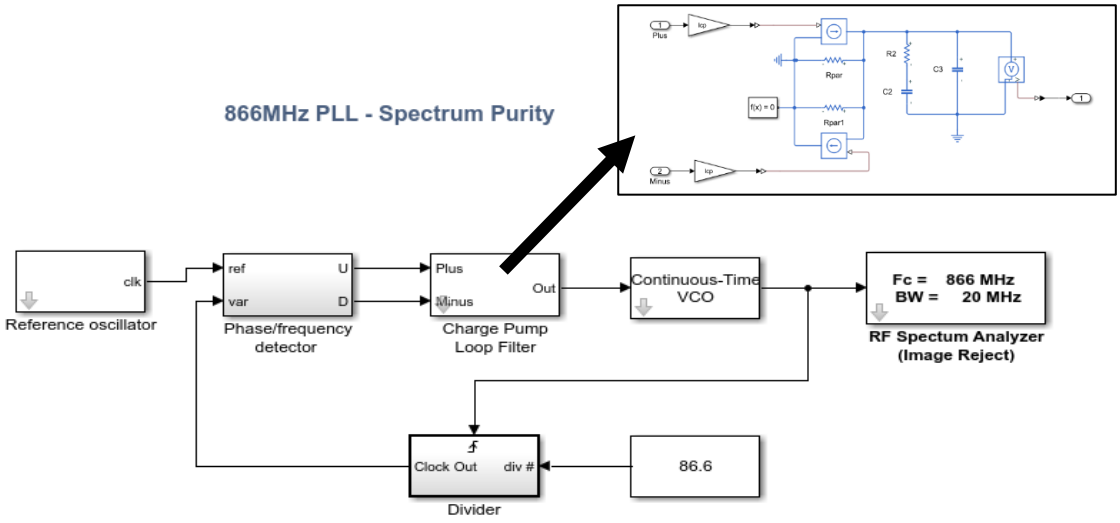

Figure 3.23 Block diagram of PLL frequency synthesis

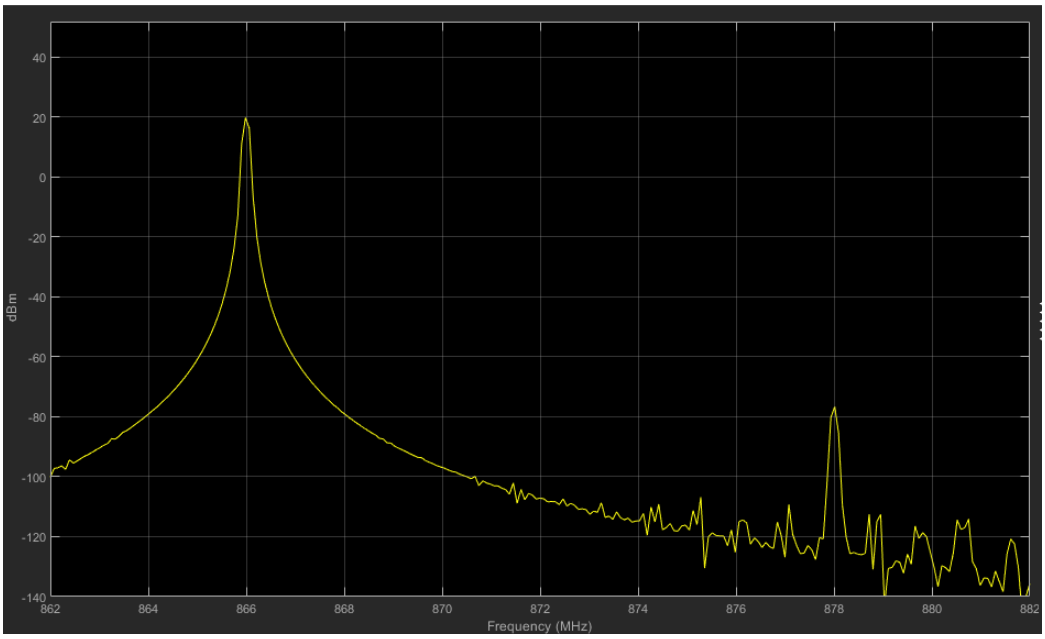

Figure 3.24 Spectrum of the design PLL frequency synthesis

According to the simulated output spectrum, the spur tone of the frequency synthesis is -76 dBm, and it locates on 878 MHz, which is outside the RFID operation band. Inside the operation band, there is no system impairment. Thus, the PLL spectrum is pure enough for the RFID system.

In conclusion, a type II 3rd order PLL frequency synthesis has been designed and its performance has also been measured for a passive RFID reader. This designed synthesis can achieve all the requirements including lock time, phase noise level, and spectrum purity according to the verification tests.

3.6.2.2. Limits and Discussion

In the proposed RFID system, the reference signal of 10 MHz is generated in the central system and then transmitted to frequency synthesis over a twisted-pair cable. Therefore, it is necessary to examine the effects of cable transmission and also determine the cable length limits for system implementation.

For transmission of the 10 MHz reference signal over a Cat5e cable, the dominant effect for the signal is the insertion loss. Based on the standard TIA-568-C.2 [136] for 100 m Cat5e twisted-pair cable, the insertion loss of the signal can be estimated following the equation below:

$$1.02 \times \left(1.808\sqrt{f} + 0.017f + \frac{0.2}{\sqrt{f}}\right) + 4 \times 0.02\sqrt{f} + 0.0003f^{1.5} \qquad (3.22)$$

where f is the signal frequency. With simple calculation, the attenuation for a 10 MHz single over 100 m Cat5e is 7.1 dB.

For most frequency synthesis systems, there is a minimum SNR level for the input reference signal to retain proper operation of the phase detector. This is because the phase detector may produce an incorrect phase error, which will result in an unstable loop or long settling time. Take PLL frequency synthesis ADF4350 as an example, the minimum power of the reference input is – 32 dBm. If assumed that the cable quality is good and the cable attenuation is linear, for a 5 dBm reference signal, the maximum Cat5e length which can be used for the PLL is 521 m, and this length can be increased if a higher gain line driver is added.

Effect such as delay is also critical issue for the phase control accuracy. With different lengths of the Cat5e, the signal phases that reach the phase detector are different. This problem may become serious especially when multiple sub-units are connected to the central controller. Thus, instead of setting the phase offset in the controller side, it is much better to design the control functions in the phase detector so as to avoid the other impacts from the cable transmission. A simulation in terms of the output phase control has been done based on the designed system, and the result is shown in Figure 3.25. According to the result, phase control is achievable by setting a particular phase offset at the phase detector.

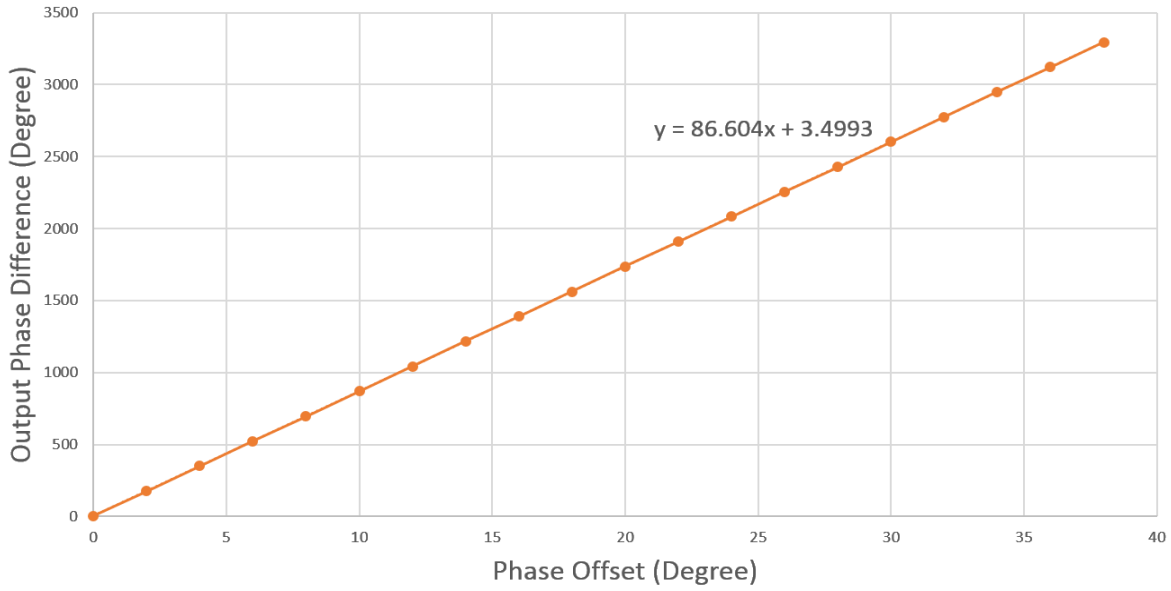

Figure 3.25 Results of the phase control at phase detector

Since crosstalk can also lead to spur problems at the RF output in a PLL frequency synthesis, it also needs to be fully considered. However, this issue often becomes serious when high frequency signals are transmitted. In the current case, only baseband signals are transmitted in surrounding pairs and, with help of the balanced transmission method, the crosstalk issue can be largely eliminated. In addition, the in-band phase noise performance is sensitive to the reference duty cycle. For example, if the duty cycle of the reference signal moves outside the range between 45% and 55%, the system suffers from 5 dB phase noise degradation [133]. However, this problem usually occurs in high data rate communication, and, with help of the differential line driver and receiver, the high slew rate capability greatly reduces the effects in terms of the phase noise.

3.7. Conclusion

This chapter first introduced the limitations of conventional UHF RFID systems in terms of their adoption for wide-area detection. A novel system configuration, which uses Ethernet cable to connect the baseband central controller and RF remote subsystem, provides a cost-effective, highly-flexible, and simply-installed solution to address this practical problem. Related theoretical models of the RFID system design have been demonstrated, such as the link budget and RF spreadsheet. In addition, the new system configuration offers a new method to achieve frequency and phase hopping by tuning the frequency of the reference tone and the phase offset of the phase detector. This new method not only can reduce the hardware cost of each subsystem but also allows the central controller to synchronise LO of those subsystems.

This initial design of the system makes it feasible to use a single RFID system to cover large-scale organisations or wide-area detection. It shows a prototype of next generation cyber-physical systems, enabling terms such as “Industry 4.0” or the “4^{th} industrial revolution”. Proper development of this new system allows it to achieve multiprotocol compatibility and supersede conventional RFID systems in the coming future.

Chapter 4

4. Measurement of Basic Link Performance

4.1. Introduction

The proposed new passive UHF RFID system operating over Ethernet cable has been modelled in a preliminary manner. Based on the simulation results, this new system should have a similar detection capability to conventional systems since the only difference between them is the use of near baseband communication. However, to practically determine the system performance, features such as its transmission spectrum, receiver sensitivity, and detection range have to be experimentally measured. Furthermore, in order to fully understand the merits and limitations of this new system, comparisons of some specifications between the new and conventional RFID systems are needed. With the help of these understandings, further improvements and future development directions of such systems will become clear. Therefore, this chapter reports these experimental measurements and makes suggestions concerning the basic link of the new system.

In the subsequent subchapters, the available functions of this new system will be introduced, and the blocks relating to those functions will be explained and discussed. A series of practical experiments will then be conducted to measure the overall system performance and identify limitations in the central controller, remote subsystem, and Ethernet cable.

4.2. System Basic Functionalities

Generally, RFID readers are controlled via an interface or panel in a PC or embedded system. The available functionalities of the reader are usually listed and introduced by the product vendor or developer so that users are able to properly set the desired operation features. In this new system, several control software applications are used since the baseband initialisation in the Indy R2000 chip and other parameters such as carrier frequency and output power in the RF blocks are required to be set before running an inventory.

In the central controller, the RF blocks of the Indy R2000 chip are bypassed and only low frequency modulated signals are used for the new system. Certain functions can be directly used without extra programming using the microcontroller (See Figure 4.1).

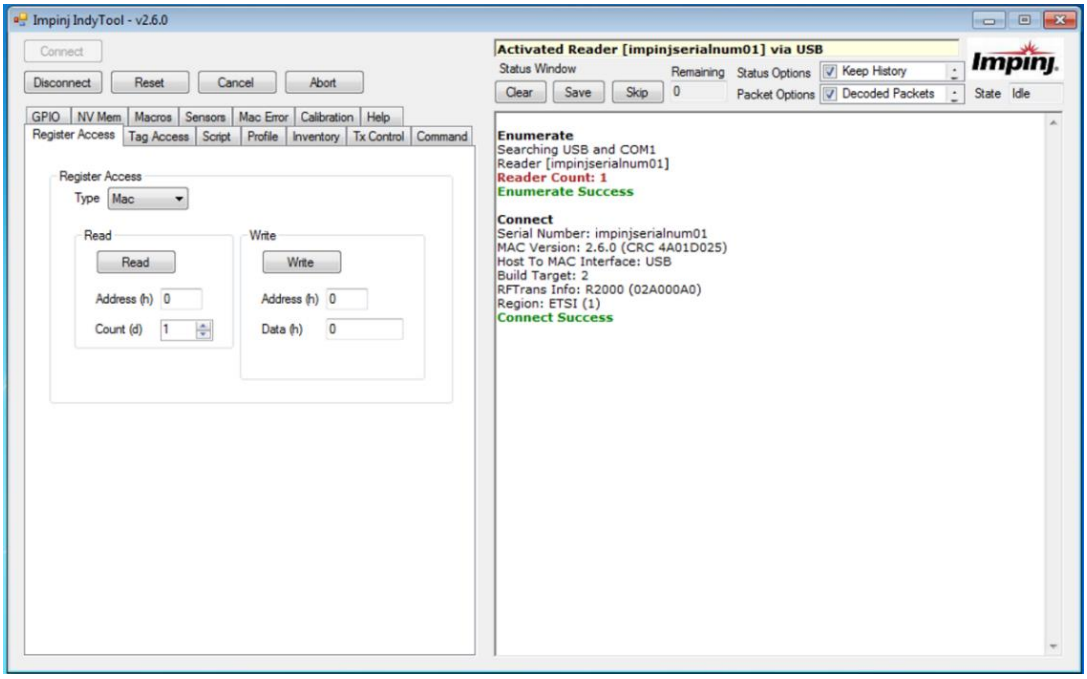

Figure 4.1 Indy R2000 chip control interface

For example, the transmission modulation scheme of the system can be set in PR-ASK or DSB-ASK by changing the operating profile in the chip. In addition, by setting the related registers in the chip, the given test pins can access different baseband points to monitor the system status. These observation ports also provide baseband output ports for the proposed new system. In this new system, the baseband communication between the Indy R2000 chip and new designed blocks are highlighted in Figure 4.2.

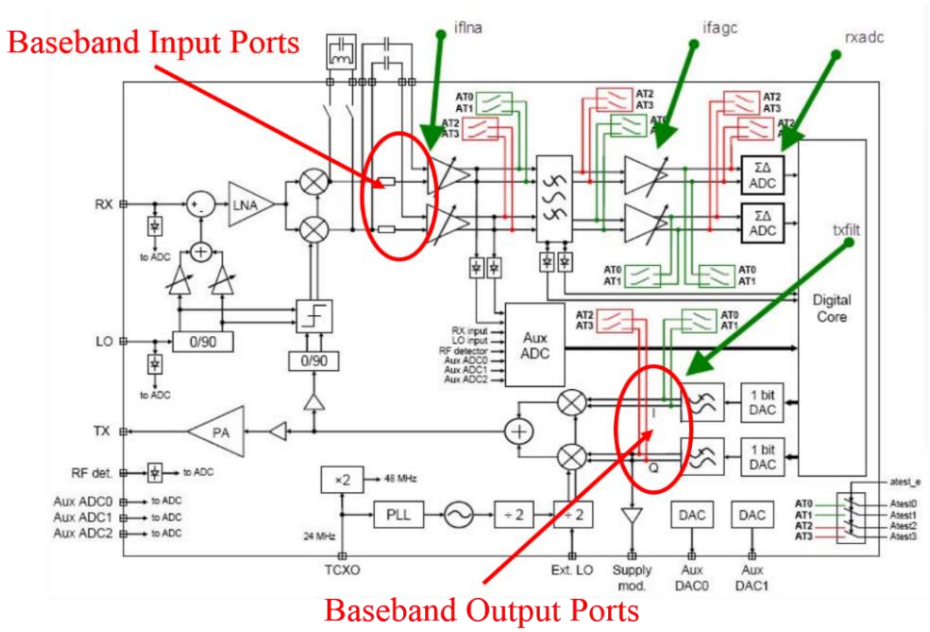

Figure 4.2 Available access points in the Indy R2000 chip

In the antenna subsystem, the carrier frequency and its hopping time are important parameters for system operation. The ADF4350 frequency synthesis chip provides a simple SPI-compatible serial interface for writing specific commands to control the chip. The interface is shown in Figure 4.3, and there are many helpful options in different registers to set the system carrier frequency.

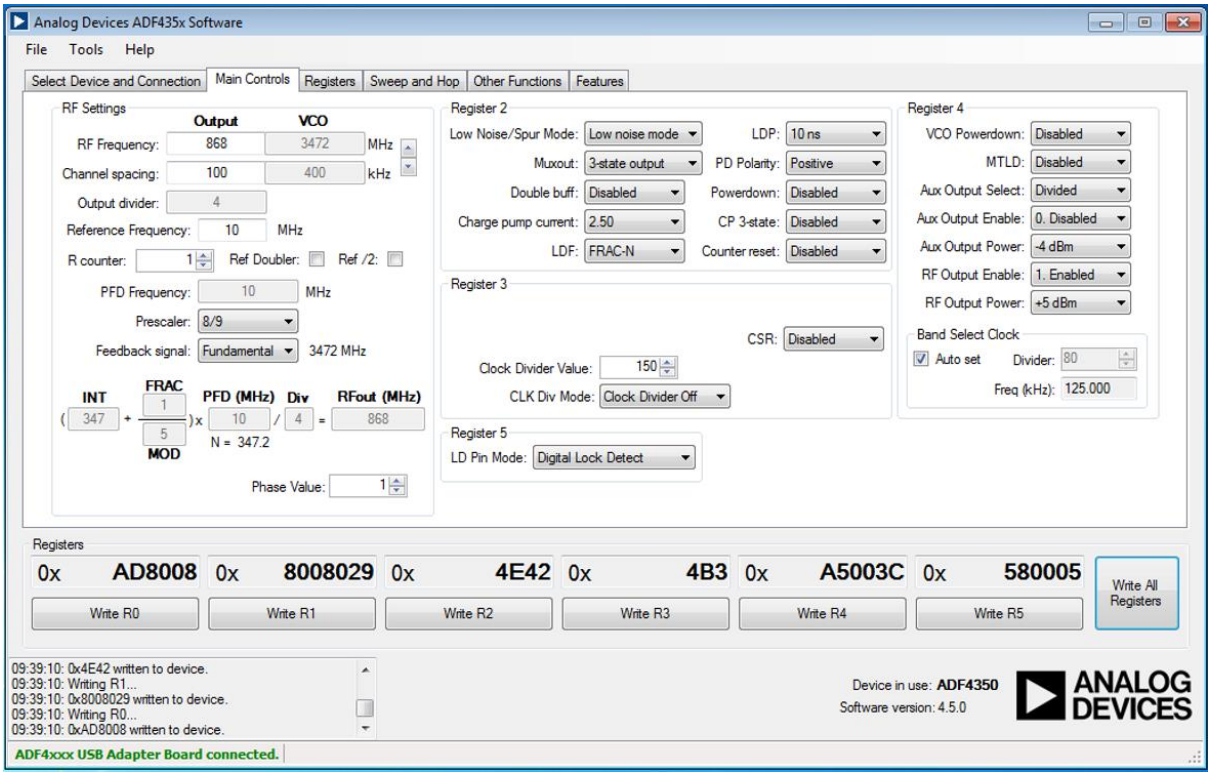

Figure 4.3 Control interface for the ADF4350 frequency interface

The only difference, which must be mentioned here, is the reference frequency of the ADF4350 chip. In the default setting, the frequency synthesis uses the internal 25 MHz crystal oscillator. However, in the new system, a 10 MHz reference signal is transmitted from the central controller. This is required to disconnect the internal oscillator output channel and then connect the input of the phase detector to the reference tone received from the twisted-pair cable.

4.3. System Performance Measurement

There are many challenges involved with the performance measurement of a radio frequency system, especially in a passive communication system. On the one hand, the complex and unpredictable wireless environment directly increases the evaluation difficulty. On the other hand, the reasons, underlying internal circuit problems, are various and usually hidden behind some abnormal results. Therefore, in order to obtain the results that are most close to the actual

values, experimental measurements are often conducted under a specific environment or sometimes are taken with the aid of other auxiliary equipment.

The measurements in this chapter are conducted to determine whether the designed system is compliant with the RFID industry standards. Also, based on the measured results, this new system is compared with other commercial RFID applications to further understand its advantages and limitations. For improving on those limitations, some discussions and suggestions are presented.

4.3.1. Baseband Signals Performance

In this new system, the Indy R2000 chip is employed to process baseband signals. This commercial RFID chip offers limited common mode pins for calibration and verification purposes. The baseband signals used in the forward link are coupled with the output of the digital-to-analog converter (DAC) via the chip headers. Before reaching the DAC, these baseband commands are all digital signals generated by the microcontroller and chip digital core obeying the Class 1 Generation 2 protocol and the ETSI standards. The analog baseband signals from the chip are only for system debug and have little ability to drive the later components. A line driver, therefore, is required after those common mode headers. Since the signals are intended to go through the twisted-pair cable, the differential output of the line driver is expected. In addition, the baseband signals need to add a DC offset of 400 mV to match the input requirement of the quadrature modulator in the subsystem.

In terms of the reverse link, down-converted low-frequency signals are received from the quadrature demodulator via a twisted-pair cable. A buffer block is applied to reject the DC component from the demodulator and pick-up noise from the cable. The filtered analog signal then goes into the chip from the pins used for the external dense reader mode (DRM) filters. Inside the chip, the received signal passes through several gain-controllable amplifiers and band-pass filters, and finally reaches the ADC. All received signals are digitised and then decoded to obtain the tag information. Figure 4.4 shows the block diagram and circuits of the Indy R2000 chip and the details of the baseband block of this new system. The system can operate the desired reader-to-tag modulation scheme and detection mode by pre-setting the related register via the software interface. As only baseband functions are applied to the new system, most of the functions for the chip RF blocks are not utilised.

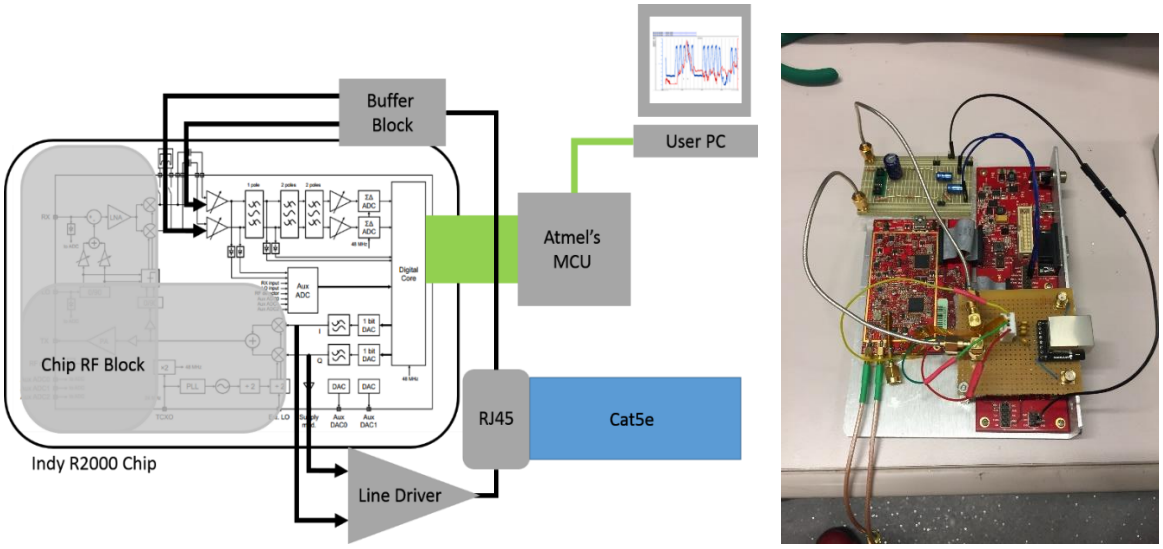

Figure 4.4 Block diagram of the baseband blocks

As the Indy R2000 chip is carefully packaged in a black box, measurements relating to determine the best initialising parameters have to be carried out. It is found that the amplitude of the analog baseband signal varies according to the initialisation of the chip output power. Figure 4.5 shows the peak-to-peak voltage (V_{bpp}) of the baseband signal over the output power setting to the chip. Based on the series of measurements, the average V_{bpp} gradually increases when the chip power setting lies from 0 dBm to 11 dBm, and it is then saturated at higher power settings, staying around 240 mV.

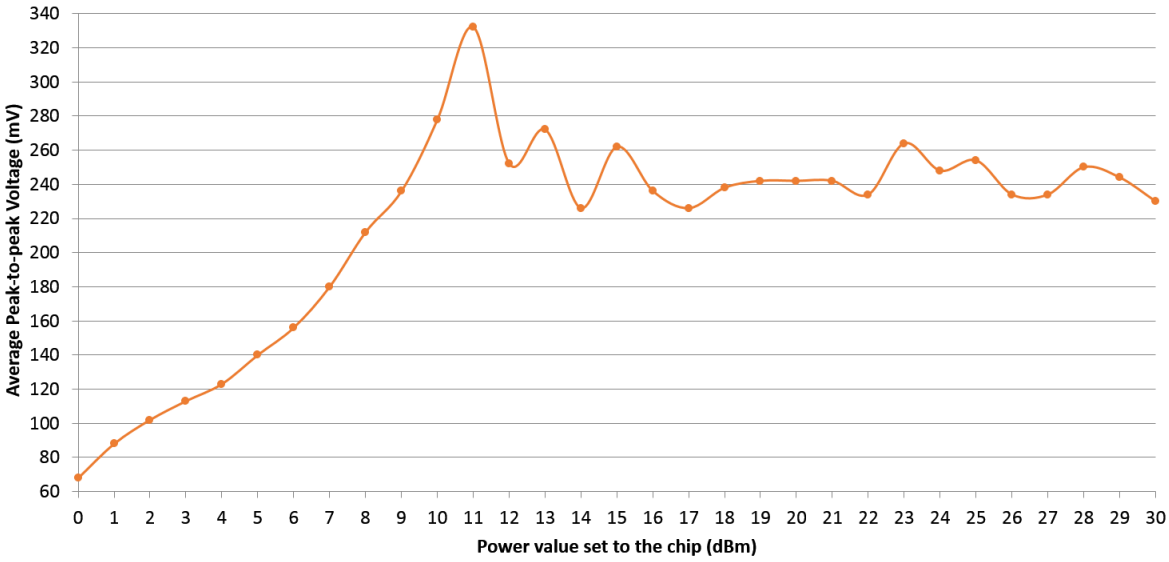

Figure 4.5 Peak-to-peak voltage of the baseband signal over the chip output power setting

Usable radio signals are therefore generated at the output of the modulator if the input signals stay in the range from 100 mV to 700 mV. A differential operational amplifier has therefore

been designed as a line driver to ensure this. The basic structure of the op-amp is shown in Figure 4.6. An AC-coupling method is used at the op-amp input to block unwanted low-frequency components including the DC part from the RFID chip. However, the cut-off frequency of this high-pass filter should be lower than the baseband frequency to successfully transmit the desired commands. Considering changes to the input voltage, the gain of this line driver is around 3 so that the amplified signals remain in the acceptable range. A mid-supply voltage of 0.4V is connected to each noninverting input of two op-amps, and therefore the output signals are biased to match the requirement. The direct advantages of applying the line driver in such configuration are the cancellation of even harmonic distortion products and swing half to achieve the required gain for each op-amp.

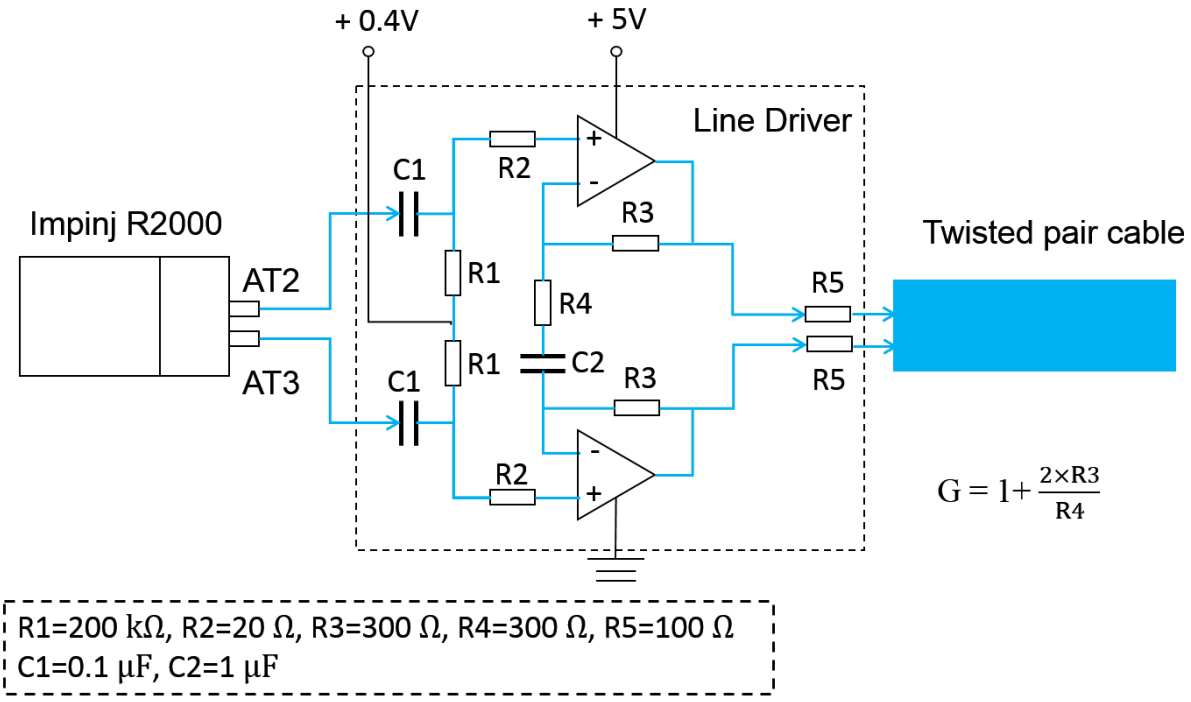

Figure 4.6 Basic structure of the line driver

Segments of the baseband signals before and after the line driver are shown in Figure 4.7 (I). In this measurement, the signal from the chip is shown in blue. The screenshot shows the baseband signal contains reader commands and DC segments, and its signal offset is around 0.83 mV. The signals in yellow are one of the line driver outputs. Their amplitude is set by the gain and the signal offset becomes 400 mV. Based on these results, the filter at the input is correctly applied since the amplified signal has almost no delay, no overshoot (III) and no baseline wandering effects (IV) occur in these DC segments. To determine the balance of the line driver outputs, two channels are measured at the same time (see Figure 4.7 (II)). The two outputs have almost the same amplification gain, and they are well biased to the desired value.

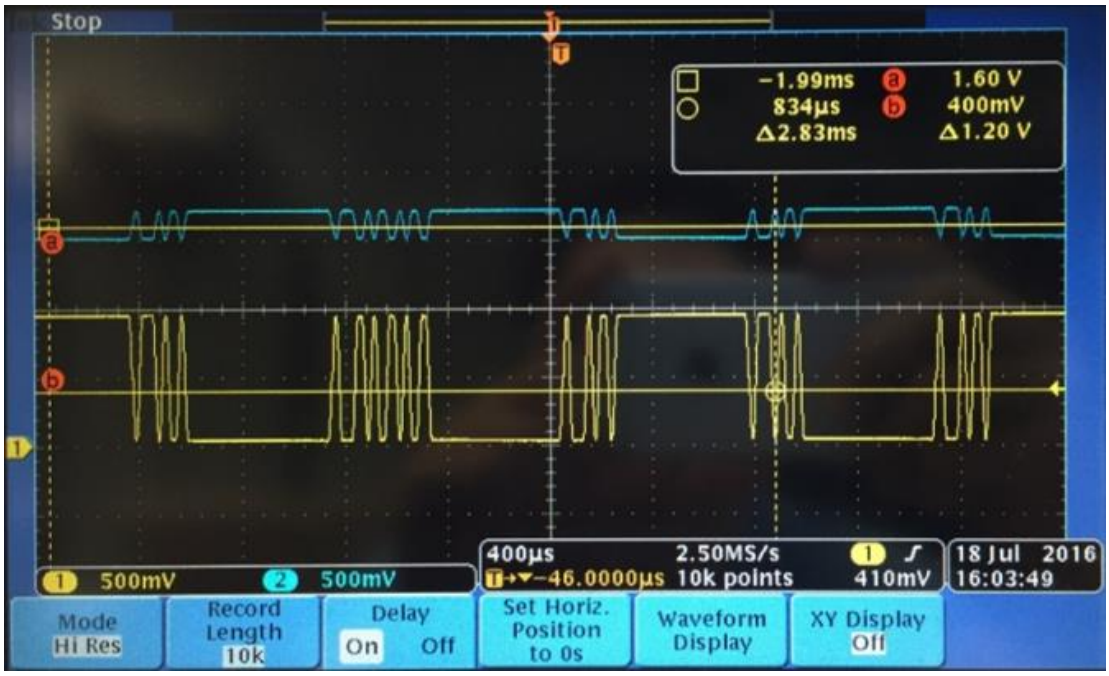
Stop
-1.99ms
834µs
Δ2.83ms
1.60 V
400mV
Δ1.20 V
400µs
2.50MS/s
10k points
410mV
18 Jul 2016
16:03:49
1 500mV
2 500mV
Mode
Hi Res
Record
Length
10k
Delay
On
Off
Set Horiz.
Position
to 0s
Waveform
Display
XY Display
Off

(I)

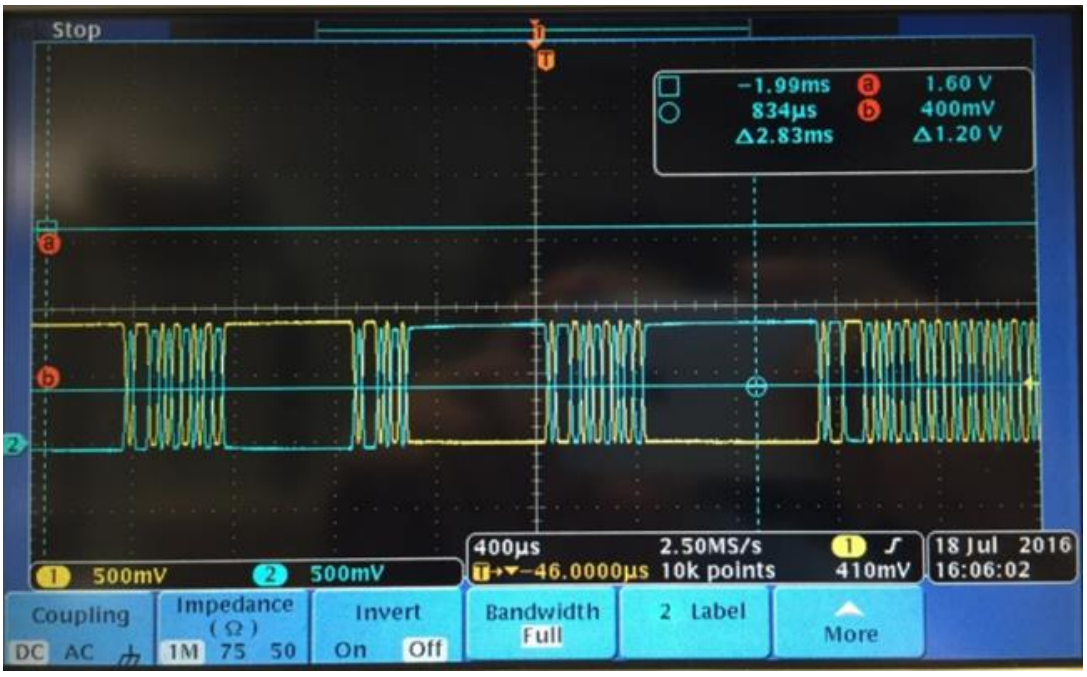
Stop
-1.99ms
834µs
Δ2.83ms
1.60 V
400mV
Δ1.20 V
400µs
2.50MS/s
10k points
410mV
18 Jul 2016
16:06:02
1 500mV
2 500mV
Coupling
DC AC
Impedance
(Ω)
1M 75 50
Invert
On
Off
Bandwidth
Full
2 Label
More

(II)

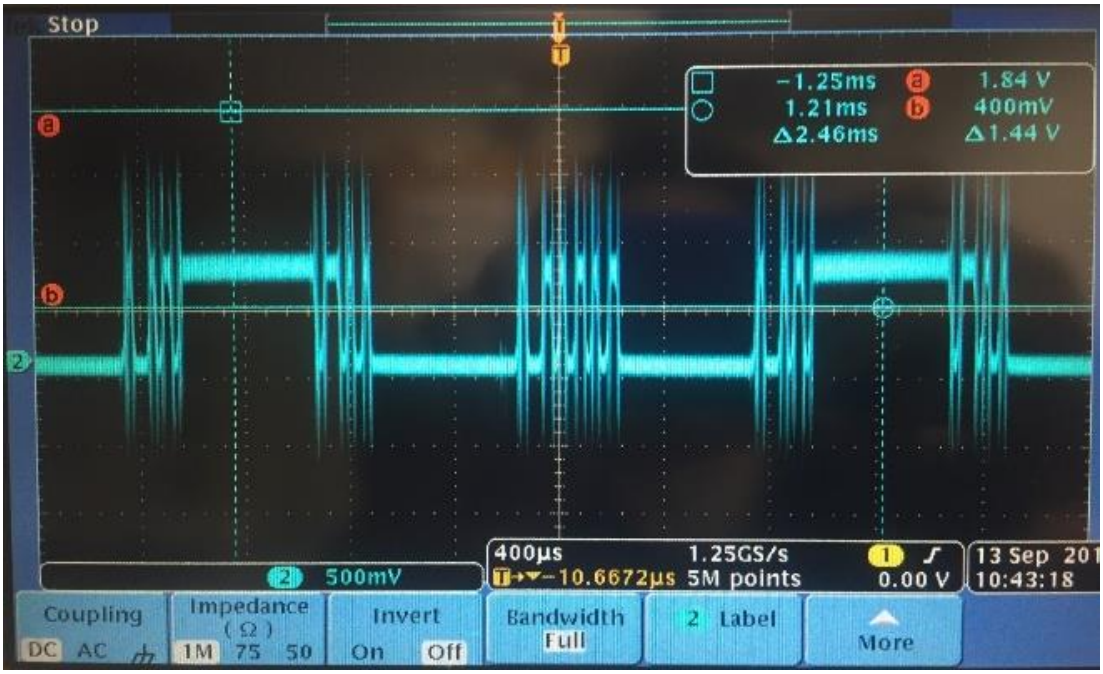

(III)

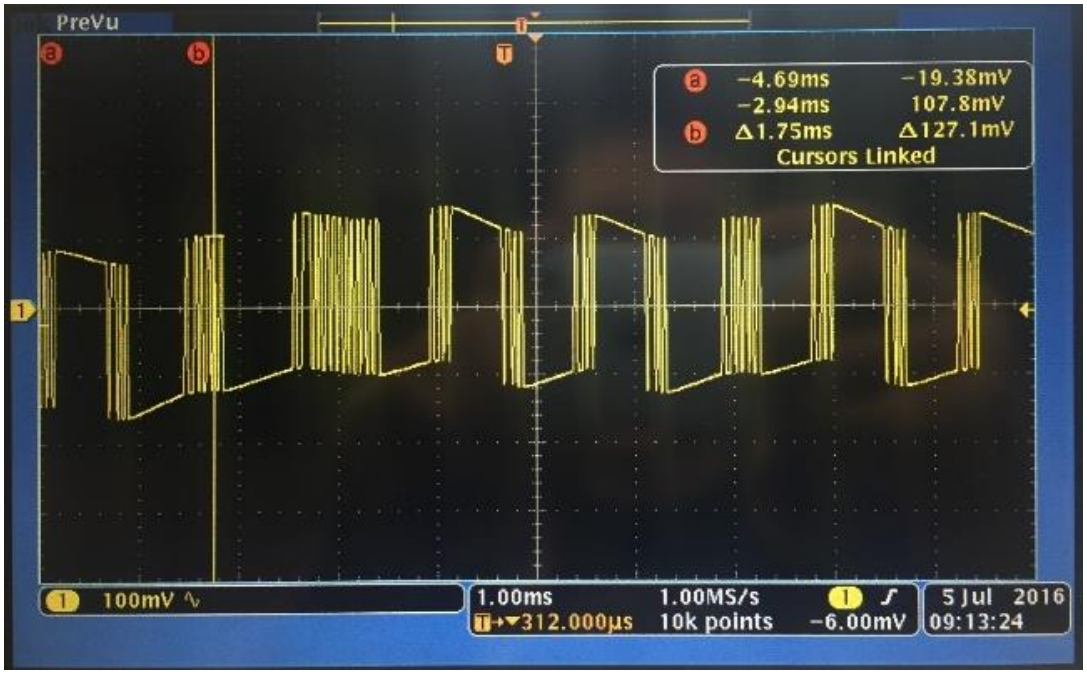

(IV)

Figure 4.7 Baseband signals before and after the line driver

In commercial systems, the internal bus or some other on-board transmission lines are used to achieve the connection between the DAC and modulator. However, in this new system, the transmission media is twisted-pair cable. Unlike the internal transmission, the effects in twisted-pair cable are more significant especially when a long-distance connection is required. Taking cable attenuation as an example, the loss becomes important since the length of the UTP

cable is much longer than the transmission line in the chip. This may reduce the signal power to an improper operation range. Based on the specification of the Indy R2000 chip, the baseband command is transmitted at a frequency of 250 kHz. Since the useful commands of the baseband signal are transmitted among DC segments and different symbol combinations lead to unstable frequency, it is difficult to directly and accurately measure the cable attenuation. Accordingly, a function generator is used to generate a 250 kHz sinusoidal wave with 2 V peak-to-peak voltage, and the attenuation loss of this Cat5e cable can be straightforwardly measured by calculating the amplitude differences between the input and output of the cable.

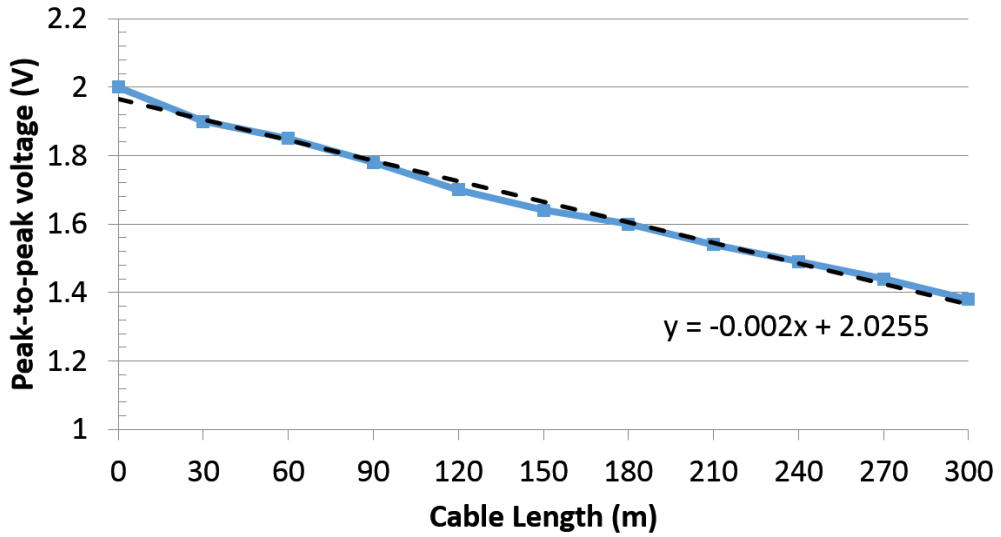

Figure 4.8 Cat5e cable attenuation measurement of 250 kHz baseband signals

Figure 4.8 shows an asymptotic dashed line as generated based on the acquired data. The slope of this asymptotic line can be referred to as the cable loss over cable length ratio, and is approximately equal to 2 mV/m (or 0.011 dB/m). This measured result is similar to the simulated value of 0.013 dB/m based on equation in Table 3.2. In order to maintain the signal power in the correct range, the maximum cable length for the baseband transmitter with an amplifier gain of 3 is around 300 metres. However, the length limit of the current configuration can be simply improved by slightly increasing the gain of the line driver.

Although the amplitude increases with the value set to the chip output power from 0 dBm to 12 dBm, in the new system the voltage stability is more important. In order to allow the baseband signals to stay in the correct range, the value for setting the output power register should be selected from 13 dBm to 30 dBm, where the amplitude of the signal is close to 240 mV. Figure 4.9 clearly shows the changes in the baseband amplitude at different stages. The purple bar

shows the range of the baseband signal that the system can obtain from the chip. The green bar illustrates the amplitude of the signal at the input of the modulator when the gain of the line drive is set to 3. The possible amplitude range is inversely proportional to the twisted-pair cable length. The blue bar shows the typical range that allows the quadrature modulator to operate properly, and the red bar presents the maximum input range for the modulator. Therefore, according to the measurements, the new system can have at least a 300 m wired connection between the central controller and antenna subsystem. This distance is much longer than the limit of the cable length (100 m) for Ethernet communication.

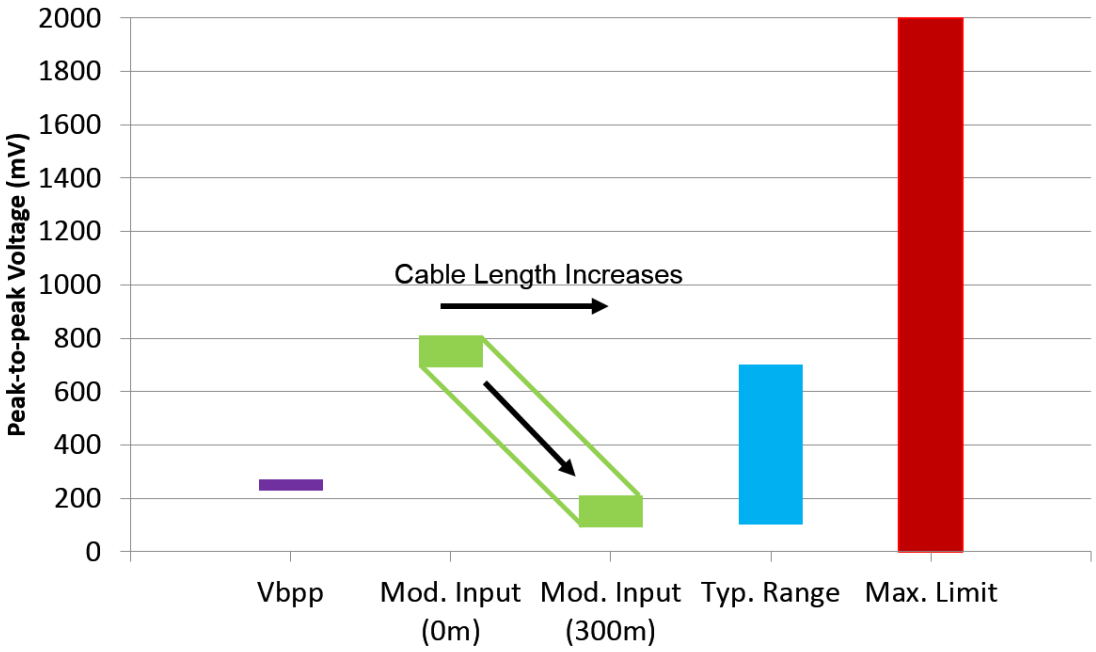

Figure 4.9 Baseband initiation range for proper operation

4.3.2. Transmission Spectrum

Highly reliable system performance requires stable and accurate transmission power and its spectrum width can perfectly suit different operating environments. Since the detection range of the passive RFID system is downlink-limited, transmission power that stays within its limit can offer the maximum coverage. However, in some cases such as a high reflection environment, too large an output power may lead to serious leakage back to the receiver. It is therefore important for the system to have a voltage-controllable RF amplifier.

In this new system, a high-gain amplifier RF5110g is applied because of its good P1dB and operating bandwidth. This RF amplifier also offers a control pin Vapc to adjust its output power

between -10 dBm and +35 dBm. With careful design, low noise and adjustable DC supply from 0.2 V to 2.6 V can be achieved by employing several voltage regulators. The input of this RF amplifier is generated by the quadrature modulator, and this signal normally has few dBm. The gain of this amplifier is normally 32 dB in the operating frequency range, and with the addition of the antenna gain, it is quite easy to exceed the standard power limit. To avoid damage due to accidentally high power, an adjustable attenuator is applied before the RF amplifier. Figure 4.10 shows the test results of the linearity of this RF amplifier at different input powers.

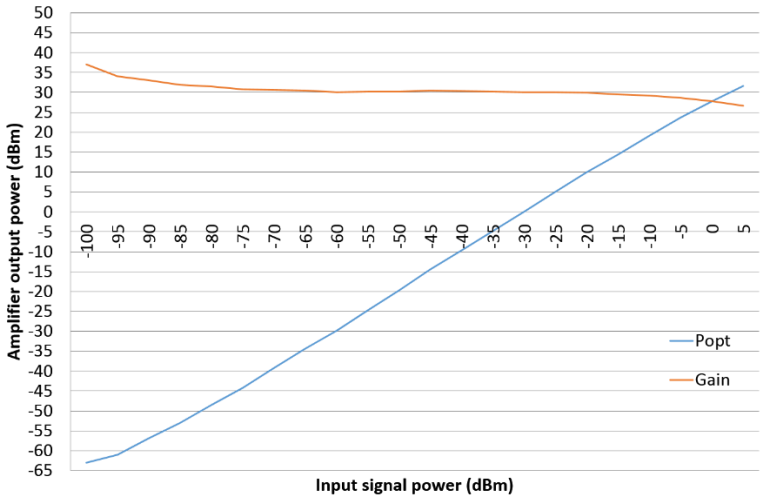

Figure 4.10 Gain linearity of the RF amplifier with different input powers

In this chapter, the measurements also involve the transmission spectrum. The ETSI offers the RFID standards and regulations to specify the requirements in terms of the transmission spectrum in European countries. The operating frequency range is only 3 MHz (from 865 MHz to 868 MHz), and this limited frequency range is divided into 4 channels with 200 kHz channel bandwidths. The transmission power from the antenna should be lower than 2 W (33 dBm), and this is the critical parameter limits the detection range of the passive tag. The regulatory authority also provides a spectrum mask for limiting the signal power in each offset frequency. Figure 4.11 shows the spectral mask based on the ETSI standard. It can be clearly seen that the power in the adjacent channel is required to stay almost 70 dB lower than the power at the carrier frequency (f_c). This restriction attempts to reduce the interference between channels and also provides for the possibility to allow multiple readers to simultaneously operate in the same detection region.

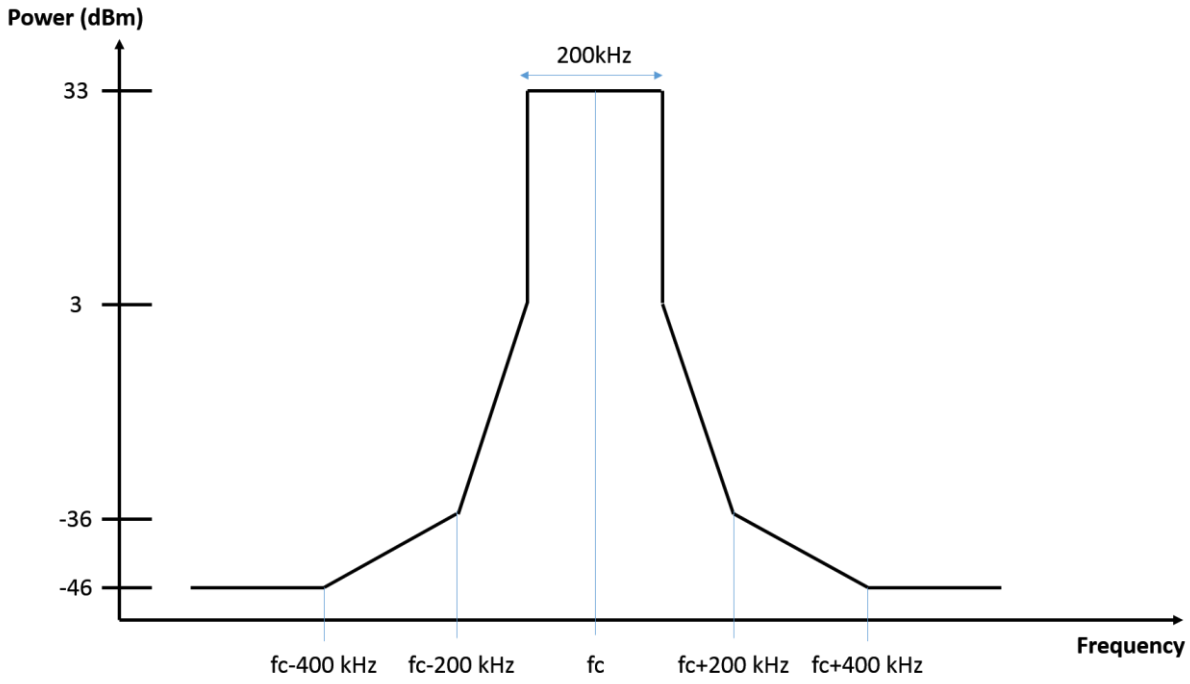

Figure 4.11 Spectral mask based on the ETSI standard

The transmission spectrum of the new system is measured by a handheld spectrum analyser N9344C from Agilent Technologies Company. In order to protect the measuring equipment and RF blocks, around 35 dB attenuation is applied and the result is shown in Figure 4.12.

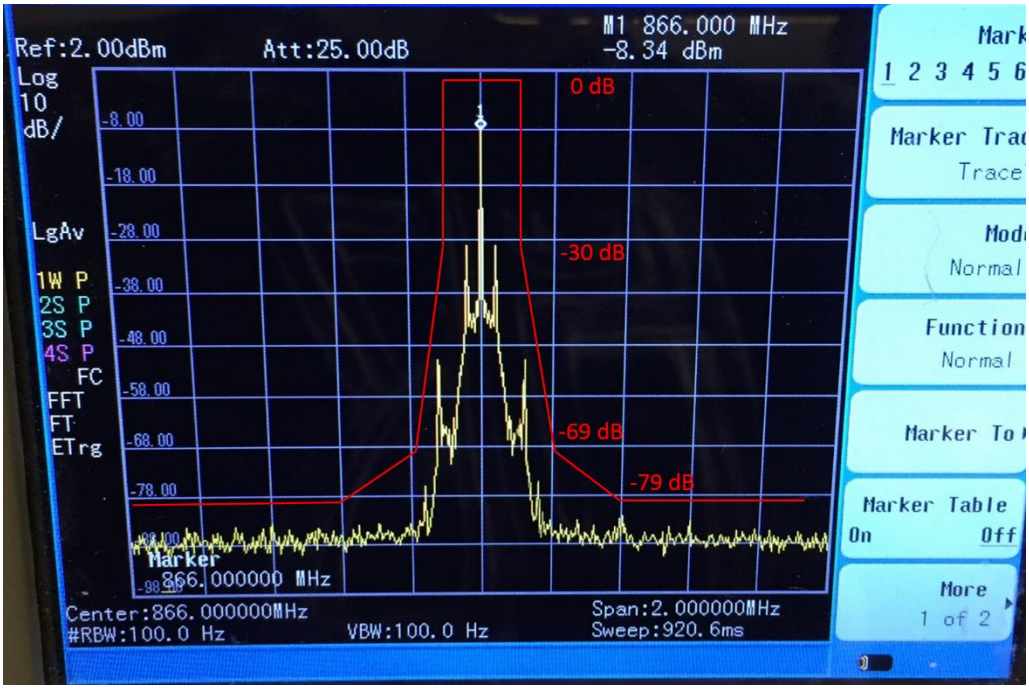

Figure 4.12 New system transmit output spectrum

Based on the measurement, the transmit spectrum of this new system nicely meets the requirements of the spectral mask. The central frequency is 866 MHz and its actual output power is -8.3 + 35 = 26.7 dBm. By adding an antenna with a gain of 6 dBi, the effective radiated power of this new system can achieve 32.7 dBm, which is close to its power limits.

4.3.3. Uplink Sensitivity

The uplink sensitivity of an RFID reader typically indicates its performance in terms of the detection range. A simple method to identify the reader sensitivity is to gradually reduce the transmission power to detect a passive tag within a fixed range and the minimum power to activate the passive tag can be used to estimate the uplink sensitivity of the reader. However, it is only possible to use this method to provide accurate and reliable results in an anechoic chamber. The anechoic chamber offers a broad space and greatly avoids external interferences. During the sensitivity measurement, only the antenna characteristics need to be considered. However, due to high expense and space requirements for using an anechoic chamber, it is difficult in many cases to use this method.

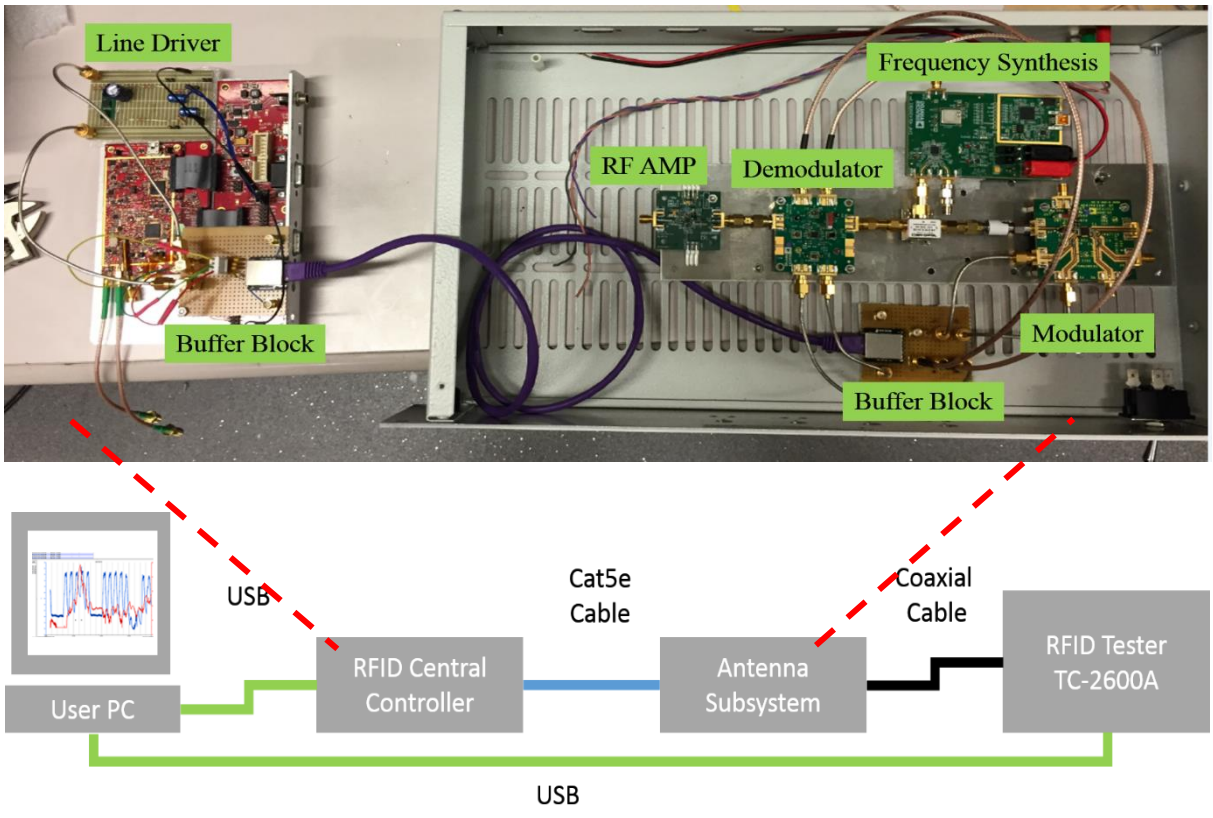

Figure 4.13 Sensitivity measurement setup based on a TC-2600A RFID Tester

A TC-2600A RFID Tester can evaluate the RFID system performance. This tester can emulate a reference tag for measuring the sensitivity of the reader itself. Unlike the previous testing method, only RF cables are required to connect the reader to the RFID Tester for this measurement, and no antenna is used (Figure 4.13). Since in practice the antenna is externally connected and its characteristics are generally given, the real uplink sensitivity of the system with an antenna can also be precisely determined.

Before introducing the approaches applied by this RFID Tester to measure the system sensitivity, it is good to understand the basic communication processes between reader and tags. Figure 4.14 states the typical processes of a successfully detected passive tag based on the link protocol. The Select command at the beginning of the process refers to a minimum delay period since the last command from the reader. If no reply is received, a new inventory round is launched in the Query stage. When the passive tag is activated, it sends a 16-bit random number to the reader. After decoding this number, the reader sends the same 16-bit number (ACK) back to the tag. The passive tag compares the ACK from the reader with its sent RN16. If the two numbers are the same, the tag transmits all the information including a protocol control bit (PC), electronic product code (EPC), and cyclic redundancy check (CRC) to the reader. Following this stage, the query stage repeats and communication with another tag starts.

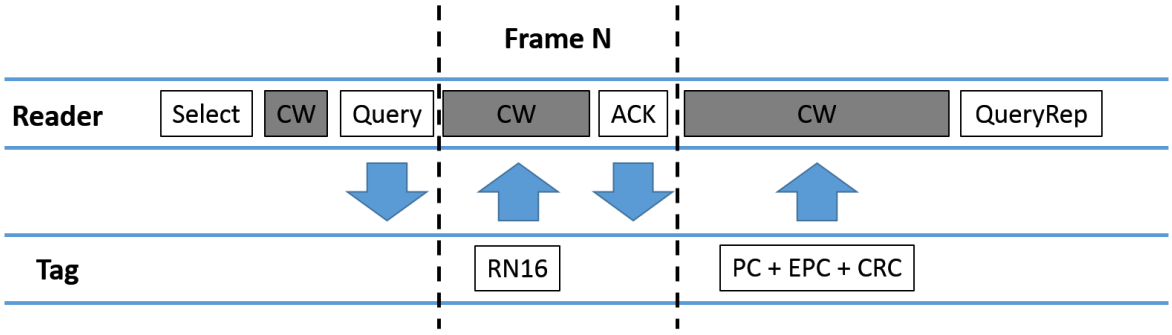

Figure 4.14 Reader sensitivity measurement scheme

In the RFID Tester, the segment of sending an RN16 and receiving an ACK is defined as a frame. When a sufficient number of frames is recorded, the bit error rate (BER) and frame error rate (FER) of the reader can be calculated using the following two equations:

$$\mathrm{BER} = \frac{number\ of\ error\ bits\ of\ RN16\ in\ ACK}{total\ number\ of\ bits\ of\ RN16\ in\ ACK} \tag{4.1}$$

$$\mathrm{FER} = \frac{number\ of\ frame\ with\ error\ bits + number\ of\ frame\ without\ response}{total\ number\ of\ frame} \tag{4.2}$$

According to this communication process, the RFID Tester can calculate the reader's bit error rate (BER) and frame error rate (FER) by comparing its RN16 signal while emulating a tag with an RN16 included in the ACK signal from the reader. After obtaining the BER or FER after a certain number of inventory rounds, the desired sensitivity of the system can then be captured by determining the minimum backscattered power for a desired BER or FER.

Figure 4.15 presents an example of measuring the sensitivity of the Indy R2000 Reader. In this measurement, the threshold of the FER is set to 45 per cent, and the inventory round of each uplink power is 200. According to the result, the FER suddenly increases when the uplink power is lower than -86 dBm. The power value relating to the intersection of the FER and the threshold (purple line) is the tested reader sensitivity, which is around -87 dBm in this example. Compared to the specifications of the R2000 RFID reader, the measured reader sensitivity is very close to the value in the datasheet. As a result, it can be concluded that this sensitivity measurement method is reliable.

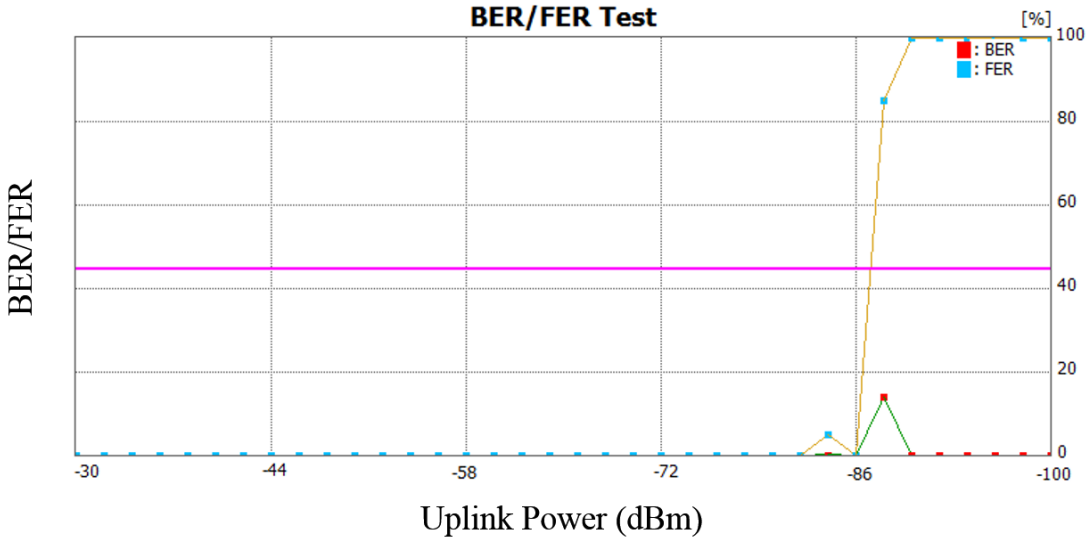

Figure 4.15 Sensitivity measurement of Indy R2000 Reader

By using the same initialisation set in the RFID tester, the sensitivity of the new system over 30 metres Cat5e cable has also been measured. As the RFID tester contains an output power error of ±1 dB when it operates in a tag mode, the average value of a certain number of sensitivity measurements is the most effective way to obtain a reliable result. Figure 4.16 presents the sensitivity measurement when a 30 metre Cat5e cable is used for the controller-subsystem connection. In this example, the maximum allowable FER is set to 45% and the uplink power changing step is set to 1. Based on the results, the reader sensitivity in this test is the uplink power at the intersection point, equal to -94.3 dBm.

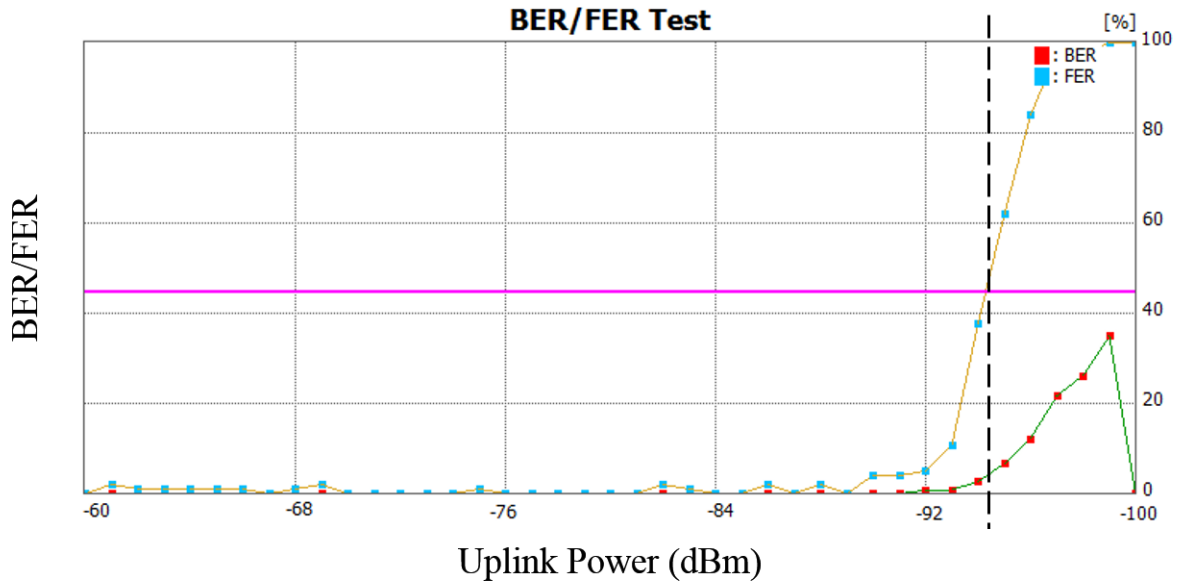

Figure 4.16 Sensitivity measurement of the new reader over 30 m Cat5e cable

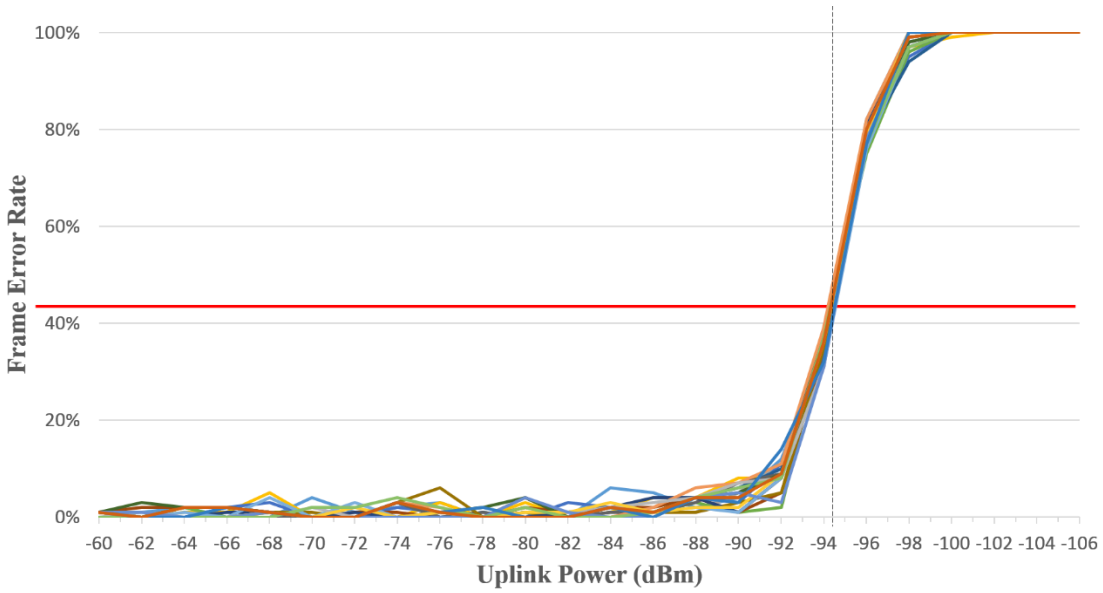

Figure 4.17 Summary of sensitivity measurements in 30 m Cat5e configuration

The results of repeating the above measurements 20 times are summarised in Figure 4.17. Although the intersection points vary in these tests, the fluctuation range is within 1 dB, which is tolerable. The average result of these 20 sensitivity values is -94.5 dBm, which is slightly better than most existing commercial readers. In addition to this merit, this new system already extends the coverage radius by 30 metres from the controller side, which is difficult to achieve using conventional RFID systems. This result shows the feasibility of this new RFID system configuration and also shows that the communication protocol in this system fully meets the RFID standards.

4.3.4. Ethernet Cable Length

It has been determined that this new system can retain high performance in terms of weak tag power detection even when a 30m Cat5e cable is used. However, it is difficult to understand the system limits with only one cable length. As a result, another series of measurements was designed to investigate the system performance when using different cable lengths. Taking into account the results regarding the cable loss of baseband signals, the maximum cable length in these measurements is set to 300 m. Considering that the impact from the cable loss is insignificant in every additional metre, the tests are planned to increase the cable length by 30 metres at a time for the ease of making different observations. In addition, in order to remain the reliability of testing results, the initial parameter and recording method is same as the initialisation in the 30m system case.

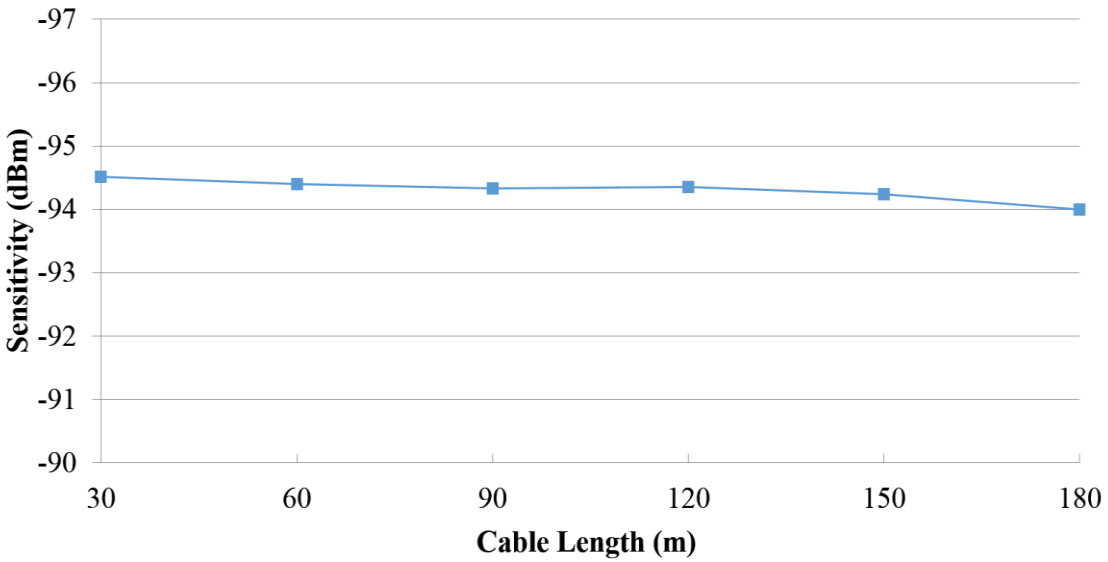

Figure 4.18 System sensitivity of different Cat5e cable length configurations

The data plotted in Figure 4.18 shows the reader sensitivity for different cable lengths. In these tests, Miller-2 PR-ASK modulation is used and a 10 MHz reference signal with a power of 10 dBm is transmitted from the central controller over the Cat5e cable. Due to the maximum input power limits of the RFID Tester, the output power of the antenna subsystem is set to +16.4 dBm at a carrier frequency of 867.4 MHz. The threshold of FER for determining the sensitivity is set at 45%. The system sensitivity for each cable length is measured 20 times, and the average sensitivity value is calculated and plotted in Figure 4.18. It is shown that the best sensitivity is - 94.5 dBm when 30 m Cat5e cable is used to connect the controller and antenna subsystem.

After increasing the length of Cat5e cable to 180 metres, the sensitivity reduces slightly to - 94 dBm. As a result, the system sensitivity is initially independent of cable length up to 180 m.

In addition to the reader sensitivity, one should investigate other performance parameters that may be affected by the long cable length. Taking the propagation delay as an example, there are several time gaps that are emphasised by the RFID protocol to allow the successful tag reading. Serious propagation delay may lead to timeout problems and lower the system detection rate. Among those time gaps, the waiting periods before and after the tag signals such as RN16 and EPC are more critical and fragile. The requirements for these time gaps are based on the baseband parameter setting. In Figure 19, the specific time gaps are pointed out and the system baseband index is also listed.

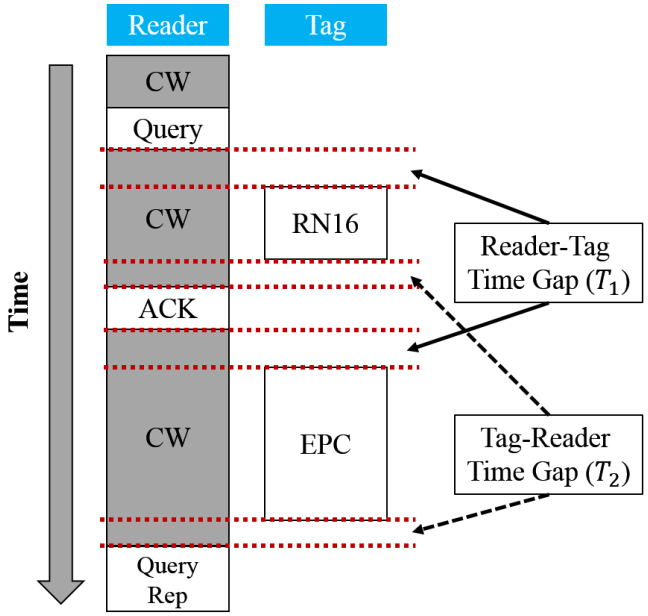

System Baseband Index

Tari (μs)	25
Pulse Width (μs)	12.5
RTcal	62.5
TRcal	85.33
DR	21.33
Tag-Reader Mod.	Miller-4
LF(kHz)	250
Data-rate ($kpbs$)	62.5
T_{pri} (μs)	4

$$\boldsymbol{T_1} = \max(RTcal, 10 \times T_{pri})$$
$$3 \times T_{pri} < \boldsymbol{T_2} < 20 \times T_{pri}$$

Figure 4.19 Link time gaps and system baseband index

When the reader sends a Query, QueryRep or other commands to the tags, the passive tags have to wait a certain time before replying with the 16-bit random number (RN16). This reader-tag time gap, T_1, is set by the larger of the value of RTcal or 10 times the symbol time (T_{pri}). Thus, using the given parameters in the above table, the reader-tag time gap in this new system is equal to the RTcal time (62.5 µs). The other time gap, T_2, is the period over which the reader has to acknowledge the tag information no more than 20 times of T_{pri}. Therefore, the tag-reader time gap should be in the range of 12 µs to 80 µs. The propagation delay of the Cat5e cable can be simply estimated based on the balanced twisted-pair telecommunication cabling and components standards. The worst case of the propagation delay in a 100 m Cat5e cable is

580 ns, and for the 180 m cable connection, the signal delay should be lower than 1 μs. Compared with the limits in those time gaps, the propagation delay is much shorter. Only when the Cat5e cable length reaches a kilometre, do the delay effects become serious.

However, this propagation delay becomes the main limitation for another interesting RFID system configuration, which may have the same long-distance detection capability as the proposed system. Instead of applying the twisted-pair cables, this RFID system directly uses a long USB cable to connect the users' PC to a conventional reader (the bottom configuration in Figure 4.20) so as to extend the system detection range. However, such a configuration is impossible to achieve over a 180 metre connection due to the fact that the delay tolerance of the USB cable is only 26 ns, which is much shorter than the time gaps in the RFID protocol. Even though the total USB length can be extended by cascading USB hubs or assembling active extension cables, the maximum distance still lies within 30 metres due to the specification limits. Therefore, it is more efficient to directly operate the RFID system over Ethernet cable rather than using the techniques such as USB over Ethernet.

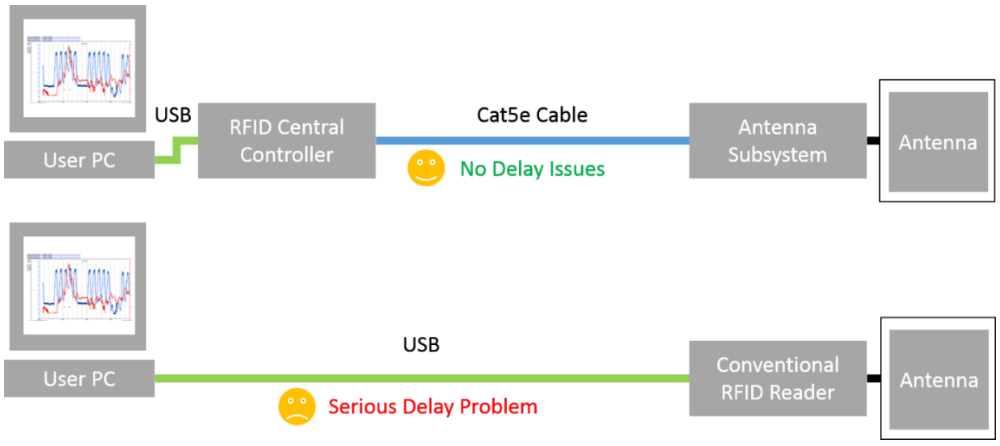

Figure 4.20 Comparison of different long-distance system configurations

Other effects such as pair-to-pair crosstalk and cable insertion loss are negligible according to the results of the sensitivity degradation. However, unlike the propagation delay, the twisted-pair cable length cannot be increased indefinitely. The critical issue, which may cause serious performance degradation, is signal incoherence due to the delay skew problem. Long twisted-pair cable is more likely to make the signals in different pairs arrive at the receiver at different times. If this time difference is significant, it requires extra signal processing techniques such as equalisation to recombine the original baseband signal. The interference immunity of twisted-pair cable is another an important aspect worthy of investigation. This is because in

practice the wireless environment is more complex, and effects such as alien crosstalk may be greater than the inside crosstalk level, which badly affects the baseband communications.

Thus, based on current analysis, for a fixed reader sensitivity such as -90 dBm, the ultimate cable length for the system can reach around 540 m when thermal noise is dominated and baseband cable loss is 0.011 dBm/m. At present, most models and specifications for twisted-pair cables are designed for Ethernet communication. However, communication over these twisted-pair cables relating to the RFID baseband is just past the start-up stage. It is important to move beyond this to achieve a full cyber-physical RFID system.

4.3.5. Practical Tag Detection

The previous measurements are based on the RFID Tester for the purpose of obtaining the actual and reliable system performance. In this subchapter, the practical tests of the proposed RFID system are conducted. Not only can this practical measurement verify the previous results, but also can it practically examine the real detection performance.

A practical demonstration of the detection range of a 300 m Cat5e connected RFID system has been carried out. Two 8.5 dBi circularly polarized antennas are deployed at a height of 1.5 m connected to an antenna subsystem in a bistatic configuration as shown in Figure 4.21 using two 2 m coaxial cables. A UPM Raflatac DogBone tag [116] can be successfully detected at the same height 6 m away from the antennas with a downlink transmission power of 31.9 dBm EIRP. Here the transmission distance is limited by the space available and is not an upper limit, but shows the potential for long-range tag reading over a Cat5e cable over 3 times the limit for standard Ethernet. The setup of this measurement is presented in Figure 21.

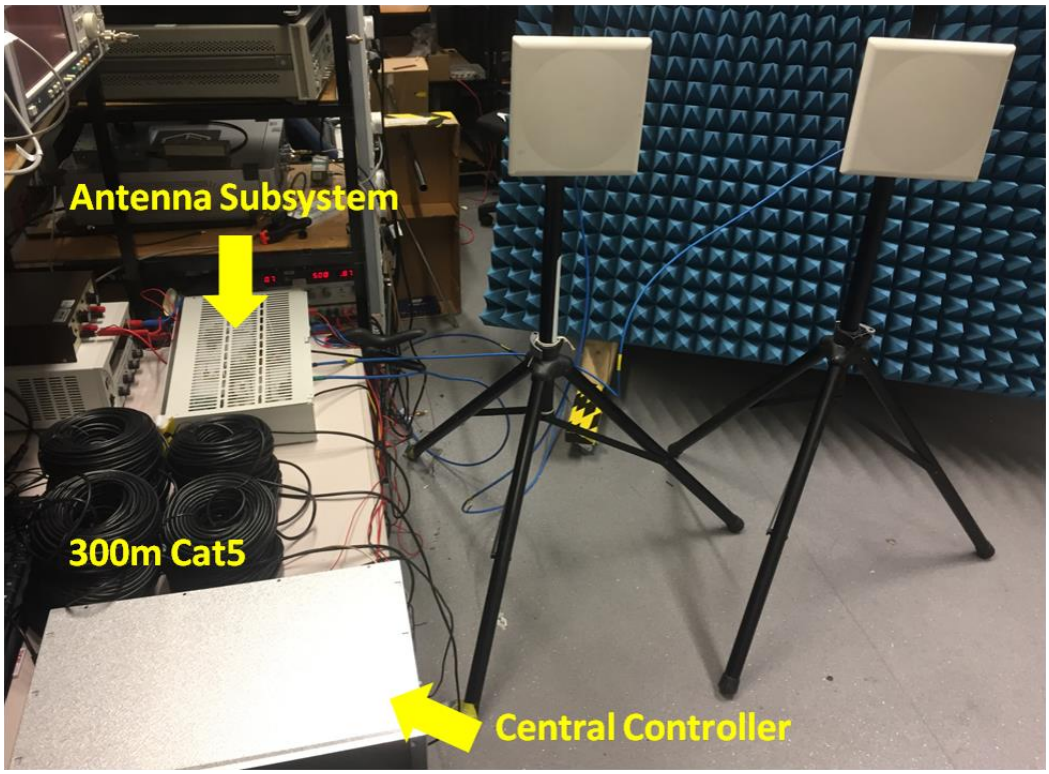

Figure 4.21 Practical tag detection of the new system

Although the practical demonstration is valid, the current system configuration suffers from a serious leakage problem. Since the RFID Tester provides perfect isolation between the transmitter and receiver ports, there was no observable leakage problem in previous measurements. The leakage problem appears at the moment of setting up the locations of two antennas. When the two antennas are placed within 0.3m on the same facing side, the system cannot detect any passive tags even though the passive tag is close to the antenna. After examining the signals at each stage, demodulator saturation, which is caused by leakage, is the dominant problem.

By gradually moving one antenna away from the other, the isolation between the transmitter and receiver increases and then the system starts to read some tags. A Vector Network Analyser (VNA) is applied to measure the Tx-Rx isolation at which the two antennas are placed with proper system operation. The result shows, for the current system configuration, that the receiver requires around 50 dB isolation from the transmitter to achieve the previous excellent system performance. Therefore, it is difficult to employ a monostatic antenna mode in the current system since most circulators or directional couplers cannot directly achieve this high isolation. To solve the leakage problems, a sophisticated leakage suppression block is needed.

4.4. Conclusions and Discussion

In this chapter, the proposed new system is measured in detail. The experimental results show that this new system is able to provide a stable and reliable transmission signal, and its power is high enough to reach the maximum regulatory limit. These excellent results are due to the excellent condition of the baseband communication between the central controller and the antenna subsystem. Through the practical tests, it is found that the uplink sensitivity of the new system is insensitive to the twisted-pair cable length, and it is shown that the reader sensitivity of this new system can achieve - 94.5 dBm over 30 m Cat5e cable, and its sensitivity remains at around - 94 dBm with 180 m Cat5e. With further investigation, the cable insertion loss, crosstalk and delay effects are also insignificant in this new configuration. This feature reveals the advantage of this proposed system configuration when compared to a USB-extended RFID system. To verify the obtained results based on the RFID Tester, a practical demonstration has been conducted. The passive tags can be successfully detected over a 6 m wireless range following 300 m of twisted-pair cable between the central controller and antenna.

This new system configuration provides high performance for long distance passive RFID applications and also reveals massive benefits for multi-antenna RFID systems. Despite its lower cable cost and high deployment flexibility, the conventional RFID reader circuit can also be simplified by sharing the digital and control blocks and communicating with remote subsystems by simply splitting and combining the desired baseband signals. However, the synchronization of the controller-subsystems communication and cable immunity may be the challenges, which require further investigation. Real tag detection also reveals the limitation of the isolation between transmitter and receiver. Therefore, a sophisticated leakage suppression is needed to achieve the full potential of this system.

Chapter 5

5. Automatic Passive Tag Detection RFID System for Long-Range Applications with Leakage Suppression

5.1. Introduction

The RFID industry has experienced fast growth in recent years and there is an urgent growing need for wide-area tracking and monitoring. The use of a distributed antenna system (DAS) greatly improves coverage compared to that of a single RFID reader. By adding frequency and phase hopping, nulls can be removed within the desired range to improve read accuracy [42]. Although the DAS configuration greatly enhances the tag received power in the worst case, it cannot avoid the leakage problems. Since RFID transmission and reception operates at the same frequency and same time, a strong transmission signal from multiple antennas is not only received by the passive tags but also by the reader receiver. The high-power transmission signal, which leaks into the receiver chain, can directly degrade the system performance. In a conventional reader, leakage problems are usually caused by limited isolation between the transmitter and receiver. In a multi-antenna RFID system, this problem becomes serious and complex due to the increasing number of leakage sources. A leakage suppression block is therefore a useful tool commonly applied in a full-duplex system to eliminate the impact of leakage. This is the focus of the research reported in this chapter.

In the following subchapters, the typical leakage types and their impacts are firstly described. After that, a brief survey of leakage suppression methods and related optimization algorithms is introduced. Following that, a design of a leakage suppression block for a passive UHF RFID system is demonstrated. The experimental comparisons between this designed system and an existing commercial system are then presented before the conclusion.

5.2. Leakage Types and Impacts

There are two antenna configurations for separating transmit and receive paths in a passive RFID system: monostatic and bistatic (Figure 5.1). The former configuration only uses one antenna for transmission and reception, since a circulator [67] or directional coupler [68] can be used to separate the reader and tag signals. In this system, the receiver may suffer from leakage problems due to imperfect isolation and a mismatch in antenna impedance. The latter

configuration can be used to alleviate the leakage problems, by using two antennas – one to transmit reader commands, and the other to receive tag signals. In this configuration, the main source of the leakage is crosstalk between the two antennas. Although a bistatic system offers better performance in terms of leakage effects, its higher cost, additional size, and lower design flexibility are accompanying issues that cannot be avoided. Reflection, which is caused by the surrounding objects, structural barriers or moving tags, is another main cause of leakage. Interference from other RF applications with close operation frequencies may also lead to serious leakage problems. For example, the receiver antenna has a large probability of capturing the transmission signals from other operating RFID readers.

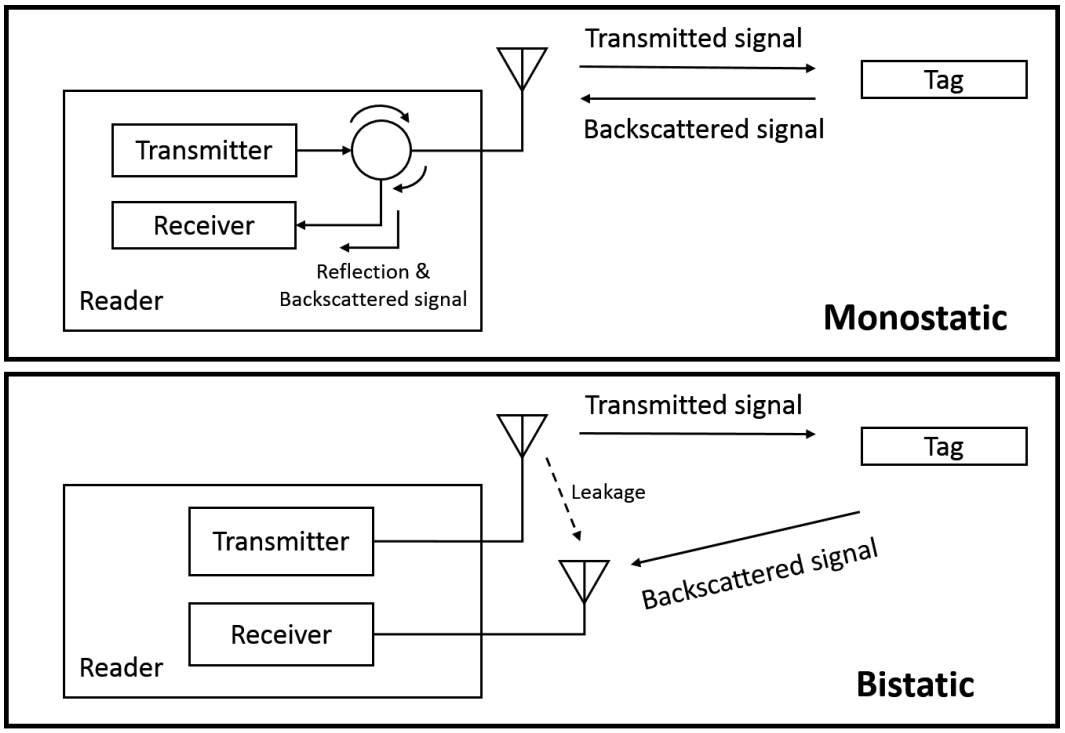

Figure 5.1 Monostatic and bistatic antenna configurations

Leakage can easily cause saturation problems, particularly as the radiation energy of the transmission signals tends to be set to the allowable maximum power (2 W ERP in Europe and 4 W ERP in the US). These strong signals may leak into the receiver and saturate or even sometimes destroy the components such as the LNA and mixer in the uplink. Saturated RF components generate nonlinear signals, which seriously affect the desired signal quality and uplink sensitivity. To avoid this saturation problem, a high dynamic range is required in both RF and baseband blocks.

The difficulty of symbol recognition or recombination is another leakage-caused problem. If the RF block continues to work, the strong leakage signal is down-converted to the baseband. As the leakage signal has the same frequency as the backscattering signals, DC-offset and unwanted noise is produced in the low-frequency stages. Owing to the complex electromagnetic environment, the leakage power may continuously vary and leads to random changes in DC-offset. This uncertain fluctuation brings considerable challenges to analog-to-digital converters.

Besides the leakage effect, the tag signal is also very easily corrupted by the phase noise associated with the local oscillator (LO), since the tag information is typically at frequencies very close to the operating frequency (less than a few hundred kilohertz from the central frequency). Leakage brings the LO phase noise to the reverse signal chain and results in a worse baseband signal SNR. In such circumstances, the system suffers high sensitivity degradation and it is impossible to fully detect weak signals until the phase noise is effectively removed.

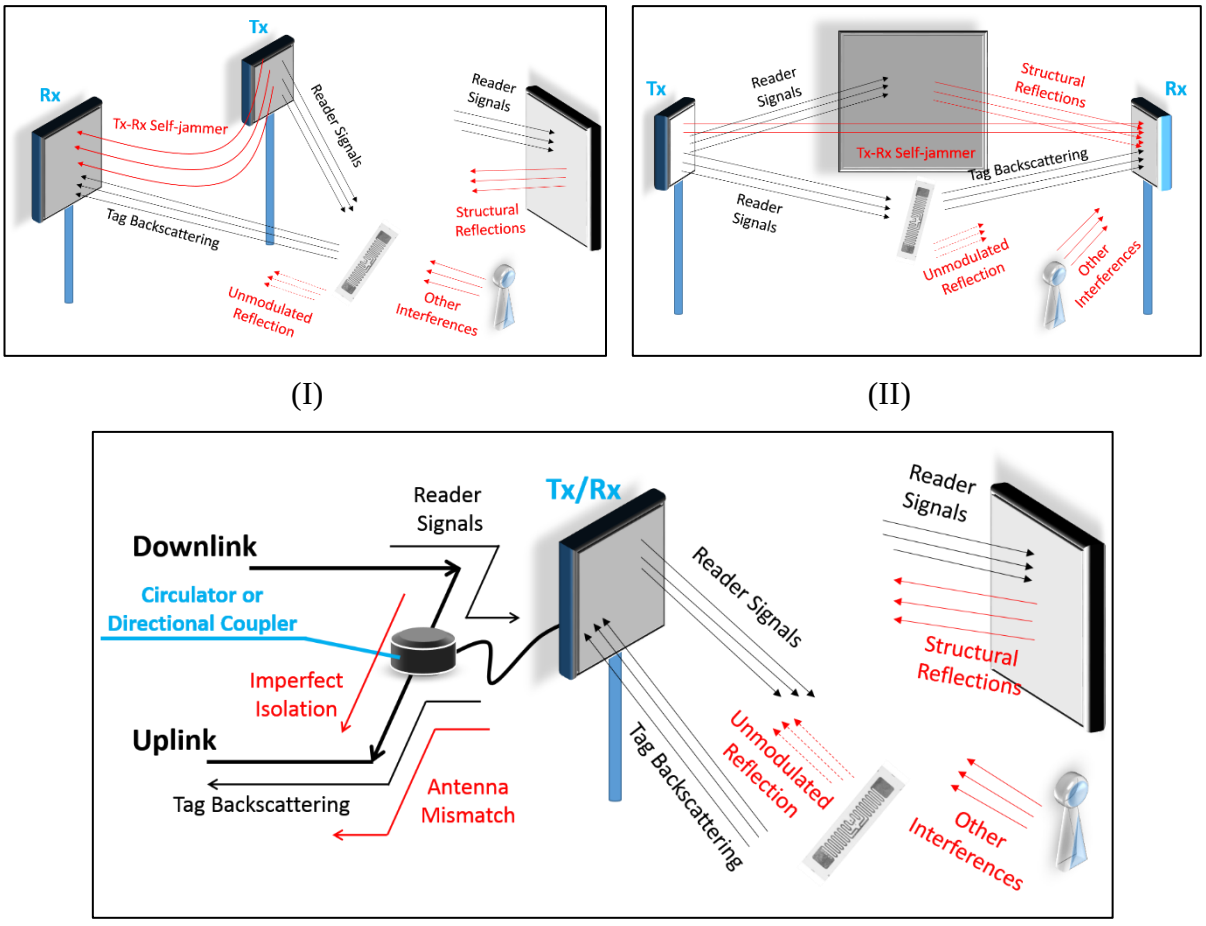

Figure 5.2 Leakage sources of different antenna configurations

All the leakage sources mentioned above in both monostatic and bistatic configurations are summarised in Figure 5.2. The unwanted signals are all highlighted in red and have to be removed so as to ensure highly-reliable operation of the system.

5.3. Leakage Suppression Methods

In the past, leakage suppression methods have been developed to improve full-duplex wireless communication systems, such as those in radar, mobile or telephone systems. RFID systems also require a leakage suppression block to enhance their sensitivity and reliability. In order to provide a low-cost and low-complexity RFID reader, mostly current commercial products adopt a direct convert receiver (DCR) configuration. Examples such as the AS399x family [138] and the R1000/R2000 family [116] have adopted the use of DCR. However, systems using such a configuration are likely to experience the unwanted effects of self-jamming. Thus, the AS399x family and R1000/R2000 family add a leakage cancellation block inside their chipset. Another popular commercial off-the-shelf product, known as software defined radio (SDR), is also widely employed to build RFID systems due to its low cost, high design flexibility, and ease of updating the system. A number of SDR applications have been devoted to RFID research since it provides easy accessibility to set system parameters, which are difficult to obtain from existing commercial readers but are very valuable for RFID protocol exploration and system measurement. However, these SDR-based RFID systems, typically do not provide a leakage suppression block. It is therefore highly desirable to build an explicit leakage canceller within the reader to improve its sensitivity and performance.

5.3.1. Basic Methods

An RFID system with a bistatic antenna configuration usually has better isolation between the transmitter and receiver than those with a monostatic configuration. This is because the isolation can be quickly improved by deploying the two specific radiation pattern antennas in the proper positions. For instance, the isolation can be around 30-40 dB when the two antennas are deployed at the same height with around a 1-metre gap [125]. However, this configuration is costly and bulky and thus it is still unpopular in RFID system design. In a monostatic RFID system, a single antenna can achieve both transmission and reception with the help of directional coupler or circulator. This system configuration saves space and reduces the cost of the system but can suffer serious leakage due to the limited isolation of the coupler and circulator. Thus, trade-offs have to be made depending on the requirements of the RFID system. If space is allowed and low-cost hardware is desired, the bistatic configuration is the better

choice to meet the required isolation. When the system must provide ease of portability and installation, a monostatic configuration with an additional leakage suppression block is an ideal option.

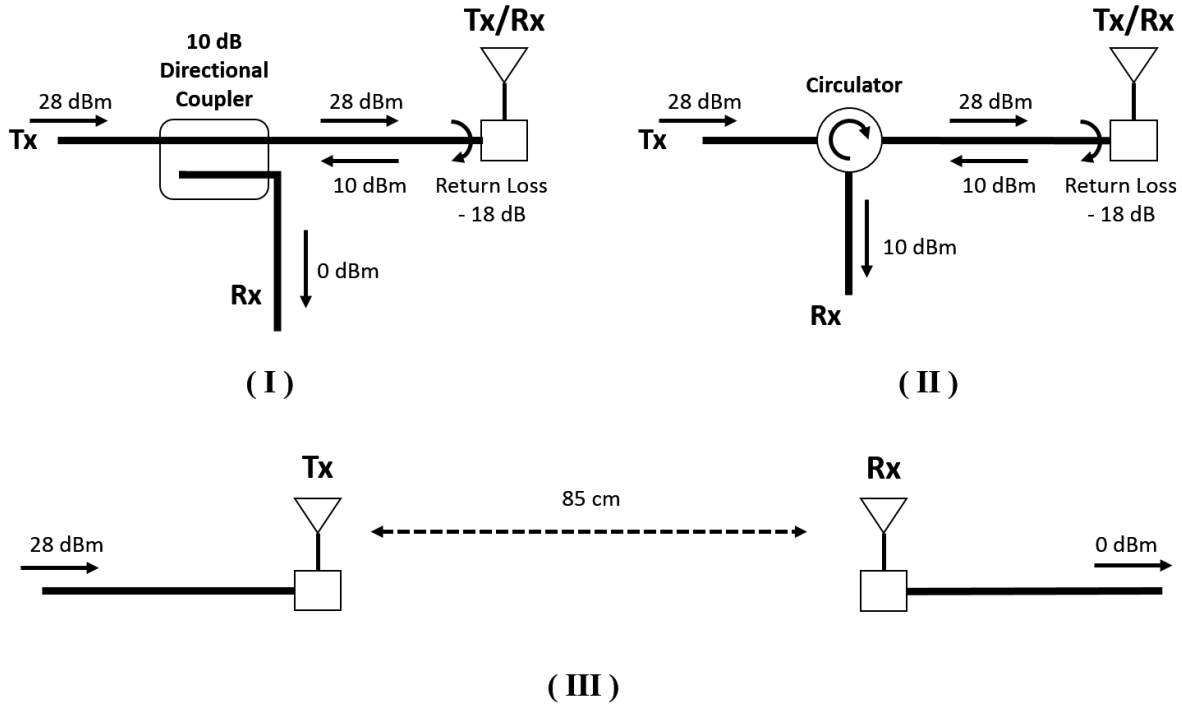

Figure 5.3 Examples of basic leakage suppression methods

Three typical examples of leakage in the circuit are presented in Figure 5.3. In the first example, a 10-dB directional coupler is applied. When the reader transmits CW signals with a power of 28 dBm, a 0-dBm (1mW) leakage is produced. In the second example, a 10-dBm self-jammer exists in the receiver chain when a circulator is employed. The leakage level in these two examples is much stronger than the backscattered tag signals. The limited isolation of the directional coupler or circulator is the main problem of the basic leakage suppression methods [139]. The bistatic case provides slightly better isolation of 28 dB when two antennas are deployed at a distance of 85 cm. This result can be better when the distance is increased, but this also results in a reduction of tag power. Thus, the basic leakage suppression methods are insufficient to handle the leakage problems.

5.3.2. Phase and Gain Control Method

Based on the above illustration and discussion, a passive RFID reader without an adaptive leakage canceller has to feature high dynamic range capabilities to address the impact of incoming leakage. Moreover, the phase noise of the LO can also leak into the uplink and

degrade the system sensitivity. To effectively handle self-jamming problems, many commercial reader systems employ a leakage canceller before the LNA and mixer using the phase and gain control method. This method is widely used since it intuitively shows how the leakage component is cancelled. The core principle of this approach is to generate a signal, which has an anti-phase but the same amplitude as the leakage signal, and add it to the received backscattered signal so as to remove the transmission leakage. Typically, the phase and gain control method is achieved by using components such as coupler, vector modulator, power detector, and microcontroller. A block diagram of a conventional canceller is shown in Figure 5.4.

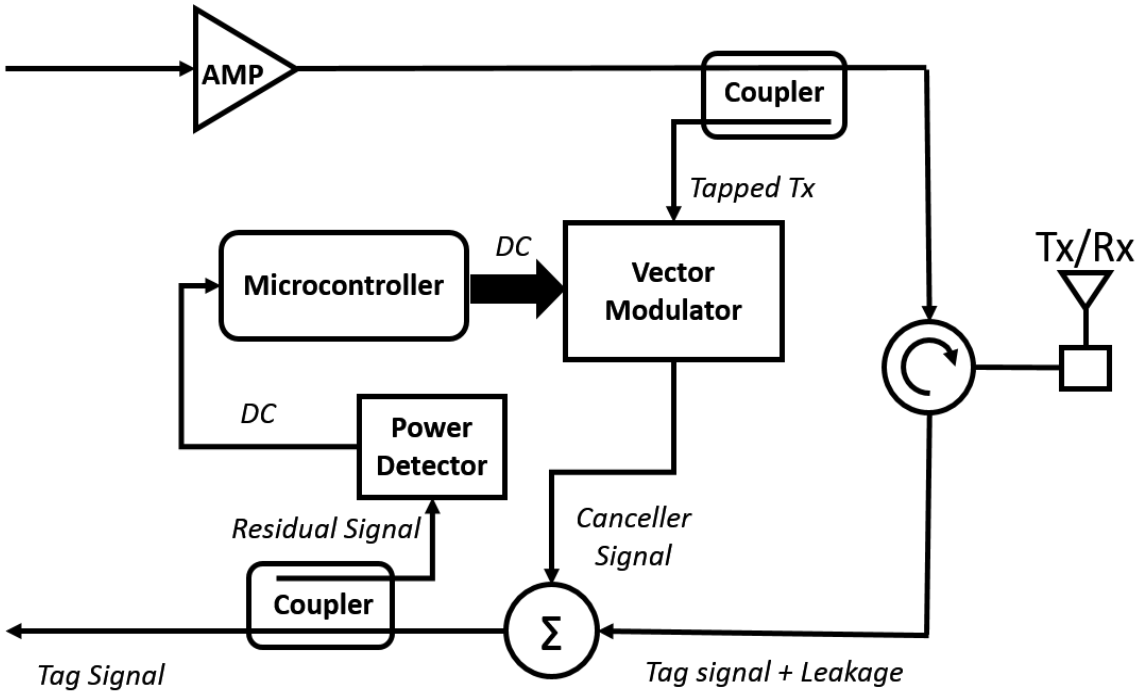

Figure 5.4 Block Diagram of phase and gain control leakage canceller [140]

In this approach, a sample of the transmission signal is tapped after the RF amplifier, and the signal is modified in the vector modulator. With help of the microcontroller, the desired cancellation signal is added to the receiving signal. The sum result of the two signals is regarded as the residual signal. The remaining leakage level can be simply detected by a power detector since the leakage level is much higher than the power of the tag signal. The residual leakage level can be represented as a voltage value, and is recorded by a microcontroller. The search algorithm in the microcontroller helps the canceller to find the optimal control for the vector modulator.

Inside the vector modulator, the tapped transmission signal is split into in-phase (I) and quadrature (Q) channels. The control signals from the microcontroller tune the gain of the amplifier in the I and Q channels, respectively. The canceller signal is the vector summation of the I and Q signals (See Figure 5.5(I)). By carefully controlling the amplitude of the I and Q signals, the magnitude and phase of the canceller signal are set as desired. Figure 5.5(II) presents an example of the vector gain representation.

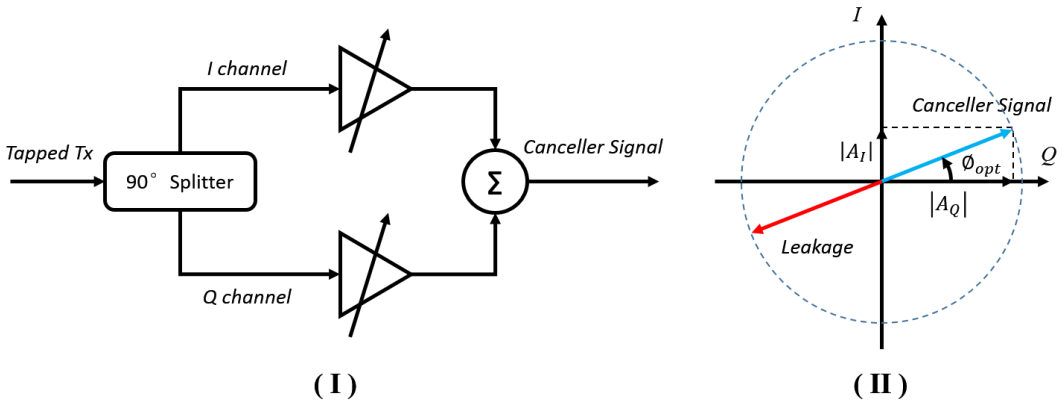

Figure 5.5 Principle of the phase and gain control methods [140]

The phase and gain control method is widely used since it is the most straightforward way to cancel the incoming leakage. The developer is able to observe the cancelling effect at each stage and set specific optimum settings. This method is superior to others in its versatility since it can eliminate the carrier power but also can cancel the intrinsic amplitude and phase noise from the reader. However, this method requires some RF components to control the gain and phase, and these components are relatively expensive. Moreover, the power consumption of the reader transceiver also becomes higher. To further understand this method, some excellent studies, and applications relating to this method can be found in [141], [142], [143], and [144].

5.3.3. Tunable Load Method

The tunable load method uses a directional coupler (Figure 5.6), where the TX signal coupled port (Port 3) is connected to a variable load. In general, the impedance of the load in each port of the directional coupler should be well matched to avoid signal reflection and attenuation. However, in this leakage cancelling method, leakage can then be largely eliminated by controlling the load impedance to reflect the specific phase and magnitude of the coupled signal to the receiver chain (port 4).

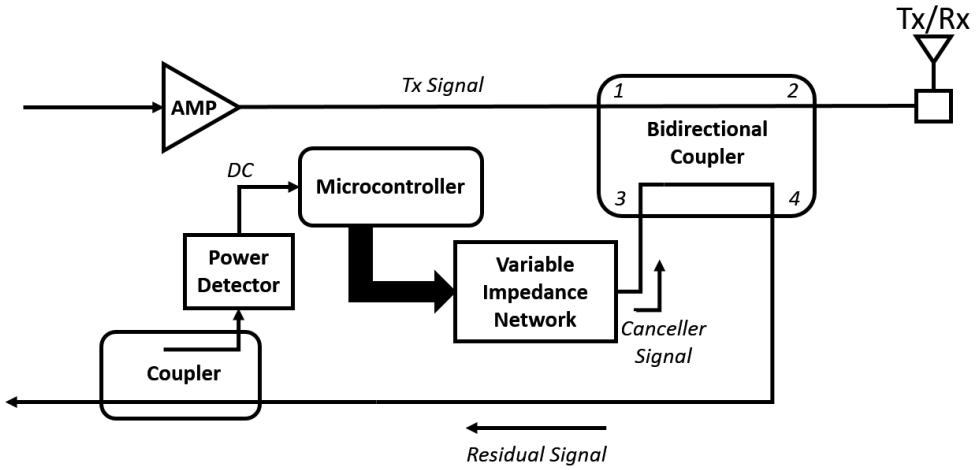

Figure 5.6 Block Diagram of the leakage canceller using the tunable load method

In the bidirectional coupler, assuming it is in the perfect condition, the transmission coefficients are equal in each port, and

$$S_{21} = S_{12} = S_{34} = S_{43} \tag{5.1}$$

In terms of the signal coupling,

$$S_{31} = S_{42} \tag{5.2}$$

Perfect isolation also leads to

$$S_{41} = S_{32} = 0 \tag{5.3}$$

Therefore the residual signal in the receiver chain can be expressed as

$$S_{res} = \mathrm{G}_1(S_{42}) + G_2(S_{21}\Gamma_a S_{42} + S_{31}\Gamma_L S_{43}) \tag{5.4}$$

where G_1 and G_2 are the amplitude coefficients, and Γ_a and Γ_L are the reflection coefficients of the antenna and tunable load, respectively. In order to obtain the desired tag signal, the return loss at the antenna should be symmetrical to the return loss at the variable impedance network, and $\Gamma_a = -\Gamma_L$. Based on Equation 5.1 and 5.2, the residual signal can be simplified to

$$S_{res} = \mathrm{G}_1(S_{42}) \tag{5.5}$$

where S_{42} represents the desired tag signal. The algorithm in the microcontroller aims to find the optimal value to allow the symmetrical return loss assumption to be tenable.

Compared to the phase and gain control method, the circuit needed to achieve this leakage cancelling approach is cheaper, composed only of low-cost PIN diodes, resistors, and capacitors. However, this variable-load method also has disadvantages. The impedance of the load may need to be recalibrated for different antenna impedances and cable lengths. In addition, many receivers using this method are only effective in counteracting on-board reflection, and other leakage sources such as environmental reflections and LO phase noise may be difficult

to remove. Furthermore, it is difficult to determine an efficient tunable method for good coverage, and therefore the scan time is hard to predict. Studies that use this method for cancelling the leakage signals include [145], [146], [129] and [147].

5.3.4. Other Leakage Cancelling Methods

Besides the above two common methods, there are also some other good methods to remove leakage signals. In [114], an RC high pass filter is used to eliminate the leakage component in the baseband. The shortcomings of this method are limited leakage suppression and long calibration time. Another effective leakage suppression method is demonstrated in [148]. This approach uses a passive mixer to reflect the leaking power. However, the settling time and its practical performance when used in an RFID system are not described. In addition to these two methods, a novel leakage suppression technique is proposed in [149] for an RFID receiver. This paper uses a dead-zone amplifier to enhance the envelope of the received signals (tag information) while suppressing the leakage. However, a reader receiver based on this method still may suffer from the saturation problem. Other interesting leakage cancelling methods for RFID systems can be found in [111], [150], [108] and [34].

5.4. Adaptive Leakage Cancellation Algorithms

Passive or static leakage cancellation blocks are ineffective for eliminating self-interference since they usually set optimal parameters beforehand or require manual adjustment for different system configurations. In practice, their operation is complicated due to the continual change of leakage level. For example, the strength of the leakage varies when performance-enhancment techniques such as frequency hopping are used. Different operational frequencies result in different leakage levels, even though the system configurations and environment are the same. If environmental factors are taken into consideration, the case becomes even worse. For instance, reflective leakage components may suddenly increase if some obstacles move close to the antenna. Due to these problems, adaptive algorithms for leakage cancellation blocks are needed. The algorithms are expected to help the canceller to quickly find the optimal settings and also keep monitoring the residual leakage to determine the canceller performance. In order to avoid degradation of the reader-tag communications and also achieve the desired isolation requirement, the canceller updating period should be as short as possible.

5.4.1. Full Search Algorithm

The most straightforward way to find the best settings for the leakage canceller is the full search algorithm. In this algorithm, all the possible combinations of the selectable parameters are

tested. The best result is the one that allows the system to obtain the minimum residual leakage in the reverse signal chain. When the scanning step of the control parameters is one, the total number of tests is equal to the number of possible combinations. For example, a leakage canceller using the phase and gain control method must have N and M settings for the phase and gain respectively. Then the total number of measurements are N × M.

This algorithm is extremely time-consuming. Both the periods for parameter initialization (Ti) and residual leakage measurement (Ts) have to be considered. Accordingly, scanning all the combinations requires an overall time of (Ti + Ts) × N × M. This low efficiency search algorithm may also sometimes lead to serious problems. Taking the frequency hopping technique as an example, if the time for overall measurement is longer than the minimum frequency hopping time, it is impossible to reach the optimal status. Therefore, some improved search algorithms have been developed to reduce the process time. Among those improved algorithms, a popular one which is applied in many commercial RFID readers and chips uses hierarchical grid partitioning to find the best point. Figure 5.7 shows a typical example using this efficient algorithm.

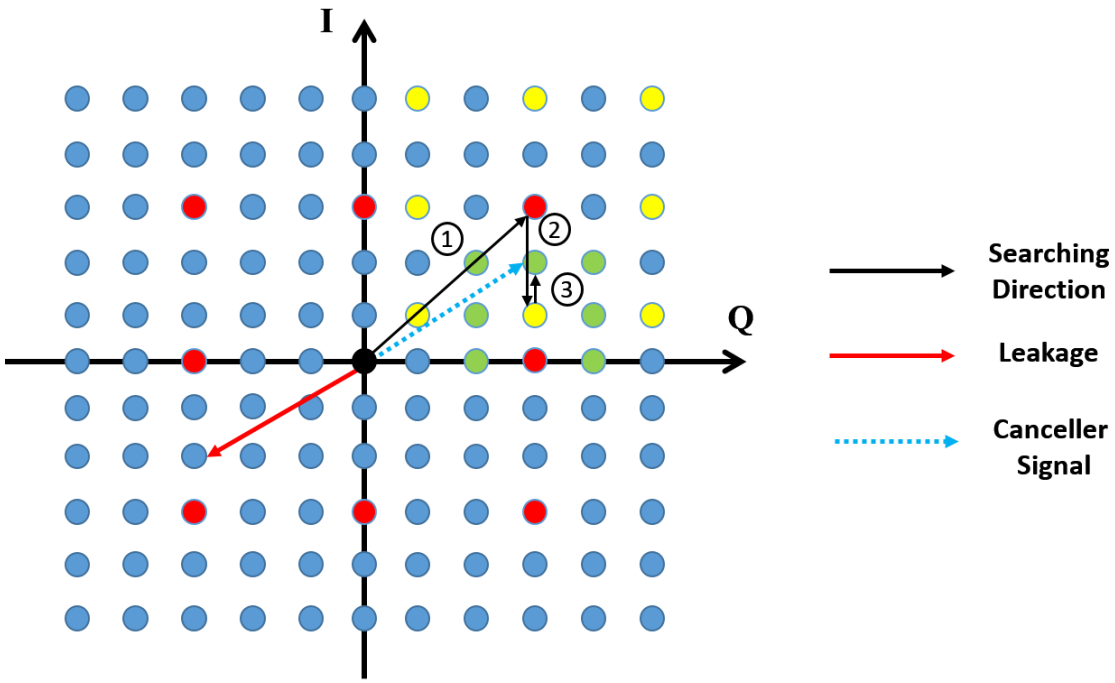

Figure 5.7 Typical example of improved full searching algorithm

Rather than measuring all the points ($N = 11^2 = 121$), this improved algorithm needs to measure only 24 points to find the optimal control value for the leakage suppression system. The first step of the algorithm is to symmetrically divide all the points into four sectors and

then to measure the central point in each sector, as well as the middle points on the axes (red points). The second step is to determine the point that offers minimum leakage component, and measure its surrounding points with half of the scale (yellow points). This process is repeated until the scale reduces to 1, and finally the optimal point can be obtained from those green points. It can be found that the scales in some searching steps are floating values. In order to obtain a quantized value for ADC and DAC to find the related point and also avoid missing points, the floating scale in the algorithm is rounded to the closest larger integer.

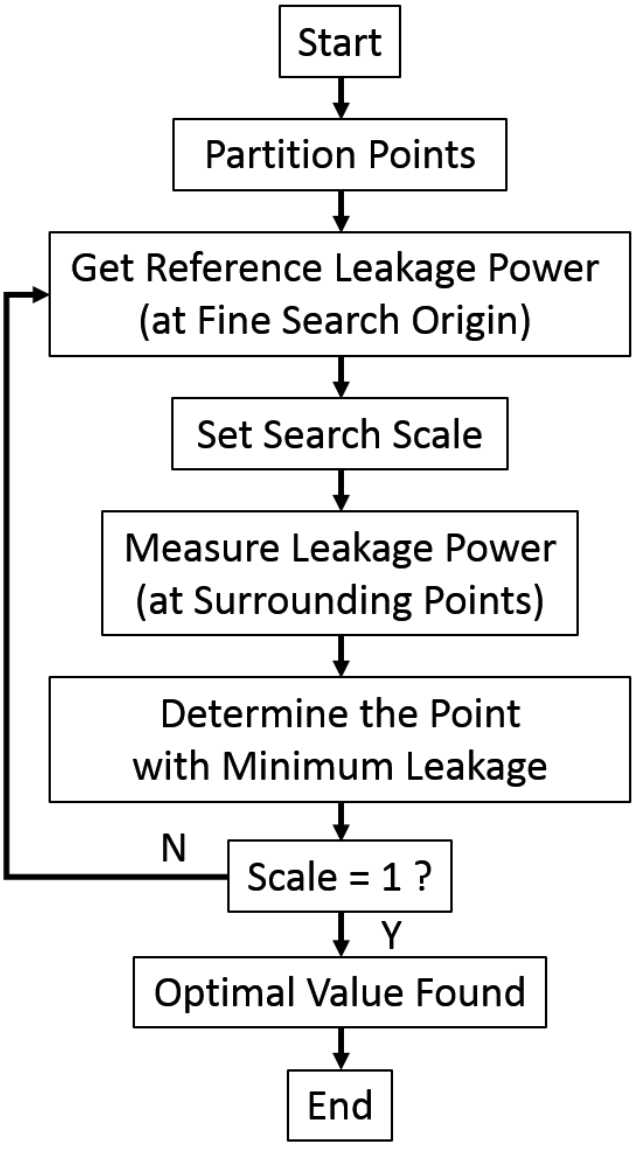

Figure 5.8 General processes of the improved full search algorithm

This improved algorithm is able to save much time in finding the optimal control value. Some similar algorithms are developed in [34] and employed in [116]. The main difference between

them is the definition of the scale, also known as the convergence rate. Hence, the general processes of this improved search algorithm can be expressed in Figure 5.3.

5.4.2. Gradient-descent Search Algorithm

The gradient-descent search algorithm also provides an efficient way to track the optimal parameters for the leakage cancellation block. Since the possible control parameters are selected from arrays, the gradient of the parameters in an array can offer great help to determine the search direction. To calculate the gradient, one random phase and gain combination (n, m) is selected as a reference point. After that, with a slight change in each parameter, two new combinations (n + δn, m) and (n, m + δm) can be obtained. The next step of this algorithm is to measure the residual leakage power of these three combinations. Following the results, the slope of the received signal strength indicator (RSSI) corresponding to the combinations can be calculated by the below equations.

$$(\nabla \mathrm{n}, \nabla \mathrm{m}) = \left[\frac{RSSI(n+\delta n,m)-RSSI(n,m)}{\delta n}, \frac{RSSI(n,m+\delta m)-RSSI(n,m)}{\delta m}\right] \tag{5.6}$$

$$\mathrm{n} = \mathrm{n} - \mu_a \times \nabla \mathrm{n} \tag{5.7}$$

$$\mathrm{m} = \mathrm{m} - \mu_b \times \nabla \mathrm{m} \tag{5.8}$$

where μ_a and μ_b are the real positive numbers and these numbers are the change steps of the parameter selection. Typically, at the beginning of the searching processes, a large step value is selected, which gradually decreases in later searching processes. This is because a large step value can save much convergence time when the number of the potential points is substantial. Step values can be held for continuous searching until the RSSI value of the new combination of points is higher than the RSSI of the reference one. This step change indicates that the optimal value has been passed in this converge direction. To continuously track the optimal parameters, the step size should be reduced and a similar search process started in the reverse direction. Theoretically, the desired control parameters can be found when the search step is at its minimum size, usually known as 1. The flow chart of this gradient descent algorithm is depicted in Figure 5.9.

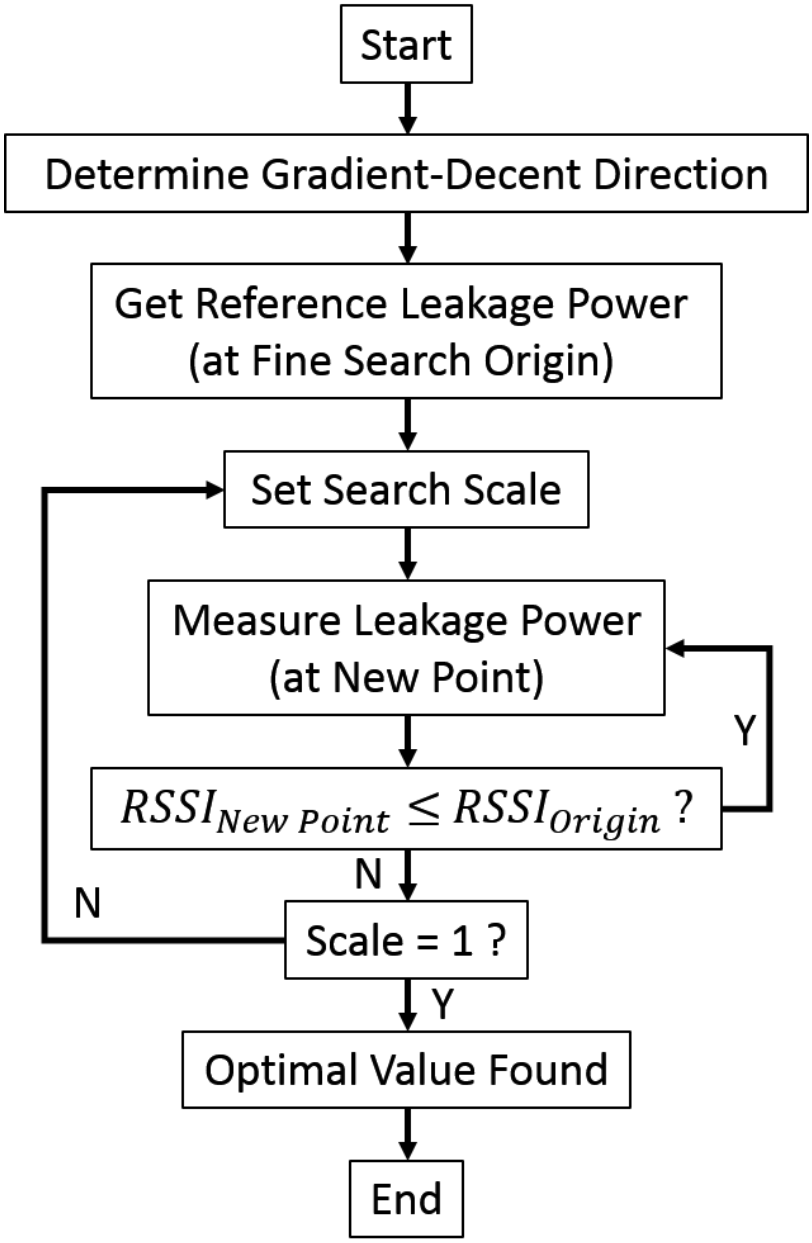

Figure 5.9 Processes of gradient-descent search algorithm

5.5. Adaptive Leakage Suppression Block Design

During the practical passive tag detection in Chapter 4, it was found that the proposed long-range RFID system has little immunity to leakage effects. Only when the leakage level is reduced to a certain value, can the system reach its potential. With help of further investigation, the dominant cause of the performance degradation in the proposed system was found to be the saturation of the quadrature demodulator. Since the maximum input power of the demodulator is around 11 dBm, it is quite easy to exceed this value when a high gain amplifier is applied in the reverse link. To solve this problem, an effective leakage suppression block (LSB) is added to the antenna subsystem (see Figure 5.10).

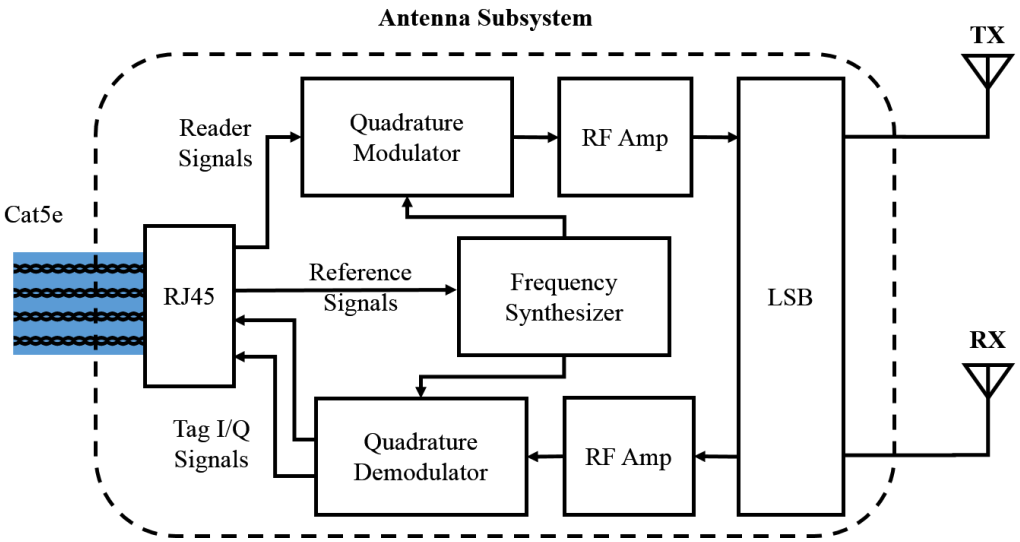

Figure 5.10 Block diagram of subsystem adding leakage suppression block

Figure 5.11 depicts a similar configuration for the leakage suppression block. In this block, instead of tapping the transmission signal, this configuration generates the canceller signal based on the carrier frequency (LO). The advantage of this configuration is its high performance in eliminating the unmodulated reflections. It also helps to remove the baseband DC-offset impacts. However, due to the variety of leakage sources, the unmatched spectrum of the canceller signal may have little effectiveness in entirely eliminating the leakage. Meanwhile, an additional amplifier may be required in this leakage suppression block due to the limited LO power. Therefore, this configuration is rarely used in many RFID readers.

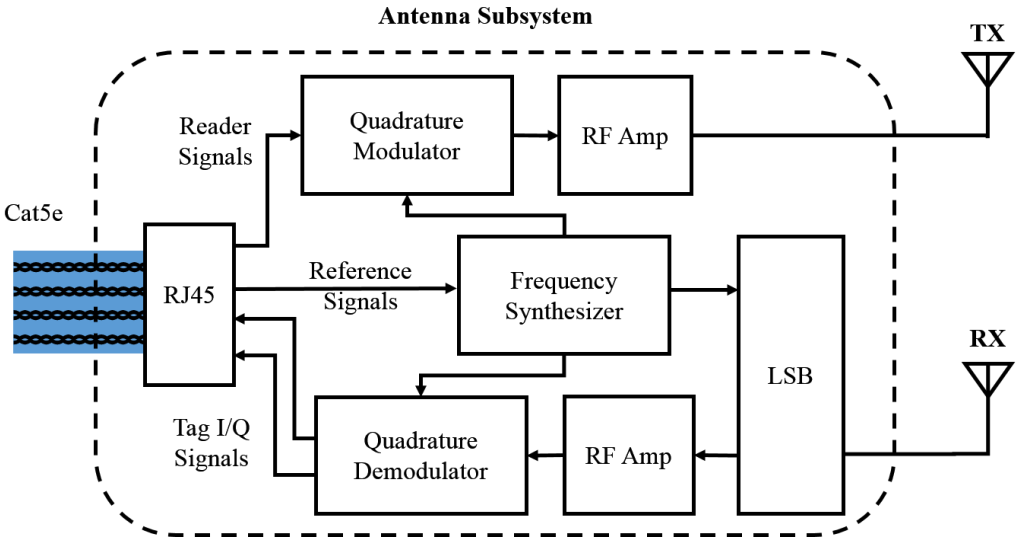

Figure 5.11 Leakage suppression block by using LO input

5.5.1. Leakage Suppression Block Structure

In the proposed antenna subsystem, the leakage suppression block is designed to apply the phase and gain control method to remove the leakage. As mentioned in previous chapters, some essential components such as vector modulator, microcontroller, and power detector are required. Figure 5.12 presents the block structure of this leakage canceller.

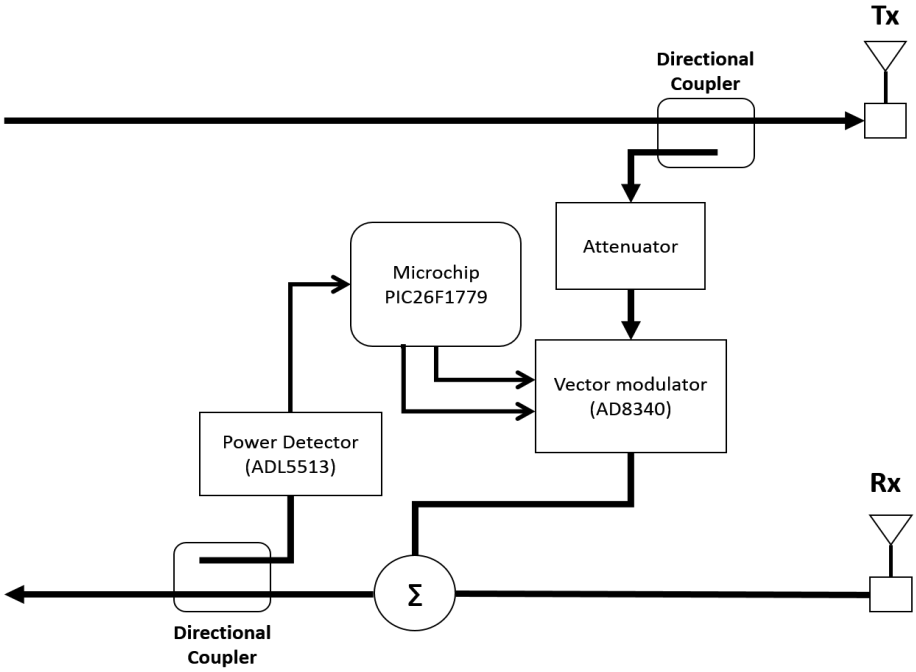

Figure 5.12 Leakage suppression block structure

To achieve the phase shifter and variable attenuator functions, an AD8340 vector modulator from the Analog Devices Company is selected. The gain can be set from its maximum of -2 dB to lower than -32 dB, and the phase can be shifted over the entire degree (0 – 360°). It provides a setpoint from 0.1 to 0.9 to guide the control input level. Here are the equations define the property.

$$Gain_{setpoint} = \sqrt{(V_I/500mV)^2 + (V_Q/500mV)^2} \tag{5.9}$$

$$Phase_{setpoint} = \arctan(V_Q/V_I) \tag{5.10}$$

where V_I and V_Q are the two control inputs. The voltage range for these two inputs is the same, operating from 0 V to 1 V.

An ADL5513 power detector is used to measure the residual leakage level. According to the specifications, its detection range in the RFID frequency band is from -62 dBm to 8 dBm and its corresponding output voltage range is from 0.6 V to 1.9 V. The voltage-power slope of this

power detector is 21 mV/dB. The detection error is less than 0.5 dB when the input RF power is in the proper range, and the response time of the power detection is around 20 ns.

Since at least two DACs and one ADC are needed to generate two control signals and receive one feedback signal respectively, a PIC16F1779 microcontroller is selected. In this control chip, there are four 10-bit DACs and one 10-bit ADC, and its operating clock rate can be up to 32 MHz. The critical task for this microcontroller is to quickly find the optimal control value using the advanced algorithm. According to its specifications, it also delivers 28 Kbytes program flash memory and 2 Kbytes data RAM for loading and operating the programme.

In terms of the rest of the RF components, a 3-dB loss power combiner is applied to add the canceller signal to the received signal. Two 10-dB directional couplers are used to separate the transmission and receiver signals. An extra attenuator is used to protect the vector modulator.

5.5.2. Applied Searching Algorithm

The designed leakage canceller block applies the improved full-scan algorithm to find the optimal control value, because this scan algorithm is efficient and reliable. The residual leakage in the receiver chain continuously decreases during the search, and its fixed processing time is good for the overall system design. In the gradient-descent algorithm, the residual leakage is fluctuant, and the optimal point may be skipped many times if the convergence rate is too fast. If the convergence rate is slowed down, the search period becomes longer, especially when the leakage canceller needs to find two optimal control points from two arrays. Accordingly, the improved full-scan algorithm becomes the natural choice.

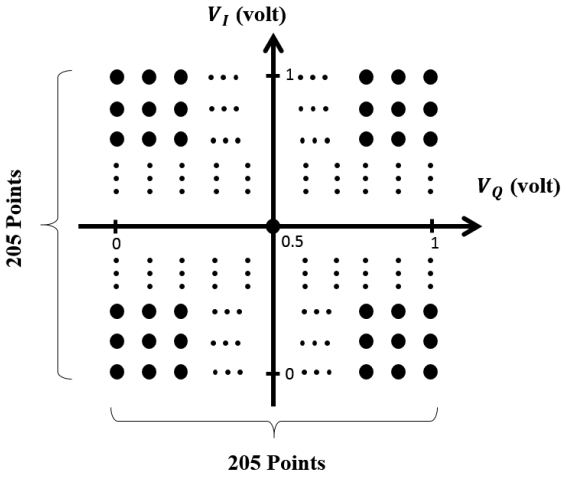

	Scale	Points	Full Search
1st	51	8	
2nd	26	8	
3rd	13	8	
4th	8	8	
5th	4	8	
6th	2	8	
7th	1	8	
Total		56	42025

Figure 5.13 Leakage suppression block structure

As stated in Chapter 5.22, the DACs inside the microcontroller have 10-bit resolution to quantise its internal reference voltage (5 V). This means, that over the voltage range 0 – 5 V, there are 1024 voltage points with an interval of 4.88 mV. To cover the whole control voltage (0 – 1 V), it requires at least 205 points (see Figure 5.13). To symmetrically partition these points in the coordinate chart, the start origin needs to be set at 0.5 V, which is equivalent to the point at (103,103). Based on this chart, it is easy to define the scales to determine the surrounding 8 points. The table in Figure 5.13 states the scale value and total measurement times based on these default parameters. This improved full-scan algorithm scans only 56 points to obtain its optimal results, whereas the conventional full-scan algorithm needs to scan 42025 points.

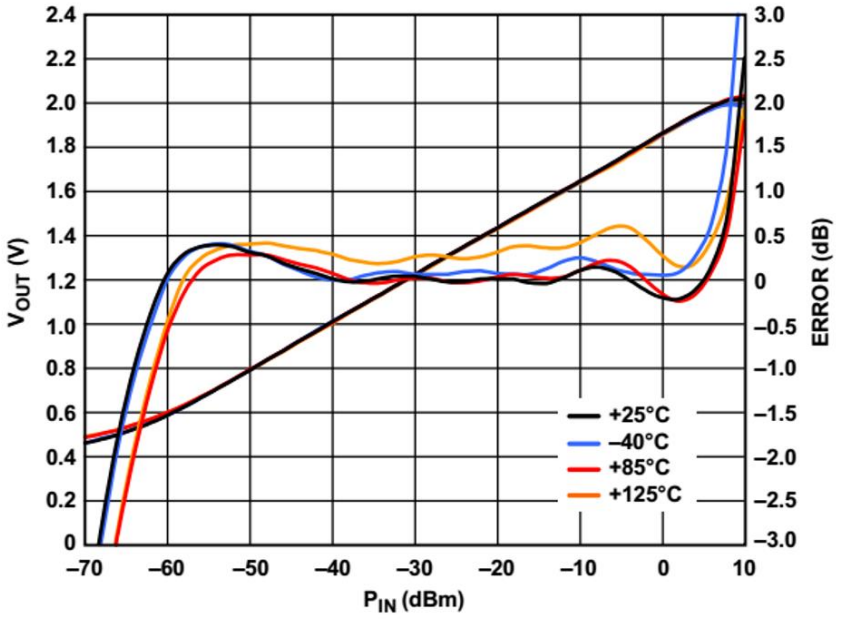

Figure 5.14 Output voltage and log conformance vs. input amplitude at 900 MHz [86]

In respect of the feedback voltage from the power detector, its linear output range is from 0.6 V to 1.9 V. Since its conversion slope is 21 mV/dB and the voltage step of the ADC is 4.88 mV, the minimum power differences that can be successfully achieved are around 0.2 dB. Figure 5.14 also shows the output error of the applied power detector. If the input power is close to its maximum or minimum limits, the error becomes serious and will result in the voltage dithering when the residual leakage reduces. To mitigate these errors, the applied algorithm increases the number of voltage samples and uses the mean value of the obtained samples to compare the power level. However, this extra sampling directly increases the search time. A trade-off between reliability and scanning time has to be made in the algorithm.

5.5.3. Suppression Effect Measurement

Since the proposed new system operates in the bistatic antenna configuration, the leakage level is largely dependent on the distance between the transmission and reception antennas. In order to reduce the environmental effects, the measurement at this stage has been conducted in a static environment with no objects moving during the testing. The Tx and Rx antennas are deployed toward the same direction with a gap of 1.5 m. The operation frequency is equal to 867 MHz, and the transmission signal is set to 26.5 dBm.

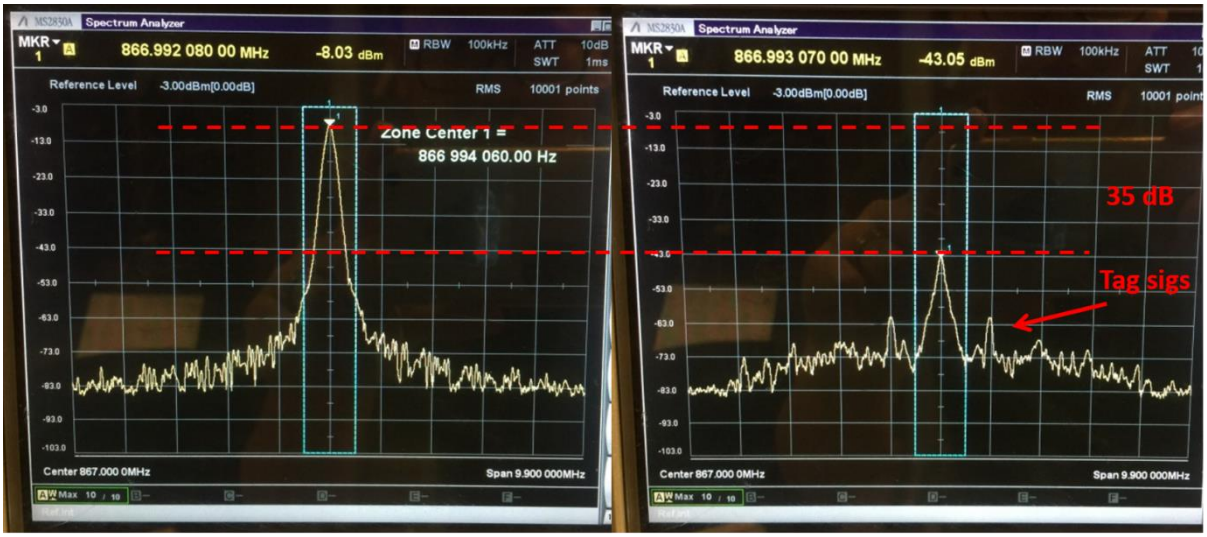

(I) **(II)**

Figure 5.15 Leakage suppression effect measurement example

Figure 5.15 plots an example of a leakage suppression effect measurement. A directional coupler is used to tap the received signal, and this signal is plotted in Figure 5.15(I). The system receiver suffers from a -8 dBm leakage signal during tag detection. This leakage level is much stronger than the received tag power. However, when the leakage suppression block starts to work, this leakage level decreases to -43 dBm over a very short time, and the tag signals can be seen in the spectrum domain (Figure 5.15(II)). The feasibility and effectiveness of this leakage canceller is proven by this result, and, in this example, it can achieve the suppression effect of 35 dB during the tag detection process. In order to obtain a reliable suppression effect result of this leakage canceller, 20 similar tests were done and the average result is plotted in Figure 5.16, which shows that the average leakage suppression effect is 36.9 dB.

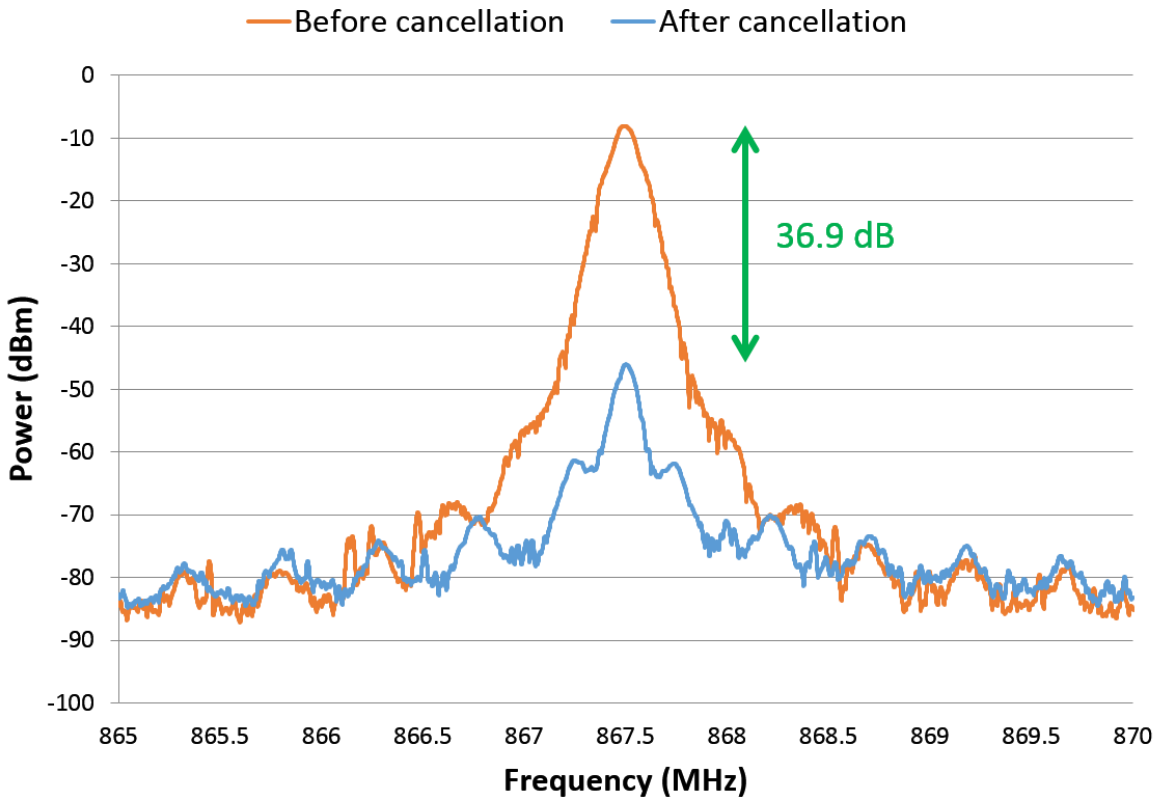

Figure 5.16 Average leakage suppression effect of the proposed canceller

However, this measurement is based on only one communication channel. In the RFID protocol, frequency hopping is required to avoid interference between different readers. As the hopping time is quite different from one reader to another, it is difficult to set a fixed time to limit the leakage canceller scanning period. However, the leakage canceller can be tested under two assumptions: one is that the hopping time is long enough for the canceller to update its optimal status, and the other is that the hopping time is shorter than the canceller scanning time.

In the first case, the performance should be similar to the measured result, since the time is long enough for the leakage canceller to retrain itself for a new carrier frequency. In order to verify this assumption, the proposed RFID system hops the carrier frequency in four channels during the operation. They are 865.7 MHz, 866.3 MHz, 866.9 MHz, and 867.5 MHz. In this test, the transmission power was increased to 32 dBm, and the leakage power measured in the receiver was -0.87 dBm. After operating the leakage canceller, as expected, the leakage in four channels all reduced to around -37.1 dBm, and the leakage suppression effect was 36.2 dBm (see Figure 5.17).

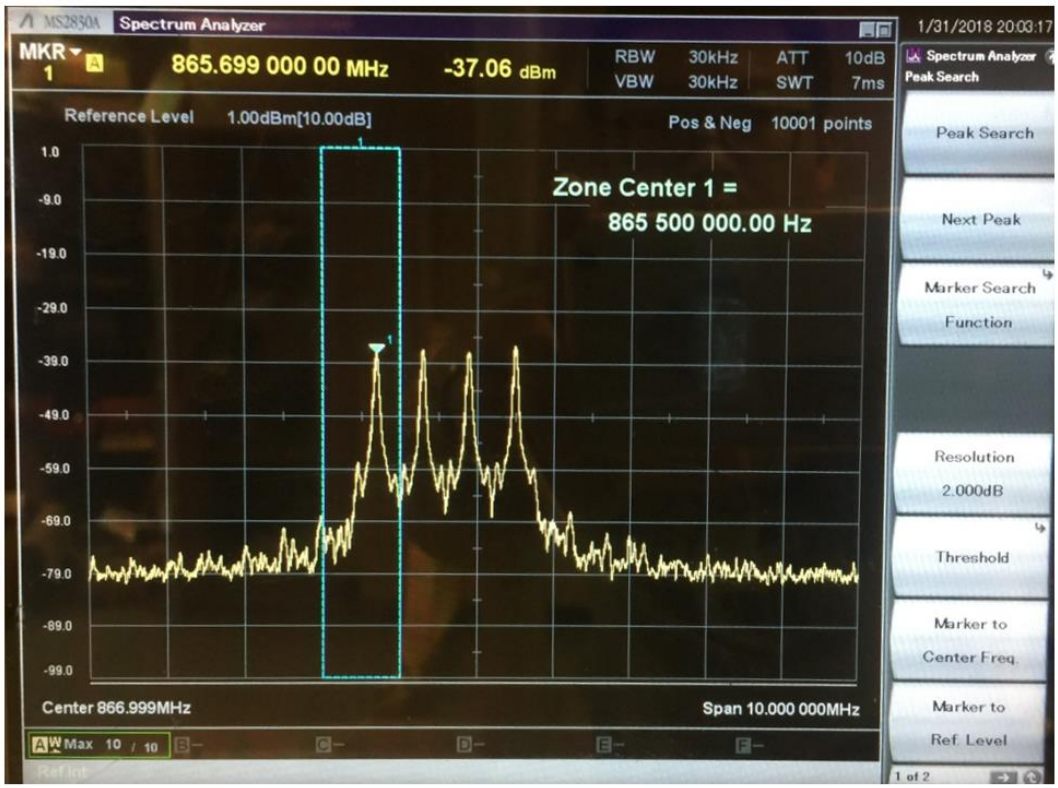

Figure 5.17 Leakage suppression effect in four channels with updating status

If the hopping time is shorter than the canceller scanning time, the leakage canceller can only be trained once, and its optimal status is fixed during the measurements. In this test, the transmission power remains at 32 dBm, and the receiver encounters a leakage of 1.63 dBm. At first, the proposed leakage canceller searches its optimal status based on the transmission signal at 866 MHz. After the settling time, the system starts to hop the operating frequency at 865.7 MHz, 866.3 MHz, 866.9 MHz, and 867.5 MHz. The result is shown in Figure 5.18. As can be seen from the figure, the leakage suppression is different in each channel. The first two channels are close to the training frequency (866 MHz), and have slightly better suppression than the other channels. Even though the leakage suppression effect at 866 MHz can still reach 37 dB, the suppression effect at 867.5 MHz is only 22 dB. Therefore, the leakage canceller is challenged when operating in such a situation.

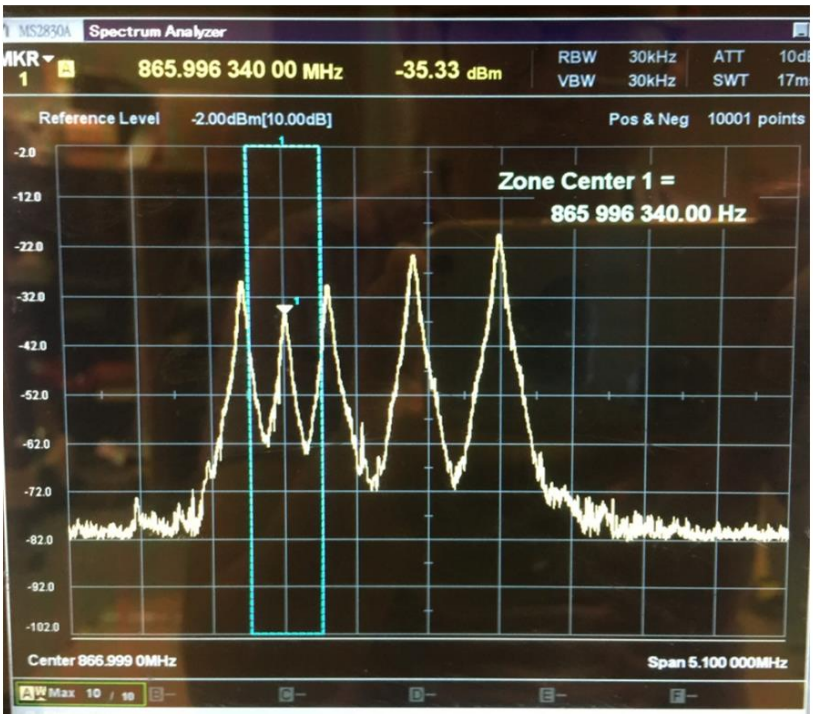

Figure 5.18 Leakage suppression effect in four channels without updating status

To ensure the leakage canceller keeps updating its optimal status, the settling time becomes critical. Based on the measurement, the proposed algorithm allows the canceller to find its optimal status within 38 ms based on 50 samples taken at each point (see Figure 5.19). According to the comparison table, this scanning speed is fast and sufficient for many commercial RFID readers to operate with the frequency hopping technique. Reducing the number of sampling times for each point can further improve the canceller settling time.

	Settling Time (ms)
[142]	330
[141]	46.5
[145]	34
This work	38

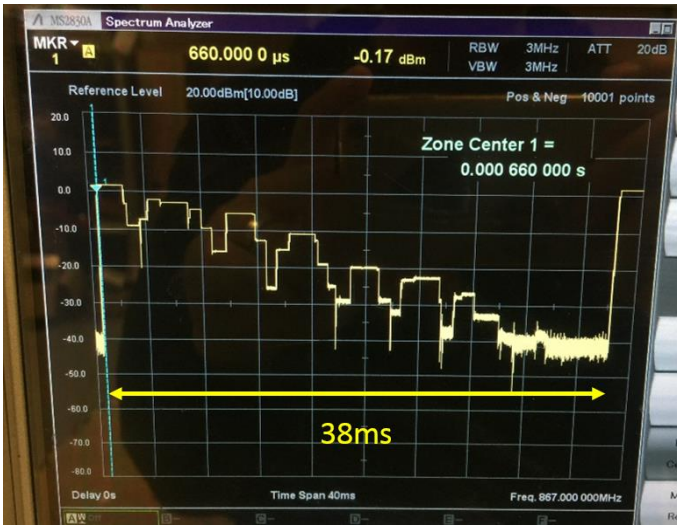

Figure 5.19 Leakage suppression block scanning time

5.5.4. Limitation and Discussion

Even though this designed leakage suppression block provides sufficient suppression for the subsystem, there is still an opportunity to improve its performance by overcoming certain limitations. The first limitation is due to the error from the power detector. When the residual leakage is reduced to its minimum level, the error becomes serious. This is because the weak signals are more sensitive to error. This problem directly leads to the failure of searching for the optimal point. Lower detection error and a higher dynamic range power detector can help to solve this problem. Applying a gain-controlled amplifier before the power detector and allowing the power detection to always occur in the low error input range is an effective and intelligent way to solve the problem. Certainly, this method requires more complex algorithms and control units.

The second limitation in the leakage canceller is the voltage resolution of the ADC and DACs. Since the block directly applies the voltage resolution (4.88 mV) based on the default setting, changes of the residual leakage can only be recognised when it is larger than 0.2 dB. In this case, most of the voltage levels are wasted. To increase the resolution, the reference voltage of the two converters can set to a lower value such as 2V, and then the voltage resolution is 2/1024 = 1.95 mV. The controller has the capability to detect a power change of more than 0.1 dB.

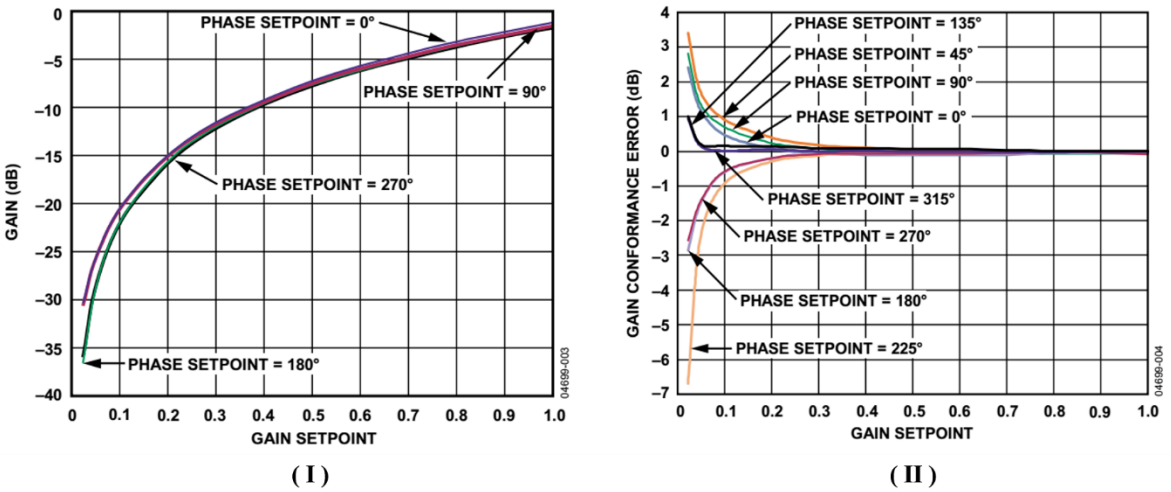

(I) (II)

Figure 5.20 Gain and phase accuracy of the vector modulator [151]

The third performance limitation comes from the vector modulator. Based on the specifications of the vector modulator in Figure 5.20(I), the gain and phase accuracy is acceptable when the gain is higher than -15 dB. This means that the power difference between the input and output

of the vector modulator should be less than 15 dB. If the difference is larger than this value, the output error is significant (Figure 5.20(II)). Therefore, an extra power detector and a variable attenuator are required to keep the vector modulator working in the proper setting range. This solution increases the hardware cost, but it is possible to provide more useful feedback signals to reduce the algorithm convergence time.

5.6. Automatic Passive RFID System with Leakage Suppression

5.6.1. Leakage Suppression of Monostatic Configuration

With the help of this leakage suppression block (LSB), the proposed RFID system is able to operate in the monostatic antenna configuration. This useful block greatly increases the flexibility of the system design since the entire RF module uses a single antenna. By simply connecting a twisted-pair cable, the remote unit is able to offer an RFID service in any place inside a building. Figure 5.21 depicts the block diagram of the antenna subsystem adding the LSB.

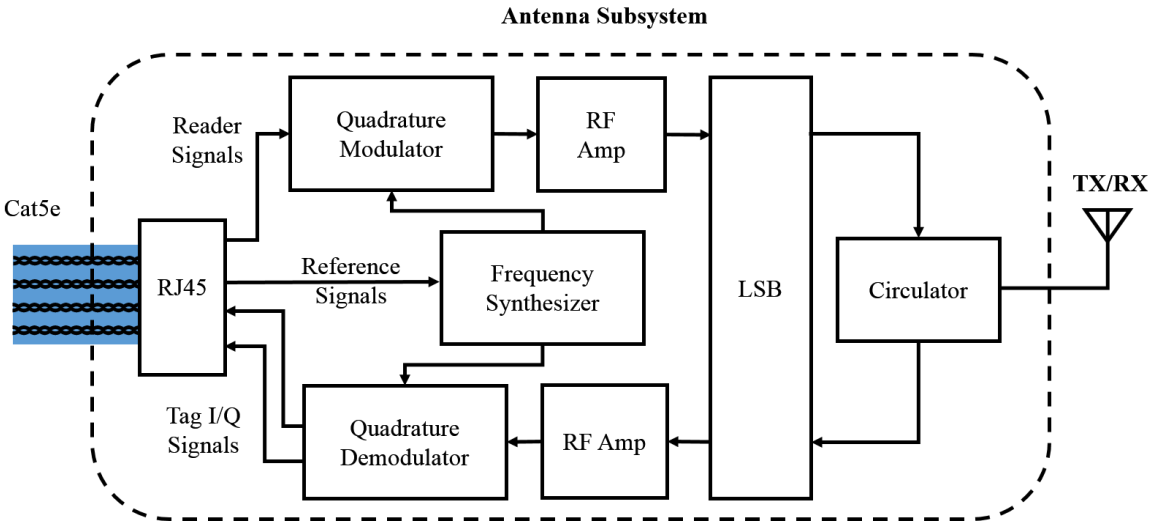

Figure 5.21 Block diagram of the new antenna subsystem

The leakage suppression effect has also been measured in this new configuration. The applied circulator provides 18 dB Tx/Rx isolation, and its insertion loss is 0.35 dB. In the test, the transmission power was set to 25 dBm, and the system operated at 866 MHz. Figure 5.22 shows that the canceller still retained its performance. This monostatic RFID system can achieve a leakage suppression of 36 dB within 38 ms.

Figure 5.22 Example of leakage suppression in the new subsystem

5.6.2. Comparison between designed and commercial RFID systems

Based on the previous practical tests, the proposed antenna subsystem suffers from a significant leakage problem when two antennas are closely installed, and its sensitivity may be lower than -60 dBm in the worst case. However, with this new subsystem, this problem has been successfully solved. With help of this proposed LCB, the new subsystem can deliver -85 dBm sensitivity over a 300 m Cat5e cable. Comparing to most RFID readers, this result is quite competitive, especially when the tag detection happens 300 m away.

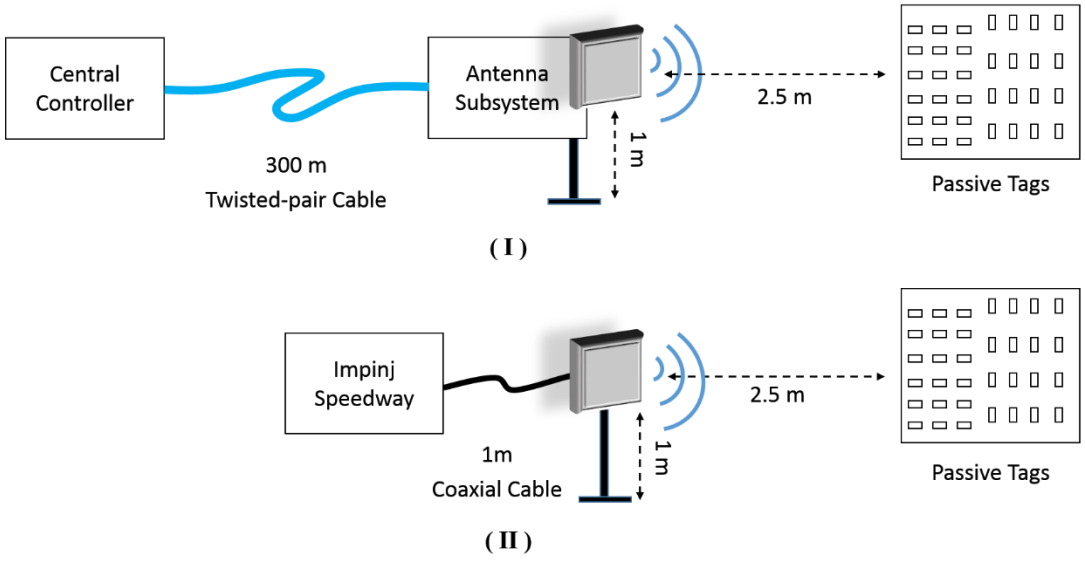

Figure 5.23 Automatic passive tag detection system configurations

In order to fully understand the real detection performance of this automatic detection system, an experimental comparison of this new system and the existing commercial Impinj Speedway RFID system was conducted. Figure 5.23 depicts the configurations of the two systems. As can

be seen from Figure 5.23(I), a 300 m twisted-pair cable is used to connect the central controller and antenna subsystem. A 6 dBic circularly polarized antenna is directly attached to the subsystem at a height of 1.5 m, and a passive tag board is placed at the same height around 2.5 m away from the antenna. There are 34 passive UPM Raflatac DogBone tags [152] attached to this board, placed in horizontal and vertical directions over 1.8 m × 2 m cardboard. Figure 5.23(II) shows that a 1 m coaxial cable is used to connect the Impinj Speedway reader and antenna. The antenna is installed at the same height, and with the same orientation as the configuration in Figure 5.23. The passive tags and board were not moved during the measurement. The transmission power in both systems was set to 20.5 dBm, and the system operated using frequency hopping.

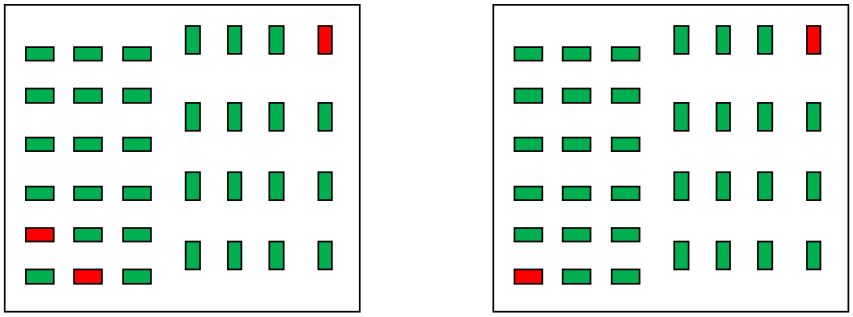

	Impinj Speedaway System	Proposed System over 300m Cat5e
Duration	3 mins	3 mins
Frequency Hopping	4 channels (865.7MHz,866.3MHz, 866.9MHz, 867.5MHz）	4 channels (865.7MHz, 866.3MHz 866.9MHz, 867.5MHz)
Rate	17.16 tags/s	57.31 tags/s
Time to see all	1.1 min	728 ms
Nulls	3	2

Figure 5.24 Measured results of two automatic tag detection systems

According to the results in Figure 5.24, the two systems provided similar detection performance. The measurements for each system were repeated 3 times, and the average value is presented in the table. Each time the tag detection operates over a 3 minute period. Those passive tags in green colour were successfully detected in the 3 measurements, whereas the tags in red colour have failed recognition at least once. In terms of the read rate, the proposed system can reach an average of 57.3 tag/s, but the commercial one reached only 17.2 tags/s. This superiority is also reflected in the time to detect all the passive tags. The designed automatic detection system

was able to obtain all the tag information within 728 ms. However, the commercial system struggled to detect some missing tags and required around 1.1 minutes to read them all.

It is also worth discussing the read range of these two systems. The given results for the proposed new system can be achieved 300 m away from the central controller, while the commercial system cannot achieve this. Based on the specification of LMR-200 coaxial cable, the cable loss is 0.4 dB/metre. For a 25 m long coaxial link, the transmission power reduces from 20.5 dBm to 10.5 dBm. Almost half of the signal power is wasted in the cable transmission. Although more advanced coaxial cables with lower attenuation can be used to reduce this loss, the cost for purchasing these cables dramatically increases the entire system budget, especially in a DAS system. Moreover, these low-loss coaxial cables are typically thicker and heavier. More details of the comparison between twisted-pair cable and coaxial cable are shown in Table 5.1. It is not difficult to find that the most cost-efficient link for large-range detection is using Cat5e cable in the system.

Table 5.1 Comparison of Cat5e cable and coaxial cables [153] [154] [155]

Cable Type		Cat5e	LMR-200	LMR-400	LMR-1700
Signal Frequency		Baseband 350 kHz	RF 900 MHz	RF 900 MHz	RF 900 MHz
Cable Loss (dB)	10 m	0.11	4	1.28	0.31
	150 m	1.65	60	19.2	4.65
	300 m	3.3	120	38.4	9.3
Weight (kg)	10 m	0.31	0.3	1	11
	150 m	4.65	4.5	15	165
	300 m	9.3	9	30	330
Approximate Price (£)	10 m	8	12.4	30.3	435.3
	150 m	120	186.6	454.5	6,530
	300 m	240	373.2	909	13,060

To compensate for the cable loss, it is also possible to use additional high-gain RF amplifiers. However, this method directly leads to higher power consumption of the system. It also a requires higher cost to cascade a high gain and high P1dB RF amplifier to maintain the system linearity. More importantly, the minimum SNR of the uplink signals is the critical parameter to allow successful decoding. It is difficult to improve this degradation in a high loss cable link. In the proposed system, a carefully designed operational amplifier can further improve the SNR of the down-converted signals before it is transmited back to the controller over a Cat5e cable. By simply doubling the magnitude of the demodulator output signals, the 300 m system sensitivity without LCB can be improved from – 94.5 dBm to – 99 dBm. This measurement proves the capability of the new system in improving the uplink SNR.

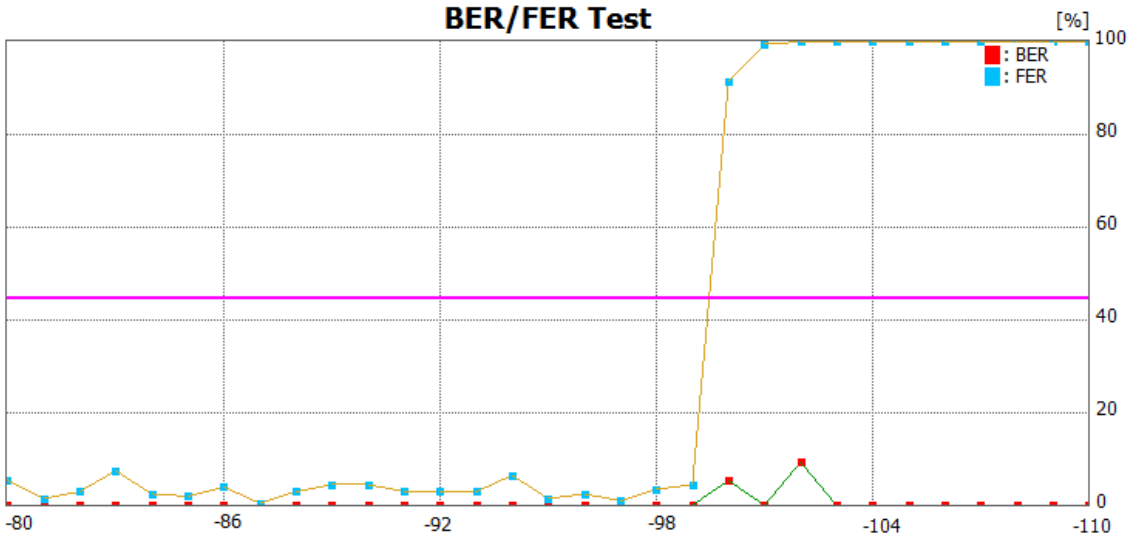

Figure 5.25 System sensitivity with an uplink amplifier

Regarding installation, twisted-pair cable can be simply plugged to an RJ45 socket to connect the link, and short cables can also be quickly cascaded using extenders. However, the coaxial cable in a conventional system needs to be screwed using specific connectors. Connector matching, limited bend radius and heavy weight greatly reduce the installation flexibility. Thus, based on this comparison study, the new automatic UHF RFID system is much superior to the conventional RFID systems for wide-area tag detection.

5.7. Conclusions

This chapter introduced leakage canceller architectures and convergence algorithms. In order to efficiently suppress the leakage in the proposed antenna subsystem, an effective leakage suppression block using a phase and gain control method has been designed. Through

measurements, this new canceller is able to deliver an average suppression of 36.9 dB, and this excellent performance remains when the system operates using frequency hopping. With help of an improved scanning algorithm, this canceller can find its optimal status within 38 ms, and this settling time can be shorter if the algorithm reduces the number of voltage samples taken at each point.

This leakage suppression block can successfully address the saturation problems of the designed subsystem, and it allows the subsystem to operate in a monostatic configuration. The sensitivity measurements have shown that the designed system can still achieve a sensitivity of -85 dBm over a 300 m Cat5e cable. Suggestions have also been given that, to further improve the leakage canceller and system performance, a higher dynamic range of the power detector and more targeted parameter settings are required. Through comparison with the Impinj Speedway RFID reader, this new automatic passive UHF RFID system has been confirmed to deliver high performance long-range passive tag detection. Particular advantages include the tag read rate and capability of uplink SNR improvement. This novel system is also superior to the conventional RFID systems in terms of link distance, link cost, and installation flexibility.

Chapter 6

6. Conclusion and Future Work

6.1. Demands for Wide-area Detection

The passive RFID market constitutes more than 80 percent of the world RFID market, and the increasing demands for wide-area detection is leading to growing research and development. The read range of a conventional passive RFID reader however is limited by its downlink power, and so for large area coverage, many readers are required. In addition to the high cost of this, the complexity of deployment and reader management, due to for example collision and leakage issues have impeded widespread adoption. The introduction of a distributed antenna configuration greatly extends the coverage of a single reader. However, this configuration has its own limitations. The RF signals to the antennas suffer from high cable loss over a long coaxial connection link. High-gain amplifiers can help to solve this issue, but in turn lead to high power consumption. In addition, the minimum uplink signal-to-noise ratio needed to demodulate the backscattering signals also limits the maximum cable length. Therefore, the use of multiple antennas configuration connected by coaxial cables is mainly appropriate for indoor applications.

The aim of this work therefore has been to develop a cost-efficient, highly-flexible, and reliable RFID system for large-area tag detection. In order to achieve this, limitations such as high cable attenuation and SNR degradation in a long cable should be overcome. Some other issues such as deployment difficulty, detection reliability and system cost should also be improved during the system design.

6.2. A Novel Passive UHF RFID System over Twisted-pair Cable

Chapter 3 has presented a new system configuration for long-range UHF RFID systems. This system consists of a central controller and an antenna subsystem, and these two modules are connected by a commonly used twisted-pair cable. Instead of carrying the carrier frequency, the twisted-pair cable is only used to transmit the low-frequency reader commands and down-converted backscattered tag signals. Because they are low frequency, these baseband signals encounter very low attenuation even though the cable is more than 100 metres long. Theoretical models such as link budgets and RF spreadsheets for this new RFID system have also been

described. The simulations confirm the feasibility of this design, and the possible limitations in each proposed block have been investigated.

In addition, a new method has been developed to achieve frequency and phase hopping by tuning the frequency and phase of the reference tone using a frequency synthesis module. The simulation results prove the feasibility and accuracy of this method. By using this new method, the cost and size of the subsystem can be further reduced, and multiple subsystems can be easily synchronised using this method for future DAS applications.

6.3. Passive RFID System in Long-Range Detection

In Chapter 4, the proposed new system has been fully measured. Based on the experimental results, this new system is able to provide stable and reliable transmission signals, and its output power is high enough to reach the maximum regulatory limit. In addition, the excellent condition of the baseband communication between the central controller and the antenna subsystem helps the system to meet the requirements of RFID industrial standards.

Through practical measurements, it has been found that the uplink sensitivity of the new system is insensitive to the length of twisted-pair cable. It was also shown that the reader sensitivity of this new system can achieve -94.5 dBm over 30 m Cat5e cable, and its sensitivity can still remain at around -94 dBm with 180 m Cat5e. According to further investigation, the cable insertion loss, crosstalk and delay effects have little effect on this new configuration. Comparison with a USB-extended RFID system, showed that the proposed system has no delay issue in its baseband communication over twisted-pair cable, while the USB-extended system cannot achieve such latency. To verify the obtained results, a practical demonstration has been conducted. Passive tags were successfully detected over a 6 m wireless range with 300 m of twisted-pair cable between the central controller and antenna.

This new system configuration delivers high performance for long distance passive RFID applications and also provides massive benefits for multi-antenna RFID systems. This proposed configuration allows a central controller and multiple subsystems to achieve the RFID DAS. Through this approach, the entire hardware cost is reduced since the baseband processes are all completed in one module. In addition, low cable loss and high deployment flexibility allow the system to achieve long-range detection where the conventional RFID systems cannot.

6.4. Long-Range Detection with Leakage Cancellation

Chapter 5 has introduced some typical leakage cancellation architectures and convergence algorithms. In order to efficiently suppress leakage in the proposed antenna subsystem, an effective leakage suppression block using phase and gain control has been designed. Through practical measurements, this new canceller was found to deliver an average leakage suppression of 36.9 dB, and this excellent performance can remain when the system operates with frequency hopping. With help of the improved scanning algorithm, this canceller can find its optimal status within 38 ms, and this settling time can be shorter if the algorithm reduces the number of voltage samples taken for each point. The overall performance of this leakage suppression block can meet the requirements of most commercial RFID readers. To further improve this suppression block, a higher dynamic range is required at the power detector along with higher resolution of the targeted parameter settings.

The leakage suppression block can successfully address the saturation problems of the designed subsystem, and allows the long-range RFID system to operate in a monostatic configuration. After adding the leakage canceller, the designed system can achieve a -85 dBm sensitivity over a 300 m Cat5e cable. A comparison study has also been conducted to evaluate the system performance. According to the results in comparison tests, the proposed long-range RFID system provides highly-reliable tag detection with a fast read rate over a 300 m Cat5e Cable, and it also shows advantages in terms of its long-range detection and installation flexibility. Therefore, an automatic long-range passive UHF RFID system with improved Tx/Rx isolation has been successfully and finally developed.

6.5. Directions of Future Work

This thesis has delivered a world-first cost-efficient, highly-flexible, and reliable passive RFID system using twisted-pair cable to address distant antennas for large-area tag detection. While significant achievements have been made to ensure its performance, more research is required to enable the system to achieve its ultimate potential in the increasingly competitive RFID market.

6.5.1. RFID DAS over Twisted-pair Cable

In Chapter 4 and Chapter 5, the proposed long-range RFID system over twisted-pair cable has been demonstrated. This system is able to provide highly-reliable detection performance. However, the demonstration only showed the reading distance that the proposed system can

achieve. Due to downlink limits, multiple subsystems are still required to achieve very large area coverage. Figure 6.1 presents the architecture of the RFID distributed antenna system using twisted-pair cable.

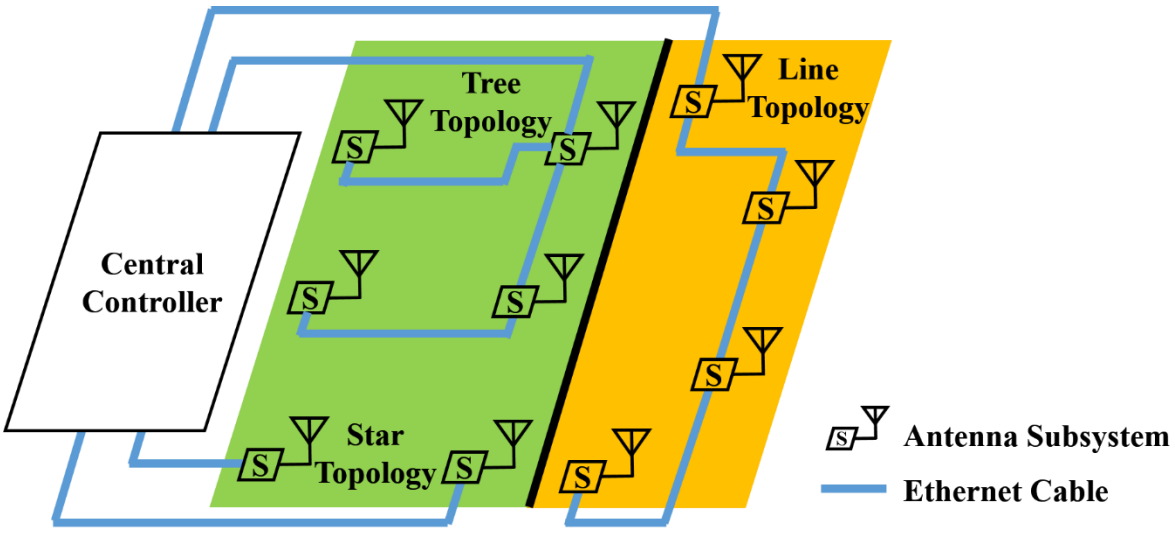

Figure 6.1 Long-range RFID DAS

Since the proposed system suffers little adverse effect from cable loss and sensitivity degradation over a long twisted-pair cable, this increases the flexibility of subsystem deployment. Figure 6.1 shows the possible topologies of the subsystems, such as star, tree or line topologies. Future studies in this direction are concentrated on baseband signal processing techniques such as equalization, synchronization, and combination, which are used to recover the tag symbols from different subsystems. In addition, the investigation of SNR tolerance for twisted-pair cable is needed to determine the maximum number of subsystems that a single cable can support in distributed configurations. However, based on the current measured results, for a DAS RFID over Cat5e cable, the maximum number of the subsystem is mainly limited by the SNR of the baseband signal in the central controller. This is because the baseband signal suffers SNR degradation in splitting the signals. Thus, the designed system can have a large number of subsystems for distributed DAS configuration. However, for a line or hybrid DAS configuration, the situation become complicated and need to be further investigated. Algorithms for efficient localization using this new system are also worthy of further development.

6.5.2. Universal Protocols RFID Subsystem

Chapter 2 demonstrated a baseband-controlled frequency and phase hopping method. Through this method, the frequency and phase of the output signal in antenna subsystem can be precisely

set to desired values so that the RFID system can operate in different frequency bands to comply with the different worldwide standards and regulations. For example, the antenna subsystem can operate in the 865 – 868 MHz band to provide tag detection in European countries, and also can operate in the 902 – 928 MHz band to deliver RFID coverage in North America. In addition to the operational frequency, other important parameters such as transmission power and communication protocols must be obeyed so as to achieve a universal protocol RFID system. In such a system, different types of tags can be detected by a single central controller, and different RFID protocols can be simultaneously applied by multiple antenna subsystems. Figure 6.2 shows an example of a universal RFID application.

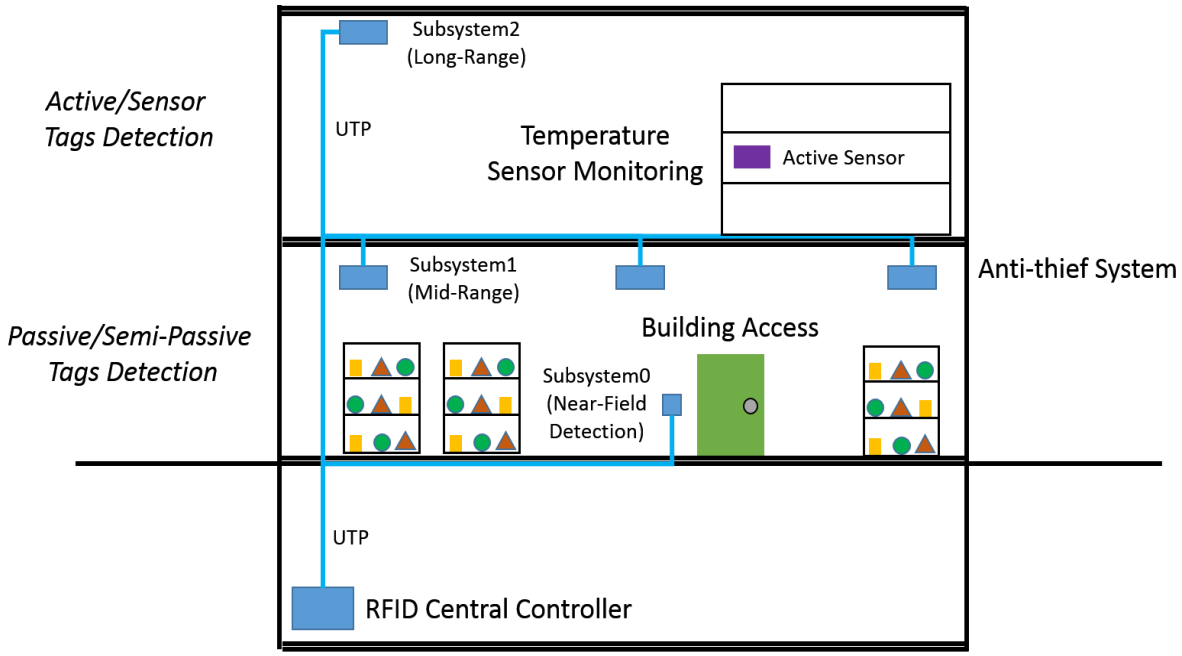

Figure 6.2 A universal protocol RFID system

In order to achieve this highly-flexible universal protocol RFID system, the current central controller should incorporate more comprehensive RFID protocols and more sophisticated interfaces to allow the different protocols to be operated at the same time. The subsystem modules can be designed in different versions for specific applications such as near-field detection, mid-range detection, and long-range detection. Studies in this direction mainly focus on developing baseband protocol combination schemes and designing low-cost, highly-reliable subsystems over twisted-pair cable for different detection range applications.

6.5.3. Multiplexing in Twisted-pair cable

In a commonly-used Ethernet cable, there are four pairs of copper wires. These four pairs are fully used by the current RFID system design: One pair is used to transmit baseband reader

commands, two pairs are used to receive the tag signals, and the last one is used to send the reference oscillator signal. However, if more control signals are needed for multiple subsystems, multiplexing techniques should be applied to increase the bandwidth use in each channel. Through this approach, the possible control functions can be centralised in the RFID central controller, and Power over Ethernet (PoE) can also be achieved.

Common approaches for analogue multiplexing are frequency division multiplexing (FDM) and time division multiplexing (TDM). Commands or signals can be sent in several distinct frequencies over four frequency channels (FDM) or can use a switch to enable the transmission and reception between controller and subsystem (TDM) in different time slots. Figure 6.3 shows the multiplexing methods for the proposed RFID system.

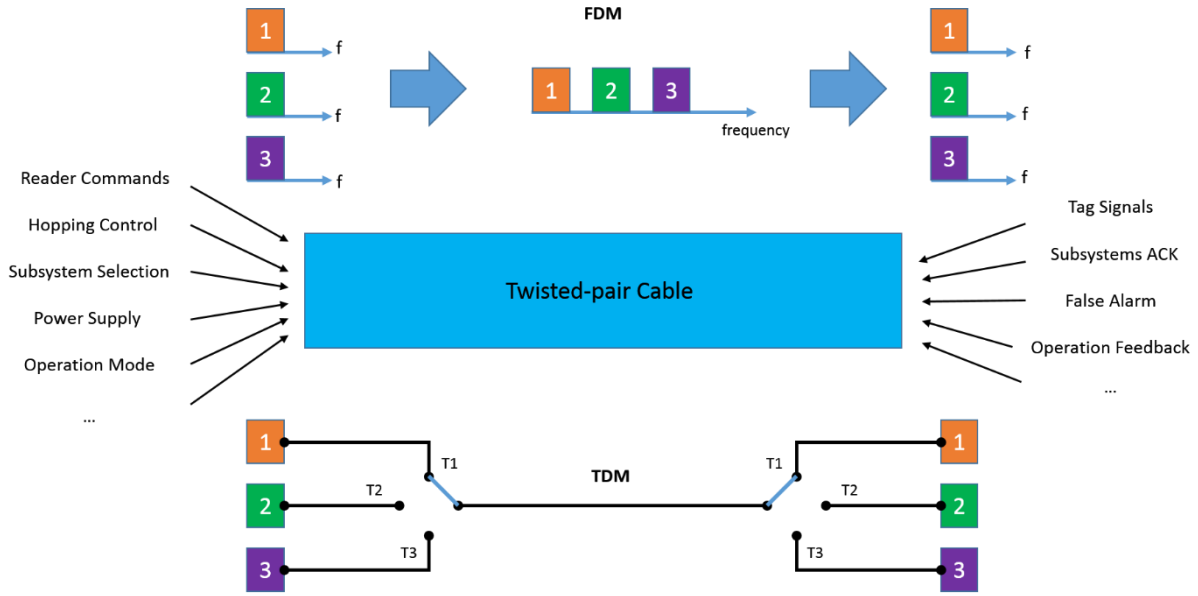

Figure 6.3 Multiplexing in twisted-pair cable

Studies here should investigate the performance degradation due to noise and other properties such as crosstalk and delay when using these multiplexing techniques. This work could be of great help to the next stage in development of the next generation digital RFID DAS.

6.5.4. Cyber-Physical RFID DAS over Twisted-pair cable

In order to achieve a next-generation cyber-physical RFID system, the central controller should be fully virtualized and realized in the web cloud, and subsystems should be able to directly communicate with an online control server through wired or wireless links. In such a digital RFID system, cable length and coverage are no longer the limitations since the subsystem can be deployed in any desired place. With help of other wireless standards and protocols, those

subsystems are able to share tag information with other subsystems or devices such as mobile phones and PCs. Figure 6.4 shows an example of the cyber-physical RFID DAS.

In this system, users are able to use their mobile phones to control the RFID systems via Internet online Cloud, and those subsystems inside a building can be controlled wirelessly by a PC. Inside the PC, a wireless RFID control card is needed to provide basic RFID physical-layer protocols. Therefore, digital RFID DAS could become one of the most important cyber-physical systems to serve society.

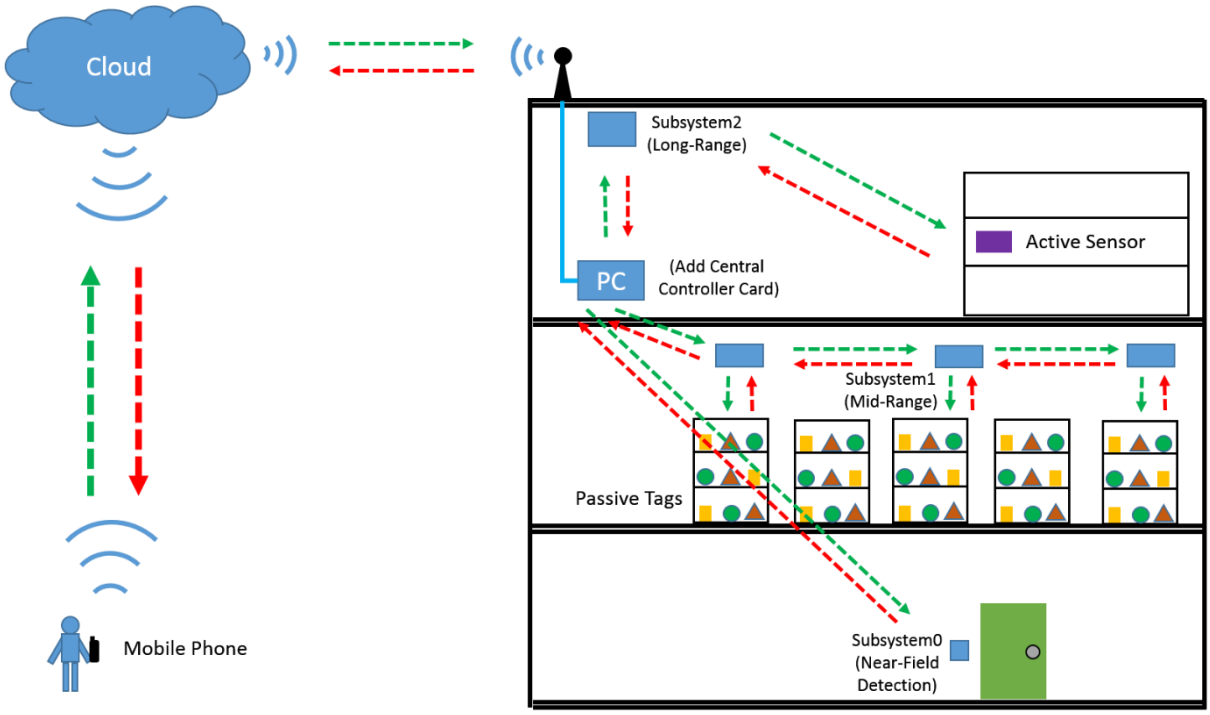

Figure 6.4 Example of the digital RFID DAS

Studies to achieve this attractive system are mainly focused on protocol design. To combine the RFID protocol with other wireless protocols such as Wifi (IEEE 802.11), it is essential fully to understand the requirements of both protocols. For example, limited package delay is tolerable in a TCP/IP network, but this delay is unacceptable in a full-duplex RFID system since it may lead to timeout and synchronisation problems. To solve such problems therefore requires careful design at the control server and physical layer. This powerful RFID system can only be achieved when a reliable cyber-physical link is established.

Appendix A

This appendix provides the details of ARM controller and R2000 Chip for system central controller. The selected control and RFID chip are both embedded in an R2000 RFID module, and this module can provide all the required baseband signals for the central controller. Figure A.1 shows the front and back side of R2000 RFID module.

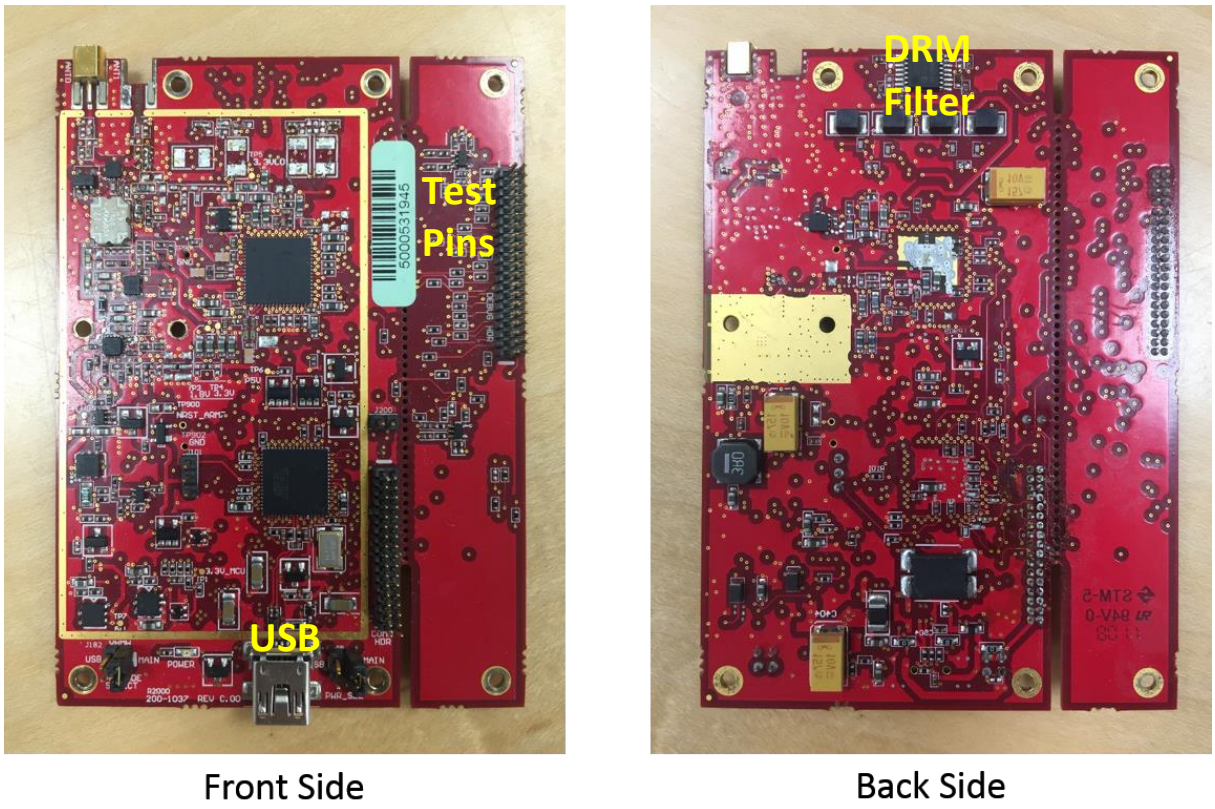

Figure A.1 Integrated R2000 RFID module

Since the RF block in the R2000 chip is bypassed, the method to obtain the baseband commands is to configure the particular registers in the ARM processor. The details of the configuration is described and its relating accessible test points from the R2000 chip are shown in Figure A.2. In this design, the downlink baseband signals can be obtained at the point just after the baseband transmission filters (red box). The baseband tag signal can also be inject back to the R2000 chip by connecting to the dense reader mode (DRM) filter pins. Thus, the baseband input and output ports on this module are determined. For more specification information, please find in the datasheet [116].

430	ANA_TEST1	R/W	11 10 9 8 7 6 5 4 3 2 1 0	rxadc_intest_i_i rxadc_intest_i_q pll_test_up pll_test_down iflna_itest iflna_qtest ifagc_iintest ifagc_qintest rxadc_intest_q_i rxadc_intest_q_q txfilt_itest txfilt_qtest			Analog test signals. pll_test_up: Set PLL charge pump up pll_test_down: Set PLL charge pump down iflna_itest: Enable IF LNA test I iflna_qtest: Enable IF LNA test Q ifagc_iintest: Enable IF AGC input test I ifagc_qintest: Enable IF AGC input test Q: rxadc_intest_q_i Enable RX ADC input test rxadc_intest_q_q I: rxadc_intest_i_i Enable RX ADC input test rxadc_intest_i_q Q txfilt_itest: Enable TX filter test I txfilt_qtest: Enable TX filter test Q
431	ANA_TEST2	R/W	1 0	adc_test atest_e			Analog test signals adc_test: Enables test feedback of AUX ADC atest_e: Enable analog test bus

(1) Register table for downlink baseband

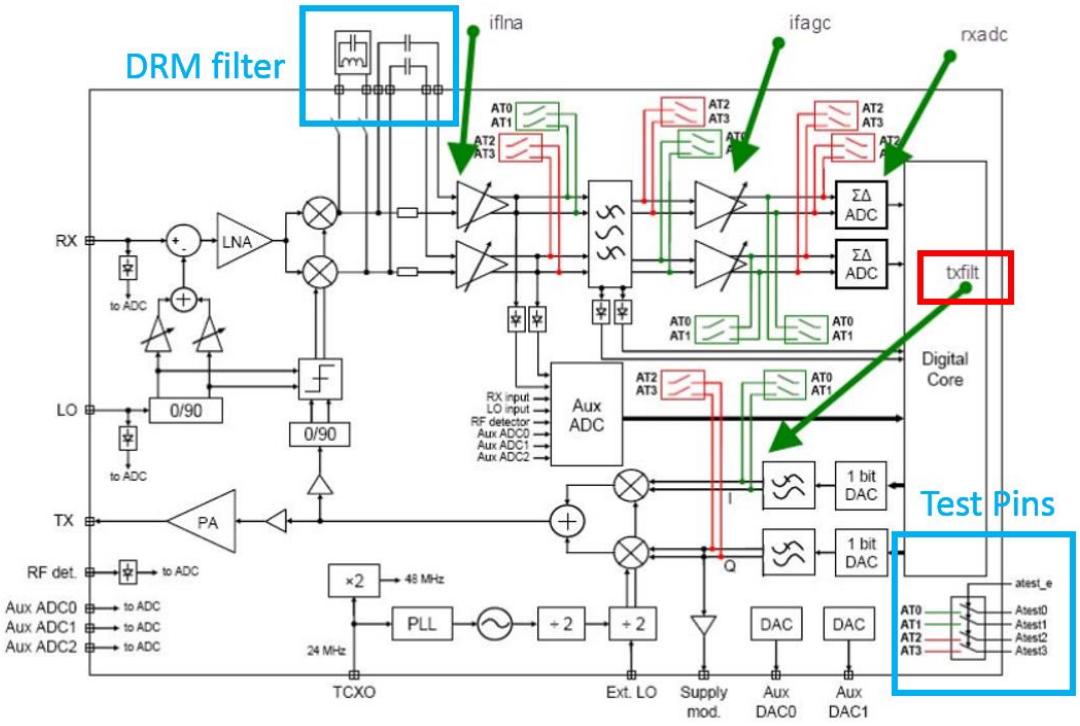

(2) Block diagram for test points and IO ports

Figure A.2 R2000 Chip block diagram and test points

Appendix B

This appendix shows the details of frequency synthesis ADF4350 and its development board. Figure B.1 provides the details of the development board that is used in the subsystem. This board including a USB connector, ADF4350 synthesiser, and internal TCXO oscillator. Accompanying software for controlling the synthesizer functions can be used via USB control port.

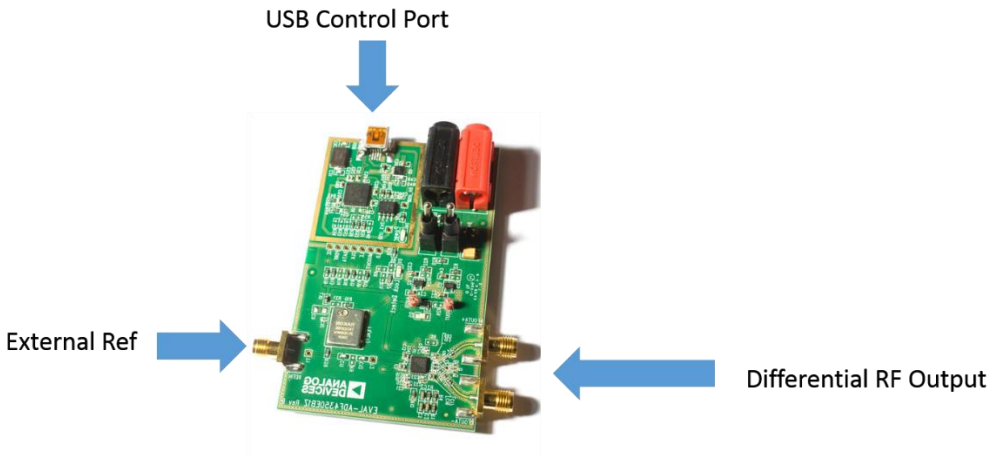

Figure B.1 ADF4350 Development board

In the designed system, the external reference signal is used. For this case, R1 and R2 have to be removed to disconnect the on-board TCXO, and R9 need to be populated with a resistor of 50 ohms (Figure B.2). Since only SMA connectors is provided in the board, extra SMA to RJ45 adaptor is needed for impedance match and connection. More specification information can be found in datasheet [133].

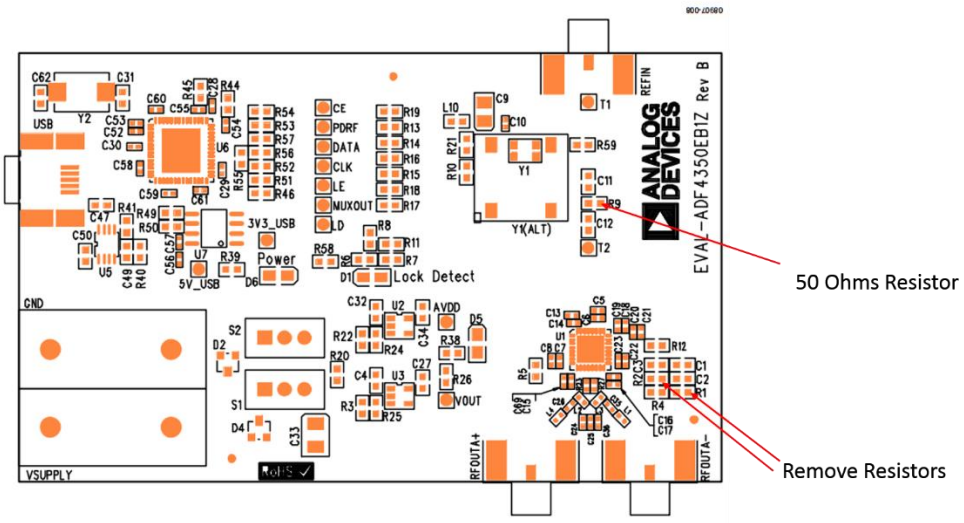

Figure B.2 ADF4350 development board circuit modification

References

[1] D. M. Dobkin, RF in RFID: UHF RFID in Practice, Elsevier Inc., 2013.

[2] C. Daily, "Unmanned supermarket," China Daily, [Online]. Available: http://www.chinadaily.com.cn/opinion/2017-07/13/content_30094968.htm. [Accessed 10 2018].

[3] R. Das, "RFID 2018-2028," IDTechEx, 2018. [Online]. Available: https://rainrfid.org/wp-content/uploads/2018/03/IDTechEx-RFID-March-_Distribute.pdf. [Accessed 09 2018].

[4] L. Boyce, "Customers CAN request not to have a contactless debit card major banks say – but at one, just 1,200 out of millions have...," This is Money, 2015. [Online]. Available: https://www.thisismoney.co.uk/money/saving/article-3214113/Customers-request-not-contactless-debit-card-major-banks-say-one-just-1-200-millions-have.html. [Accessed 09 2018].

[5] N. C. Wu, M. A. Nystrom, T. R. Lin and H. C. Yu, "Challenges to Global RFID Adoption," in *Technology Management for the Global Future - PICMET 2006 Conference*, Istanbul, Turkey, 2006.

[6] A. Abdelnour , D. Kaddour and S. Tedjini, "Transformation of Barcode Into RFID Tag, Design, and Validation," *IEEE Microwave and Wireless Components Letters* , vol. 28, no. 5, pp. 398-400, 2018.

[7] D. Ma, N. Saxena, T. Xiang and Y. Zhu, "Location-Aware and Safer Cards: Enhancing RFID Security and Privacy via Location Sensing," *IEEE Transactions on Dependable and Secure Computing* , vol. 10, no. 2, pp. 57 - 69, 2013.

[8] I. Expósito, I. Cuiñas and J. A. Gay-Fernández, "Efficient traceability solutions in the wine production by RFID and WSN," in *7th European Conference on Antennas and Propagation (EuCAP)*, Gothenburg, Sweden, 2013.

[9] M. Grabia, "Assessment of effectiveness of the use of RFID technology in selected processes at DIY retail store," in *IEEE International Conference on RFID Technology and Applications (RFID-TA)*, Tokyo, Japan, 2015.

[10] A. Badru and N. Ajayi, “Adoption of RFID in large-scale organisation — A review of challenges and solutions,” in *IST-Africa Week Conference (IST-Africa)*, Windhoek, Namibia, 2017.

[11] J. Shimbart, “Electrics, Internet and TV Wiring,” Homebuiding & Renovating, 18 04 2016. [Online]. Available: https://www.homebuilding.co.uk/electrics-internet-and-television-connections-wiring/. [Accessed 09 2018].

[12] Z. Fu, M. J. Crisp, S. Yang, R. V. Penty and I. H. White, “Long distance passive UHF RFID system over ethernet cable,” in *IEEE RFID-TA*, Warsaw, Poland, 2017.

[13] B. Lüers, B. Geck and D. Manteuffel, “24 GHz RFID transponder frontend with an equal gain baseband combining for industry 4.0 applications,” in *IEEE Microwave Conference (GeMiC), 2018 11th German*, Freiburg, Germany, Germany, 2018.

[14] M. Skilton and F. Hovsepian, The 4th Industrial Revolution, Palgrave Macmillan, Cham, 2018.

[15] J. Landt, “The history of RFID,” *IEEE Potentials*, vol. 24, no. 4, pp. 8-11, 2005.

[16] V. D. Hunt, A. Puglia and M. Puglia, RFID - A Guide to Radio Frequency Identification, Wiley-Blackwell, 2006.

[17] R. E. Floyd, “RFID in Animal-Tracking Applications,” *IEEE Potentials*, vol. 34, no. 5, pp. 32-33, 2015.

[18] E. C. Jones and C. A. Chung, RFID in LOGISTICS: A Practical Introduction, CRC Press, 2007.

[19] M. F. Wolff, “Retrospective: The genesis of the integrated circuit: How a pair of U.S. innovators brought into reality a concept that was on many minds,” *IEEE Spectrum*, vol. 13, no. 8, pp. 45-53, 1976.

[20] J. DeLorenzo and J. DiFranco, “Response of a linear FM matched filter to gated noise,” *Proceedings of the IEEE*, vol. 54, no. 6, pp. 905-906, 1966.

[21] B. Violino, Artist, *The History of RFID Technology*. [Art]. RFID JOURNAL, 2005.

[22] Y. Mehrjerdi , “RFID: A Bibliographical Literature Review with Future Research Directions,” *Industrial Engineering & Production Research*, vol. 25, no. 2, pp. 151-190, 2014.

[23] A. Rida, L. Yang and M. Tentzeris, RFID-Enabled Sensor Design and Applications, Artech House, 2010.

[24] W. Arnold, “The toll highway faces automation,” *Electronics,* p. 74, 1973.

[25] A. Koelle, S. Depp and R. Freyman, “Short-range radio-telemetry for electronic identification, using modulated RF backscatter,” *Proceedings of the IEEE,* vol. 63, no. 8, pp. 1260-1261, 1975.

[26] K. Ashton, “That ‘Internet of Things’ Thing,” RFID Journal, 2009. [Online]. Available: http://www.rfidjournal.com/articles/view?4986.

[27] C.-T. Huang, L.-W. Lo, W.-l. Wang and H.-L. Chen, “A study for optimizing the reading rate of RFID tagged cartons in palletizing process,” in *Industrial Engineering and Engineering Management,* Singapore, Singapore, 2008.

[28] S. Guo, Z. Zhou, J. Li, Q. Xiang and Z. Li, “Applications of Soft Computing in RFID System: A Review,” in *Control and Decision Conference (CCDC),* Qingdao, China, 2015.

[29] V. Paredes, “Mojix Delivers Next Generation STAR System with World’s Longest-Range Passive Tracking Capabilities,” Mojix, 5 6 2012. [Online]. Available: https://www.mojix.com/mojix-delivers-next-generation-star-system-with-worlds-longest-range-passive-tracking-capabilities/.

[30] S. Antipolis, “New UHF spectrum available for RFID and short range devices,” ETSI, 13 3 2014. [Online]. Available: http://www.etsi.org/news-events/news/761-2014-03-news-uhf-spectrum-available-for-rfid-and-short-range-devices.

[31] R. RFID, “RAIN RFID,” RAIN RFID, [Online]. Available: https://rainrfid.org/.

[32] E. Ngai, K. K. Moon, F. J. Riggins and C. Y. Yi, “RFID research: An academic literature review (1995–2005) and future research directions,” *Production Economics,* vol. 112, no. 2018, pp. 510-520, 2008.

[33] C.-C. Chao, J.-M. Yang and W.-Y. Jen, “Determining technology trends and forecasts of RFID by a historical review and bibliometric analysis from 1991 to 2005,” *Technovation,* vol. 27, no. 2007, pp. 268-279, 2007.

[34] A. J. S. Boaventura and N. B. Carvalho, “The Design of a High-Performance Multisine RFID Reader,” *MICROWAVE THEORY AND TECHNIQUES,* vol. 65, no. 9, pp. 3389-3400, 2017.

[35] A. Bothe, C. Schraeder and N. Aschenbruck, “An UHF RFID Performance Evaluation Architecture based on Traces from a Software Defined Transceiver,” in *IEEE RFID Technology and Applications Conference (RFID-TA)*, Tampere, Finland, 2014.

[36] M. Warnke, G. Rösnick, G. Smietanka, S. Brato and J. Götze, “Hybrid Extension of a Flexible Software Defined RFID Reader,” in *Smart Objects, Systems and Technologies (Smart SysTech)*, Dortmund, Germany, 2014.

[37] O. Martens, A. Liimets and A. Kuusik, “Synchronization algorithm for RFID-reader and its implementation,” in *Advances in Wireless and Optical Communications (RTUWO)*, Riga, Latvia, 2015.

[38] L. Sun, J. Liu, G. Hui and X. Mao, “The Design and Implementation of A RFID Reader Based on MFRC531,” in *Computer Science and Network Technology 3rd International*, Dalian, China, 2013.

[39] C. Tang, Z. Tang, Y. Yang and Y. Zhan, “Design of UHF RFID Reader Based on AS3991,” in *IEEE RFID-TA*, Guangzhou, China, 2010.

[40] G. W. a. D. W. Q. Lei, “Design of a handheld UHF RFID reader for The Internet of Things,” in *Computer and Management (CAMAN)*, Wuhan, China, 2011.

[41] a. Q. Z. L. Liu, “Design and Implementation of a Long-Range RFID Reader,” in *Electronic Measurement & Instruments (ICEMI)*, Chengdu, China, 2011.

[42] S. Sabesan, M. Crisp, R. Penty and I. White, “Wide Area Passive UHF RFID System Using Antenna Diversity Combined With Phase and Frequency Hopping,” *Antennas and Propagation,* vol. 62, no. 2, pp. 878-888, 2014.

[43] H. H. Su, J. Zhang and M. S. Tong, “Design of chipless RFID tag based on surface acoustic wave,” in *Electromagnetics Research Symposium - Fall (PIERS - FALL)*, Singapore, 2018.

[44] Q. Zhang, T. Han, B. Zhang, G. Tang, Y. Huang, T. Omori and K.-y. Hashimoto, “Frequency domain FEM analysis of reflector scattering characteristics for SAW tags,” in *Ultrasonics Symposium (IUS)*, Tours, France, 2016.

[45] M. M. Khan, F. A. Tahir, M. F. Farooqui, A. Shamim and H. M. Cheema, “3.56-bits/cm 2 Compact Inkjet Printed and Application Specific Chipless RFID Tag,” *Antennas and Wireless Propagation Letters*, vol. 15, pp. 1109-1112, 2015.

[46] C. Herrojo , J. Mata-Contreras , F. Paredes , A. Núñez , E. Ramon and F. Martín, "Near-Field Chipless-RFID System With Erasable/Programmable 40-bit Tags Inkjet Printed on Paper Substrates," *Microwave and Wireless Components Letters,* vol. 28, no. 3, pp. 272-274, 2018.

[47] A. Vena , E. Perret , D. Kaddour and T. Baron, "Toward a Reliable Chipless RFID Humidity Sensor Tag Based on Silicon Nanowires," *Microwave Theory and Techniques ,* vol. 64, no. 9, pp. 2977-2985, 2016.

[48] A. E. Abdulhadi and T. A. Denidni, "Self-Powered Multi-Port UHF RFID Tag-Based-Sensor," *Radio Frequency Identification ,* vol. 1, no. 2, pp. 115-123, 2017.

[49] N. Kaur, D. S. Velandia, W. Whittow, D. Barwick, E. Iredia, N. Parker, N. Porter, P. P. Conway and A. A. West, "Design and Performance of a Flexible Metal Mountable UHF RFID Tag," in *Electronic Components and Technology Conference (ECTC),* San Diego, CA, USA, 2015.

[50] C. Cremoux, A. Boyer and K. Dhia, "Reliability of active RFID tag immersed in water for "Preventing infant abduction" application," in *Antennas and Propagation in Wireless Communications (APWC),* Palm Beach, Netherlands Antilles, 2014.

[51] M. Le, T. P. Dong, T. Vuong and Q. Nguyen, "A Circularly Polarized Passive RFID Tag on Wall," in *Applied Electromagnetics (APACE),* Johor Bahru, Malaysia, 2014.

[52] P. Parthiban, B.-C. Seet and X. Li, "Low-cost low-profile UHF RFID reader antenna with reconfigurable beams and polarizations," in *IEEE International Conference on RFID (RFID),* Phoenix, 2017.

[53] T. Deleruyelle, P. Pannier, J. Alarcón, M. Egels and E. Bergeret, "Multi-standard UHF and UWB antennas for RFID applications," in *the Fourth European Conference on Antennas and Propagation,* Barcelona, Spain, 2010.

[54] J. Virkki, X. Chen , T. Björninen and L. Ukkonen, "Embroidered antennas and antenna-electronics interfaces for wearable RFID tags," in *IEEE MTT-S International Microwave Workshop Series on Advanced Materials and Processes for RF and THz Applications (IMWS-AMP),* Pavia, Italy, 2017.

[55] S. Sabesan, M. Crisp, R. V. Penty and I. H. White, "Demonstration of improved passive UHF RFID coverage using optically-fed distributed multi-antenna system," in *IEEE International Conference on RFID,* Orlando, FL, USA, 2009.

[56] R. Langwieser, G. Lasser, A. L. Scholtz and M. Rupp, "Comparison of multi-antenna configurations of an RFID reader with active carrier compensation," in *IEEE International Conference on RFID-Technologies and Applications*, Sitges, Spain, 2011.

[57] T.-H. Dao, M.-T. Le and Q.-C. Nguyen, "Indoor localization system using passive UHF RFID tag and multi-antennas," in *International Conference on Advanced Technologies for Communications (ATC 2014)*, Hanoi, Vietnam, 2014.

[58] L. Catarinucci, D. D. Donno, L. Mainetti, L. Palano, L. Patrono, M. L. Stefanizzi and L. Tarricone, "Integration of UHF RFID and WSN technologies in healthcare systems," in *IEEE RFID Technology and Applications Conference (RFID-TA)*, 2014, 2014.

[59] R. Correia and N. B. Carvalho , "Ultrafast Backscatter Modulator With Low-Power Consumption and Wireless Power Transmission Capabilities," *IEEE Microwave and Wireless Components Letters,* vol. 27, no. 12, pp. 1152 - 1154, 2017.

[60] H. Cheng, . W. Ni and N. Li, "A systematic scheme for designing RFID systems with high object detection reliability," in *International Conference on Information Science, Electronics and Electrical Engineering*, Sapporo, Japan, 2014.

[61] P. Liu, W. Liu, Q. Li, M. Duan, Y. Wang and Y. Dai, "A research on tracing code of culture of food safety traceability based on RFID and improved EPC," in *International Conference on Logistics, Informatics and Service Sciences (LISS)*, Sydney, NSW, Australia, 2016.

[62] W. Yao, C. Chu and Z. Li, "The Adoption and Implementation of RFID Technologies in Healthcare: A Literature Review," *Medical System,* vol. 36, no. 6, pp. 3507-3525, 2012.

[63] C. Costa, F. Antonucci, F. Pallottino, J. Aguzzi, D. Sarria and P. Menesatti, "A Review on Agri-food Supply Chain Tractability by Means of RFID technology," *Food Bioprocess Technology,* vol. 6, no. 2, pp. 353-365, 2013.

[64] D. Bonter and E. Bridge, "Applications of radio frequency identification (RFID) in," *Field Ornithology,* vol. 82, no. 1, pp. 1-10, 2011.

[65] V. Peppa and S. Moschuris, "RFID technology in supply chain management: a review of the literature and prospecting adoption to the Greek market," *Engineering Education,* vol. 15, no. 1, pp. 61-68, 2013.

[66] M. Chan and X. Zhang, "Experiments for Leveled RFID Localization for Indoor Stationary Objects," in *11th International Conference on Information Technology*, 2014.

[67] D. Simard, K. Bouchard, S. Gaboury, B. Bouchard and A. Bouzouane, "Accurate Passive RFID Localization system for Smart Home," in *3rd International Conference on Network Embedded Systems for Every Application*, 2012.

[68] C. Chang, W. Chen and T. Cheng, "A Secure RFID Mutual Authentication Protocol Conformation to EPC Class 1 Generation 2 Standard," in *10th International Conference on Intelligent Information Hiding and Multimedia Signal Processing*, 2014.

[69] G. Wang, Y. Wang and Y. Li, "Authentication Protocol of RFID System Based on Security Policy," in *3rd International Conference on Instrumentation, Measurement, Computer, Communication and Control*, 2013.

[70] D. Sun and J. Zhong, "A Hash-Based RFID Security Protocol for Strong Privacy Protection," *Transactions on Consumer Electronics*, vol. 58, no. 4, pp. 1246-1252, 2012.

[71] M. Mubarak, J. Manan and S. Yahya, "A Critical Review on RFID System towards Security, Trust, and Privacy (STP)," in *7th International Colloquium on Signal Processing and its Applications*, 2011.

[72] W. Chen, "A Feasible and Easy-to-Implement Anticollision Algorithm for the EPCglobal UHF Class 1 Generation-2 RFID Protocol," *Automation Science and Engineering, IEEE*, vol. 11, no. 2, pp. 485-491, 2014.

[73] I. Broz, N. Bako, Z. Butkovic and A. Baric, "RFID UHF Protocol Implementation in Distributed Sensor Networks," in *International Convention on Information and Communication Technology, Electronics and Microelectronics*, 2015.

[74] P. Solic, J. Radic and N. Rozic, "Early Frame Break Policy for ALOHA-Based RFID System," *Automation Science and Engineering, IEEE*, vol. 2015, no. 99, pp. 1-6, 2015.

[75] R. Want, "An introduction to RFID Technology," *Pervasive Computing, IEEE*, vol. 5, no. 1, pp. 25-33, 2006.

[76] A. Hashemi, A. H. Sarhaddi and H. Emami, "A Review on Chipless RFID Tag Design," *Electronics Engineering*, vol. 7, no. 2, pp. 68-75, 2013.

[77] D. Wang and W. Ip, "Review on Modelling and Optimization Problems about RFID Technology and Applications," in *Control and Decision Conference,* 2013.

[78] A. Buffi, P. Nepa and R. Cioni, "SARFID on drone: Drone-based UHF-RFID tag localization," in *IEEE International Conference on RFID Technology & Application (RFID-TA)*, Warsaw, Poland, 2017.

[79] H. H. Su, J. Zhang and M. S. Tong, "Design of chipless RFID tag based on surface acoustic wave," in *Progress in Electromagnetics Research Symposium - Fall (PIERS - FALL)*, Singapore, Singapore, 2017.

[80] Atlas, "HANDHELD RFID READERS," Atlas , 2019. [Online]. Available: https://www.atlasrfidstore.com/handheld-rfid-readers/. [Accessed 09 2019].

[81] Keonn, "RFID robot for automatic inventory: AdvanRobotTM," AdvanRobotTM , 2019. [Online]. Available: https://www.keonn.com/systems/view-all-2/inventory-robots.html. [Accessed 09 2019].

[82] R. 24-7, "WILL DRONES CHALLENGE FIXED AND HANDHELD RFID READERS IN RETAIL?," RFID 24-7, 08 2014. [Online]. Available: http://rfid24-7.com/article/will-drones-challenge-fixed-and-handheld-rfid-readers-in-retail/. [Accessed 09 2019].

[83] P. M. Senadeera, N. S. Dogan, Z. Xie, H. S. Savci, I. Kateeb and M. Ketel, "Recent trends in RFID transponders," in *IEEE Southeastcon*, Jacksonville, FL, USA, 2013.

[84] J. Wang, C. Zhang and . Z. Wang, "A Low Power Low Cost Fully Integrated UHF RFID Reader with 17.6dBm Output P1dB in 0.18 um CMOS Process," in *IEEE Radio Frequency Integrated Circuits Symposium,* 2010.

[85] D. Oyeka, M. Ziai, J. Batchelor, E. Parker, V. Romaguera and S. Yeates, "Developing Inkjet Printing to enable low cost UHF RFID transfer tattoo tags," in *IEEE Antennas and Propagation Society International Symposium,* 2013.

[86] EPCglobal, "Class 1 Generation 2 UHF Air Interface Protocol Standard Version 1.0.9," EPCglobal, 2005. [Online]. Available: http://www.epcglobalinc.org. [Accessed 09 2019].

[87] E. Global, "EPC™ Radio-Frequency Identity Protocols Class-l Generation-2 UHF RFID Protocol for Communications at 860 MHz-960MHz," EPC Global, 2006. [Online]. Available: http://www.epcglobalinc.org. [Accessed 09 2019].

[88] E. T. S. I. (ETSI), "Regulatory status for using RFID in the EPC Gen 2 band (860 to 960 MHz) of the UHF spectrum," ETSI, 2014. [Online]. Available: http://www.gs1.org/docs/epc/UHF_Regulations.pdf. [Accessed 09 2019].

[89] D. Kim and . J. Yeo, "Dual-Band Long-Range Passive RFID Tag Antenna Using an AMC Ground Plane," *Antennas and Propagation,* vol. 60, no. 6, pp. 2620-2626, 2012.

[90] I. Mayordomo, R. Berenguer, A. Alonso, I. Fernandez and I. Gutierrez, "Design and Implementation of a Long-Range RFID Reader for Passive Transponders," *Microwave Theory and Techniques,* vol. 57, no. 5, pp. 1283-1290, 2009.

[91] L. Liu and Q. Zhang, "Design and Implementation of a Long-Range RFID Reader," in *10th International Conference on Electronic Measurement & Instruments,* 2011.

[92] S. Sabesan, M. Crisp, R. Penty and I. White, "An error free passive UHF RFID system using a new form of wireless signal distribution," in *RFID IEEE International Conference,* 2012.

[93] S. Sabesan, M. Crisp, R. Penty and I. White, "Passive UHF RFID interrogation system using wireless RFID repeater nodes," in *IEEE RFID International Conference,* 2013.

[94] S. Ahn, J. Park and J. Kim, "BoMR: A Booster for Mobile RFID Readers," in *International Conference on ICT Convergence,* 2011.

[95] L. Liu and S. Lai, "Aloha-based anti-collision algorithms used in RFID system," in *Wireless Communications, Networking, and Mobile Computing International Conference,* 2006.

[96] H. Vogt, "Efficient object identification with passive RFID tags," in *Pervasive Computing, Springer Berlin Heidelberg,* 2002.

[97] M. Kodialam and T. Nandagopal, "Fast and reliable estimation schemes in RFID systems," in *12th International Conference on Mobile computing and networking,* 2006.

[98] K. Finkenzeller, RFID-Handbook Fundamentals and Applications in Contact less Smart Cards and Identification, Wiley and Sons, 2003.

[99] J. Choi, D. Lee and H. Lee, "Query tree-based reservation for efficient RFID tag anti-collision," *Communications Letter,* vol. 11, no. 1, pp. 85-87, 2007.

[100] X. Liu, Z. Qian, Y. Zhao and Y. Guo, "An Adaptive Tag Anti-Collision Protocol in RFID Wireless Systems," *IEEE Communications, China,* vol. 11, no. 7, pp. 117-127, 2014.

[101] M. Jakeem, K. Raahemifar and G. Khan, "Novel Modulo based Hloha Anti-Collision Algorithm for RFID Systems," in *IEEE International Conference on RFID,* 2014.

[102] W. Chen, "An Accurate tag estimated method for improving the performance of an RFID anti-collision algorithm based on dynamic frame length ALOHA," *Automatic Science and Engineering,* vol. 6, no. 1, pp. 9-15, 2009.

[103] H. Chung, H. Mo, N. Kim and C. Pyo, "An advanced RFID system to avoid collision of RFID reader, using channel holder and dual sensitivities," *Microwave and Optical Technology Letters,* vol. 49, no. 11, pp. 2643-2647, 2007.

[104] J. Eom, S. Yim and T. Lee, "An efficient reader anticollision algorithm in dense RFID networks with mobile RFID readers," in *IEEE Transactions on Industrial Electronics,* 2009.

[105] M. Bueno-Delgado, R. Ferrero, F. Gandino, P. Pavon-Marino and M. Rebaudengo, "A Geometric Distribution Reader Anti-Collision Protocol for RFID Dense Reader Environments," *Automatic Science and Engineering,* vol. 10, no. 2, pp. 296-306, 2013.

[106] Z. Li, H. Yang, J. Li, C. He and J. Zhou, "An Enhanced Neighbor-friendly Reader anti-collision Algorithm in Mobile RFID Networks," in *4th IEEE International Conference on Information Science and Technology,* 2014.

[107] S. Jung, M. Kim and Y. Yang, "A Reconfigurable Carrier Leakage Canceler for UHF RFID Reader Front-Ends," *Circuits and System I: Regular papers, IEEE,* vol. 58, no. 1, pp. 70-76, 2011.

[108] M.-S. Kim, S.-C. Jung, J. Jeong, H. Kin, M. Seo and J. Ham, "Adaptive TX Leakage Canceler for the UHF RFID Reader Front End Using a Direct Leaky Coupling Method," *IEEE Transactions on Industrial Electronics ,* vol. 61, no. 4, pp. 2081 - 2087, 2014.

[109] J. Jung, H. Roh, J. Kim, H. Kwak, M. Jeong and J. Park, "TX leakage cancellation via a micro controller and high TX-to-RX isolation covering an UHF RFID frequency band of 908-914 MHz," *IEEE Microwave and Wireless Components Letters,* vol. 18, no. 10, pp. 710-712, 2008.

[110] T. Xiong, X. Tan, J. Xi and H. Min, "High TX-to-RX isolation in UHF RFID using narrowband leaking carrier canceller," *IEEE Microwave and Wireless Components Letters,* vol. 20, no. 2, pp. 124-126, 2010.

[111] S.-C. Jung, M.-S. Kim and Y. Yang, "Baseband Noise Reduction Method Using Captured TX Signal for UHF RFID Reader Applications," *IEEE Transactions on Industrial Electronics,* vol. 59, no. 1, pp. 592 - 598, 2012.

[112] Q. Peng, C. Zhang, X. Zhao, X. Sun, F. Li, H. Chen and Z. Wang, "A Low-cost UHF RFID system with OCA tag for short-range communication," *Industrial Electronics,* vol. 62, no. 7, pp. 4455-4465, 2015.

[113] N. Usachev, V. Elesin, A. Nikiforov and V. Telets, "Behavioral Approach to Design Universal UHF RFID Reader Transceiver ICs," in *29th International Conference on Microelectronics,* 2014.

[114] Q. Peng, C. Zhang, H. Song and Z. Wang, "A Low-cost, low-power UHF RFIDreader transceiver for mobile applications," in *IEEE RFIC Symp. Dig.*, 2012.

[115] L. Ye, H. Liao, F. Song, J. Chen, J. Zhao, R. Liu, C. Wang, C. Shi, J. Liu, R. huang and Y. Wang, "A Single-chip CMOS UHF RFID reader transceiver for Chinese mobile applications," *Solid-State Circuits, IEEE,* vol. 45, no. 7, pp. 1316-1329, 2010.

[116] Impinj, "Types of the RFID systems," 2017. [Online]. Available: https://www.impinj.com/about-rfid/types-of-rfid-systems/.

[117] Microsemi, "Understanding 802.3at: PoE Plus Standard Increase Available Power," Microsemi, 2011. [Online]. Available: https://www.streakwave.com/powerdsine/Understanding_802_3at_PowerDsine.pdf.. [Accessed 09 2019].

[118] J. Rodas, V. Barral, C. Escudero and R. Langwieser, "A Solution for Optimizing Costs and Improving Diversity of RFID Readers," in *19th International Conference on Systems, Signals and Image Processing*, 2012.

[119] Q. Lei, G. Wang and D. Wang, "Design of a handheld UHF RFID reader for the Internet of Things," in *International Conference on Computer and Management*, 2011.

[120] H. Li, H. Wang, Z. Shang, Q. Li and . W. Xiao, "Low-power UHF Handheld RFID Reader Design and Optimization," in *8th World Congress on Intelligent Control and Automation*, 2010.

[121] A. A. M. Salen, A. R. JR. and R. S. Roman, "Distributed Antennas for Indoor Radio Communications," *IEEE Transactions on Communications,* vol. 35, no. 12, pp. 1245-1251, 1987.

[122] V. G.-G. Buendía, S. Kenny, S. K. Podilchak, G. Goussetis, A. Costanzo and P. Nicole, "Smart cable for Radio Frequency Identification in aeronautical applications," in *10th European Conference on Antennas and Propagation (EuCAP)*, Davos, Switzerland, 2016.

[123] Y. Wang, N. Zhang and L. Jin, "The hardware design and implementation of four-channel UHF RFID reader based on Impinj R2000," in *6th IEEE International Conference on Software Engineering and Service Science (ICSESS)*, Beijing, China, 2015.

[124] Mojix, "STAR™ RFID READER," Mojix, 2018. [Online]. Available: https://www.mojix.com/star-content/. [Accessed 09 2018].

[125] PervasID, "Space Ranger 9100™ System," PervasID, 2018. [Online]. Available: http://www.pervasid.com/products/. [Accessed 09 2018].

[126] A. S. Bakhtiar, M. S. Jalali and S. Mirabbasi, "A high-efficiency CMOS rectifier for low-power RFID tags," in *IEEE International Conference on RFID (IEEE RFID 2010)*, Orlando, FL, USA, 2010.

[127] J. Zhang, G. Tian, A. M. J. Marindra, A. I. Sunny and A. B. Zhao, "A Review of Passive RFID Tag Antenna-Based Sensors and Systems for Structural Health Monitoring Applications," *Sensors (Basel)*, vol. 17, no. 2, pp. 1-33, 2017.

[128] NXP, "UCODE," NXP, 2018. [Online]. Available: https://www.nxp.com/products/identification-and-security/smart-label-and-tag-ics/ucode:MC_50483. [Accessed 09 2018].

[129] M. Koller and R. Küng, "Adaptive carrier supression for UHF RFID using digitally tunable capacitors," in *European Microwave Conference*, Nuremberg, 2013.

[130] Microchip, "AT91SAM7S256," Microchip, 2018. [Online]. Available: https://www.microchip.com/wwwproducts/en/AT91SAM7S256. [Accessed 09 2018].

[131] A. Devices, "AD8349," Analog Devices, 2018. [Online]. Available: http://www.analog.com/en/products/ad8349.html#product-overview. [Accessed 09 2018].

[132] A. Devices, “ADL5380,” Analog Devices, 2018. [Online]. Available: http://www.analog.com/en/products/adl5380.html#product-overview. [Accessed 09 2018].

[133] A. Devices, “ADF4350,” Analog Devices, 2018. [Online]. Available: http://www.analog.com/en/products/adf4350.html. [Accessed 09 2018].

[134] Qorvo, “RF5110G,” Qorvo, 2018. [Online]. Available: https://www.qorvo.com/products/p/RF5110G#parameters. [Accessed 09 2018].

[135] IEEE, “IEEE Standard for Ethernet,” IEEE , 2018. [Online]. Available: https://standards.ieee.org/standard/802_3-2018.html. [Accessed 09 2018].

[136] T. Standard, “TIA-568-C2 Standard,” TIA, 2009. [Online]. Available: http://innovave.com/wp-content/uploads/2016/01/TIA-568-C.2.pdf. [Accessed 09 2018].

[137] . W. F. Egan, Frequency Synthesis by Phase Lock, John Wiley & Sons, 2011.

[138] AMS, “AS399x family,” AMS, [Online]. Available: https://ams.com/search#/as399. [Accessed 09 2018].

[139] B. You, B. Yang, X. Wen and L. Qu, “Implementation of Low-Cost UHF RFID Reader Front-Ends with Carrier Leakage Suppression Circuit,” *International Journal of Antennas and Propagation,* vol. 2013, no. 11, pp. 1-8, 2013.

[140] A. Boaventura, J. Santos, A. Oliveira and N. B. Carvalho, “Perfect Isolation: Dealing with Self-Jamming in Passive RFID Systems,” *IEEE Microwave Magazine* , vol. 17, no. 11, pp. 20 - 39, 2016.

[141] K. Kapucu, M. Pauli and C. Dehollain, “A Fast Active Leakage Cancellation Method for UHF RFID Readers,” in *IEEE International Conference on RFID,* 2017.

[142] I. Mayordomo and J. Bernhard, “Implementation of an adaptive leakage cancellation control for passive UHF RFID readers,” in *IEEE International Conference on RFID,* 2011.

[143] D. P. Villame and J. S. Marciano, “Carrier suppression locked loop mechanism for UHF RFID readers,” in *IEEE International Conference on RFID,* Orlando, 2010.

[144] J.-W. Jung, H.-H. Roh, J.-C. Kim, H.-G. Kwak, M. S. Jeong and J.-S. Park, “TX Leakage Cancellation via a Micro Controller and High TX-to-RX Isolations Covering

an UHF RFID Frequency Band of 908–914 MHz," *IEEE Microwave and Wireless Components Letters* , vol. 18, no. 10, pp. 710 - 712, 2008.

[145] E. A. Keehr, "A low-cost, high-speed, high-resolution, adaptively tunable microwave network for an SDR UHF RFID reader reflected power canceller," in *IEEE International Conference on RFID*, Orlando, 2018.

[146] A. J. S. Boaventura and N. B. Carvalho, "The Design of a High-Performance Multisine RFID Reader," *IEEE Transactions on Microwave Theory and Techniques,* vol. 65, no. 9, pp. 3389 - 3400, 2017.

[147] T. Brauner and X. Zhao, "A Novel Carrier Suppression Method for RFID," *IEEE Microwave and Wireless Components Letters* , vol. 19, no. 3, pp. 128 - 130, 2009.

[148] Q. Guo, Z. Sun, J. Liu, J. Huang, Y. Wang, X. Tan and H. Min, "A Novel Adaptive Leakage Suppression Method for UHF RFID Reader," in *IEEE International Conference on RFID*, 2017.

[149] S.-S. Lee, J. Lee, I.-Y. Lee, S.-G. Lee and J. Ko, "A new TX leakage-suppression technique for an RFID receiver using a dead-zone amplifier," in *International Solid-State Circuits Conference Digest of Technical Papers*, San Francisco, 2013.

[150] W. Xi, Y. Qing, B. Zhang , L. Zeng, J. Li and J. Zhang, "A novel method of carrier suppression for UHF RFID readers," in *2014 3rd Asia-Pacific Conference on Antennas and Propagation*, Harbin, 2014.

[151] A. Devices, "AD8340 Datasheet," Analog Devices, [Online]. Available: http://www.analog.com/en/products/ad8340.html#product-overview. [Accessed 09 2018].

[152] U. tag, "UPM Raflatax DogBone Datasheet," UPM, [Online]. Available: http://www.fastrfid.com/raflatac/UHF/tech_speck_3001572_letter.pdf. [Accessed 09 2018].

[153] T. M. Systems, "LMR-200," Times Microwave Systems, 2018. [Online]. Available: https://www.timesmicrowave.com/documents/resources/LMR-200-UF.pdf. [Accessed 09 2018].

[154] T. M. Systems, "LMR-400," Times Microwave Systems, 2018. [Online]. Available: https://www.timesmicrowave.com/documents/resources/LMR-400.pdf. [Accessed 09 2018].

[155] T. M. Systems, “LMR-1700,” Times Microwave Systems, 2018. [Online]. Available: https://www.timesmicrowave.com/documents/resources/LMR-1700.pdf. [Accessed 09 2018].

[156] R. Rezaiesarlak and M. Manteghi, “Design of Chipless RFID Tags Based on Characteristic Mode Theory (CMT),” *Antennas and Propagation,* vol. 63, no. 2, pp. 711-718, 2015.